Cancer Theranostics with Nano-enabled Bacterial Bots

A Thesis Submitted in Partial Fulfilment of

the Requirements for the Award of the Degree of

Doctor of Philosophy

By

Debashree Debasmita

To

Indian Institute of Technology Guwahati

Centre for Nanotechnology

Indian Institute of Technology Guwahati

Guwahati-781039, Assam, India

Table of Contents

DECLARATION

I hereby declare that the research work embodied in the thesis entitled "**Cancer Theranostics with Nano-enabled Bacterial Bots**" is the outcome of work carried out by me under the supervision of Prof. Siddhartha Sankar Ghosh and Prof. Arun Chattopadhyay, Centre for Nanotechnology, Indian Institute of Technology Guwahati, Assam, for the award of the degree of Doctor of Philosophy. To the best of my knowledge and belief, the current thesis has not been submitted for any degree, diploma, associateship etc. of any institute or university elsewhere.

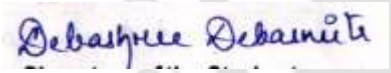

Debashree Debasmita (176153004)

Centre for Nanotechnology

Indian Institute of Technology Guwahati

Guwahati-781039 Assam India

February, 2023

Guwahati

Indian Institute of Technology Guwahati

CERTIFICATE

This is to certify that the thesis entitled "**Cancer Theranostics with Nano-enabled Bacterial Bots**", being submitted to the **Indian Institute of Technology Guwahati** by **Debashree Debasmita** (Roll No: **176153004**) for the award of the degree of **Doctor of Philosophy** in **Nanotechnology** is a bonafide record of research work carried out by her. The information and the data reported by her are solely the results of her original findings. She has meticulously carried out the investigations and followed the guidelines of the laboratory. This work has not been submitted elsewhere for any degree or diploma.

Dr. Siddhartha Sankar Ghosh
Professor
Department of Biosciences and Bioengineering
Indian Institute of Technology Guwahati
Guwahati-781039, Assam, India

Prof. Arun Chattopadhyay
Department of Chemistry
Indian Institute of Technology Guwahati
Guwahati-781 039, INDIA

Prof. Siddhartha Sankar Ghosh

Thesis Supervisor

Department of Biosciences and Bioengineering

Indian Institute of Technology Guwahati

Guwahati-781039, Assam, India

Prof. Arun Chattopadhyay

Thesis Supervisor

Department of Chemistry

Indian Institute of Technology Guwahati

Guwahati-781039, Assam, India

Dedicated to my parents

and to all those people who contributed directly and indirectly towards the fulfilment of my dreams

Acknowledgement

My foremost sincere gratitude is towards the people who made this journey reach its destination, my supervisors, Prof. Siddhartha Sankar Ghosh and Prof. Arun Chattopadhyay.

I am grateful towards Prof. Siddhartha Sankar Ghosh for providing me this wonderful opportunity of diving in to the world of research, offering the best research facilities, encouraging me to participate in conferences, always making sure that I complete my thesis work on time and for the support he has provided throughout the tenure.

I am indebted towards Prof. Arun Chattopadhyay for being my inspiration forever; his constant support has been my driving force throughout the PhD tenure. I am grateful for all the efforts he has made to help me complete my thesis work. I thank him for always believing in me and bringing the best out of me every time.

I extend my gratitude towards my doctoral committee members and viva-voce committee members Prof. Lal Mohan Kundu (Chairman), Prof. Tapas Kumar Mandal, Dr. Partho Sarathi G. Pattader, Prof. Ashis Kumar Mukherjee, Dr. Akshai Kumar A. S, Dr. Rajiv K. Kar, Prof. Siddhartha Sankar Ghosh and Prof. Arun Chattopadhyaya for their periodic evaluations, valuable suggestions and inputs.

I am grateful to Centre for Excellence in Nanoelectronics and Theranostic Devices, Central Instrumentation Facility, Centre for Nanotechnology, Centre for Excellence DBT Programme Support Biosciences and Bioengineering, and Department of Chemistry for supporting, meeting the essential requirements and providing me all the facilities to pursue my thesis work. I thank all the staff members of Centre for Nanotechnology (especially Dr. Pranjoli Das) for extending their help as and when required.

My gratitude towards all my former seniors from Centre for Nanotechnology (Dr. Upashi Goswami, Dr. Deepanjalee Dutta, Dr. Aditi Bannerjee, Dr. Bandhan Chatterjee, Dr. Anitha T Simon and Dr. Kasturi Gogoi), Department of Biosciences and Bioengineering (Dr. Neha Arora, Dr. Anil Bidkar, Dr. Srirupa Bhattacharyya, Dr. Rajib Shome) and Department of Chemistry (Dr. Srestha Basu) for their efforts to build a wonderful research environment and passing on to all the juniors.

My sincere gratitude towards all my current lab mates (Konika, Arupam, Hirak, senior Sayantani, Sawna, Sujisha, junior Sayantani, Muktashree, Plaboni, Shilpi, Thiru, Arisha, Basab, Dr. Mihir, Dr. Srimonto, Manideepa, Priya, Archismita, Arin, Ujjala, Shamim, and Santonu) for their cooperation and support for maintaining a great working environment. I thank Tarik for extending his helping hand.

I am grateful to the universe for gifting me with the best family and in-laws. My foremost gratitude for my late mother (Kalpita Pradhan) for showering her blessings forever, being the coolest mother, always believing that "I can do anything" and always pushing me to achieve big. I am grateful to my father (Akshaya Kumar Pradhan) for being the most supportive and liberal parent and being there always. I can never thank enough my elder sisters (Tapoti Taponwita and Yogati Yogabrata), my brother-in-laws (Srikanta Swain and Binata Khuntia) for raising me as their child and being there for me all the time. I thank my late father-in-law (Dr. Tapas Bhattacharjee) for showering his blessings on me, my mother-in-law (Purnima Bhattacharjee) for her patience and support and my sister-in-law (Madhushree Chatterjee) for being a friend and a sister to me. My lovely nieces (Urvi, Aarvi and Dhairavi), my dear nephew (Dev) and my pets Dubloo and Dingroo and other furry friends of IIT Guwahati campus for cheering me up in my darkest days.

I express my gratitude towards my best half, my husband, Dr. Basu Bhattacharjee, for being my "forever constant" and supporting me unconditionally throughout, being my biggest critic, for being my "go to person" and standing beside me always through my thick and thins. I thank him for putting his efforts to push me ahead to pursue my dreams and bringing so much to my life.

Lastly, I thank all those wonderful people (Yasmita, Ishani, Swati, Richa, Shuchishloka, Dr. Abhilipsa Das, Dr. Raghunand Tirumalai, Dr. Rajesh Kumar, Dr. Chaitanya Veena Yeruva, Prof. Animesh Mohapatra, Jaya Rajappan, Aditya kumar Panda, Arjun Sahoo, Dr. B.C Dwivedy, Anjum Mallick and Prof. Sachidananda) who have made their conscious and unconscious efforts to help me reach here.

Abbreviations

AFM: Atomic force microscopy

AuNCs: Gold (Au) nanoclusters

AuNPs: Gold (Au) nanoparticles

BHI: Brain heart infusion growth medium

BCG: Bacillus-Calmette-Guerin

CAFs: Cancer associated fibroblasts

CFU: Colony forming unit

CLSM: Confocal laser scanning microscopy

DCs: Dendritic cells

DCFHDA: 2',7'-Dichlorofluoresceindiacetate

DCFH: 2',7'-Dichlorodihydrofluorescein

DCF: 2',7'-Dichlorofluorescein

DMEM: Dulbecco's modified eagle medium

EBV: Epstein-Barr-Virus

ECM: Extracellular matrix

EDX: Energy dispersive X-ray

EGFR: Epidermal growth factor receptor

EMT: Epidermal to mesenchymal transition

EPR: Enhanced permeation and retention

EPS: Extra polymeric substance

ER: Oestrogen receptor

FESEM: Field emission scanning electron microscopy

GFP: Green fluorescence protein

HER-2: Human epidermal growth factor receptor -2

HPV: Human papilloma virus

LAB: Lactic acid bacteria

LPS: Lipopolysaccharide

MALT: Mucosa associated lymphoid tissue

MIC: Minimum inhibitory concentration

MOI: Multiplicity of infection

MPA: 3- Mercaptopropionic acid

MRI: Magnetic resonance imaging

MRSA: Multi-drug resistant *Staphylococcus aureus*

MRS: deMan Rogosa Sharpe medium

MTX: Methotrexate

$NADP^+$: Nicotinamide adenine dinucleotide phosphate

OMVs: Outer membrane vesicles

PAMPs: Pathogen associated molecular patterns

PDT: Photodynamic therapy

PET: Positron emission tomography

PGN: Peptidoglycan

PTT: Photothermal therapy

RBCs: Red blood cells

RFP: Red fluorescence protein

ROS: Reactive oxygen species

SAED: Selected area electron diffraction

SCFA: Short chain fatty acid

SDS-PAGE: Sodium dodecyl-sulphate -polyacrylamide gel electrophoresis

TEM: Transmission electron microscopy

TLR: Toll-like receptor

TME: Tumour microenvironment

TNF-α: Tumour necrosis factor α

XPS: X-ray photoelectron spectroscopy

XRD: X-ray diffraction

Abstract

The contemporary cancer therapeutics are being strategically designed to obtain improved outcomes as compared to the conventional methods. The primary challenges faced by the conventional mode of therapies such as surgeries, radiation therapies, and later chemotherapy are difficulty in tumor accessibility, undesirable impact on normal cells, ineffectiveness towards cancer stem cells, missing the targets, rapid drug release prior to reaching the targets, poor pharmacokinetics of drugs, and resistance development to the therapy. In order to focus on the improvements, target specificity through small molecules, aptamers, antibodies, nucleic acid, stimuli sensitive polymers have been developed. Coating of the drug with polymers and loading the drugs on nano-carriers for enhanced bioavailability, slower release and safety from immune attacks have also been introduced. Developing methods for immunotherapy are also being practiced. Gradually the newer methods such as gene therapy, immunotherapy, and combined therapies have overtaken the conventional methods. Although these methods have shown improved results in comparison to the previous methods but the threat imposed by the cancer stem cells and drug resistance are still continuing. The advent of bacteria-mediated therapy has shown some light towards a path of developing a resistance – free cancer therapy. Since, the anaerobic bacteria preferably colonize in the hypoxic areas of the tumor and act on the core of the tumor, hence, there is a better opportunity for the bacteria to eradicate the stem cells and prevent relapse of cancer. The attenuated strains achieved through genetic engineering and over-expression of endotoxins and therapeutic genes have generated hopes for a better future of cancer therapeutics. The commonly used strains are *Salmonella, Bifidobacterium, Clostridium, E. coli* and Lactic acid bacteria (LAB). The bacteria-based therapy can have two usages, first as a therapeutic entity and second as a delivery vehicle. The anti-cancer effects of the bacteria can be inherent or can be inculcated through genetic modifications of endotoxin gene, pro-drug activating enzymes, siRNA, shRNA based silencing, and immune system evoking via over-expression of cytokines specifically activating T-cells and macrophages. The anti-biotic susceptibility, suitability for genetic manipulation, and low immunogenicity are required criteria for bacteria to be a therapeutic agent. The risk factor associated with the bacteria-mediated therapy is controlling the growth and number of bacteria after the therapeutic regimen is over. A few studies have been reported on these aspects and a lot more is yet to be explored. In order to avoid the adversities of using a pathogenic strain, the shift can be made towards opting for

safer strains that do not require genetic manipulation and have inherent anticancer effects. The safest option is to use human gut friendly bacteria. The gut bacteria play a pivotal role in drug actions, resistance and overall health of an individual. The gut microbes, which have inherent anti-cancer properties are *Streptococcus pyrogenes, Mycobacterium bovis*, *Serratia marcescens*, *Lactobacillus plantarum*, *Lactobacillus rhamnosus* GG, *Lactobacillus acidophilus, Salmonella, Clostritidium, Bifidobacterium and E. coli*. Out of this vast range of bacterial strains the, *Lactobacillus* are among the safest strains as they are non-pathogenic. This could solve the safety issues of using attenuated pathogenic strains. The *Lactobacillus* strains are anti-tumorigenic naturally and are antibiotic susceptible, making them suitable as an anti-cancer agent and also as a carrier. The current dissertation work was up-taken to explore the potential of wild type *Lactobacillus rhamnosus* as a living bacbot that could function as a theranostic agent having anti-cancer effects mediated by an anti-cancer drug methotrexate and their inherent abilities in annihilating cancer tumours.

Chapter 2

In this chapter, the gold nanoclusters were synthesized on the outer surface of living *Lactobacillus rhamnosus* using chemical synthesis method. The synthesis was carried out using $HAuCl_4$ and 3-mercaptopropioic acid. The nanoclusters formation was standardized in such a way that the bacteria remained intact, alive and viable after the synthesis. The characterization study included, spectroscopic analysis (UV, photoluminescence, X-ray Photoelectron Spectroscopy), X-ray diffraction, microscopy analysis (confocal laser scanning microscopy, transmission electron microscopy, field emission scanning electron microscopy, atomic force microscopy), and energy dispersive X-ray analysis. The synthesized gold nanoclusters were approximately 1.3 nm in size and had rendered fluorescence to the living bacteria making them traceable. These bacteria were named as Lac_AuNC. The doubling time of the bacteria is 1.1 h and the incubation time is 48 h. The Lac_AuNC were inoculated in to fresh medium and were allowed to divide and produce progenies. These progenies were again made to divide and this was continued for six-subsequent sub-cultures. All the progenies were collected and their TEM images revealed that their surfaces had large aggregates of gold nanoclusters in the form of spheres. The size of the spheres was varying but the number of the spheres was decreasing as the cell division progressed. The observations could be attributed to the membrane remodeling occurring during cell division that contributes towards the aggregation of the nanoclusters. The decrease in the number of these spheres could be attributed

to the loss of some portions of the cell membrane with each cell division. That led to loss of some gold nanoclusters along with the lost portions of the membrane. The confocal microscopy images of the progenies show gradual absence of fluorescence and decrease in amount of gold in XPS analysis support the theory. Thus, this study was one of its kind were a detailed analysis of fate of the gold nanoclusters after cell division of the parent generations were studied. Such studies focus light on the after effects of the use of nanoclusters in therapy.

Chapter 3

This chapter summarizes the development of therapeutic bacbot and their role as anti-cancer therapeutic module. The Lac_AuNC were used to encapsulate methotrexate (MTX) on them. The characterization studies such as spectroscopic and microscopic analysis confirmed the synthesis of bacbots. These bacbots were used to treat on monolayer of both cancerous and non-cancerous cell lines. The effect of the bacbots were more profound on the cancerous cells than the non-cancerous cells. The cells chosen were from different origins in order to determine the specificity of the bacbots. The bacbots were further treated on spheroids of the cancer cells and showed a dose depended effect on them. The effects of control bacteria and Lac_AuNC were nearly similar suggesting that the inherent anti-cancer properties of the bacteria were undisturbed by the synthesis of gold nanocluster. However, after a certain concentration the effects were stagnant suggesting a threshold of effect was reached by the bacteria which might be due to presence of a limited number of receptors on the cells or release of metabolites. The dose dependent effect of bacbots shows the synergistic effect of the MTX and bacbots in only 6 h of treatment. This study is important as the efficiency of the bacbts were determined both qualitatively and quantitatively moreover, this study shows the possibilities of developing bacteria-based therapeutic modules without genetic engineering. The safer wild-type strains also have potential to be used as a carrier or anti-cancer agent.

Chapter 4

This chapter summarizes the effect of the bacbots on the biofilm formed by *S.aureus*. The study was up taken as the biofilm formation by *S.aureus* pose threat to the cancer patients due to their immunocompromised state and co-morbidity. The bacbots were incubated with biofilms and their viabilities were determined with crystal violet assay. The effect of bacbots were dose dependent and showed synergistic of MTX and bacbots. The spectroscopic and microscopic analysis support the findings. The importance of this study is to explore the dual efficiency of the bacbots. This study

reveals that the designed bacbots are active against bot cancer and secondary infections caused by the pathogen.

Chapter 5

This chapter summarises the major conclusions and discusses the future prospects of the current thesis work.

Chapter 1

Introduction

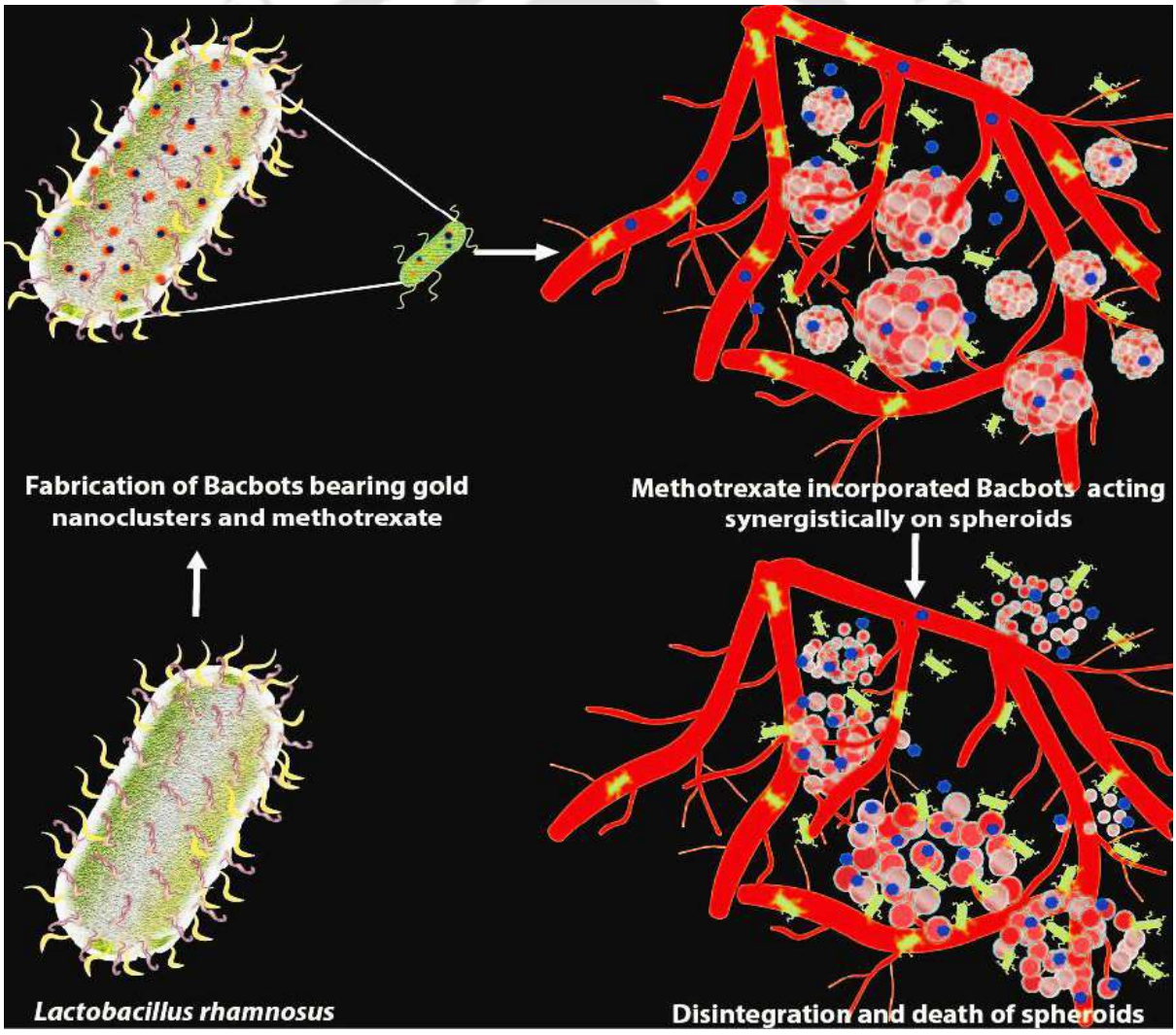

1.1 Introduction to cancer

The global health concern raised by cancer is due to the high mortality rate. Nearly one in every six deaths caused globally are due to cancers. The most common forms of cancers are breast cancer, lung cancer, prostate cancer, and colon cancer; however, the list is even longer [1,2]. The root cause of cancer is mutations in an individual at the genetic level. But, many mutations occur at the somatic levels also [3] . There are over 1000 mutagens identified that leads to development of cancer. Some of the mutagens are chemicals, radiations or biological agents but they all act via alterations in the genome of the individual. The cancer is primarily an uncontrollable growth of cells. There exists a well-regulated cell division mechanism in normal cells, but the unregulated cell divisions (caused by mutagen induced alterations of genome) of certain cells lead to formation of mass of cells, known as tumours. Thus, these cells are clones as they grow from the same cell. The tumour cells attain certain abilities such as proliferation, evade immune response, be non-responsive to anti-proliferative signals, initiate angiogenesis, resisting apoptosis, altering cell metabolism, and tumour promoting inflammation. These abnormal traits allow the cancer cells to persistently grow, divide, metastasize and resist immune attacks and therapies.

Cancer comprises of three phases; first phase is initiation where the abnormalities in the cells initiate the uncontrolled cell division. Second is promotion that comprises of tumour growth the third phase is progression that leads to metastasis [4]. The tumours that remain restricted to the site of their origin are called as benign tumours. Those tumours that can migrate away from their site of origin, relocate and metastasize are called metastatic tumours. Metastasis is lethal and causes more than 90% of deaths from cancer. Metastasis begins with dissemination of clusters of cancer cells and the nature of the primary tumour determines the nature of the metastatic tumour. The cells undergo an epidermal to mesenchymal transition (EMT) where the epidermal cells those otherwise remain connected to basement membrane transform to have mesenchymal like migratory properties. According to studies, the EMT also contributes to chemoresistance. The metastasis is a complex process. Prior to the initiation of metastasis, the cancerous cells communicate to the other tumorigenic cells by sending microRNA through exosomes to induce EMT and malignancy in them. Further, remodelling of extracellular matrix (ECM) supports the metastatic cells to settle the ground for secondary tumours. The tumour cells disrupt the endothelium of the vasculature and intravasation takes place. Apart from adhesion molecules of the ECM, organotropism also plays vital role in colonisation [5]. The former studies also reveal that the distant colonisation of the cells are microenvironment and genetics specific. The extravasation of these cells occurs by rupturing the vesicles and escaping to newer sites. The migrating cells generate stress in the nearby surrounding tissues and cause irregular compression and dilation of blood vessels around the tumours. This creates high interstitial pressure and leakage of drugs or even formation of edema occurs as a consequence. The abnormal cells exert pressure on the other cells and induce tumorigenesis. The cancer cells crosslink the extracellular matrix and become stiff to external forces. This stiffness is seen more in cancerous cells than in normal cells hence; the stiffness of cells is considered to be a hallmark of cancer [6]. Another important hallmark of cancer is inflammation whether it supports the initiation of tumour or proliferation and is case specific. The other primary hallmarks of cancer are sustained proliferative signalling, acquiring replicative

immortality, resistance to apoptosis/cell death, inducing angiogenesis, active invasion, and resisting growth suppression [7,8]. The metastatic tumours possess more threat than the benign tumours as they can invade to other areas and organs through blood circulation and may lead to tumours in various distant sites. The metastasis of tumours also causes relapse of certain tumours. The tumour microenvironment (TME) of cancer cell plays a vital role in the continued survival and dissemination of cells by constantly interacting with the tumour cells. It consists of cancer cells, cancer stem cells, ECM and associated stroma [9]. During the tumour development, the haematopoiesis is also disrupted and any immature immune cells are released to the circulation and reach the tumour sites and they aid in tumour suppression. The generation of dendritic cells is also hampered and decreases in patients with cancer as compared to a healthy normal individual [10]. Reactive oxygen species (ROS) are pro-tumorigenic but beyond the threshold it is cytotoxic. The tumour cells develop strategies to shift the threshold of ROS, to avoid senescence or apoptosis [11]. When we discuss about the cancer relapse, the primary reason is dedifferentiation of non-cancerous stem cells into cancerous stem cells. Thus, these cells gain the advantage of pluripotency. This interconversion of cells enables drug resistance [12]. Additionally, the cancer stem cells contribute to metastasis, radiation resistance, heterogeneity and recurrence. They have the ability to arrest G0 phase of cell cycle and form tumours by self-renewal and differentiation into any cell type. These were first identified in leukemia. They form the bulk of the tumour. The cancer stem cell can divide into one cancer stem cell and one daughter cell or two cancer stem cells [13]. Thus, cancer is controlled by multiple factors and various mechanisms are developed within the abnormal cells in order to stay immortal and proliferate.

1.2 Cancer Therapeutics

A relay of events and experiments have led to the current development in cancer therapy. Previously, the treatment comprised of surgeries only. The drawback of having surgeries as the only options are their incompetency to reduce the risk of recurrences as surgeries were difficult to perform on remote sites. Thus, the remnant cancer cells could relapse into new tumours. Gradually, the inefficacy of up - taking only surgical methods were noticed in great numbers and the need of a better therapy came into existence. Further, radiation therapy was highly encouraged as a mode of therapy and was performed in combination with surgery also. This too couldn't solve the issues due to side effects in the surrounding normal cells. The next level of treatment regimens included chemotherapy where, a targeted drug/ a chemical compound was intravenously injected to specifically attack the tumour cells. The term 'chemotherapy' was coined by Paul Ehrlich in 1900. He was the first person to screen drugs on animal models and this expedited the development in cancer chemotherapy. Until 1960s, surgery and radiation therapy were considered the only option for cancer. But soon the drop in their success rate and the advent of chemotherapy diverted the custom of cancer therapy. The experimental studies supported the multidimensional attack by combinatorial drugs on the cancer cells and this encouraged the implementation of a combination of chemotherapy after surgical removal of tumour or radiation therapy. For years, this has become the standard protocol for treatment of cancer. Approximately, it took four decades to develop model systems for testing the drugs and the first tumour transplant in the mouse accelerated this screening after 1910. Hormone therapy especially in breast cancer was a promising approach. By

1958, 5-fluorouracil was already known but the effects of most of the drugs on the normal cells was a concern. The earliest victory of the combination of surgery and chemotherapy was seen in testicular cancer in mid-1974 [14].

Chemodynamic therapy is another approach of using a catalytic agent to convert peroxide to hydroxyl radical and induce apoptosis in tumours. The metals (Fe, Mn, Cu) are used to generate hydroxyl radicals at the tumour sites although the mode of action is target specific there are certain limitations. The decomposition of peroxide takes place at higher pH, the acidic pH doesn't support chemodynaic therapy fully. Another hindrance is production of higher amounts of reducing agents by tumour microenvironment. So, the best way to use this therapeutic agent is to combine with other methods such as chemodynamic therapy with photodynamic/photothermal therapy, chemotherapy, starvation therapy or gas therapy [15]. In fact, the first combined chemotherapy was applied on leukemia with a combination of prednisone, vincristine, 6-mercaptopurine, and methotrexate. This too led to a list of complications. Some of the major concerns were the miss-targeting of the drugs and affecting the normal cells, burst release of the drugs that prevented prolonged effects of drugs and led to repeated shots of the drug, less bioavailability of these molecules in some cases. The quest to develop therapies for cancer and associated complexities has led to establishing some new age options. These include combining multiple therapies together instead of monotherapy. The most common combinations are first removing the tumour by

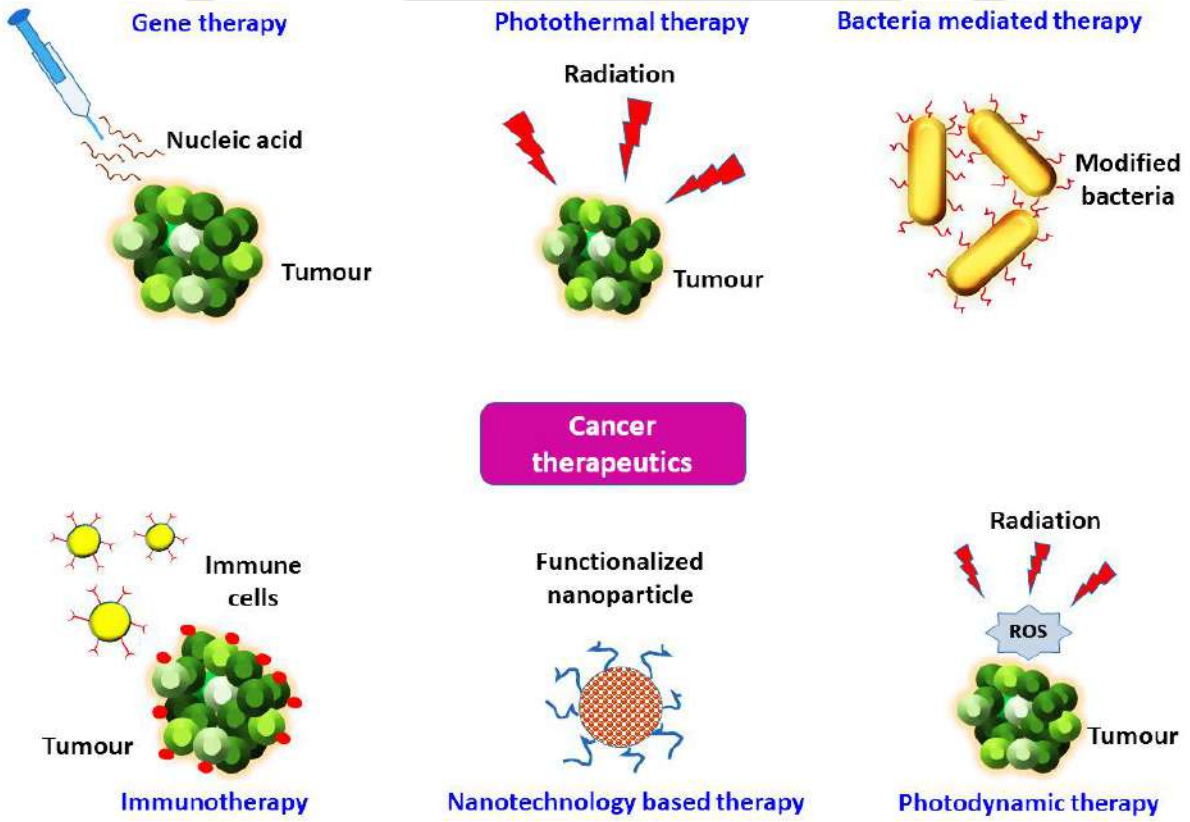

Figure 1.1. Schematic representation of different types of advanced cancer therapeutics.

surgery and then re-enforcing the effects of the surgery by chemotherapy. This enhances the overall effect of the therapy as the removal of tumour by surgeries is supported by the chemotherapy for further reducing the risk of the recurrences. Most of these include surgery diagnosed by magnetic resonance imaging (MRI), ultrasonography, X-ray or endoscopy. However, the success of combination therapies also bears the risk of side-effects to the normal cells. The chemotherapy has so far been an effective mode of treatment and to overcome the drawbacks a bulk of strategies has been opted. The most used techniques are fabricating the drug with target specific moieties like biomarker specific antibodies, aptamers, siRNA, small molecules etc. Some strategies were developed in order to elevate the bioavailability of the drug by coating the drug with a hydrophobic polymer for a sustained release and stability in the blood streams. A customisable therapy for cancer would be the best suited way to eradicate it; however, developing an individual specific treatment regimen is quite arduous. Moreover, these cancer cells also develop strategies to resist the effect of the drugs used and thus emerge as drug resistant cancer cells. This acts as a limiting factor for any therapeutic entity.

The pioneering approach to counter the drug resistance was to use a combined dose of more than one drug having unrelated mechanism of action. For nearly 50 years, the formula worked towards better killing however, gradually this too was saturated. This paved the route for levelling up the treatments by targeted therapies. The initial success was achieved by targeting epidermal growth factor receptor (EGFR), human epidermal growth factor receptor (HER-2), and oestrogen receptor (ER). Further, this targeting extended up to immunotherapy. Early detection, drug screening on cell lines, analysis of the tumour size, tumour ability, localization and growth of tumour can help in combating resistance[16] . A small amount of reactive oxygen species (ROS) is required for smooth functioning of certain cellular metabolism. A group of enzymes convert these superoxides (peroxide, hydroxyl, superoxide) in to water and oxygen (back in to their reduced state). If the amount of ROS increases or decreases in a cell (the optimum amount of ROS generated in a cell is $1.5*10^5$ oxidative hits /day) then the cell undergoes oxidative stress. This is associated to cancer. Excessive ROS generation occurs in cancer cells as a by-product of high rate of glycolysis. This can be detrimental to the cell as ROS degrades nucleic acids, proteins, and lipids. ROS activates calcium channels and thus has a vital role in cell proliferation. The notable fact is, ROS after a threshold, can induce apoptosis by interfering with certain intracellular pathways. According to studies, the ROS levels in the range of 100 µM to 1 mM in the solid tumours promote tumour progression, metastasis, tumour survival and autophagy. However, further elevation of ROS in cancer cells makes them more susceptible to cell death in comparison to the normal cells. Since, ROS impacts the cells in various pathways, the therapies targeting the levels of ROS production and scavenging are also in light. Certain silica based nanoparticles were shown to regulate the ROS levels and countering the alterations of cancer cells to avoid apoptosis [17]. The best combination therapies working on elevating ROS levels are photodynamic therapy and chemodynamic therapy [18].

Similar to ROS, the tumour microenvironment (TME) can also be targeted as this undergoes remodelling during cancer metastasis due to acidosis, hypoxia and angiogenesis. Thus, targeting the TME tactfully is also an option for therapy. Some of the probable targets could be

preventing vascularisation, inducing immune responses in tumour associated fibroblasts and macrophages, exosomes. For example, incyclidine, antibody Fab 3369, and JNJ0966 that are used for targeting the metalloprotienases of extracellular matrix. Topotecan targets tumour hypoxia by inhibiting topoisomerase I and thus, impacts the cellular activities induced by hypoxia such as angiogenesis, macrophage associated with TME, cell proliferation and glucose metabolism. Acidic pH favours cancer cells so a combination of radiation therapy with Acetazolamide targeting carbonic anhydrase and cancer cells has been in clinical trials [19]. Further, the new age model for cancer therapy is nanomedicine. The combination of gene therapy (bearing genes that are tumour suppressors, or activate immune response against tumour) with chemotherapy helps in target specific delivery of gene and the synergistic effects of the drug additionally acts on the tumour cells [20].

1.3 Role of Nanotechnology in Cancer Therapy

A vast shift in the field of therapy has been brought by the emergence of nanotechnology and their fusion with the existing methods in upgrading the therapeutic regimen. There has been a plethora of documentation on various nano-sized carriers and complexes that has curbed the therapeutic constraints. The primary advantage of using nano-carrier system is attaining bioavailability and solubility of drug, targeted release of drugs, and longer retention in blood circulation. Apart from these, rapid detection of biomarkers leading to cancer diagnosis have become possible due to nanoparticles. They are mostly internalized by endocytosis and the larger nanoparticles are up taken by phagocytosis and experience less efflux [21]. The use of nanocarriers for therapies might seem to resolve the issues faced by other mode of therapies but in reality, the nanocarriers experience challenges such as being caught up by the immune cells, extravasation from the blood vessels, and a dense extracellular tumour matrix prevents intrusion of nanocarriers. Despite the modifications, only 0.7% of the nanocarriers successfully reach the tumour sites [22]. There has been extensive research on the efficacy of nanoparticles for cancer therapies. The advantage of nanoparticles over other conventional methods is their small sizes that provide them with various properties and help cross the biological membrane barriers. According to some studies, the shape of the nanoparticle also determines its competency for example, rod shaped nanoparticles are up taken more conveniently than the sphere-shaped nanoparticles. Sometimes this internalization is cell-type specific. They are internalized into the cells by endocytosis commonly. The nanoparticles could be either organic nanoparticles or inorganic nanoparticles. Some of the commonly used inorganic nanoparticles are metal nanoparticles such as gold or silver. Iron oxide nanoparticle bearing magnetic properties is an appropriate choice for imaging and external magnetic field guided targeted therapy. These nanoparticles showcase various physical and chemical properties that allow them to sometimes escape the immune responses due to their small size. These nanoparticles act on the tumour cells by adapting various pathways such as mitochondrial or cell cycle dysfunction, generation of reactive oxygen species and inducing apoptosis [23]. There are experimental proofs that nanoparticles have been successful in targeted-therapy, biomarker-mapping, gene therapy, molecular imaging etc. The major application of nanoparticles in cancer therapy could be divided in to detection or therapy [24].

Quantum dots, nanoshells and gold nanoparticles are mostly known for detection of biomarkers of cancers. Whereas, liposomes, dendrimers, polymeric micelles and carbon nanotubes are known more for therapeutic purposes. Liposomes are nano-sized amphiphilic spheres of lipoproteins. These liposomes have a hydrophobic tail and a hydrophilic head. These are popular drug carriers where the hydrophobic drug molecules need to be supplied at the targets. A size range of 4000 kDa to 500 nm of liposome is seen to swim in the vasculature and reach the targets. The liposomes larger than 100 nm can easily get eliminated by the immune systems. Tuneable liposomes can deliver drugs in response to change in pH, magnetic field, redox potential or ultrasonic waves. Apart from liposomes, lipid-based nano-emulsions and lipid nanoparticles have been synthesized. Carbon nanotubes (single walled or multi walled) are known to be suitable non-invasive methods of drug delivery. Polymeric nanoparticles are 10-1000 nm in size and they can self-assemble to form amphipathic spheres. The dendrimers are spherical structures where equally spaced branches of polymers are placed. They accommodate large quantity of drugs. Different types of drugs can bind to dendrimers with different chemical groups [25]. Although nanotechnology has not been clinically in use up till now but it is in commercial use in the form of sensing devices [26], imaging and diagnostic methods. As discussed, a pivotal advantage of using nanoparticles is their high surface to volume ratio. This provides space for incorporating antibodies, aptamers, small molecules, biomarker specific peptides etc. Thus, diagnosis of the abnormalities by detecting the biomarkers is made easier. The biomarkers can be a protein, carbohydrate or a nucleic acid that is being expressed by the cancer cells and are found in the body fluids (saliva, blood, urine, tears). The most common biomarker detectors are gold nanoparticles, quantum dots and polymer dots. The supremacy of nanoparticle over other therapeutic moieties lies in the nano-ranged size of 10-150 nm. The nanoparticle can extravasate from the poorly formed blood vessels near the tumour site and thus escape what??? to deposit and retain at the tumour site, this is called enhanced permeation and retention (EPR) effect. This was established about 30 years ago. The deposition of nanoparticles via EPR effect is also known as passive deposition. The fabrication of nanoparticle (using aptamers, antibodies, proteins, polymers) for tumour specific deposition is called active deposition [27]. The quantum dots have been used for imaging of tissues in murine models as they are photostable and their photoluminescence can be tuned as per the requirement. The less penetrable nanoparticles were replaced by quantum dots having florescence in near-infrared region. Mercaptodecanoic acid coated gold nanoparticles have been used for imaging and detection of tumour initiation sites and microvasculatures. The nanoparticles are sometimes used to carry RNA to either upregulate or downregulate genes. The cationic lipid nanoparticles are conventionally used as RNA is negatively charged. This also enables easy uptake of RNA through lipid bilayer in the cells. This easy bio-delivery also accompanies easy degradation of the nucleic acid and clearance. The natural and synthetic polymers are used to form nanoparticles to enhance the biocompatibility and easy loading of nucleic acid for targeted therapy. Some nanoparticles are coated with biomembranes derived from cells such as red blood cells (RBCs) [28]. The prodrugs are small molecules with chemotherapeutic abilities that remain masked. On interaction with a specific stimulus (specific enzyme, biomarkers) the prodrug gets converted to an active compound. They are more soluble and can easily get internalized [29].

The major drawback of the nanocarriers is their inability to reach the hypoxic cores of the tumours. These cores are developed due to the lack of sufficient oxygen supply to such distant sites. These core areas provide propensity to the cancer cells to become stem like cells and thus relapse happens. The heterogeneity of tumours also possesses challenges for the nanocarriers. The leaky vasculature, dense microvasculature surrounding the tumour, macrophages availability of the region, interstitial fluid pressure are the key deciding factors of the efficiency of the nanocarriers[30] . If the nanoparticles are of size more than 10 nm then the renal clearance from the body pose threat. When in the circulation, the nanoparticles often get surrounded by proteins present in the blood and this corona of protein often attracts immune attacks. PEGylation is done in order to retain the nanoparticle for longer durations in the circulation. The reliability of nanoparticle for the outcomes of imaging and cytotoxicity is a risk factor in commercializing them. Fluctuating results due to biological factors and individual specific challenges make their use uncertain. Scaling up of the synthesis of nanoparticles is a huge call in to question as batch wise preparation of nanoparticles might also have minor deviations in terms of the thickness of the coatings or size. These minor errors can make major fluctuations in the outcomes. Most of the studies done on exploring the ability of the nanoparticle for detection is done in laboratory and majority of them are unrealistic in terms of implementing them in hospitals. The conversion of laboratory-based experiments to a point-of-care device is a great barrier. Before deploying nanoparticle-based therapy, their bioavailability, toxicity, and pharmaco-kinetics must be studied in depth [31,32]. For example, nanoshells can be used for imaging without any toxicity but their larger size limits their roles. Sometimes, these nanoparticles fail to discriminate the uncontrolled growth of cancer cells and rapidly dividing normal cells and miss-targeting occurs.

1.4 New Age Therapies of Cancer

1.4.1 Cancer Immunotherapy

Immunotherapy for cancer works on the principle of eliciting immune response for surveillance and killing the tumour cells. Mostly this method is supportive for haematological tumours but the effectiveness in solid tumours is not up to the level as the solid tumours are heterogeneous and also the TME varies for each type of tumour. The cellular immunotherapy is currently pursued in the research, where the manipulated immune cells are injected into the patients. This method can be specific (T-cell, CD8 or CD4 mediated) or non-specific (lymphocyte, cytokine, macrophage mediated). Immune check points are mostly targeted as they control the over-activation of T-cells in normal condition. These check points are targeted to activate T-cells. The cytokines can also be targeted as they are directly associated with activating the immune cells. There are three phases of cell immunotherapy, first is elimination that is followed by equilibrium and third phase is escape. In the elimination stage, the innate and adaptive immunity becomes hyper active and eliminate the tumour cells by recognising the antigens. The remaining tumour cells maintain an equilibrium and these which develops resistance against immunotherapy can escape. The vaccines are known to trigger the immune systems against diseases. The vaccines for cancer comprise of lysate of tumour cells, tumour antigens, dendritic cells or mRNAs. These components are recognised by the immune cells and they progress towards attacking the cancer cells. The immunotherapy is achieved by various delivery systems such as - injections at local tumours, nanoparticle based

delivery systems, PEGylation of the immunomodulatory agent, hydrogel, and liposomes [33]. Biomaterials to locally induce immune response can also be implanted. There are limiting factors for immunotherapy such as the immunity of the individual, microflora, TME heterogeneity, drug used and also the mutations of tumour cells. The uneven compression of blood vessels near tumours and high interstitial fluids makes even the cancer vaccines less effective. The resistance to immunotherapy develops by activating mechanisms to escape immune response such as by down-regulating antigen expression, deploying immune regulatory cells, proliferations of cells with only up regulating the production of proteins having immune response evading abilities [34]. The after effects of immunotherapy include production of cytokines leading to leakages in the capillaries and sepsis. Sometimes multi-organ failure is also seen. Dermatological and pulmonary toxicity and Hepatitis are also expected to occur as an additional effect [35]. Autoimmunity limits the use of immunotherapy although many drugs for immunotherapy has been approved now a day. The first approved immunotherapeutic agent was interferon-α (cytokine) in 1986.

1.4.2 Ferroptosis

In recent times, a newer mode of cancer therapy has emerged which is an iron-based therapy causing lipid peroxidation and subsequent cell death. The iron dependency of cancer cells makes them vulnerable to ferroptosis. The change in the cell shape is seen and the mitochondria shrinks after peroxidation of lipid this makes ferroptosis distinct from other regulated cell deaths like necrosis, apoptosis or pyroptosis. Additionally, the nucleus remains intact [36]. The loss of cell membrane integrity and blebbing are absent in ferroptosis. The lipid peroxidation alters the redox balance between oxidants and anti-oxidants and hence, develops membrane disruption. Iron (II and III) can react with peroxide and generate ROS by Fenton reaction. Ferroptosis can be controlled by certain genes such as p53, GPX4, and SLC7A11 [37]. The combined effect of ferroptosis and chemotherapy works synergistically to combat drug resistance. This can be combined with photothermal therapy as the rise in temperature leads to accelerated fenton reaction. Ferroptosis can also be combined with magnetic resonance imaging (MRI) such that the targeting will be image guided for precision and the fenton reaction generated ions will increase the contrast of imaging [38].

1.4.3 Gene therapy

In gene therapy the targeted nucleic acid, gene, siRNA, miRNA or oligonucleotide is delivered to the target site both *in vivo* and *ex vivo*. In case of *in vivo* therapy, the genes are sent to the targeted location by delivery system and in ex vivo method the tumour cells of the patients are derived and cultured. They are subjected to gene editing followed by placing them back to the patient's body. The process is highly specialised and specific to individuals. There are multiple delivery routes of in vivo gene delivery depending on the location of the tumour and easy accessibility such as nasal, intravenous, oral, transdermal, ocular etc. The limitations of the therapy are phagocytic uptake, nuclease susceptibility, biological barriers, immune response and renal clearance. The non-invasive nature makes it more feasible for cancer therapy. The viral vectors are considered appropriate for gene delivery but the immunogenicity and the limited loading capacity are matter of concern. Here, the use of nanoparticles as gene delivery vehicle comes as a rescue. However, the low

transfection efficiency and systemic clearance of the nanoparticles are the limitations. Gene therapy can be used to develop vaccination for cancer; suicide genes, cytokine genes, or gene targeting angiogenesis or promoting proliferations can be transfected into tumour cells. The non-viral gene delivery methods include microinjections, electroporation, ultrasound mediated microbubble, polymers, and liposomes. Other than the viruses, certain bacterial strains are also used such as *Bifidobacterium, Listeria, Clostridia* etc [39].

The conventional therapies have shown saturation in their efficacy due to the multivariate mutations in cancer cells. The remotely originated tumours are difficult to target using the old methods. The emergence of chemotherapy initially boosted the therapeutic outcomes but the heterogeneous TME, hypoxic cores, efflux mechanism, immune suppression by cancer cells led to develop resistance to chemotherapy. The changes made to combat this resistance were mostly based on combining more therapies together for targeting the tumours from various mechanisms. The use of more than one drug having different mode of action, using PTT or PDT with chemotherapy, using surgery, radiation and chemotherapy together and many more combinations were applied. The success rates were although considerable but the relapsing of tumours generated by cancer stem cells still remains a challenge. The non-conventional methods such as gene therapy or immunotherapy are not cost effective and moreover, they are mostly effective when customised as per the patients' conditions and tumour heterogeneity. They are associated with many unwanted health effects sometimes causing autoimmunity, or non-specificity. The physiological barriers, immune system reactions, TME pose multiple challenges to be addressed. Some of these challenges were greatly dealt by the contribution of nanotechnology in therapy. The high surface to volume ratio, possible tuning in shape, size, features according to biomarkers, small size, EPR effect and extravasation from blood vessels made nanoparticles the ideal therapeutic option both as an individual therapeutic module and also as nano-carriers. In spite of having advantages over many non-conventional methods the scalability, renal clearance, lack of precision in pharmacokinetics of nanoparticles and uncertainty in implications of nanoparticle-based therapies in clinical trials beyond diagnostics made room for their improvement. Thus, now the hope shifted towards using biological agents for therapy in order to have self-propelling, chemotactically driven, target specific entities that could be easily manipulated genetically and fabricated with functionalized materials for additional features. These bio-agents were anaerobic microbes that can swim towards the tumours by virtue of their hypoxic cores. The entirely new field of cancer therapy generated on introducing bacteria-mediated cancer therapy which is a currently active topic of research showing potential to beat majority of the challenges of other therapies.

1.5 Bacteria-based cancer therapy

The word 'bacteria' brings an idea of danger or disease. But in reality, not all bacteria are detrimental; some are the so-called 'good bacteria'. The advanced cancer therapy has harnessed the potential of bacteria and utilises their pathogenicity for the benefits [40]. The first ever bacteria-based cancer therapy was performed by William B. Coley when he injected *Streptococcus* into the sarcoma patients and noticed reduction in tumour. According to studies conducted by Neil S. Forbes, approximately 10^4 times more *Salmonella typhimurium* colonizes in the tumours, due to their affinity for hypoxia than the normal cells. Other than hypoxia, which is the absence of sufficient

oxygen in tumours (1-4%), the bacteria also get attracted towards the TME, sometimes the unevenly compressed blood vessels surrounding the tumours tend to trap these bacteria and the leaky vasculature helps escaping them. The facultative anaerobes have advantage over obligate anaerobes as they can reach both oxygenated and hypoxic areas of the tumour. The surge in tumour necrosis factor α (TNF-α) was observed in a study after systemic administration of *Salmonella*. After careful neutralisation of TNF-α, a delay in tumour accumulation of the bacteria was observed [41,42,43,44].

In 2005, for the first time, auxotrophic *Salmonella* was demonstrated to replicate in tumour. The bacteria are known to effectively regress prostate, ovarian, pancreatic, and lung cancer [45]. The anaerobes are best suited for this purpose due to their affinity towards less oxygen and ability to thrive in anoxia. In an experiment, spores of *Clostridium* were injected to mice bearing tumours and lethality was seen within 48 h of administration. The mice without any tumour could survive leading to the conclusion that the spores could germinate in hypoxia of tumours and released toxins causing lethality. However, the healthy mice were saved by the immune response. This experiment also showed that the spores could reach to the tumour sites via blood vessels ruling out the necessity of intra-tumoral injection of spores/bacteria. Studies reveal that the luminescent bacteria selectively accumulated in the tumor sites in mice model and increased luminescence was seen indicating the bacterial growth and reproduction within the tumor. This therapeutic approach showed delayed tumor growth in human lung cancer cell induced in mice[46]. The bacteria dwelling in our system secrete their own products that act as immunosuppressors or carcinogens at times. The selective silencing of bacterial products offers a target specific approach to shut down the bacterial toxins mediated tumorigenesis and immunosuppression.

The commonly used bacterial strains for cancer therapies are *Salmonella*, *Clostridium*, *Pseudomonas*, *E.coli*, *Bifidobacterium*, and *Listeria*, lactic acid bacteria (LAB). In the mid of 1990s, safer strains were developed by genetic engineering and modifications of these wild type strains by attenuation. For example, the endotoxin gene removal from *Clostridium* made the strain safer. The deletion of *msbB* gene in *Salmonella* and *E. coli* rendered attenuation as this gene was responsible for myristoylation of lipid A of lipopolysaccharide (LPS) causing 10^4 times reduction in toxicity. Inducing auxotrophism by gene manipulation can also enhance specificity for TME and less impact on normal cells. The bacteria-based therapy is an amalgamation of chemistry, material science, biology and engineering. The autonomous properties of the bacteria remain intact while upgrading the capabilities of the bacteria through fabrication and engineering. The addition of cytokine expressing genes such as TNFα, IL-12, IL-1B can uplift their immunogenicity and enhance T-cell mediated immune responses. This hybrid system has enhanced delivery capabilities, effective diagnostics and therapeutic efficacy. The bacteria can directly be used to target the tumour or can be used as a delivery vehicle. The ideal bacterial vector must be motile, non-pathogenic, easy to genetically manipulate, have tumour specificity, ability to multiply in TME and susceptible to antibiotics. In fact, motility and antibiotic susceptibility in bacteria make them superior to viral delivery vehicles. The bacteria will not disperse randomly with blood stream due to motile nature and their numbers can be controlled using suitable antibiotics. The non-immunogenicity of the bacteria is a required feature as this will provide safety to the entire therapeutic module. The

tumours create an immuno-supressing environment by attracting the nearby macrophages by chemotaxis and then the abilities of the macrophages are made incompetent as soon as they reach the hypoxic areas. Thus, the macrophages become non-phagocytic. Similarly, T-cells also lose their competency and the TME becomes immune suppressant region helping the tumours to survive [47].

The attenuation of the virulent strains is crucial as the safety of the patient is necessary. The virulent genes are edited from the organism and the recombinant attenuated strains are prepared. The bacteria can also be made auxotrophic for metabolites or amino acids that are essential for the bacteria but are richly available only in TME. The gene editing leaves the bacteria incapable of synthesizing the amino acid but is compelled to depend on the TME, thus, drives tumour colonization and multiplication in tumours. Often the selected recombinant gene that is engineered has toxicity for the cancer cells but the secretion of the product needs to be conjugated to a secretory protein for the proper regulation. So, that along with the secretory protein the actual recombinant product reaches the tumour via secretions [48]. The most commonly used strain is *Salmonella* as they have toxicity, tumour specificity and fast migration in body fluids. This can be conjugated with PTT or any other methods like nanoparticle or liposomes encapsulating drugs for combating tumour. *E. coli* modified to express catalase and loaded with black phosphorous quantum dots enhanced the ROS generation on NIR illumination; this combined therapy proved the potential of live *E. coli* as a carrier and toxic therapeutic entity. *Clostridium* novyi-NT is a recombinant strain that showed tumour regression when gold nanoparticles were coated on them. The *Listeria monocytogenes* is another bacterium highly tumour specific and has the ability to interfere with the phagolysosomal fusion and delivers the therapeutic payload in to the cytoplasm of the tumour cells [49]. The bacteria can be used for RNA interference, pro-drug activation, expressing tumour antigens, gene delivery and for diagnostics and imaging such as magnetic resonance imaging (MRI). The attenuated *Salmonella typhimurium* VNP2009 strain as already mentioned is the most well-known bacterial species to be used for cancer therapy. It has inspired subsequent development of many *Salmonella* strains where mutation was focused on reduction in virulence without hampering their tumor specificity. Similarly, mutated *Listeria monocytogenes* were also designed that could induce anti-tumor activity with attenuated virulence. Once the mutated bacteria are injected into the blood circulation, their actions are observed in tumors in various ways which are species specific. *Salmonella* spp. can directly induce apoptosis; up regulate connexin-43 that establishes gap junctions between tumor cells and dendritic cells. The activation of both dendritic cells (DCs) and macrophages leads to surge in interleukin-1β. *Listeria* spp. targets the tumor cells by activating nicotinamide dinucleotide phosphate oxidase and simultaneously increases calcium levels inducing high levels of reactive oxygen species (ROS). *Salmonella* spp. has always been seen as a potential anti-cancer entity as it can selectively grow in hypoxic areas which makes it suitable to be used for this purpose, but its virulence is so much that it cannot be used directly without having undergone attenuation. Earlier VNP20009 was designed for the purpose later A1 strain was derived from the same ATCC1408 strain. Sometimes the virulent genes are deleted and at times the strains are developed by inducing auxotropic mutations. They are even designed in a way such that they can be controlled by external factors like radiations, magnetic field, temperature etc. The *Salmonella* strain KST0649 was subjected to certain modifications to

derive an oxytolerant strain KST0650. This strain showed nearly 20 times more tumor invasion as compared to the parent strain KST0649; this was designed to be controlled externally via radiation, a radiation sensitive promoter bearing plasmid was inserted into the system for this activity[50]. The tumor targeting bacteria could be modified in many ways including engineering prodrug activating enzymes. The *E. coli DH5α* strain was engineered to express β-glucoronidase enzyme and luxCDABE; the lux gene helped to illuminate the bacterial colonies and thus led to the real time tracking of the bacteria, at the same time the glucuronidase enzyme converts the anticancer prodrug 9ACG to 9AC. There has been an expansion in the scope of bacteria-based-bots. Fabricating the bots with molecules sensitive to alterations in their physical environment (pH, temperature, magnetic or electric field) and then deploying these as intracellular sensors. Such bots report extensive details on the intracellular processes like host-pathogenesis, endocytosis and phagocytosis [51].

Clostridium spp. secretes toxins that can disturb the membrane integrity and interfere in cellular mechanisms as well[52-53]. The most challenging part of cancer therapy are targeting specificity, improper tissue penetration and limited drug availability to the cancer cells. To overcome these, a potential therapeutic option is to genetically engineer bacteria, which themselves are small robot-like systems that can swim on their own by virtue of their flagella. They can swim towards the tumor microenvironment via chemotaxis. The bacteria when reach the target specifically delivers the payloads to the tumors. In doing so the amount of drug availability also increases and specific therapy is also achieved. These therapeutic bacteria can be visualized using a magnetic resonance imaging (MRI) or a positron emission tomography (PET) scan. So, it is a comparatively convenient option to track the movement of the therapeutic substance. The genetic engineering also allows external control of the drug release, tracking and targeting. The obligate anaerobes such as *Clostridium and Bifidobacterium* can reach the anoxic areas of the tumors by sensing the oxygen deprivation. These anoxic areas comprise of cells that are unresponsive to the drugs. The facultative anaerobes such as *Salmonella* reach the tumors via different mechanisms. They can get entrapped in the chaotic vasculatures of the tumors and eventually swim to the targets; they can chemo-tactically be drawn towards the tumor micro environment; the bacteria can sense the concentrations of serine, ribose and aspartate and accordingly penetrate the tissues. Some other strains move towards tumors by following inflammation; the inherent property of tumor cells to escape immune reaction attracts bacteria to hide in such immune suppressed areas. The bacteria can either have their natural mechanism to kill tumors whether by producing toxins or by delivering the payloads like cytokines, pro-drugs, pro- enzyme activators, specific shRNAs etc[54]. The bacteria mediated cancer gene therapy is thus a method to invade tumors more specifically and the motile nature of the live bacteria makes it a self-propelling system. As per studies, 95% portions of the tumors are hypoxic and only rest of the 5% of the cells are dividing, the partial pressure of oxygen in normal tissues range from 24-66 mmHg whereas in cancer cells this range is 10-30 mmHg and in a majority portion it is below 2.5 mmHg, which indicates existence of hypoxic areas within the tumors. Those bacteria which can target the hypoxic areas and invade the tumors and sometimes reside in the tumors, they draw their nutrition from the necrotic areas of the tumors, and are the ones which could be used for target specific cancer gene

therapy. So, the anaerobes either facultative or obligate were opted to be designed genetically as compared to other microbes.

In practice, the oral intake of bacteria-based therapeutic module face challenges as the therapeutic bacteria is to mask them from acidic gastric pH and the other routes elicit immune responses. The first barrier is stomach acid followed by antibacterial secretions of the intestine; the peristaltic movement of the gut also eliminates the foreign entity and the gut associated lymphoid tissues (GALT) also aids elimination. If a bacterial strain is able to overcome these barriers, then only it can penetrate the tissues. For this to happen, the strain has to be highly pathogenic. However, the pathogenicity and immune system attacks can be escaped by genetic modifications. The immune regulatory proteins can be engineered in the bacteria, and expression of therapeutic genes in attenuated strains. The bacteria can be modified to respond to external stimuli. Dosage determination, biosafety, and scalability are some of the bottle-necks. The primary attractive property of the bacteria for therapeutic use is their self-propulsion. The modifications are mainly based on designing a safe strain, efficient viability retention of the bacteria in TME and providing additional features to the bacteria for smooth targeting and killing. The chemical conjugation of bacterial surface with sulfhydryl, carboxyl or amine groups helps in the interaction with nanoparticles. For example, conjugating an attenuated bacterium with magnetic nanoparticle can generate ROS and easily penetrate through tumours. Thus, the fabrication will bring better outcomes than only bacteria or only nanoparticle acting on tumours. By genetic engineering, secretion of metabolites, adhesion abilities, and targeting can be upregulated or downregulated based on the need. These days advanced genetic editing using CRISPR-Cas system are also in trend. In a study, the bacteria were coated with RBC membrane to protect them from the physiological conditions inside the body. The results were encouraging and stated the formation of safer bacteria with coating than the uncoated bacteria as these triggered fewer immune responses. The membrane coatings additionally aid in encapsulating drugs such as doxorubicin [55]. In another study, the bacteria *Caulobacter crescentus* alone had shown anti-tumour activity. Some bacterial strains have anti-angiogenesis properties. Some other can induce alteration in immune responses by releasing heat shock proteins, immune checkpoint inhibitors or producing lipopolysaccharides [56]. One of the most used modified strains of *Salmonella typhimurium* 14028 is *Salmonella enterica* serovar Typhimurium VNP20009 [57]. It is an auxotrophic mutant that is safer and tumour targeting [58]. The strain was also used orally to deliver therapeutic DNA to the GALT where the DNA was transcribed and immune response was initiated without reaching the tumour [59,60].

The hyper production of extracellular matrix by tumour cells creates a dense network around them acting as a fence against immune interventions and drug accessibility. The fibrous connective tissues make a congested extra cellular matrix where limited supply of blood occurs in core areas and thus, a hypoxic environment is created. This physical barrier promotes resistance to therapeutic entities. The cancer associated fibroblasts (CAFs) are targets for cancer therapeutics. Degrading them or inhibiting their production can help in reducing the gridlock and easy passage of drugs. Deploying the live bacteria carrying therapeutic proteins or hyaluronidase (acts on hyaluronic acid produced by CAFs that promotes resistance) are of great importance and has seen the platform of clinical trials. The use of nanoparticles is often eliminated by the hepatobiliary

channels of the body but using a facultative anaerobe to reach through the dense ECM is easier. The hypoxia-affinity, leaky vasculatures and immuno-deficient periphery supports colonisation of the bacteria. *E. coli* Nissle, an oral probiotic was used to genetically engineer the therapeutic genes and has also been in to clinical trials. In another study, this strain was engineered for hyper-vesicularization and the outer membrane vesicles (OMV) so produced by them were able to deliver the hyaluronidase combined with fusion proteins for degradation of hyaluronic acid. This modified strain could successfully induce remodelling of stroma and inducing immunotherapy by targeting the immune checkpoints [61]. Bacteria can serve as raw materials for delivery vehicles, synthesis of nanoparticles, vaccines etc [62].

The tumour hypoxia affinity of bacterial strains had pushed them to clinical trials Phase I. But unfortunately, due to undesired additional effects the trials showed the bacteria themselves are not an agent capable enough for tumour eradication. Thus, combining the anti-tumour properties of bacteria with that of the other therapies would level up the efficiency overall. The combination of PTT and bacteria have expedited the tumour eliminations, which was otherwise not satisfactory with PTT alone. Salmonella VNP20009 was used as a carrier of the PTT generating material for deeper penetration and distribution into the tumours, especially for larger size (more than 200 mm^3). The bacteria have inherent tissue penetration ability as they are a pathogenic strain and have tumour colonisation affinity [63]. Sometimes bacteria can enhance the effects generated by the chemotherapy. In a study, the higher ROS production was seen by the genetically modified *E. coli* having doxorubicin conjugated on it. This hybrid system was capable of eliciting immune response simultaneously in different tumour models and project a greater impact [64].

1.5.1 Combined action of nanotechnology and bacteria-mediated cancer therapy

The combination of nanotechnology and bacteria has also shown improved outcomes. The conjugated nanoparticles over bacteria act synergistically by enhancing the effect of the therapeutic agent and also the therapy overall. Mostly this combination brings increased bioavailability of the therapeutic entity, longer retention in body fluids and controlled drug release and the bacteria also aid in easy tumour colonisation. The advancement in nanotechnology especially in the field of medicine has generated several options for targeted therapies such as delivering silencing agents against the toxin, stimuli responsive killing of lethal microbes, direct blocking of bacterial toxins etc. The studies on nanoparticles suggest that, the abilities of nanoparticles to enter the chaotic vasculature while escaping the enzymatic degradation due to protective coatings and penetrating the tumor cells due to enhanced permeability and retention effect is the reason behind using them extensively for the cancer therapies. The modifications that are being carried out are designing of stimuli responsive nanoparticles, which can be either used in monotherapies or in combination with other therapies as well. Further modifications are based on designing biological barrier penetration abilities for better outputs. The LPS of gram-negative bacteria provides virulence to it; the LPS binding protein plasmid was combined with protamine to form a nanoparticle, and further it was encapsulated with polymer coating. This was injected to mice bearing orthotropic tumor as a result of this the LPS binding protein blocked the LPS from activating TLR4 receptors and facilitated T-cell infiltration to the tumor sites thus tumor regression was seen. The deletion of cancer-causing bacteria (*F. nucleutum, H. pylori*; gut microbiota) using nanotechnology is a

promising therapeutic option. PLGA nanoparticles carrying antibiotics against *H. pylori* were designed such that the nanoparticles were coated with membranes of gut epithelial cells. This approach was based on interaction between the nanoparticle and the bacteria and via receptors already present in the membrane. This worked against the bacteria with considerable target specificity as compared to non-targeted therapy[65].

The nanoparticles/ nanocarriers can carry protein, genes, mRNA, image contrasting agent etc. For example, *Magnetospirillum magneticum* (AMB-1) loaded with indocyanin green nanoparticles were responsive to external magnetic field and also to radiation. The thermo-sensitive liposomes bearing doxorubicin attached to the surface of *Salmonella* showed combined effect on tumours [66]. The route of administration could be intravenous, intratumoral, oral, nasal depending on the need and accessibility. The bacteria are self-propelling system that can swim through the blood, tissues, mucus following gradients of chemical signals (chemotaxis), magnetic fields (magnetotaxis), pH (pH taxis) or even light (phototaxis). These abilities aid in nanoparticle penetrations in to the targets. The conjugation of nanoparticle on to the bacteria can be antibody mediated, aptamer based, hydrophobic or covalent interaction based. Less immunogenic nanoparticles like PLGA nanoparticles could be conjugated to Salmonella VNP20009. In fact, studies suggest that PLGA nanoparticles of different sizes can be loaded on the same bacteria making a bio-hybrid system. However, the linkage chemistry of nanoparticle to the bacteria and size of the nanoparticle determines the motility and attachment density of the nanoparticle [67]. The pharmacokinetics (absorption, distribution, metabolism and excretion) of the therapeutic entities are of utmost importance. Any non-fulfilment of pharmacokinetics leads to incomplete tumour killing and remainder product causes resistance [68,69]. The bacteria can also be used to expedite the efficiency of nanocarriers by guiding them to tumour hypoxia. These nanocarriers can be bound to the live bacteria by surface chemistry and the premature drug release or miss-targeting can be controlled. Magnetotactic bacteria, *Magnetococcus marinus* MC-1 was used to deliver drug loaded liposome to the hypoxic core [45].

1.5.2 Bacteria-mediated Cancer Immunotherapy

The immortality of tumours is achieved by low antigenicity that masks them from immune attacks and tumorigenicity that leads to high proliferation rate. The major limitation of cancer immunotherapy is suppression of CD8+ T cells by the tumour cells. This blockage can be released by cytokine release [70]. The only approved bacteria mediated cancer immunotherapy is Bacillus Calmette-Geurin (BCG) mediated immunotherapy of urinary bladder cancer. The common strains specific for immunotherapy are *Salmonella*, *Clostridium* and *Bifidobacterium*, which are anaerobic bacteria [71]. The constituents of bacteria such as nucleic acids, lipopolysaccharide (LPS) and flagellum are recognised by the macrophages and dendritic cells and thus are immunogenic and have potential for cancer immunotherapy. The increased concentration of LPS results in cytokine release and activation of toll like receptors (TLR) and nuclear factor kappa B (NF-kB) leading to dendritic cell maturation. When live bacteria are injected into the blood stream these distribute randomly everywhere and within a span of few hours are eliminated by the immune cells. The chemotaxis mediated colonization of remaining bacteria in tumour occurs in hypoxic cores. The dense ECM protects these bacteria from the action of immune cells. As these bacteria

divide and multiply in the tumour cores, they activate the immune system of the host and the tumour cells are attacked. The mechanism of provoking the immune system is strain specific and also tumour specific. The elevated levels of Ca^{2+} ions within the cells and the activation of nicotinamide adenine dinucleotide phosphate ($NADP^{+}$) generate ROS and causes cell killing on intervention of *Listeria* into the tumours. Additionally, ROS also activates T-cell and the suppressor cells deployed by the tumour cells are attacked by *Listeria* making the tumour sites

susceptible. Cell membrane destabilizing toxins like phospholipases and haemolysins are secreted by *Clostridium*. By injecting *Salmonella* into the blood stream apoptosis is induced in the cancer cells and they also act by activation of autophagy and upregulating gap junction production between cancer cells and adjacent dendritic cells. The tumour antigens are passed to the dendritic cells via these gap junctions followed by activation of cytotoxic T-cells. The bacteria on genetic manipulation and surface modification can reach the tumour and release the payload in the tumour vicinity. The immunogenicity of *Salmonella* is due to its flagellum; it is recognised by the receptors of immune cells as Pathogen Associated Molecular Pattern (PAMP). When in vivo, the bacteria

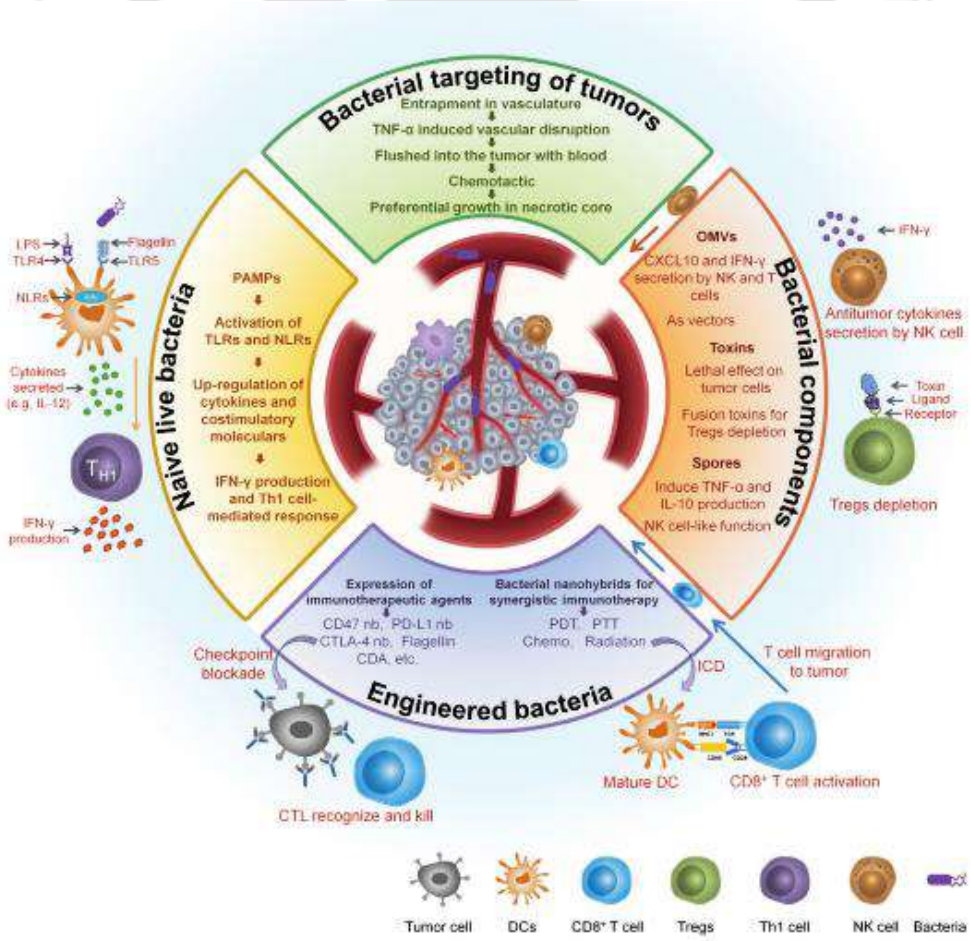

Figure 1.2. Schematic representation of bacteria induced cancer immunotherapy depicting different strategies of bacteria for eliciting immune response. Reprinted from John Wiley and Sons. Reference 73.

follow strict regulations on synthesis of flagella to avoid recognition by immune cells. Although, the flagella are the main part of *Salmonella* that provides motility, adherence and invasion abilities. Thus, the flagellum is a target for immunomodulatory responses [72]. The *E. coli* strain was fabricated with antigen that was specific for an over-expressed receptor on cancer cells. By gene manipulation, a lysis circuit was incorporated in the bacteria. The antigen- receptor mediated tumour localization occurred and following the recognition the lysis circuit activated and the immune reactions were awakened by the lysed bacteria. The immune checkpoint inhibitors can be used to elicit immune response [73]. Some studies suggest *E. coli* could be a replacement to *Salmonella* as there were no *E. coli* found in liver and spleen of tumours bearing mice model on simultaneous injection of *Salmonella* and *E. coli*. In another experiment, on simultaneous injection of these two strains in C57BL/6 mice, the tumour accumulation ability of both the strains were found to be similar. However, the enzyme linked immunosorbent assay (ELISA), polymerase chain reaction (PCR) and western blot analyses of the lysed tumours revealed that the activation of cytokines was seen in case of only *Salmonella* [74]. This suggests *Salmonella* is more appropriate than *E. coli* for eliciting immune response. The bacteria primarily activate CD8+ and CD4+ T-cells [75]. The heat shock proteins released by *Clostridium* activates cytokines (Interleukin-12) and toll-like receptors (TLRs) [76]. Other than the commonly used bacteria, certain naturally fluorescent bacterial strains were also explored for their tumour targeting abilities. *Rhodobacter sphaeroides* 2.4.1 is such a strain that on intravenously injected in to mice with tumours, showed higher penetration and the fluorescence from those deeper ends of the tumours were brighter than the green fluorescence protein (GFP) and red fluorescence protein (RPF) expressing *E. coli*. Such studies provide evidences that strains of bacteria having natural potential must be encouraged over genetically modified strains [77]. *Bifidobacterium breve* engineered to express IL-24 showed tumor reduction in head and neck tumor xenograft mice. The IL-24 is a member of IL-10 family and activates apoptosis of tumor cells [78].

A few studies have shown that using non-pathogenic strains (*E. coli* strain K-12) and accumulating gold nanoparticles (AuNPs) on them can induce PTT on exposure to near infrared rays (NIR). *Bifidobacterium longum*, a non-pathogenic anaerobe, was genetically modified to perform cloning within the tumor cells. The bacteria selectively resided in the tumor once injected into the system and divided too. Initially when injected, the bacteria were seen all over but within a few hours they located themselves near and within the tumor. This indicated that the tumor hypoxic micro environment provided shelter for the bacteria to grow. The bacteria could be eliminated by administering antibiotics[79]. The avirulent strain of *Samonella*, SLΔppGpp, also attacks tumor cells by activating the immune cells via eliciting the cytokines.These studies encourage the use of non-pathogenic strains for bacteria based therapies in order to increase the overall safety of the treatment process [80].

1.5.3 Role of gut microbiome in bacteria mediated cancer therapy

The human gut microbiota comprises of archaea, protozoa, fungi, bacteria and protozoan viruses. Most of these residents live as commensals within the human body. Sometimes a few of them gain pathogenicity and become foes for the system. The gut microbiota also maintains mutualism with the host by carrying out metabolism of certain substances, synthesis of vitamins, protection against pathogens, restricting growth of pathobionts and by supporting hematopoiesis. An intact gut

microbiota helps in maintaining a sound health and homeostatic state. The gut microbiota composition is influenced by genetics of the host, exposure to the pathogens, lifestyle of the individual, colonization of microbes at the time of birth, intake of antibiotics, diseases that occurred to the host. The microbiota evolves up to a few years after birth till maturation after that its composition remains nearly constant. Some modifications may occur as per the diet and lifestyle of the individual. This microbial consortium brings out many changes to the drugs that are taken orally or intravenously, most of these include hydrolysis, reduction, removal of functional groups, amine formation, acetylation etc[81]. There are a number of bacteria in the gut of an individual such as *Akkermansia muciniphila*, which is an anaerobe and strictly remains associated with the mucus lining of the gut. It utilizes the mucus layer to extract carbon and nitrogen sources for itself. It is usually present in healthy guts along with *Methanobrevebacter smithili*, *Gordonibacter* spp. and *Faecalibacterium prausnitzli*. *A. muciniphilia* is capable to produce short chain fatty acid (SCFA), which has immunoregulatory activities. It can at times act as a pathogen too. The gut microbiota comprises of 5% of *F. prausnitzli*, alone. It produces butyrate that maintains gut homeostasis by regulating the colonocytes. Lower concentration of this bacterium is found to be associated with colorectal cancer, inflammatory bowel disease and irritable bowel syndrome. A non- filamentous rod-shaped bacterium, *Bifidobacterium,* comprises of less than 1% of the total gut microbiota. It is also found in oral cavity and reproductive tracts of female individuals. These bacteria break down the sugars into lactate, acetae or ethanol. *Bacteriodes fragilis* is another bacterial species, which catabolizes carbohydrates. It has immunoregulatory activities and it can influence the distant lymph nodes too. There are some other strains of bacteria that are found in the gut but very less information is available regarding their exact function. These are *Enterococcus hirae Burkholderia cepacia, Eubacterium limosum, E. faecium and C. aerofaciens*[82]. The microbiota, the host immune system and the tumor cells interact among themselves and this interaction determines the fate of the tumor progression[83]. It is estimated that a sum total of 3×10^{13} microbes reside in a human host.

The shift in microbiota composition, called as dysbiosis, in healthy and cancer patients depicts the role of microbes in causing diseases. The colorectal cancer is the third most common cancer worldwide. The fecal samples of colorectal cancer patients contain bacterial strains such as *Enterococcus faecalis, Bacteroides fragilis*, *Streptococcus gallolyticus*, *Escherichia coli*, *Fusobacterium nucleatum*, *Peptostreptococcus, Porphyromonas*, *Parvimonas* and *Prevotella* spp. Presence of *F. nucleatum* is considered as a bacterial biomarker of colorectal cancer. Thus the role of bacteria in maintaining homeostasis and causing disease is vital[84]; this is a complex role because sometimes the microbiota acts as a pro-carcinogen and sometimes it exhibits anticancer effects. The transfer of fecal matter to the lower gut of patients suffering from inflammatory bowel disease is a potential therapy option. This is because the healthy individual bears a consortium of bacteria that supports homeostasis and the diseased individual bears a disrupted microbiota. The fecal matter transplantation restores the stable microbiota consortium in the patients thus helps in recovery[85]. The gut microbiota influences the health of an individual by producing substances that metabolize nutrients and toxins as well as provide protection against the pathogens. There is also co-existence of a group of microbes that are pivotal cancer-causing pathogens, responsible for almost 20% of the cancer cases worldwide. These are *Helicobacter pylori*, *Fusobacterium nucleatum,* Epstein- Barr

virus (EBV) and Human papilloma virus (HPV). The *Salmonella typhi* is a potential causative organism of biliary cancer whereas *Helicobacter pylori* cause gastric cancer and mucosa associated lymphoid tissue (MALT-lymphoma). There is a mutual effect prevailing between cancer and the microbiota, either the microbe can initiate the cancer or the tumor progression can itself alter the microbial composition.

Microbes also provide a platform for cancer therapy, *Streptococcus pyrogenes, Mycobacterium bovis*, *Serratia marcescens*, *Lactobacillus plantarum*, *Lactobacillus rhamnosus* GG, *Lactobacillus acidophilus Salmonella, Clostritidium, Bifidobacterium and E. coli* have shown to mediate anticancer effects. The BCG vaccine provided the first ever microbe-based cancer therapy that was approved for therapeutic purposes in 1990, which is an attenuated *Mycobacterium bovis* strain. Probiotic supplements strengthen the natural defense mechanisms of the body by inducing apoptosis or by activating N-K cells. Bacterial toxins show anti-cancer activities as well for example doxorubicin, which is a well-known anticancer drug. Bacterial pathogen associated molecular patterns (PAMPs) can be used as an adjuvant in vaccines to elicit immune responses against cancer causing viruses, one such example is use of monophosphoryl lipid A derived from *Salmonella enterica*, against cervical cancer[86]. It has been observed that the microbiota of a tumor is different from that of a healthy tissue indicating the role of microbiota dysbiosis in cancer. As per studies, certain species of bacteria can promote inflammatory state that triggers cancer development by increased production of reactive oxygen species (ROS), release of proinflammatory toxins, counter acting on anti-tumor functions of the immune system or by interfering with the normal cell signaling pathways as well. Some strains have the ability to modify the chemistry of the drugs resulting in alteration of its efficacy (either increasing or decreasing); the Gamma proteobacteria, found in pancreatic cancer, produces an isoform of cytidine deaminase that downregulates the activity of gemcitabine. Tumor microbiota can also influence the expression of receptors on cancer cells and immune cells as well. They can induce tumor suppressive cytokine signaling. In China, more than 2000 years ago, fecal matter was administered to patients orally with acute diarrhea, even during World War II; camel stool was used for the same by the soldiers. Now days, fecal matter transplantation is done via colonoscopy mostly. The use of probiotics as a supplement has also shown changes in the tumor microbiota of the patients. The co-administration of 5- fluoro uracil and *Lactobacillus rhamnosus* exhibited better outcomes in colon cancer treatment[87]. Some of the obligatory and facultative anaerobes display affinity towards the tumors and choose to move and reside inside the tumors due to the hypoxic areas present in them. The use of live attenuated bacteria for therapeutics is the result of these studies. These tumor targeting bacteria can also act as reliable delivery systems as they can easily be internalized by virtue of their inherent feature to escape from the immune responses. The payloads could be drugs, RNAs, pro-drug converting enzymes, immunomodulators or even cytokines. The use of genetically modified bacterial species can further add up to its efficacy.

1.6 Secondary bacterial infections during Cancer

The immunity of a patient is vulnerably challenged during the cancer development and progression. The person usually becomes immunocompromised and invites various pathogenic attacks despite the use of antibiotics and hygienic surrounding. The bacterial pneumonia is a prominent threat for such cancer patients causing 10% of total cancer associated mortalities. The major pathogenicity is observed in hematology associated cancers such as leukemia where 30% mortality is due to pneumonia. Studies suggest that in case of hematopoietic stem cell transplant for treatment of leukemia, 80% chances of pneumonia infections are there. Neutropenia, malnutrition, chemotherapy induced immunosuppression, dysbiosis, and damaged skin or epithelium induce these secondary infections in cancer patients [88]. The pathogen enters the body through airways or hematological transplants from infected individuals. Before reaching the alveolar region, the pathogens are usually swept by the mucosal linings. The pneumonia pathogenicity is affected by the malignancy, treatment, pre-existing infections and co-morbidity of the patient. Chemotherapy generated derangements of leukocytes also favors localization of the pathogen. Current treatment includes vaccination of the patients against pneumonia but the timing of the doses and the durability vary. The antibiotics are also prescribed for such patients but the dose timings are the bottle necks as there is less consistency in the outcomes of antibiotic therapy moreover, drug resistant strains also pose threat [89]. Similar to *Streptococcus pneumoniae* another deadly bacterial infection is caused by *Staphylococcus aureus*, a gram-positive bacterium causing nosocomial infection. The organism causes sepsis, toxic shocks, and sometimes leads to pneumonia. The multi-drug resistant *Staphylococcus aureus* are even more contagious and dangerous. According to a survey, 96% of the blood samples of patients infected with blood stream infection (BSI) were positive for *Staphylococcus.* Most of the isolates from the samples were resistant to ciprofloxacin [90, 91]. *Staphylococcus aureus* can also regulate cancer metastasis by regulating neutrophil infiltration into lungs [92]. According to an extensive study conducted for nearly 2 years on cancer patients' blood, pus, and sputum the bacterial cultures isolated contained 18% *Klebseilla* spp., 17% *Pseudomonas* spp., 14.7% *E.coli*, and 13.7% *Staphylococcus aureus*. The most common infection in these patients was BSI. In most of the studies in developed countries, the mortality from these infections in cancer patients is 70% by the gram-positive bacteria. In studies up taken in the developing countries, the gram negative bacteria has more dominance [93,94]. Since, the secondary infections are a threat to the cancer patients and adds on to their sufferings, methods must be developed to counter the effect of these pathogens. Although vaccines and antibiotic therapies are being implicated into their treatment regimen but the emergence of resistant strains makes the treatment tougher and sometimes incomplete. Moreover, since the dose timings are not standardized, due to heterogeneity among patients, they give varying outcomes making the process less reliable. This calls for the development of a more dependable and all-inclusive method for dealing with the resistant strains.

1.7 Relevance of the current dissertation

As elaborately discussed, the failure of the conventional cancer therapies led to the remodeling of the then existing facilities and built the substratum for the modern and non-conventional cancer therapies. The major bottle necks of the conventional and non-conventional therapies are the

interference of host immune system in identifying and eliminating the therapeutic entities before reaching the targets. The immediate release of the payload by the delivery vehicles, their poor pharmacokinetics and the various mechanisms that are developed by the tumor cells to create a secured area preventing the invasion of immune cells need to be addressed on an urgent basis. The available literatures reveal the unique properties of facultative and anaerobic bacteria that have the potential to beat these challenges as the bacteria itself has the ability to invade into the tumors preferentially, and multiply over there. Thus, the bacteria are more suitable therapeutic agents than the other methods. The genetic engineering of desired genes, mRNA, miRNA, siRNA, shRNA, cytokine expressing genes, endotoxin expressing genes have practically aided in the quality improvement of the bacteria-based therapy. The primary issues faced by this mode of therapy is the pathogenicity of the bacteria used. Although the virulent genes are deleted by gene editing of the bacterial strains but there has been no definite study revealing their no after effects on the hosts post intravenous injection. Moreover, there are shortage of evidences of these strains not regaining their pathogenicity by any means that could confirm their safety. Few articles are available on use of wild-type non-pathogenic strains of bacteria that generate the curiosity to uptake the challenge of using a wild-type non-pathogenic gut bacteria *Lactobacillus rhamnosus* as a drug delivery vehicle for a well-known anti-cancer drug methotrexate. The current dissertation work is an amalgamation of nanotechnology and bacteria-mediated therapy. The wild-type gut bacteria were used in order to address the issue of the pathogenicity. The *Lactobacillus rhamnosus* being a human friendly strain resides in the gut in human. Thus, it is a part of the microbiome. Moreover, studies have confirmed the presence of inherent anti-tumor effect of the bacteria. These properties are helpful in addressing the issues stated above as *Lactobacillus rhamnosus* can be a replacement for the genetically modified strains for having deleterious effect on tumor. A previous work reported from our group was used as a base for developing the *Lactobacillus rhamnosus* based fluorescent drug delivery vehicle. Taking inspiration from this work[95] we have fabricated gold nanoclusters of size 1.3 nm (approx.) on the surface of the live *Lactobacillus rhamnosus*. The methotrexate drug was loaded on top of it keeping the bacteria alive, motile and able to divide. These are addressed as 'bacbots'. The process of development of the delivery vehicle was standardized in order to keep the anti-tumor properties of the bacteria intact. The highlight of the studies is explained in detail in the following chapters. The gold nanoclusters synthesized on the live *Lactobacillus rhamnosus* were passed down the generations on cell division. These nanoclusters were seen to aggregate in the form of spheres and their numbers reduced down the generation. The study was extensively carried out for 262 cell divisions (six subsequent sub-cultures of the parent bacteria at the interval of 48 h of incubation; cell doubling time of the bacteria being 1.1 h). This study is unique as there are no reports on the passage of nanoclusters or nanoparticles fabricated on the bacteria to their progenies. The study holds a lot of importance as this shows the after effects of the nanotechnology combined bacteria-based therapies. An idea about the persistence of the nanoparticles/ nanoclusters can be extracted from this study. The details have been discussed in chapter 2 of the thesis. The next study was up taken to validate the effect of the bacbots on cancer cells. The results are profound on different types of cancer cell lines - HeLa and HT29. The studies were up taken on monolayer of cells and also on the 3D-spheroids of these cancer cells. The bacbots have shown excellent synergistic effect of drug and inherent anti-cancer properties of the bacteria on the spheroids as well in a dose depended

manner. The specificity of the bacbots towards the cancerous cells as compared to the non-cancerous cell lines provides evidence of their efficiency. The details of the study are provided in chapter 3. Since, the cancer is associated with secondary bacterial infections by *Staphylococcus aureus*, these bacbots were also applied on biofilms of *Staphylococcus aureus*. The results showcased 85% of the eradication of the biofilms at lower concentrations of the bacbots.

1.8 References

(1) Mattiuzzi, C.; Lippi, G. Current Cancer Epidemiology Glossary. *J. Epidemiol. Glob. Health.* **2019**, *9* (4), 217–222.

(2) Ferlay, J.; Colombet, M.; Soerjomataram, I.; Parkin, D. M.; Piñeros, M.; Znaor, A.; Bray, F. Cancer Statistics for the Year 2020: An Overview. *Int. J. Cancer.* **2021**, 149 (4), 778–789.

(3) Varmus, H. The New Era in Cancer Research. *Science.* **2006**, *312* (5777), 1162–1165.

(4) Rakoff-Nahoum, S. Why Cancer and Inflammation? *Yale J. Biol. Med.* **2006**, *79* (3–4), 123–130.

(5) Fares, J.; Fares, M. Y.; Khachfe, H. H.; Salhab, H. A.; Fares, Y. Molecular Principles of Metastasis: A Hallmark of Cancer Revisited. *Signal Transduct. Target. Ther.* **2020**, *5* (1).

(6) Nia, H. T.; Munn, L. L.; Jain, R. K. Physical Traits of Cancer. *Science.* **2020**, 370 (6516).

(7) Hanahan, D.; Weinberg, R. A. Hallmarks of Cancer: The next Generation. *Cell.* **2011**, *144* (5), 646–674.

(8) Marco, E. Semblanza de Ada Raquel Aular Alfonzo. *An. Venez. Nutr.* **2013**, *26* (1), 62.

(9) Hanahan, D. Hallmarks of Cancer: New Dimensions. *Cancer Discovery.* **2022**, 31–46.

(10) Hiam-Galvez, K. J.; Allen, B. M.; Spitzer, M. H. Systemic Immunity in Cancer. *Nat. Rev. Cancer.* **2021**, *21* (6), 345–359.

(11) Hayes, J. D.; Dinkova-Kostova, A. T.; Tew, K. D. Oxidative Stress in Cancer. *Cancer Cell* **.2020**, *38* (2), 167–197.

(12) Senga, S. S.; Grose, R. P. Hallmarks of Cancer—the New Testament. *Open Biol.* **2021**, *11* (1), 0–2.

(13) Yang, L.; Shi, P.; Zhao, G.; Xu, J.; Peng, W.; Zhang, J.; Zhang, G.; Wang, X.; Dong, Z.; Chen, F.; Cui, H. Targeting Cancer Stem Cell Pathways for Cancer Therapy; *Springer US*, **2020**, 5.

(14) DeVita, V. T.; Chu, E. A History of Cancer Chemotherapy. *Cancer Res.* **2008**, *68* (21), 8643–8653.

(15) Wang, X.; Zhong, X.; Liu, Z.; Cheng, L. Recent Progress of Chemodynamic Therapy-Induced Combination Cancer Therapy. *Nano Today.* **2020**, 35, 100946.

(16) Vasan, N.; Baselga, J.; Hyman, D. M. A View on Drug Resistance in Cancer. *Nature.* **2019**, *575* (7782), 299–309.

(17) Perillo, B.; Di Donato, M.; Pezone, A.; Di Zazzo, E.; Giovannelli, P.; Galasso, G.; Castoria, G.; Migliaccio, A. ROS in Cancer Therapy: The Bright Side of the Moon. *Exp. Mol. Med.* **2020**, *52* (2), 192–203.

(18) Ding, Y.; Pan, Q.; Gao, W.; Pu, Y.; Luo, K.; He, B. Reactive Oxygen Species-Upregulating Nanomedicines towards Enhanced Cancer Therapy. *Biomater. Sci.* **2022**.

(19) Roma-Rodrigues, C.; Mendes, R.; Baptista, P. V.; Fernandes, A. R. Targeting Tumor Microenvironment for Cancer Therapy. *Int. J. Mol. Sci.* **2019**, 20 (4).

(20) Chen, T.; Xu, J.; Zhu, L.; Yan, D. Cancer-Cell-Membrane-Camouflaged Supramolecular Self-Assembly of Antisense Oligonucleotide and Chemodrug for Targeted Combination Therapy. *Nanoscale*. **2022**.

(21) Khademi, R.; Mohammadi, Z. Nanoscale Advances Therapeutics in Acute Lymphoblastic Leukemia: A Systematic Review of Preclinical Studies †. *Nanoscale Adv.* **2023**, **5**, 571-595.

(22) Hui, Y.; Yi, X.; Hou, F.; Wibowo, D.; Zhang, F.; Zhao, D.; Gao, H.; Zhao, C. X. Role of Nanoparticle Mechanical Properties in Cancer Drug Delivery. *ACS Nano*. **2019**, *13* (7), 7410–7424.

(23) Chugh, H.; Sood, D.; Chandra, I.; Tomar, V.; Dhawan, G.; Chandra, R. Role of Gold and Silver Nanoparticles in Cancer Nano-Medicine. *Artif. Cells, Nanomedicine Biotechnol.* **2018**, *46* (1), 1210–1220.

(24) Sahu, A.; Choi, W. Il; Tae, G. Recent Progress in the Design of Hypoxia-Specific Nano Drug Delivery Systems for Cancer Therapy. *Adv. Ther.* **2018**, *1* (4), 1800026.

(25) Jin, C.; Wang, K.; Oppong-Gyebi, A.; Hu, J. Application of Nanotechnology in Cancer Diagnosis and Therapy - A Mini-Review. *Int. J. Med. Sci.* **2020**, *17* (18), 2964–2973.

(26) Das, S. Sensors & Diagnostics Diagnosis of Cancer Using Carbon Nanomaterial- Based Biosensors. *Sensors & Diagonostics*. **2022**.

(27) Zhang, W.; Taheri-Ledari, R.; Ganjali, F.; Mirmohammadi, S. S.; Qazi, F. S.; Saeidirad, M.; KashtiAray, A.; Zarei-Shokat, S.; Tian, Y.; Maleki, A. Effects of Morphology and Size of Nanoscale Drug Carriers on Cellular Uptake and Internalization Process: A Review. *RSC Adv.* **2022**, *13* (1), 80–114.

(28) Lin, Y. X.; Wang, Y.; Blake, S.; Yu, M.; Mei, L.; Wang, H.; Shi, J. RNA Nanotechnology-Mediated Cancer Immunotherapy. *Theranostics.* **2020**, *10* (1), 281–299.

(29) Han, H.; Wang, H.; Jangili, P.; Li, M.; Wu, L.; Zang, Y.; Sedgwick, A. C.; Li, J. The Design of Small-Molecule Prodrugs and Activatable Phototherapeutics for Cancer Therapy. *Chem Soc Rev.* **2023**,52, 879-920.

(30) Chen, H.; Zhang, W.; Zhu, G.; Xie, J.; Chen, X. Rethinking Cancer Nanotheranostics. *Nat. Rev. Mater.* **2017**, *2* (17024).

(31) Zhang, Y.; Li, M.; Gao, X.; Chen, Y.; Liu, T. Nanotechnology in Cancer Diagnosis: Progress, Challenges and Opportunities. *J. Hematol. Oncol.* **2019**, *12* (1), 1–13.

(32) Sharifianjazi, F.; Jafari Rad, A.; Bakhtiari, A.; Niazvand, F.; Esmaeilkhanian, A.; Bazli, L.; Abniki, M.; Irani, M.; Moghanian, A. Biosensors and Nanotechnology for Cancer Diagnosis (Lung and Bronchus, Breast, Prostate, and Colon): A Systematic Review. *Biomed. Mater.* **2022**, *17* (1).

(33) Riley, R. S.; June, C. H.; Langer, R.; Mitchell, M. J. Delivery Technologies for Cancer Immunotherapy. Nature Reviews Drug Discovery. *Springer US.* **2019**, 175–196.

(34) Tan, S.; Li, D.; Zhu, X. Cancer Immunotherapy: Pros, Cons and Beyond. *Biomed. Pharmacother.* **2020**, 124.

(35) Kennedy, L. B.; Salama, A. K. S. A Review of Cancer Immunotherapy Toxicity. *CA. Cancer J. Clin.* **2020**, *70* (2), 86–104.

(36) Liang, C.; Zhang, X.; Yang, M.; Dong, X. Recent Progress in Ferroptosis Inducers for Cancer Therapy. *Adv. Mater.* **2019**, *31* (51), 1–25.

(37) Xu, T.; Ding, W.; Ji, X.; Ao, X.; Liu, Y.; Yu, W.; Wang, J. Molecular Mechanisms of Ferroptosis and Its Role in Cancer Therapy. *J. Cell. Mol. Med.* **2019**, *23* (8), 4900–4912.

(38) Yin, W.; Chang, J.; Sun, J.; Zhang, T.; Zhao, Y. Nanomedicine-Mediated Ferroptosis Targeting Strategies for Synergistic Cancer Therapy. *J. Mater. Chem. B*, **2023**, 11, 1171-1190.

(39) Yadav, A. C.; Gopisankar, M. G. Gene Therapy. Introd. to Basics Pharmacol. Toxicol. Vol. 1 Gen. Mol. *Pharmacol. Princ. Drug Action* .2019, 1, 319–328.

(40) Taniguchi, S.; Fujimori, M.; Sasaki, T.; Tsutsui, H.; Shimatani, Y.; Seki, K.; Amano, J. Targeting Solid Tumors with Non-Pathogenic Obligate Anaerobic Bacteria. *Cancer Sci.* **2010**, *101* (9), 1925–1932

(41) Leschner, S.; Westphal, K.; Dietrich, N.; Viegas, N.; Jablonska, J.; Lyszkiewicz, M.; Lienenklaus, S.; Falk, W.; Gekara, N.; Loessner, H.; Weiss, S. Tumor Invasion of Salmonella Enterica Serovar Typhimurium Is Accompanied by Strong Hemorrhage Promoted by TNF-α. *PLoS One.* **2009**, *4* (8).

(42) Chen, J.; Yang, B.; Cheng, X.; Qiao, Y.; Tang, B.; Chen, G.; Wei, J.; Liu, X.; Cheng, W.; Du, P.; Huang, X.; Jiang, W.; Hu, Q.; Hu, Y.; Li, J.; Hua, Z.-C. Salmonella-Mediated Tumor-Targeting TRAIL Gene Therapy Significantly Suppresses Melanoma Growth in Mouse Model. *Cancer Sci.* **2012**, *103* (2), 325–333.

(43) Xu, W.; Zhou, T.; Zhou, J.; Qiang, Z.; Zhang, J.; Hua, Z. Attenuated Salmonella VNP20009 Mutant (ΔhtrA) Is a Promising Candidate for Bacteria-Mediated Tumour Therapy in Hosts with TNFR1 Deficiency. *Lett. Appl. Microbiol.* **2018**, *67* (1), 97–103.

(44) Felgner, S.; Pawar, V.; Kocijancic, D.; Erhardt, M.; Weiss, S. Tumour-Targeting Bacteria-Based Cancer Therapies for Increased Specificity and Improved Outcome. *Microb. Biotechnol.* **2017**, *10* (5), 1074–1078.

(45) Jahanban-Esfahlan, R.; de la Guardia, M.; Ahmadi, D.; Yousefi, B. Modulating Tumor Hypoxia by Nanomedicine for Effective Cancer Therapy. *J. Cell. Physiol.* **2018**, *233* (3), 2019–2031.

(46) Cheng, C.; Lu, Y.; Chuang, K.; Hung, W.; Shiea, J.; Su, Y.; Kao, C.; Chen, B.; Roffler, S.; Cheng, T. Tumor-Targeting Prodrug-Activating Bacteria for Cancer Therapy. *Cancer Gene Ther.* **2008**, (6):393-401.

(47) Ryan, R. M.; Green, J.; Lewis, C. E. Use of Bacteria in Anti-Cancer Therapies. *BioEssays.* **2006**, *28* (1), 84–94.

(48) Liang, K.; Liu, Q.; Kong, Q. New Technologies in Developing Recombinant-Attenuated Bacteria for Cancer Therapy. *Biotechnol. Bioeng.* **2021**, *118* (2), 513–530.

(49) Liang, S.; Wang, C.; Shao, Y.; Wang, Y.; Xing, D.; Geng, Z. Recent Advances in Bacteria-Mediated Cancer Therapy. *Frontiers in Bioengineering and Biotechnology.* **2022**, 1–20.

(50) Gao, S.; Jung, J.; Lin, S.; Jang, A.; Zhi, Y.; Ahn, K. B.; Hyun-jung, J.; Lim, J. H.; Guo, H.; Choy, H. E.; Lim, S. Development of Oxytolerant Salmonella Typhimurium Using Radiation Mutation Technology (RMT) for Cancer Therapy. *Sci Rep.***2020**, *10*(1), 3764.

(51) Wang, Z.; Wang, L.; Bian, H.; Huang, Z.; Zhang, X.; Xiao, Y. Outer Surface-Labeled Bacteria as Live Sensors Accurately Quantitating Interfacial PH: A Smart Technique for Antimicrobial Resistance. *ACS Nano*; **2022**, *16*(11), 18344–18354.

(52) Duong, M. T.; Qin, Y.; You, S.; Min, J. Bacteria-Cancer Interactions: Bacteria-Based Cancer Therapy. *Exp. Mol. Med.* **2019**, *51*(12), 1-15.

(53) Cronin, M.; Stanton, R. M.; Francis, K. P.; Tangney, M. Bacterial Vectors for Imaging and Cancer Gene Therapy: A Review. *Cancer Gene Ther.* **2012**, *19* (11), 731–740.

(54) Forbes, N. S. Engineering the Perfect (Bacterial) Cancer Therapy. *Nat. Rev. Cancer.* **2010**, *10* (11), 785–794.

(55) Li, Z.; Wang, Y.; Liu, J.; Rawding, P.; Bu, J.; Hong, S.; Hu, Q. Chemically and Biologically Engineered Bacteria-Based Delivery Systems for Emerging Diagnosis and Advanced Therapy. *Adv. Mater.* **2021**, *33* (38), 1–29.

(56) Pan, H.; Zheng, M.; Ma, A.; Liu, L.; Cai, L. Cell/Bacteria-Based Bioactive Materials for Cancer Immune Modulation and Precision Therapy. *Adv. Mater.* **2021**, *33* (50), 1–22.

(57) Johnson, S. A.; Ormsby, M. J.; Wessel, H. M.; Hulme, H. E.; Bravo-Blas, A.; McIntosh, A.; Mason, S.; Coffelt, S. B.; Tait, S. W. G.; Mowat, A. M.; Milling, S. W. F.; Blyth, K.; Wall, D. M. Monocytes Mediate Salmonella Typhimurium-Induced Tumor Growth Inhibition in a Mouse Melanoma Model. *Eur. J. Immunol.* **2021**, *51* (12), 3228–3238.

(58) Suh, S. B.; Jo, A.; Traore, M. A.; Zhan, Y.; Coutermarsh-Ott, S. L.; Ringel-Scaia, V. M.; Allen, I. C.; Davis, R. M.; Behkam, B. Nanoscale Bacteria-Enabled Autonomous Drug Delivery System (NanoBEADS) Enhances Intratumoral Transport of Nanomedicine. *Adv. Sci.* **2019**, *6* (3).

(59) Jia, L.-J.; Wei, D.-P.; Sun, Q.-M.; Huang, Y.; Wu, Q.; Hua, Z.-C. Oral Delivery of Tumor-Targeting Salmonella for Cancer Therapy in Murine Tumor Models. *Cancer Sci.* **2007**, *98* (7), 1107–1112

(60) Fu, W.; Lan, H.; Liang, S.; Gao, T.; Ren, D. Suicide Gene/Prodrug Therapy Using Salmonella-Mediated Delivery of Escherichia Coli Purine Nucleoside Phosphorylase Gene and 6-Methoxypurine 2′-Deoxyriboside in Murine Mammary Carcinoma 4T1 Model. *Cancer Sci.* **2008**, *99* (6), 1172–1179.

(61) Thomas, S. C.; Madaan, T.; Kamble, N. S.; Siddiqui, N. A.; Pauletti, G. M.; Kotagiri, N. Engineered Bacteria Enhance Immunotherapy and Targeted Therapy through Stromal Remodeling of Tumors. *Adv. Healthc. Mater.* **2022**, *11* (2), 1–31.

(62) Liu, L.; Wu, J.; Gao, J.; Lu, X. Bacteria-Derived Nanoparticles: Multifunctional Containers for Diagnostic and Therapeutic Applications. *Adv. Healthc. Mater.* **2020**, *9* (22).

(63) Chen, W.; Guo, Z.; Zhu, Y.; Qiao, N.; Zhang, Z.; Sun, X. Combination of Bacterial-Photothermal Therapy with an Anti-PD-1 Peptide Depot for Enhanced Immunity against Advanced Cancer. *Adv. Funct. Mater.* **2020**, *30* (1), 1–13.

(64) Sun, M.; Ye, H.; Shi, Q.; Xie, J.; Yu, X.; Ling, H.; You, S.; He, Z.; Qin, B.; Sun, J. Both-In-One Hybrid Bacteria Suppress the Tumor Metastasis and Relapse via Tandem-Amplifying Reactive Oxygen Species-Immunity Responses. *Adv. Healthc. Mater.* **2021**, *10* (21), 2100950.

(65) Song, W.; Anselmo, A. C.; Huang, L. Nanotechnology Intervention of the Microbiome for Cancer Therapy. *Nat. Nanotechnol.* **2019**, *14* (12), 1093–1103.

(66) Yin, T.; Diao, Z.; Blum, N. T.; Qiu, L.; Ma, A.; Huang, P. Engineering Bacteria and Bionic Bacterial Derivatives with Nanoparticles for Cancer Therapy. *Small.* **2022**, *18* (12), 2104643.

(67) Zhan, Y.; Fergusson, A.; McNally, L. R.; Davis, R. M.; Behkam, B. Robust and Repeatable Biofabrication of Bacteria-Mediated Drug Delivery Systems: Effect of Conjugation Chemistry, Assembly Process Parameters, and Nanoparticle Size. *Adv. Intell. Syst.* **2022**, *4* (3), 2100135.

(68) Alfarouk, K. O.; Stock, C. M.; Taylor, S.; Walsh, M.; Muddathir, A. K.; Verduzco, D.; Bashir, A. H. H.; Mohammed, O. Y.; Elhassan, G. O.; Harguindey, S.; Reshkin, S. J.; Ibrahim, M. E.; Rauch, C. Resistance to Cancer Chemotherapy: Failure in Drug Response from ADME to P-Gp. *Cancer Cell Int.* **2015**, *15* (1), 1–13.

(69) Zargar, A.; Chang, S.; Kothari, A.; Snijders, A. M.; Mao, J.; Wang, J.; Hernández, A. C.; Keasling, J. D.; Bivona, T. G. Overcoming the Challenges of Cancer Drug Resistance through Bacterial-mediated Therapy. Chronic Dis. *Transl. Med.* **2019**, *5* (4), 258–266.

(70) Osuna-Pérez, J.; García-Ferreras, R.; Veiga, E. From Cellular Microbiology to Bacteria-Based next Generations of Cancer Immunotherapies. Cell. Microbiol. 2020, *22* (4), e13187.

(71) Al-Ramadi, B. K.; Fernandez-Cabezudo, M. J.; El-Hasasna, H.; Al-Salam, S.; Attoub, S.; Xu, D.; Chouaib, S. Attenuated Bacteria as Effectors in Cancer Immunotherapy. *Ann. N. Y. Acad. Sci.* **2008**, *1138* (1), 351–357.

(72) Felgner, S.; Spöring, I.; Pawar, V.; Kocijancic, D.; Preusse, M.; Falk, C.; Rohde, M.; Häussler, S.; Weiss, S.; Erhardt, M. The Immunogenic Potential of Bacterial Flagella for Salmonella-Mediated Tumor Therapy. *Int. J. Cancer.* **2020**, *147* (2), 448–460.

(73) Huang, X.; Pan, J.; Xu, F.; Shao, B.; Wang, Y.; Guo, X.; Zhou, S. Bacteria-Based Cancer Immunotherapy. *Advanced Science.* **2021**, 1–22.

(74) Phan, T. X.; Nguyen, V. H.; Duong, M. T.-Q.; Hong, Y.; Choy, H. E.; Min, J.-J. Activation of Inflammasome by Attenuated Salmonella Typhimurium in Bacteria-Mediated Cancer Therapy. *Microbiol. Immunol.* **2015**, *59* (11), 664–675.

(75) Stern, C.; Kasnitz, N.; Kocijancic, D.; Trittel, S.; Riese, P.; Guzman, C. A.; Leschner, S.; Weiss, S. Induction of CD4+ and CD8+ Anti-Tumor Effector T Cell Responses by Bacteria Mediated Tumor Therapy. *Int. J. Cancer.* **2015**, *137* (8), 2019–2028.

(76) Sedighi, M.; Zahedi Bialvaei, A.; Hamblin, M. R.; Ohadi, E.; Asadi, A.; Halajzadeh, M.; Lohrasbi, V.; Mohammadzadeh, N.; Amiriani, T.; Krutova, M.; Amini, A.; Kouhsari, E. Therapeutic Bacteria to Combat Cancer; Current Advances, Challenges, and Opportunities. *Cancer Med.* **2019**, *8* (6), 3167–3181.

(77) Kwon, S. Y.; Jiang, S.-N.; Zheng, J. H.; Choy, H. E.; Min, J.-J. Rhodobacter Sphaeroides, a Novel Tumor-Targeting Bacteria That Emits Natural near-Infrared Fluorescence. *Microbiol. Immunol.* **2014**, *58* (3), 172–179.

(78) Wang, L.; Vuletic, I.; Deng, D.; Crielaard, W.; Xie, Z.; Zhou, K.; Zhang, J.; Sun, H.; Ren, Q.; Guo, C. Bifidobacterium Breve as a Delivery Vector of IL-24 Gene Therapy for Head and Neck Squamous Cell Carcinoma in Vivo. *Gene Ther.* **2017**, *24* (11), 699–705.

(79) Yazawa, K.; Fujimori, M.; Amano, J.; Kano, Y. Therapy: Selective Localization and Growth in Hypoxic Tumors. *Cancer Gene Ther.* **2000**, *7* (2), 269–274.

(80) Wang, L.; Qin, W.; Xu, W.; Huang, F.; Xie, X.; Wang, F.; Ma, L.; Zhang, C. Bacteria-Mediated Tumor Therapy via Photothermally-Programmed CytolysinA Expression. *Small.* **2021**, *17* (40), 2102932.

(81) Roy, S.; Trinchieri, G. Microbiota: A Key Orchestrator of Cancer Therapy. *Nat. Rev. Cancer* .**2017**, *17* (5), 271–285.

(82) Routy, B.; Gopalakrishnan, V.; Daillère, R.; Zitvogel, L.; Wargo, J. A.; Kroemer, G. And General Health. *Nat. Rev. Clin. Oncol.* **2018**, *15*(6):382-396.

(83) Elinav, E.; Garrett, W. S.; Trinchieri, G.; Wargo, J. The Cancer Microbiome. *Nat. Rev. Cancer.* **2019**, *19* (7), 371–376.

(84) Wong, S. H.; Yu, J. Gut Microbiota in Colorectal Cancer: Mechanisms of Action and Clinical Applications. Nature Reviews Gastroenterology and Hepatology. *Springer US*. **2019**, 690–704.

(85) Tsilimigras, M. C. B.; Fodor, A.; Jobin, C. Carcinogenesis and Therapeutics: The Microbiota Perspective. *Nat. Microbiol.* **2017**, *2*, 1–10.

(86) Zitvogel, L.; Daillère, R.; Roberti, M. P.; Routy, B.; Kroemer, G. Anticancer Effects of the Microbiome and Its Products. *Nat. Rev. Microbiol.* **2017**, *15* (8), 465–478.

(87) Helmink, B. A.; Khan, M. A. W.; Hermann, A.; Gopalakrishnan, V.; Wargo, J. A. The Microbiome\, Cancer, and Cancer Therapy. *Nat. Med.* **2019**, *25*, 377–388.

(88) Carney, D. N.; Fossieck, B. E. J.; Parker, R. H.; Minna, J. D. Bacteremia Due to *Staphylococcus aureus* in Patients with Cancer: Report on 45 Cases in Adults and Review of the Literature. *Rev. Infect. Dis.* **1982**, *4* (1), 1–12.

(89) Wong, J. L.; Evans, S. E. Bacterial Pneumonia in Patients with Cancer: Novel Risk Factors and Management. *Clinics in Chest Medicine. Elsevier*, **2017**, 263–277.

(90) Ahmed, N.; Baruah, F.; Grover, R. Staphylococcal Blood Stream Infections in Cancer Patients. *Ann. Med. Health Sci. Res.* **2015**, *5* (3), 226.

(91) Gotland, N.; Uhre, M. L.; Sandholdt, H.; Mejer, N.; Lundbo, L. F.; Petersen, A.; Larsen, A. R.; Benfield, T. Increased Risk of Incident Primary Cancer after *Staphylococcus aureus* Bacteremia: A Matched Cohort Study. *Medicine (Baltimore)*. **2020**, *99* (17), e19984.

(92) Qi, J. L.; He, J. R.; Liu, C. B.; Jin, S. M.; Gao, R. Y.; Yang, X.; Bai, H. M.; Ma, Y. B. Pulmonary *Staphylococcus aureus* Infection Regulates Breast Cancer Cell Metastasis via Neutrophil Extracellular Traps (NETs) Formation. *MedComm*. **2020**, *1* (2), 188–201.

(93) Bhat, S.; Muthunatarajan, S.; Mulki, S. S.; Archana Bhat, K.; Kotian, K. H. Bacterial Infection among Cancer Patients: Analysis of Isolates and Antibiotic Sensitivity Pattern. *Int. J. Microbiol.* **2021**, *2021*, 8883700.

(94) Worku, M.; Belay, G.; Tigabu, A. Bacterial Profile and Antimicrobial Susceptibility Patterns in Cancer Patients. *PLoS One*. **2022**, *17*, 1–17.

(95) Goswami, U.; Basu, S.; Paul, A.; Ghosh, S. S.; Chattopadhyay, A. White Light Emission from Gold Nanoclusters Embedded Bacteria. *J. Mater. Chem. C*. **2017**, *5* (47), 12360–12364.

Chapter 2

Hierarchical Passage of Gold Nanoclusters in Living Bacteria

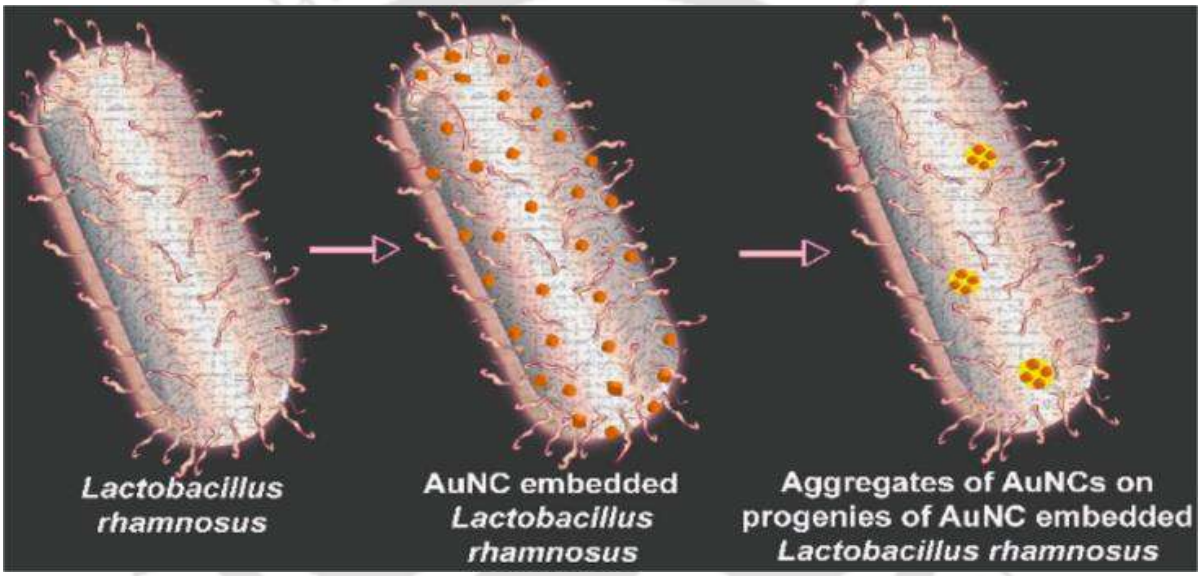

This chapter has been published in *ACS Applied Biomaterials*

(https://pubs.acs.org/doi/10.1021/acsabm.2c00315)

Abstract

The gold (Au) nanoclusters chemically synthesized on the cell surface of living *Lactobacillus rhamnosus* render them photoluminescent. Importantly, the bacteria were viable and the clusters were passed down the generations with the loss of luminescence in the first sub-culture onwards. Moreover, the clusters were agglomerated into spherical structures on the order of 100-200 nm on the cell surfaces of the bacteria of all six sub-cultures studied. There was no indication of the formation of plasmonic Au nanoparticles in the larger structures. The results indicated the important role of bacterial cell wall remodeling in transforming the smaller Au nanoclusters into larger aggregates down the generations. That the clusters remained on the cell surface of bacteria for several generations may hold important implications for using nanoparticle-studded bacteria in healthcare especially in theranostics.

2.1 Introduction

The principles and practices of synthetic and materials chemistry and functional components of living species -in combination – may provide novel opportunities in designing advanced drug delivery and therapy platforms. In particular, an ideal vehicle that not only efficiently encapsulates cargos or itself acts as therapeutic agent but also addresses the challenges of targeting, specificity, host immune response and undesirable burst release is desirable. An important choice in this regard would be living bacteria. For example, the current technology allows genetically engineered bacteria for efficient killing of tumors especially when combined with other therapeutic modalities such as nanomaterials-based drugs, photothermal and photodynamic therapies. The use of bacteria for carrying out biomedical applications such as genetic engineering-based therapy, enzyme-prodrug therapy and bio-imaging are promising alternatives[1,2,3]. For example, genetically engineered attenuated live bacteria – when administered orally - deliver therapeutic DNA to targeted tissues[4]. Also, anti-body targeted bacteriobots act as theranostics agents in hypoxic tumor cores[5]. Nanoparticle loaded live bacteria also work as non-viral gene delivery system[6]. Photothermal metal nanoparticles in bacteria help express gene in tumors upon exposure to NIR radiation. [7]

Additionally, facultative anaerobic bacteria get attracted towards cancer cells by chemotaxis and thus are more effective over other strains for targeting both hypoxic and aerobic tumor sites[8]. Moreover, these bacteria are attenuated for developing programmed delivery vehicle, at tumor sites, to promote cytotoxicity or to express immunomodulators that help in eliciting innate immune response against the tumors [9,10,11]. Thus, bacterial species such as *Listeria monocytogenes, Clostridium, Salmonella typhimurium* and *Bifidobacterium* have been used for developing self-propelling delivery systems[12,13]. Further, gut microbiota provides an important choice for therapeutic bacteria as they are reported to influence the overall tumor microenvironment and thus affect the treatment outcomes[14,15,16]. Also, *Lactobacillus* strain is known to accumulate in tumor sites leading to their regression[17]. The achievements of BCG immunotherapy stems from the ability of the bacteria to draw their nutrition from necrotic tumor cells and the hypoxic sites within the tumors that also provide them protection from immune clearance[18]. The success of bacteria mediated therapy provides impetus to pursue the combination of nanoscale materials, molecular

drugs and bacteria in theranostics. A possible way forward is to synthesize nanoscale particles on the living bacterial cell wall followed by incorporation of drug molecules on the nanoparticles.

However, this can be challenging as the peptidoglycan (PGN) - consisting of alternate chain of *N*-acetylglucosamine and *N*-acetylmuramic acid interlinked by β-1,4 bond - may prevent the nanoparticles from bonding to the surface or their high turnover rate may knockout the nanoparticles from the cell walls. For example, *Lactobacillus acidophilus* and *Neisseria gonorrhoea* have the rate of cell wall turnover 25- 50% per generation[19]. Further, the PGN layer is lysed by autolysins[20] and there is a delay of one generation during the renewal of new strands in gram positive bacteria[21]. Recent results suggest that the nanoparticles could indeed be synthesized on the cell walls of bacteria. For example, white light emission from the combination of the bacterial proteins and Au nanoclusters on the cell walls of green fluorescent protein expressing bacteria was recently reported[22] However, pursuit of synthesis of nanoparticles on living bacteria and understanding their fate in several generations of bacteria are vital to future success of any combination therapy as described above. Such reports are still awaited.

In this chapter, the synthesis of Au nanoclusters on the *Lactobacillus rhamnosus* (MTCC 1408) by chemical reduction of the parent salt has been reported. The results indicated that the bacteria were alive following the formation of the luminescent clusters on their cell walls. In addition, the clusters were transferred to several generations of progenies. Importantly, the so-synthesized clusters were aggregated on the cell walls of the progenies with loss of luminescence after a few generations,

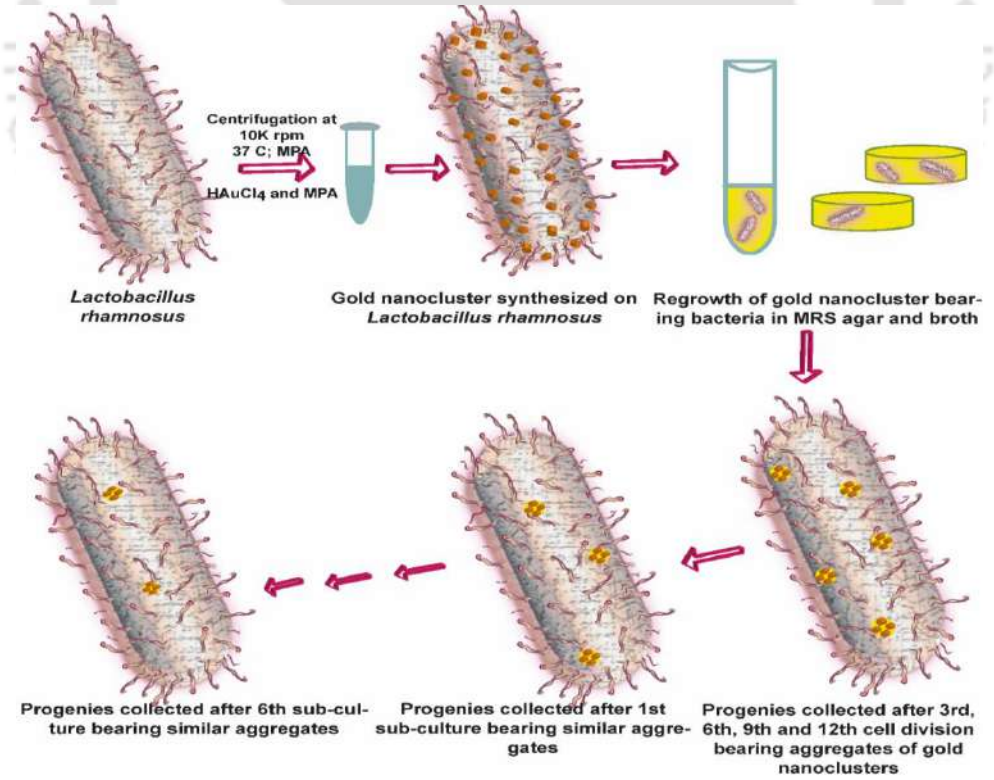

Scheme 2.1. Schematic representation of synthesis of gold nanoclusters on live and viable *Lactobacillus rhamnosus* cell surface using chemical reduction method and subsequent aggregation of the nanoclusters on the cell surface of the progenies as described in the legends.

suggesting the effect of cell wall remodelling in subsequent generations. The idea of the growth of Au nanoclusters on the bacterial cell wall and their generational fate is described briefly in Scheme 2.1.

2.2. Materials and Methods

2.2.1. Growth curve of *Lactobacillus rhamnosus*

The doubling time of the *Lactobacillus rhamnosus* was determined by measuring the optical density of the bacteria after an interval of 3 h for a duration of 48 h. The analysis was carried out by taking the logarithmic values of the optical density against the different time points. The doubling time was found to be 1.1 h.

2.2.2. Sample preparation for characterization studies

The control bacteria, gold nanocluster bearing bacteria and the progenies were centrifuged at 10K rpm for 5 min and then were re-dispersed in double autoclaved deionised water. The process was performed thrice. The obtained samples were diluted and further used for the characterization studies.

2.2.3. Determination of Colony Forming Unit/mL before and after synthesis

The quantification of bacteria before and after synthesis was carried out by taking *Lactobacillus rhamnosus* from late log phase followed by serially diluting the culture and spreading on MRS agar plates. These agar plates were incubated for 48 h at 37 °C and then the colonies of bacteria were counted. The cfu/mL of *Lactobacillus rhamnosus* was found to be 10^9 cfu/mL. The similar procedure was followed to calculate the cfu/mL after synthesis; it was found to be 10^8 cfu/mL.

2.2.4. Spectroscopy analysis

The UV-visible spectroscopy analysis was carried out in Jasco V-630 spectrophotometer. The fluorescence spectroscopy analysis was done using Fluoromax-4 (Horiba Jobin Yvon). The excitation wavelength used was 320 nm for all the samples.

2.2.5. Field Emission Transmission Electron Microscopy, Energy Dispersive X-ray analysis and Elemental mapping analysis

The diluted samples were drop cast on carbon coated copper mesh and were allowed to dry. The analysis as carried out in Jeol 2100F FETEM. The EDX and elemental mapping analyses were also performed to confirm the presence of Au.

2.2.6. Field Emission Scanning Electron Microscopy

The samples were drop cast on aluminium foil for the analysis and were dried. The analysis was performed in Jeol JSM-7610.

2.2.7. Atomic Force Microscopy

The samples were diluted using double autoclaved deionised water and were drop cast on clean glass slide for drying. The analysis was carried out in Oxford Cypher S atomic force microscope.

2.2.8. Confocal Laser Scanning Microscopy

The prepared samples were imaged by CLSM (Zeiss, LSM 880) using laser at 405 nm.

2.3. Results and Discussion

The Au nanoclusters were synthesized by incubation of the growth medium free late log phase grown culture of *Lactobacillus rhamnosus* (MTCC 1408; 10^9 cfu/mL) with HAuCl4 and 3-mercaptopropionic acid for 3 min at 37 °C . The synthesis was confirmed first by the appearance of luminescent orange color when observed above a UV transilluminator (with excitation at 312

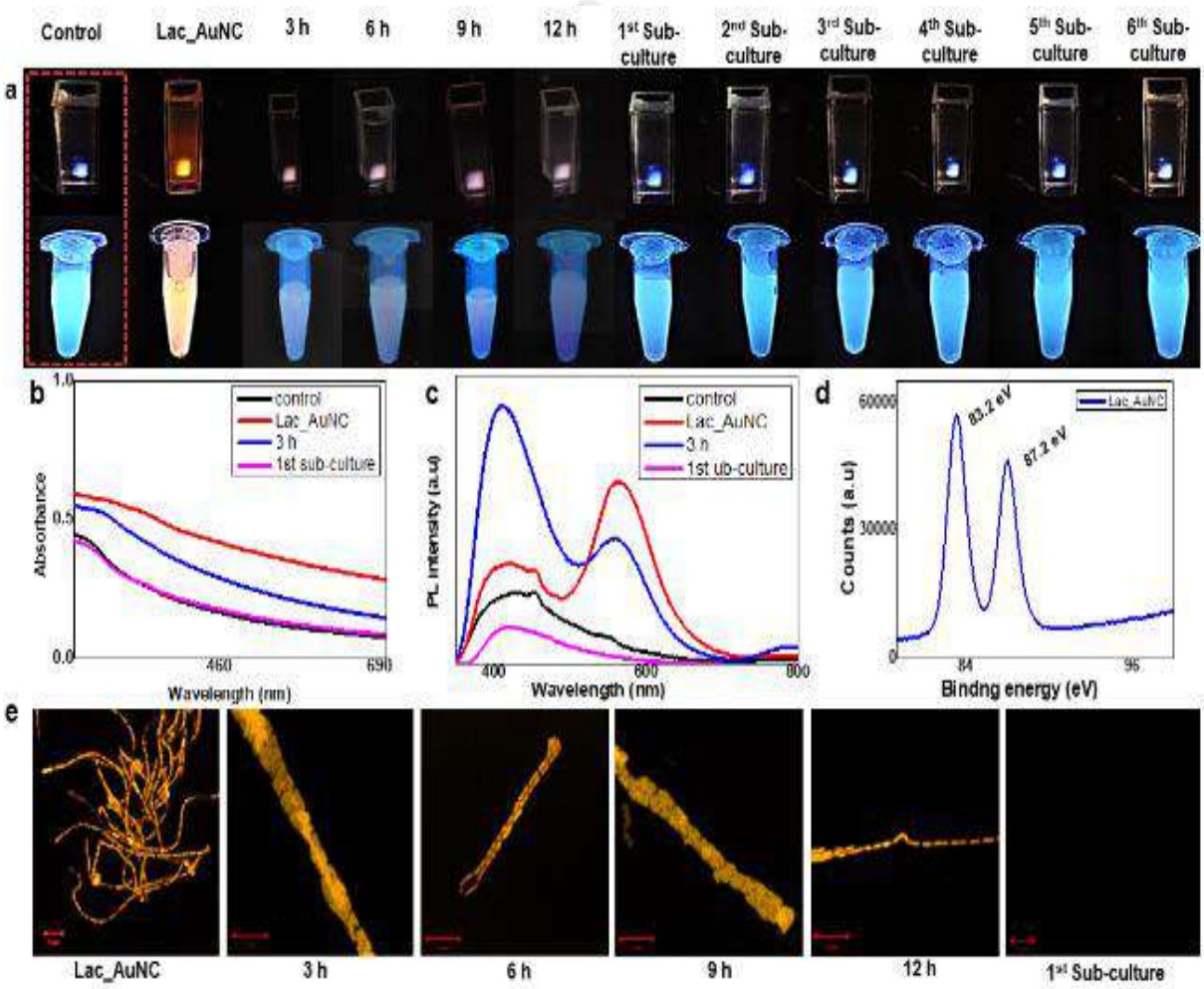

Figure 2.2. (a) Transilluminator visualization of gold nanocluster-studded *Lactobacillus rhamnosus* and their progenies of subsequent cell divisions after 3 h, 6 h, 9 h,12 h and 1st to 6th sub-cultures (each sub-culture was carried after 48 h of incubation). (b) UV-visible spectra of control *L.rhamnosus*, Lac_AuNC and its progenies collected after 3 h and 1st sub-culture.(c) Photoluminescence spectra of control *L.rhamnosus*, Lac_AuNC and its progenies collected after 3 h and 1st sub-culture. (d)XPS analysis of Lac_AuNC showing binding energy peaks at 83.2 eV and 87.2 eV(e)confocal laser scanning microscopy images of Lac_AuNC and its progenies collected after 3 h, 6 h, 9 h, 12 h and 1st sub-culture showing disappearance of fluorescence after 1st sub-culture of Lac AuNC.

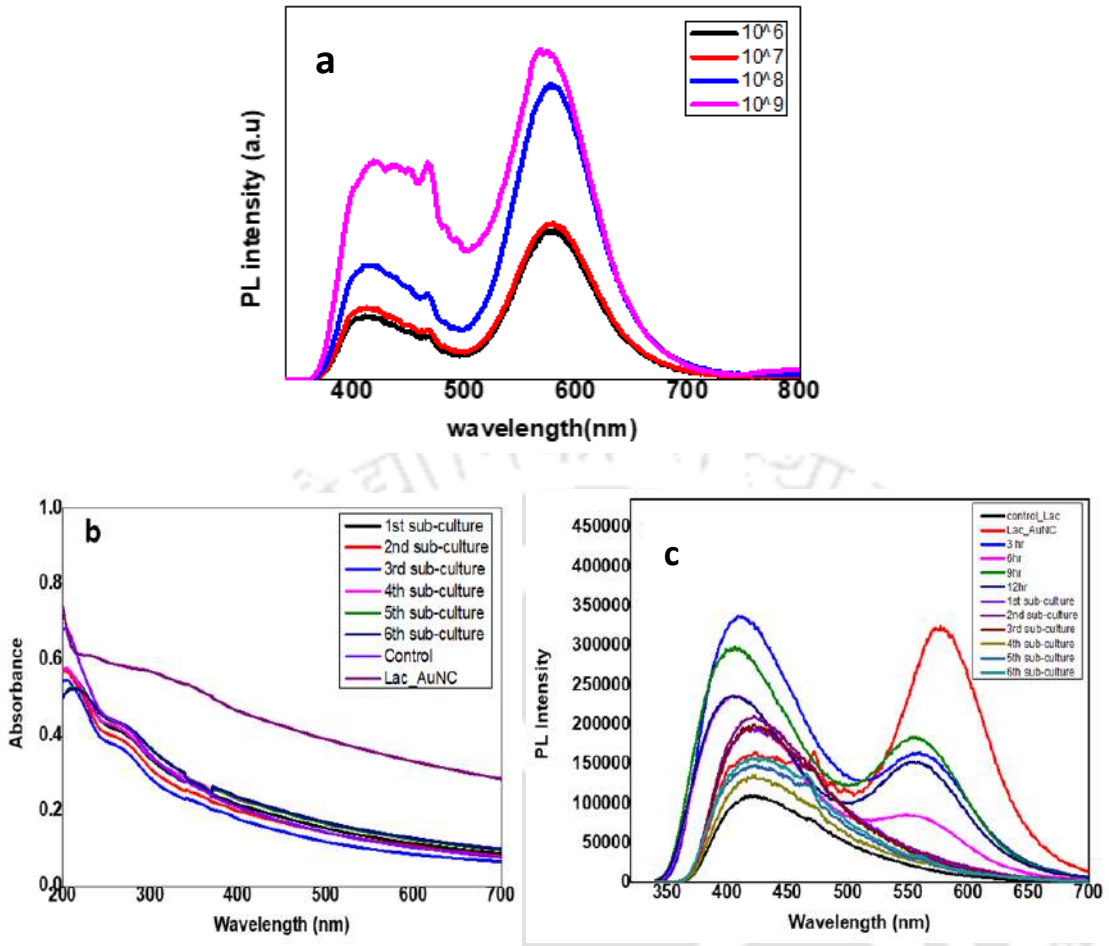

Figure 2.3. Spectroscopy analysis (a) Photoluminescence spectra of Lac_AuNC with different concentrations of bacteria taken for synthesis , (b) UV absorbance spectra (c) photoluminescence spectra of control, AuNC embedded bacteria (Lac_AuNC) and their progenies collected after 3 h, 6 h, 9 h, 12 h and 1st to 6th sub-cultures.

nm) (Figure 2.2a). The color dimmed increasingly with time following incubation and was lost in the first sub-culture and was absent in subsequent cultures too (Figure 2.2a).

UV-vis spectrum of the resulting medium consisted of a broad peak in the range of 200-400 nm and the absence of a peak at 520 nm that is characteristic of Au nanoparticles (due to surface plasmon resonance) discounted their formation (Figure 2.2b). Similar observations were made in all sub-cultures (Figure 2.4c). Importantly, photoluminescence spectrum of the medium consisted of a peak at 420 nm (when excited with 320 nm radiation), due to the amino acid residues of the proteins in bacteria. On the other hand, a second and more intense peak at 580 nm also appeared in the spectrum, indicating the formation of Au nanoclusters that was absent in the control bacteria (Figure 2.2c and Figure 2.3a).

Further, the luminescence spectrum of the *Lactobacillus rhamnosus* consisted of a single peak at 420 nm owing to the proteins (Figure 2.2c). The peak at 580 nm disappeared in the first and subsequent sub-cultures of bacteria whereas the peak at 420 nm was persistent (Figure 2.2c and

Figure 2.3c). X- ray photoelectron spectroscopy (XPS) of the cluster-studded patent cells indicated the presence of Au (0) with peaks at 83.2 and 87.2 MeV (Figure 2.2d). Confocal laser scanning microscopy (CLSM) of the Au nanocluster studded bacteria also supported the formation of the clusters with the presence of characteristic emission in the orange when excited by 405 nm laser (Figure 2.2e). Importantly, individual bacterium appeared luminescent orange on its entire body, indicating that indeed Au nanoclusters were attached to the bacteria. Overall, the results from the above experiments suggested that Au nanoclusters with emission in the orange were formed on the *Lactobacillus rhamnosus*. Further, the luminescence on the bacteria (upon incubation, doubling time of bacteria being 1.1 h) persisted for at least 12 h (Figure 2.2e, Figure 2.4); however, that was lost in the first (Figure 2.2e and Figure 2.5) and subsequent sub-cultures.

Transmission electron microscopy (TEM) images (Figure 2.6b, Figure 2.7 and Figure 2.8) of the drop-cast product medium revealed the presence of intact bacteria studded with nanoscale particles of size 1.3 $\pm$ 0.4 nm (Figure 2.9). Images of control bacteria were devoid of such structures (Figure 2.4a). The presence of Au spread across the bacterial body was supported by elemental mapping performed using energy dispersive X-ray spectroscopy (Figure 2.4h). Additionally, field emission scanning electron microscopy (FESEM) study (Figure 2.10) supported the presence of intact bacteria in the product medium. Thus, Au nanoclusters with characteristic photoluminescence were produced possibly on the cell walls of the bacteria. whereas, there were no such deposits seen in case of the control *Lactobacillus rhamnosus*. Atomic force microscopy (AFM) studies revealed that the Au nanocluster studded bacterial surfaces had higher roughness as compared to the control bacteria (Figure 2.11).

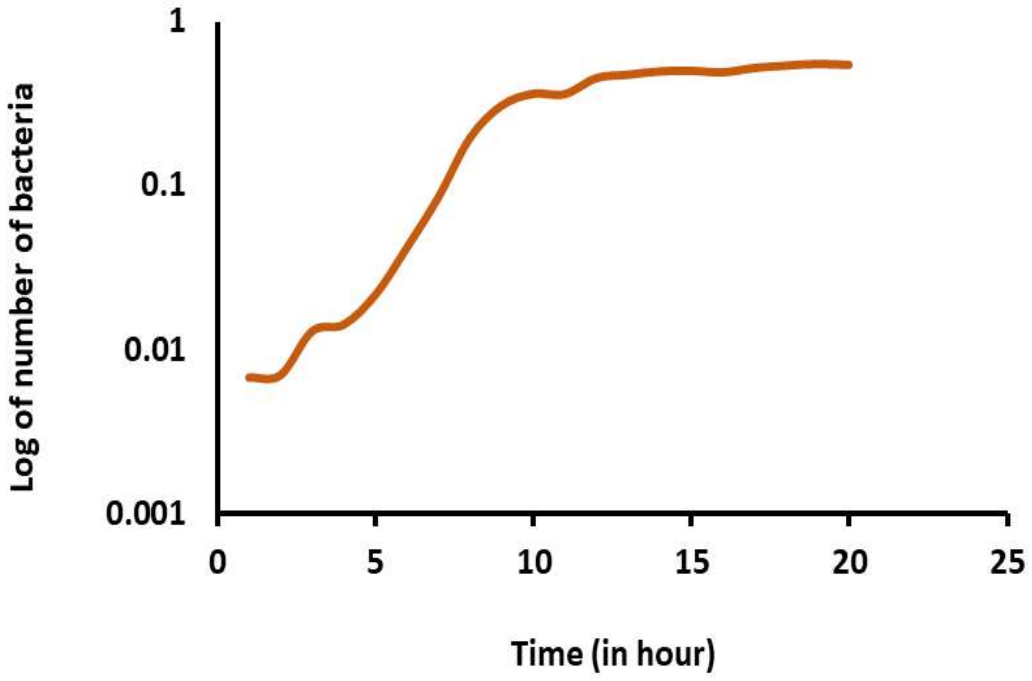

Figure 2.4. Growth curve. Growth pattern of *Lactobacillus rhamnosus* grown at 37 °C for 48 h.

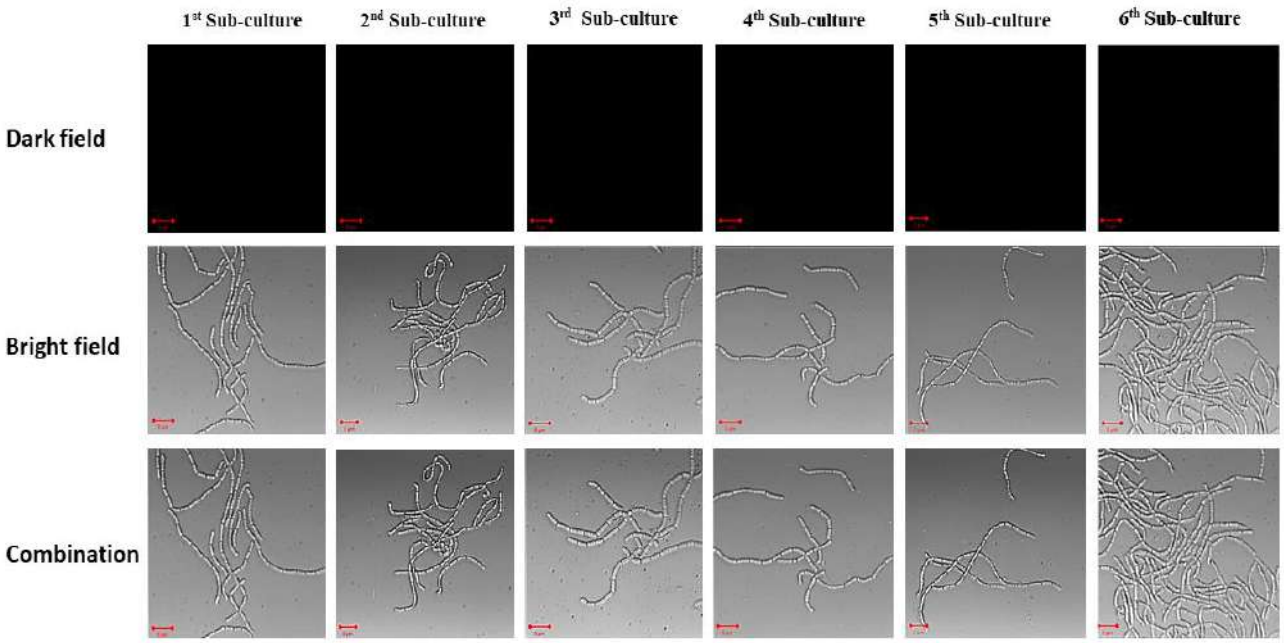

Figure 2.5. Confocal laser scanning microscopy. CLSM images of progeny bacteria grown from 1st to 6th sub-culture of Lac_AuNC as described in the legends.

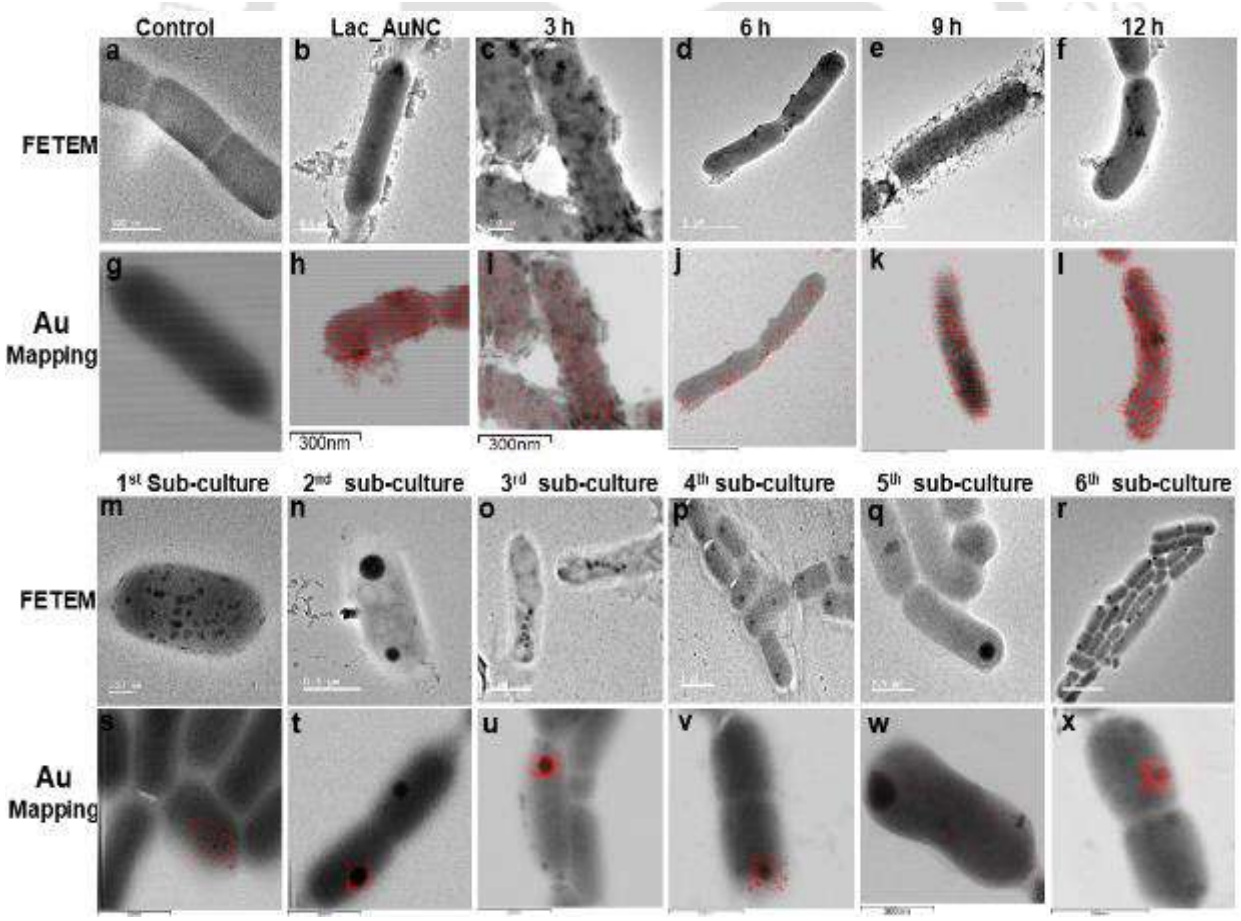

Figure 2.6. TEM images and respective elemental mapping analysis of 'Au' in control *Lactobacillus rhamnosus*, Lac_AuNC and its progenies collected after 3 h, 6 h, 9 h, 12 h and 1st to 6th sub-culture.

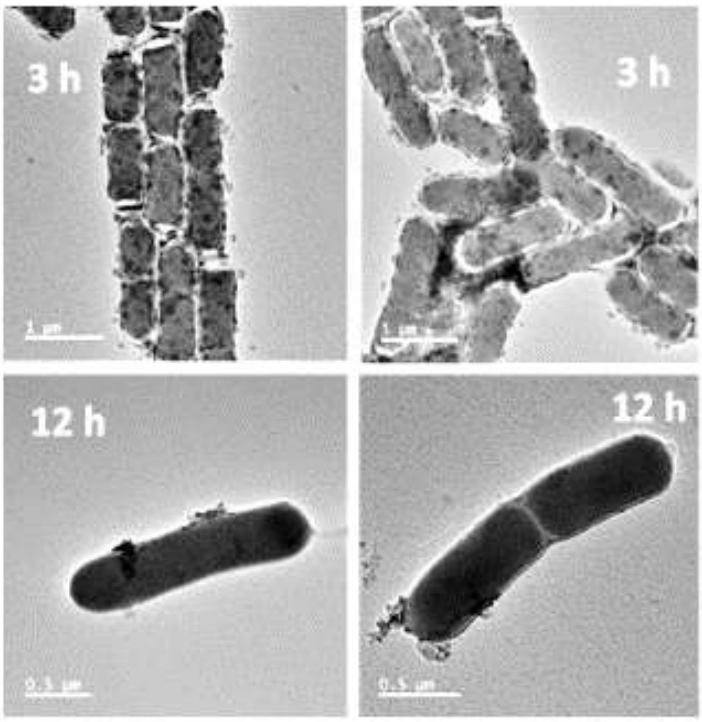

Figure 2.7. FETEM images of progenies of Lac_AuNC collected after 3 h and 12 h of incubation.

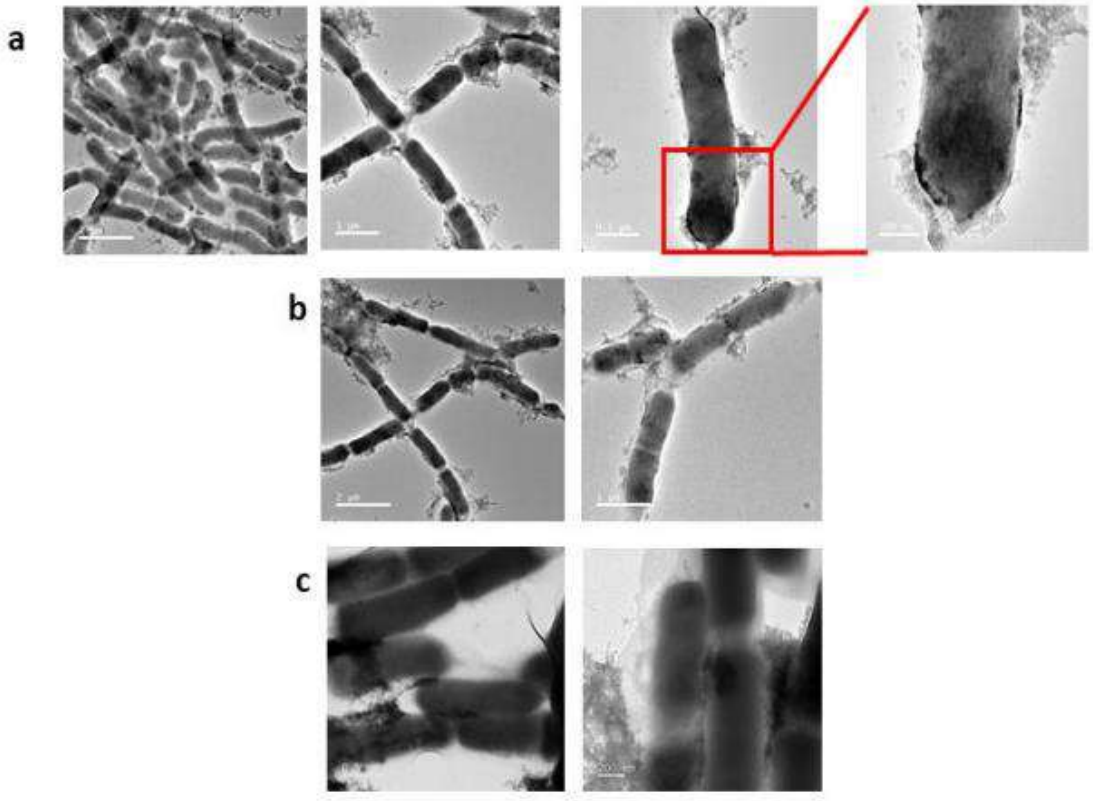

Figure 2.8 (a) FETEM images of Lac_AuNC (taken on same day as Figure 2.4) (b) and (c) FETEM images of Lac_AuNC (taken on different days).

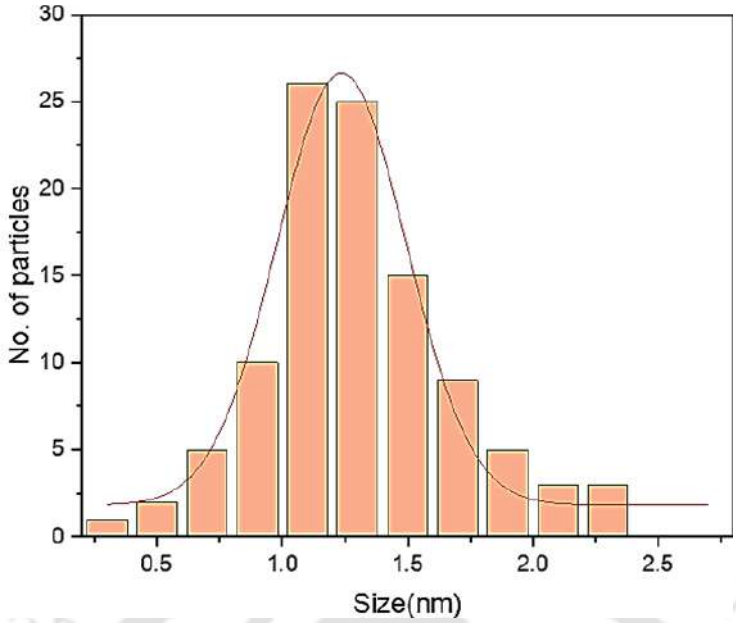

Figure 2.9. Size distribution. Average size of gold nanoclusters formed on *Lactobacillus rhamnosus* (Lac_AuNC; 1.31±0.36 nm). The size distribution calculation was done using several TEM images and involving about 100 particles.

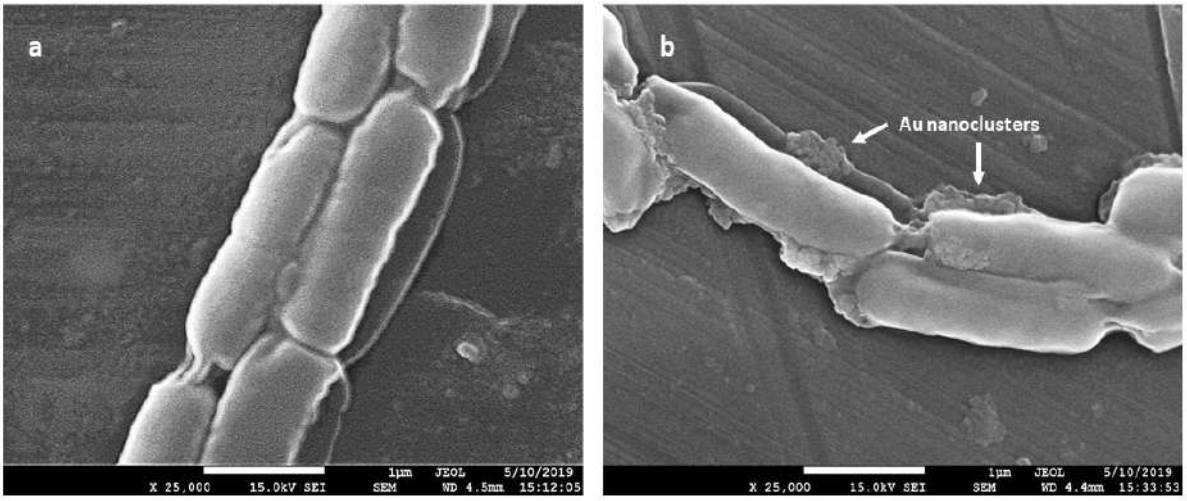

Figure 2.10. Field emission scanning electron microscopy images of (a) control *Lactobacillus rhamnosus* (Lac_AuNC) bacteria and (b) gold nanocluster bearing *Lactobacillus rhamnosus* (Lac_AuNC).

Thus, suggesting the presence of the clusters on the outer cell wall surfaces. An important point in the investigation was to find the viability of Lac_AuNC. This was pursued by first inoculating 1% of these bacteria in fresh medium and then incubating for up to 48 h at 37 °C. The observation of the turbidity of the medium suggested the division of the cells and, thus, the viability of the bacteria containing Au nanoclusters. In order to confirm the results, the broth medium was spread on MRS

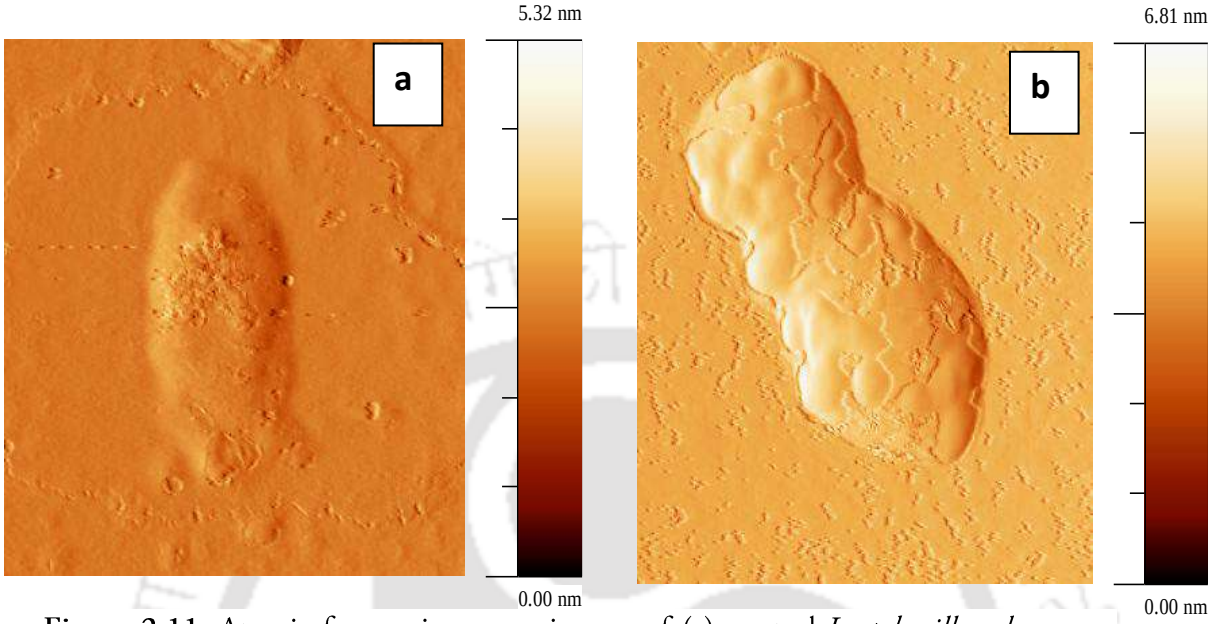

Figure 2.11. Atomic force microscopy images of (a) control *Lactobacillus rhamnosus* (Lac_AuNC) bacteria and (b) gold nanocluster bearing *Lactobacillus rhamnosus* (Lac_AuNC).

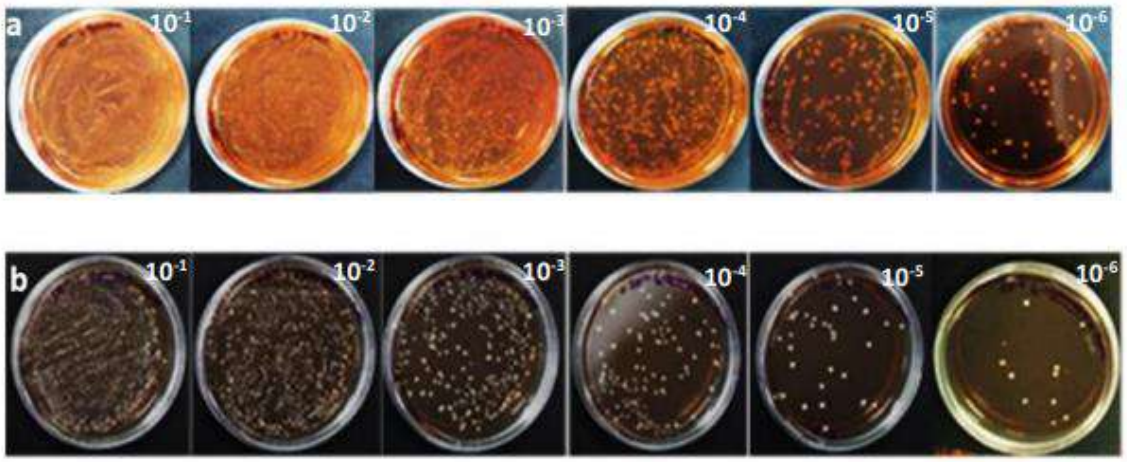

Figure 2.12 Colony forming unit/mL (a) MRS agar plates containing bacterial colonies obtained after plating serial dilutions (as described in the legends) of control *Lactobacillus rhamnosus* (10^9 cfu/mL) and (b) colonies obtained after plating serial dilutions of gold nanocluster bearing *Lactobacillus rhamnosus* (Lac_AuNC; 10^8 cfu/mL).

agar plates and the progeny cell colonies were observed to have grown into 10^8 cfu/mL in 48 h (Figure 2.12). Progenies obtained by reinoculation of Lac_AuNC into six subsequent subcultures indicated the presence of Au in all of them.

However, the number of bacteria with Au in them went down after each subculture. For example, the TEM images in combination with elemental mapping of the first subculture (Figure 2.6m and 2.6s) indicated that the progeny cells consisted of agglomerated Au particles that were present in a few spots on the bacteria. On the other hand, there was also the presence of bacteria without Au. TEM images showed the presence of those nanoparticle-like structures in members of all these subcultured progeny cells (Figure 2.6c-f and 2.6n-r). However, the number of bacteria with Au in them went down after each sub-culture. For example, the TEM images in combination with elemental mapping of the first sub-culture (Figure 2.6m and Figure 2.6s) indicated that the progeny cells consisted of agglomerated Au particles that were present in a few spots (typically one or two spots of agglomerated Au particles on each bacterium) on the bacteria.

However, the number and distribution pattern were different and the number was reduced as passing down. The average size of the aggregates of all the sub-cultures ranged between 95.23±11.57 μm to 220.60±89.99 μm; there was no consistent change in size observed down the generations. The images of the bacteria could not be taken at higher resolutions as the samples wee biological and tended to burn rapidly. The resolution below 10 nm was difficult to achieve. The EDX analysis (Figure 2.13 to Figure 2.19) and elemental mapping analysis revealed the presence of 'Au' on these particles (Figure 2.6i-l and t-x)

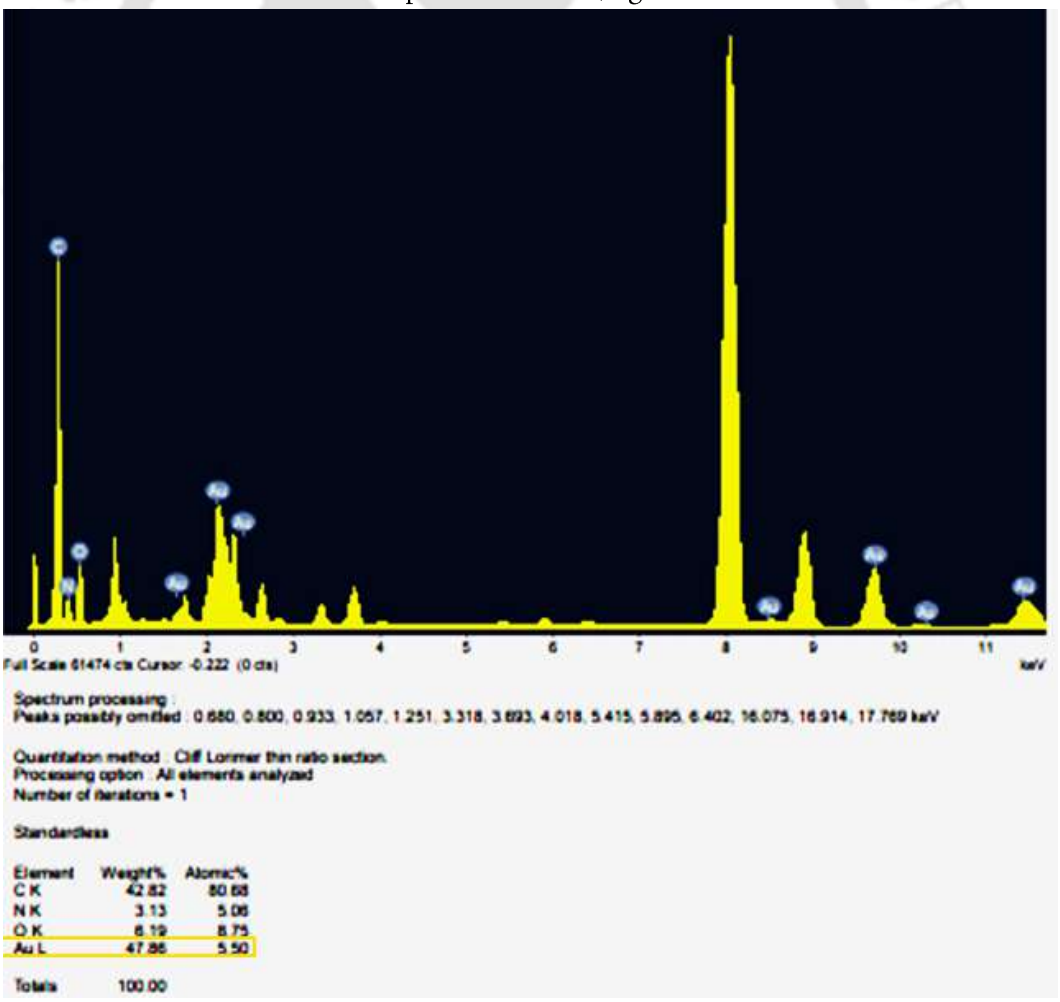

Figure 2.13. Energy dispersive X-ray analysis. Results of EDX analysis of Lac_AuNC.

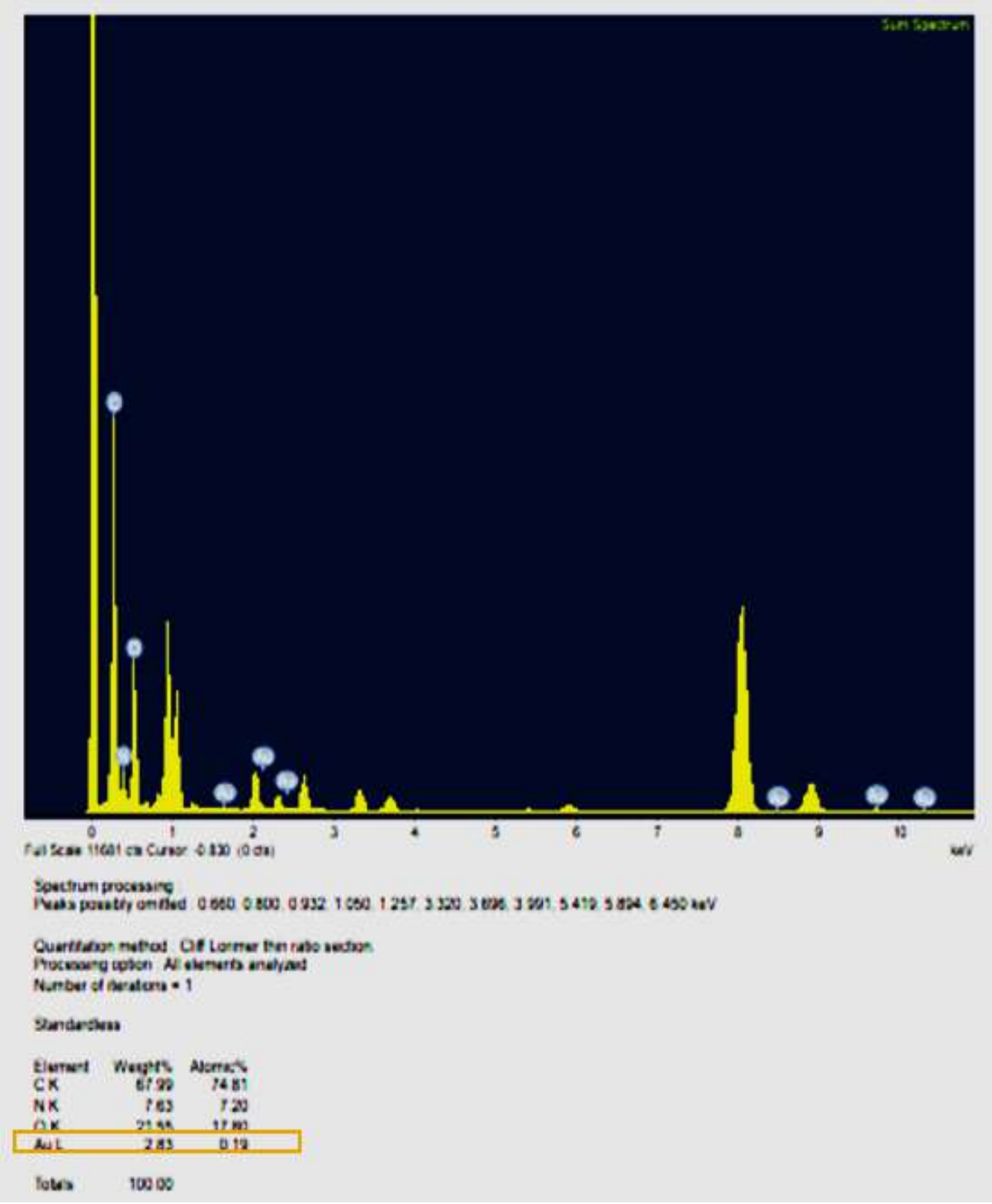

Figure 2.14. Energy dispersive X-ray analysis. Results of EDX analysis of progeny bacteria grown after 1st sub-culture of Lac_AuNC.

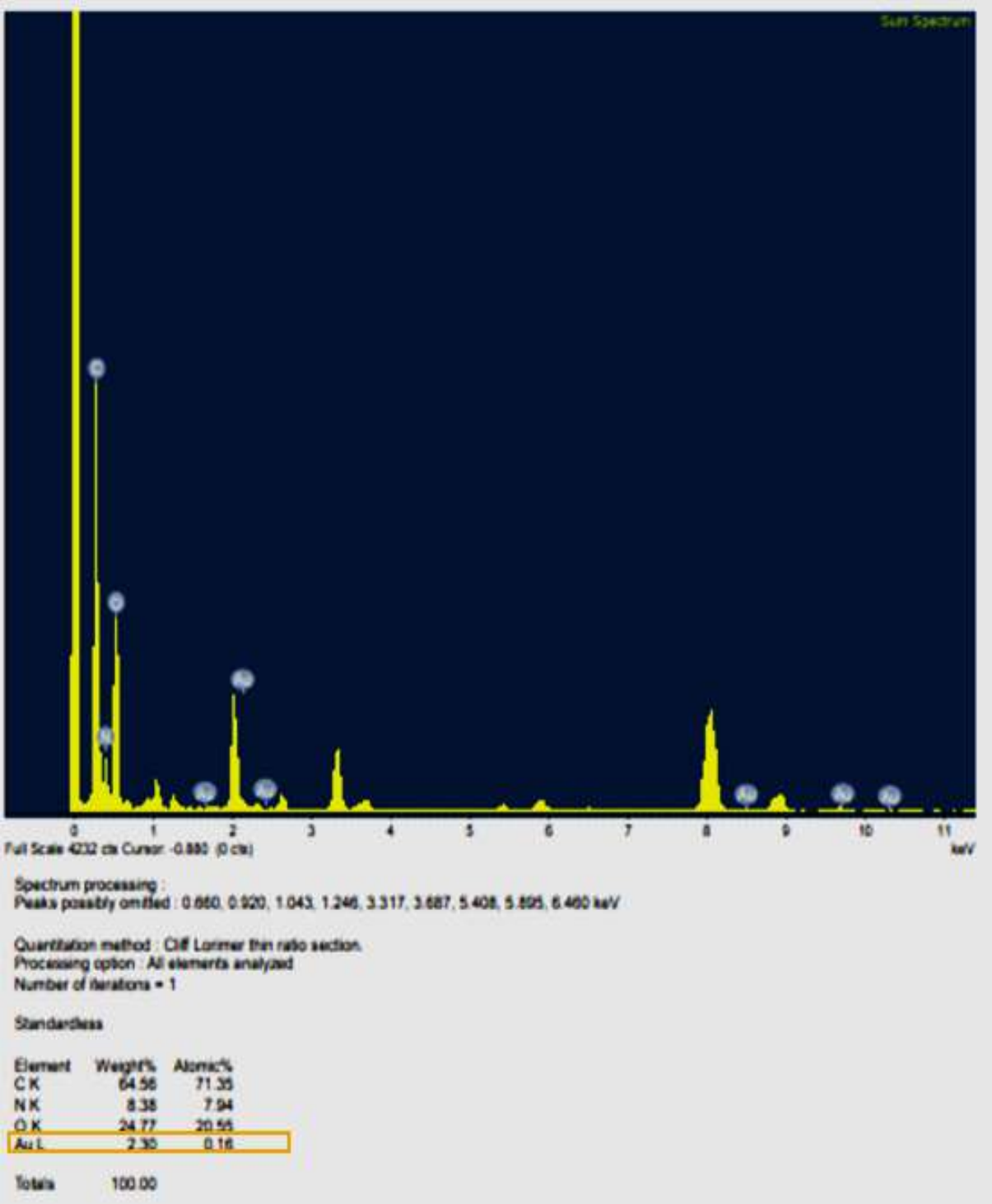

Figure 2.15. Energy dispersive X-ray analysis. Results of EDX analysis of progeny bacteria grown after 2nd sub-culture of Lac_AuNC.

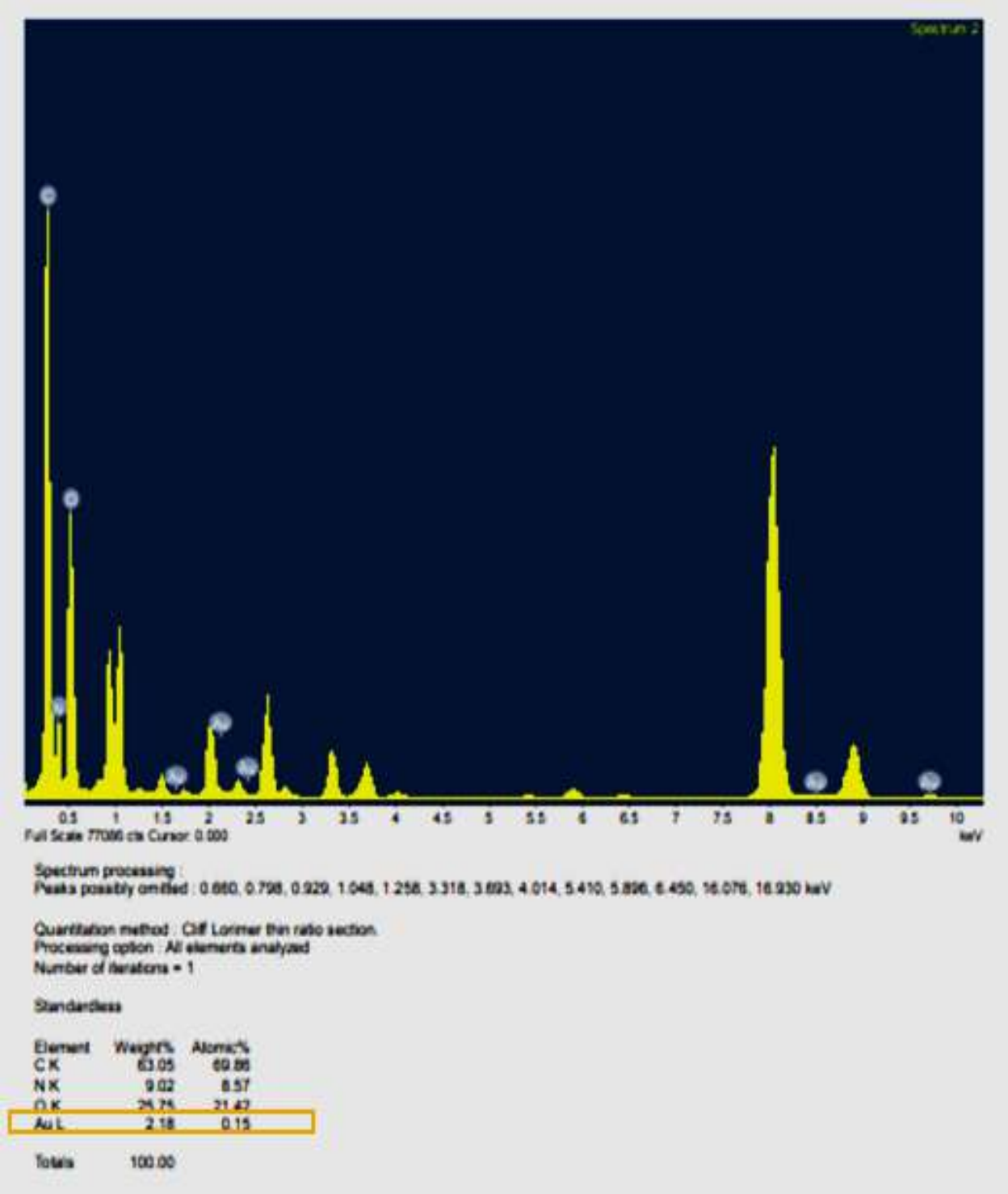

Figure 2.16. Energy dispersive X-ray analysis. Results of EDX analysis of progeny bacteria grown after 3rd sub-culture of Lac_AuNC.

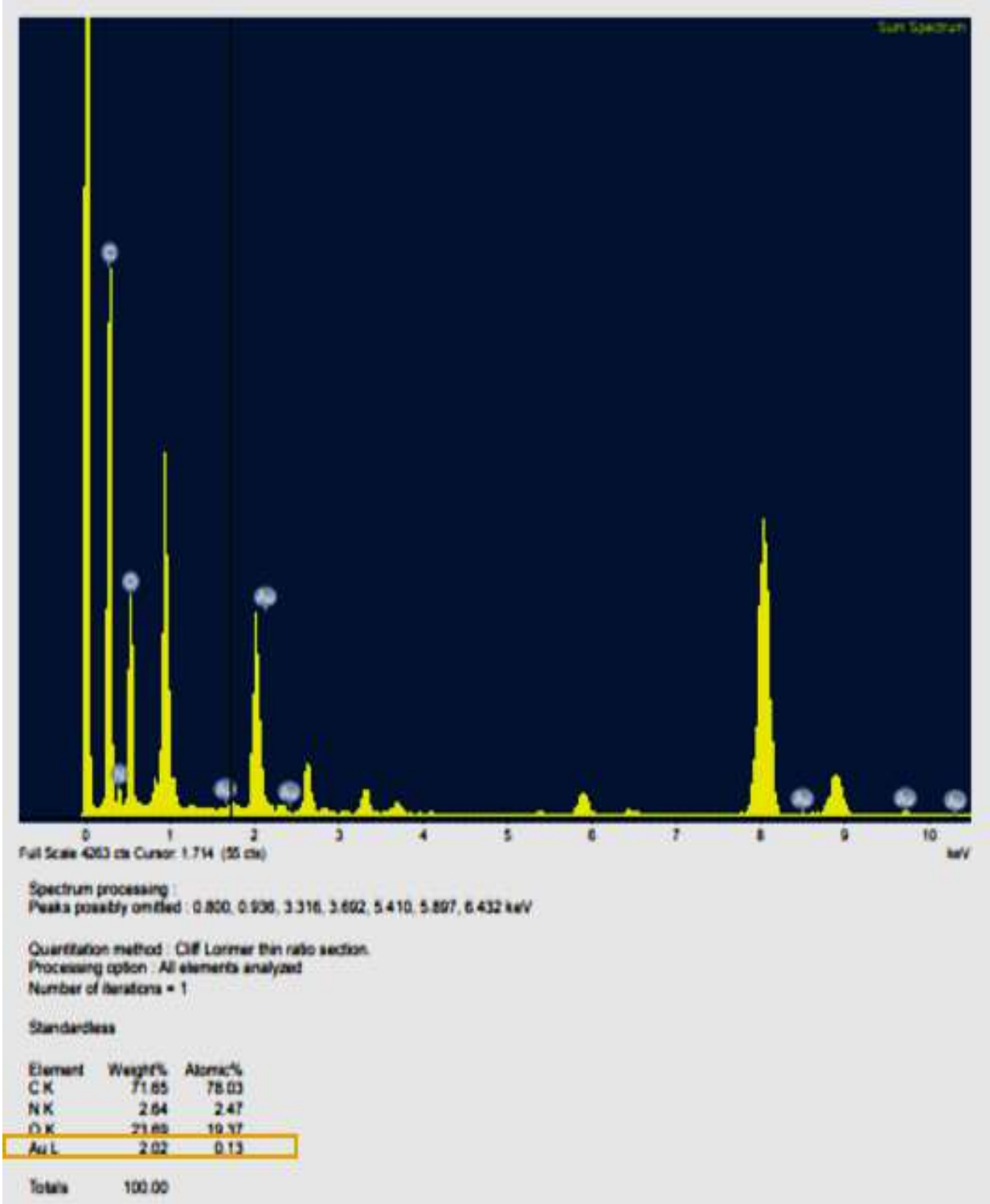

Figure 2.17. Energy dispersive X-ray analysis. Results of EDX analysis of progeny bacteria grown after 4th sub-culture of Lac_AuNC.

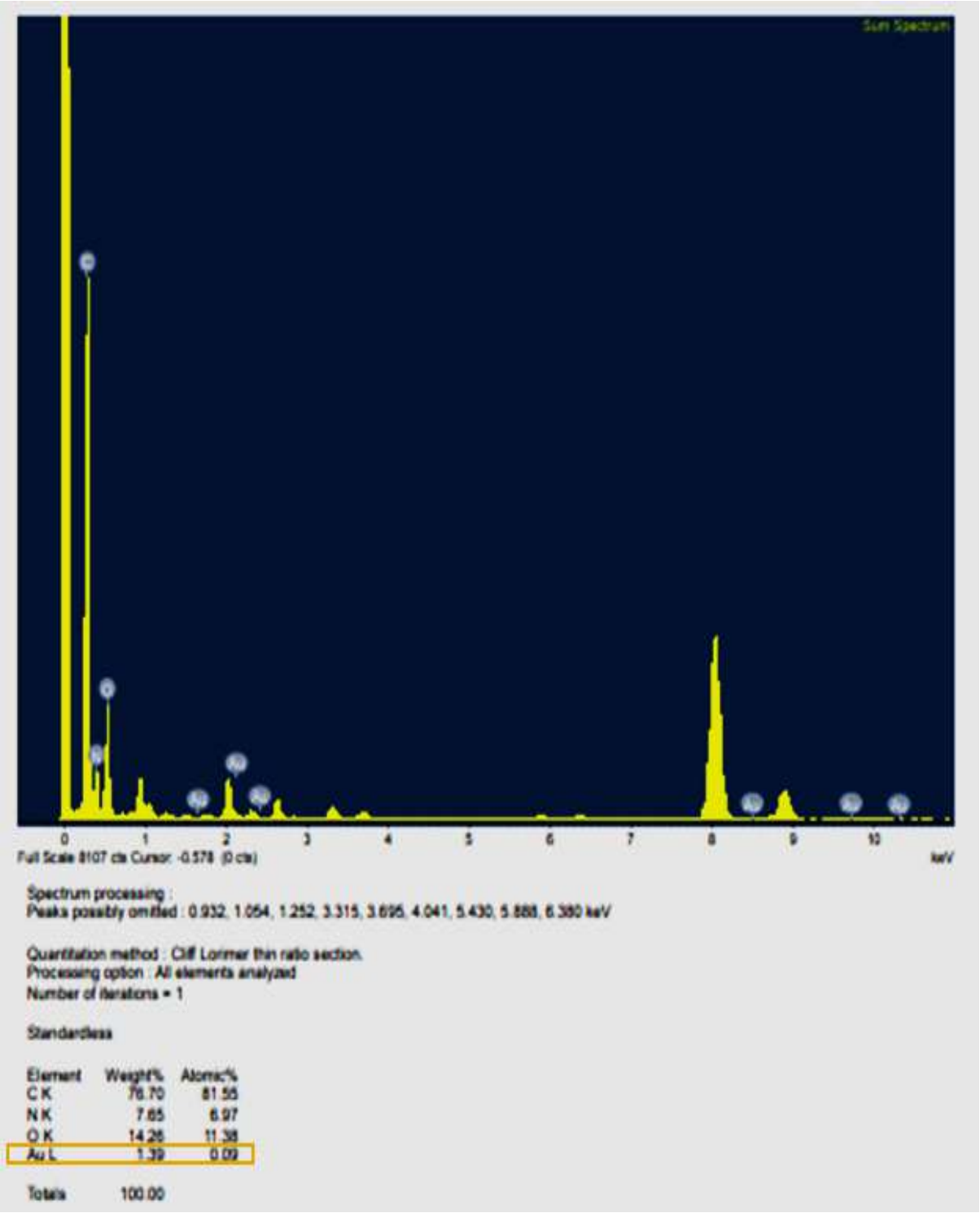

Figure 2.18. Energy dispersive X-ray analysis. Results of EDX analysis of progeny bacteria grown after 5thsub-culture of Lac_AuNC.

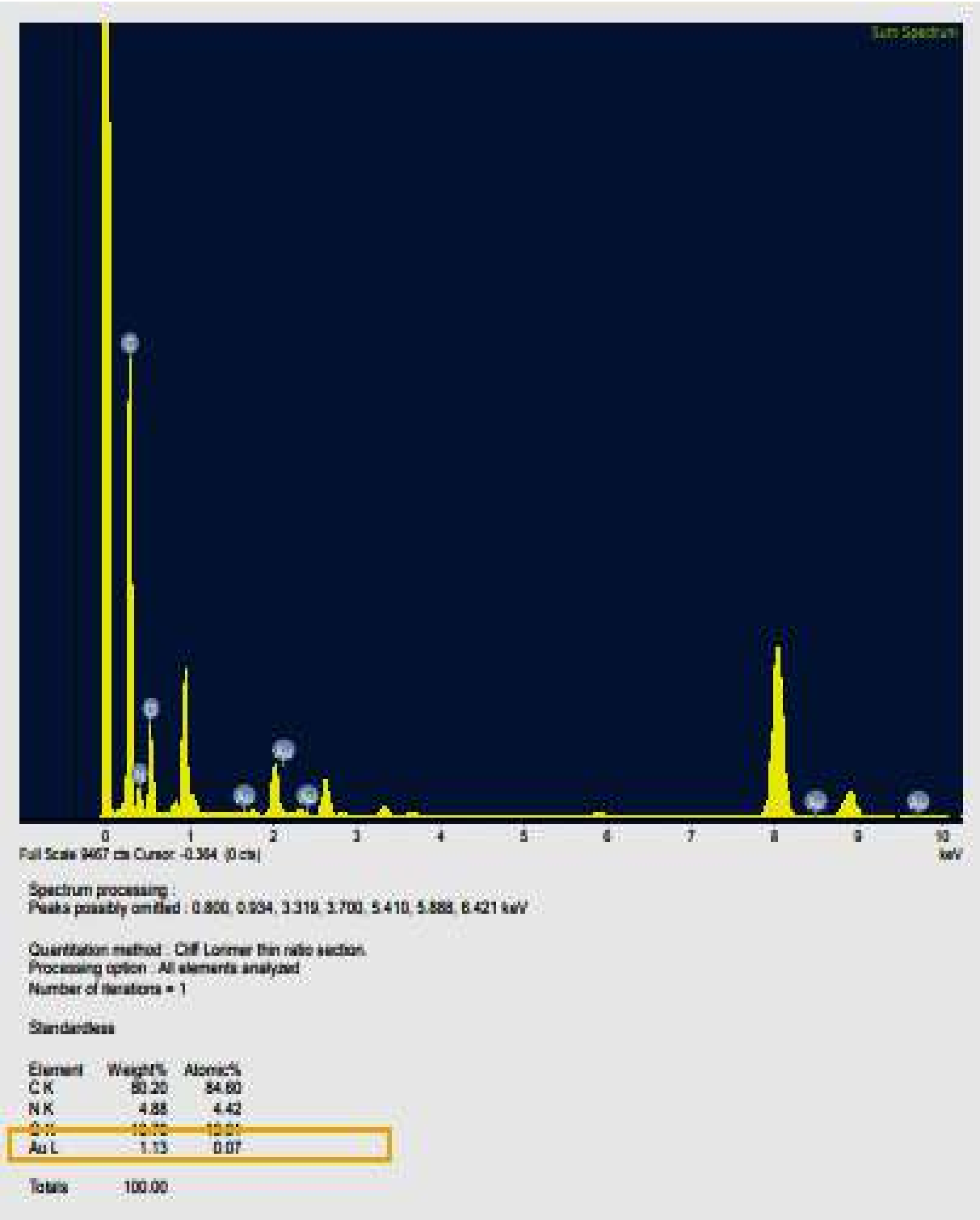

Figure 2.19. Energy Dispersive X-ray analysis. Results of EDX analysis of progeny bacteria grown after 6thsub-culture of Lac_AuNC.

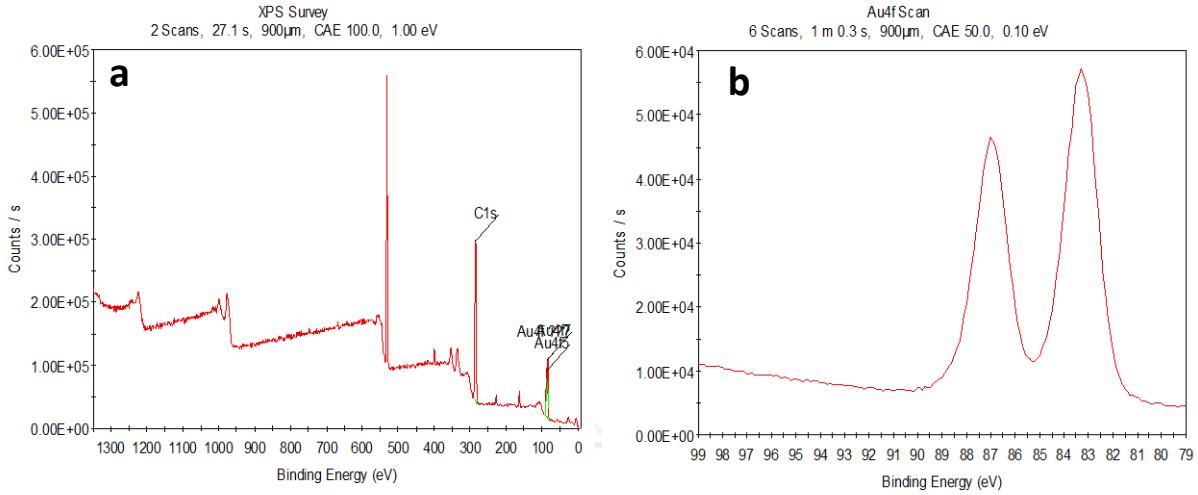

Figure 2.20. X-ray photoelectron spectroscopy analysis. (a) XPS survey spectrum and (b) Au4f scan part of the spectrum of gold nanocluster bearing *Lactobacillus rhamnosus*(Lac_AuNC).

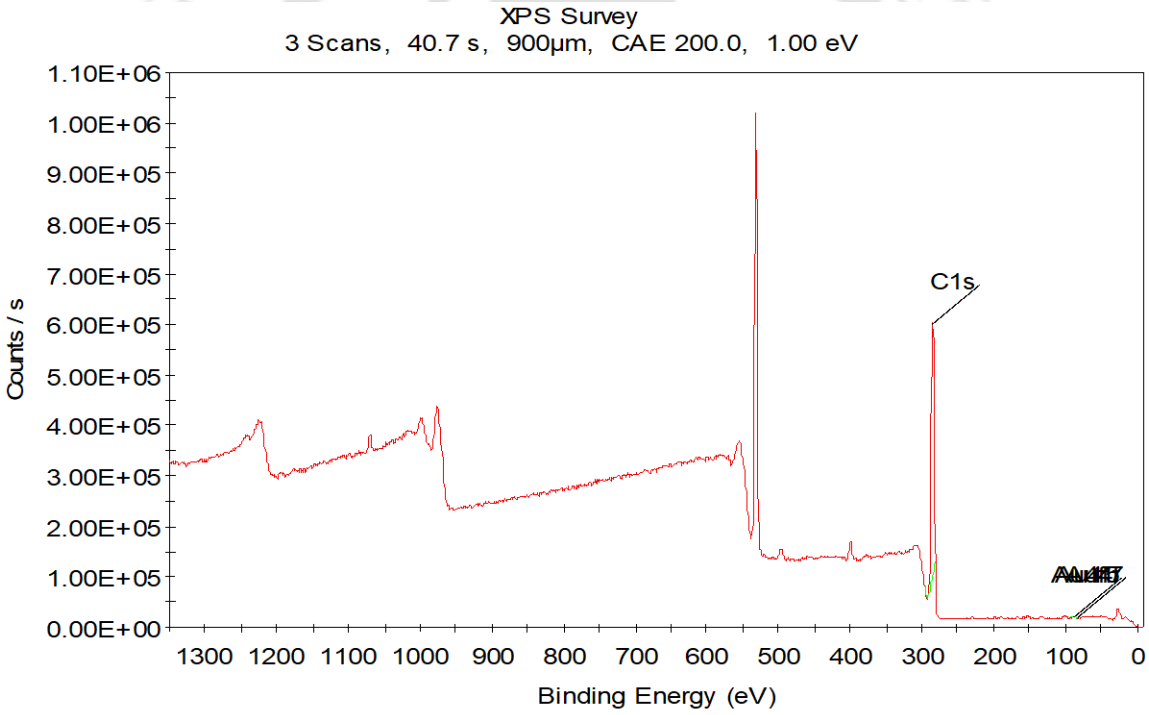

Figure 2.21. X-ray photoelectron spectroscopy analysis. XPS survey spectrum of progeny bacteria grown after 1st sub-culture of Lac_AuNC.

But for further confirmation the progeny cells of all sub-cultures along with the control bacteria were lyophilized and were subjected to further analysis by XPS. The result confirmed the presence of Au4f5 (Figure 2.2d and Figure 2.20) in the lyophilized cultures. However, the presence of Au in the 3rd sub-culture to 6th sub-cultures were too low to be detected (Figure 2.20 to Figure 2.26). UV-vis spectrum of the cultures (Figure 2.3b) representing subsequent progenies did not exhibit any peak that is characteristic of localized surface plasmon resonance of Au nanoparticles, thus discounting the formation of larger agglomerated particles from the clusters.

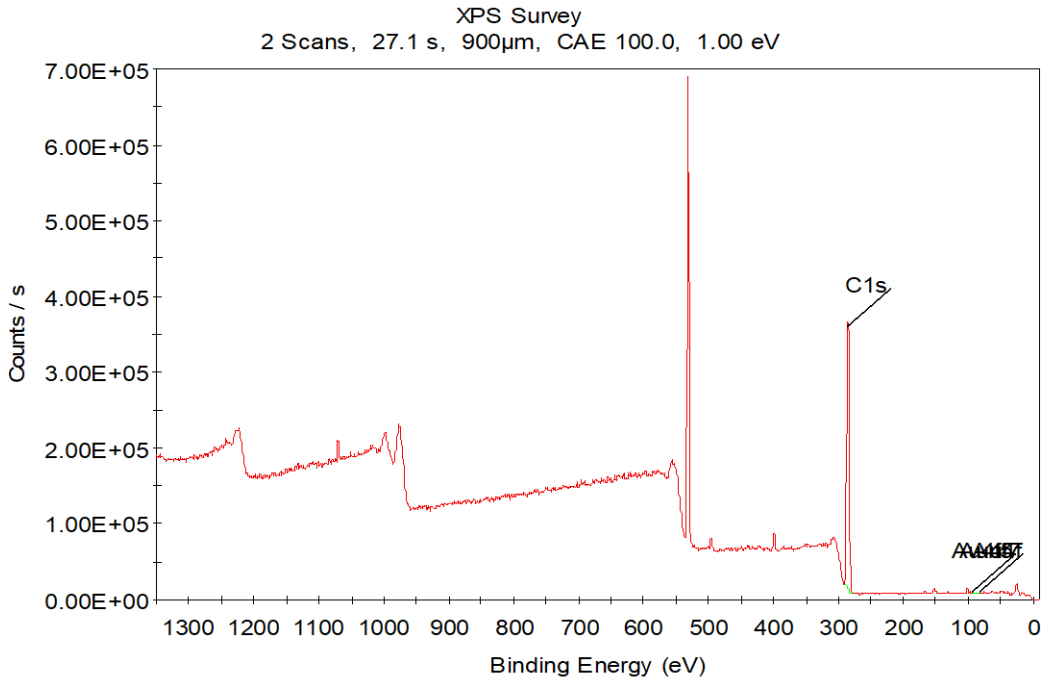

Figure 2.22. X-ray photoelectron spectroscopy analysis. XPS survey spectrum of progeny bacteria grown after 2nd sub-culture of Lac_AuNC.

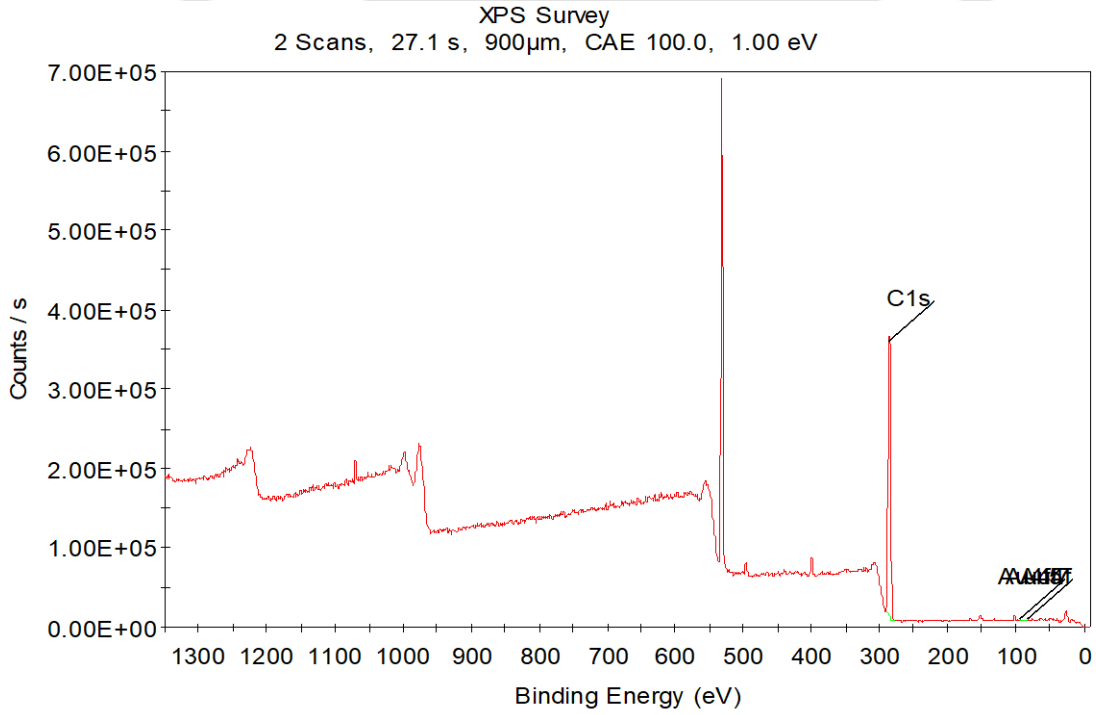

Figure 2.23. X-ray photoelectron spectroscopy analysis. XPS survey spectrum of progeny bacteria grown after 3rd sub-culture of Lac_AuNC.

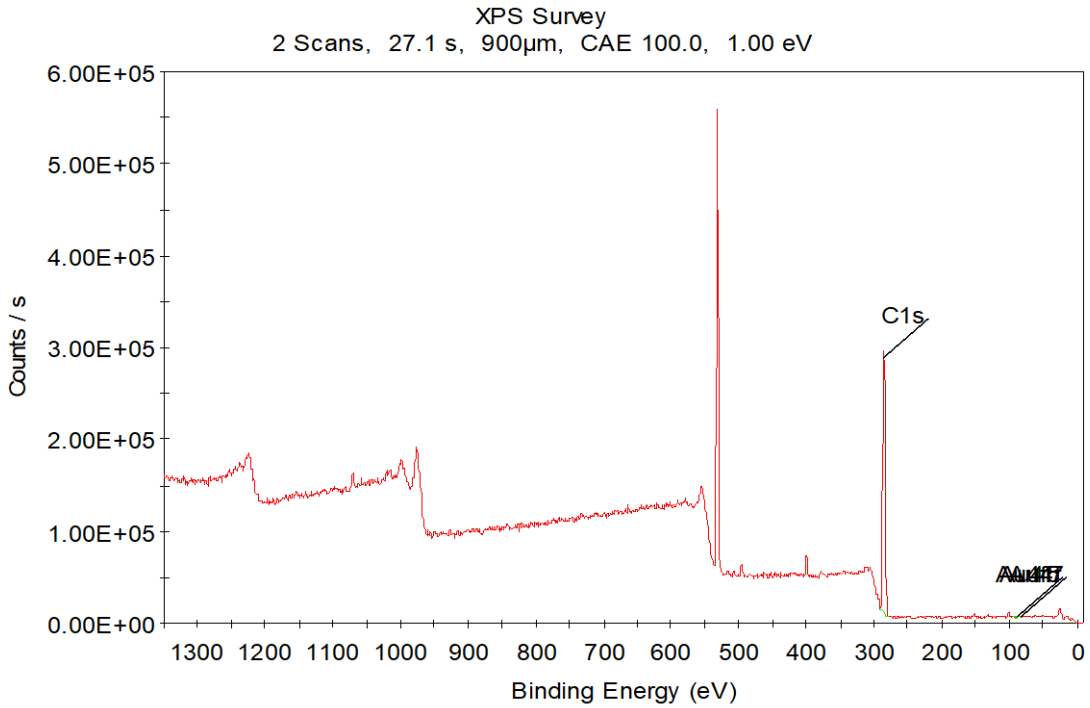

Figure 2.24. X-ray photoelectron spectroscopy analysis. XPS survey spectrum of progeny bacteria grown after 4th sub-culture of Lac_AuNC.

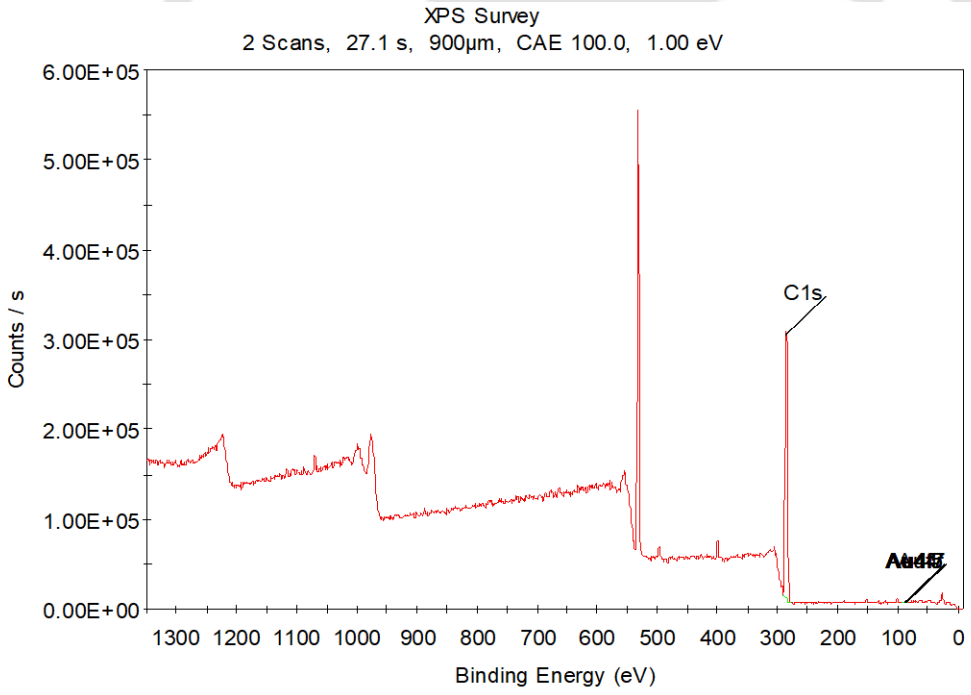

Figure 2.25. X-ray photoelectron spectroscopy analysis. XPS survey spectrum of progeny bacteria grown after 5th sub-culture of Lac_AuNC.

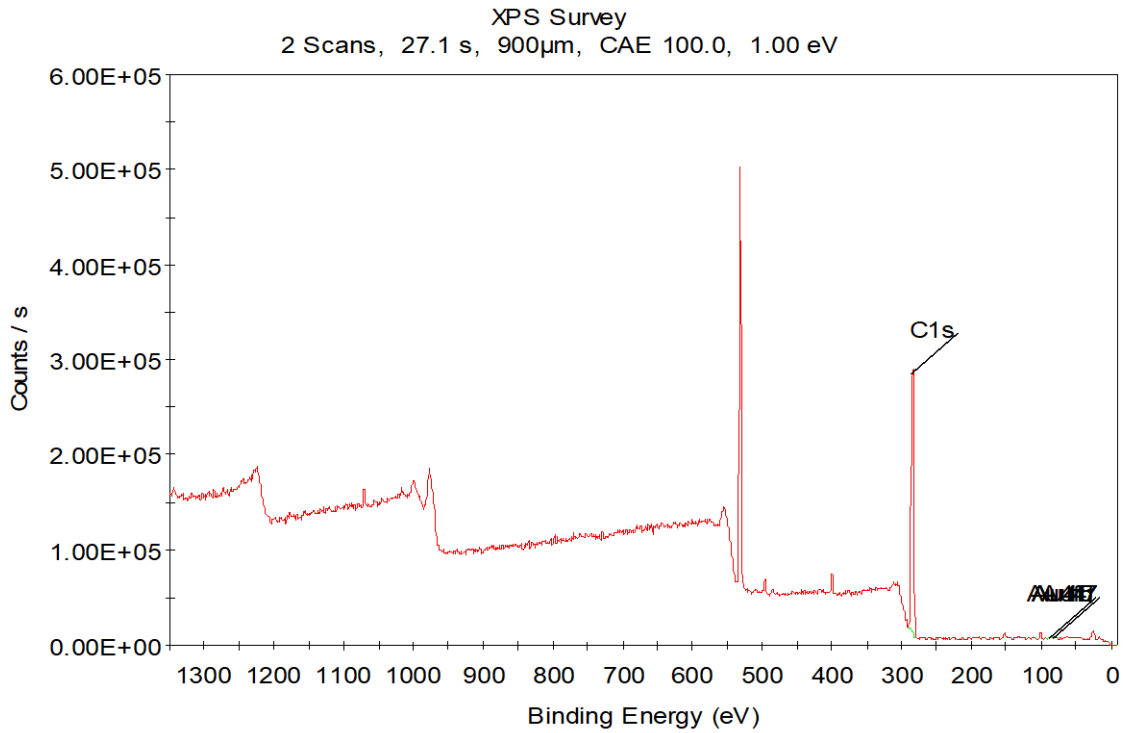

Figure 2.26. X-ray photoelectron spectroscopy analysis. XPS survey spectrum of progeny bacteria grown after 6th sub-culture of Lac_AuNC.

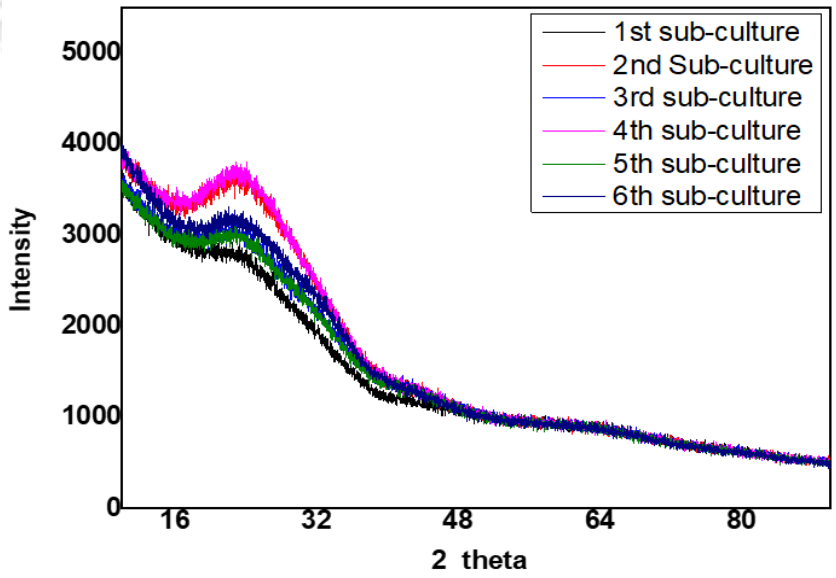

Figure 2.27. X-ray diffraction analysis. X-ray diffraction pattern of progeny bacteria grown from 1st to 6th sub-culture of Lac_AuNC as described in the legends.

Similarly, X-ray diffraction and selected area electron diffraction analyses did not indicate the formation of crystalline Au nanoparticles (Figure 2.27, Figure 2.28 and Figure 2.29). Overall, the Au nanoclusters formed on the bacteria were passed on the next generations as agglomerated particles without being converted into plasmonic Au nanoparticles.

That the clusters were passed down the generations and were not agglomerated might reflect the membrane remodeling of the bacteria in which a certain percentage of the original cell wall was passed down the next generation along with the clusters. An important aspect of the investigating passage of nanoclusters is to understand the effect of Au nanoclusters on genomic DNA and proteins across generations of bacteria. This was pursued by isolating the genomic DNA[23] of the original Au nanocluster studded bacteria and of all six sub-cultures mentioned above and control bacteria. The agarose gel electrophoresis results (Figure 2.30) of the isolated DNA of all generations did not indicate any qualitative changes that had occurred at the genomic level Further, the whole protein was also isolated from all of those cultures and the SDS-PAGE (Figure 2.31) revealed that there had been no qualitative change to the protein profiles of any of these cells of any generation. Thus, the results indicated that the synthesis of Au nanoclusters on the bacteria and subsequent reproduction for six generations did not alter the quality of the genome of the bacteria. It could be that the Au nanoclusters were embedded on the outer cell walls of bacteria and thus they did not affect the genome.

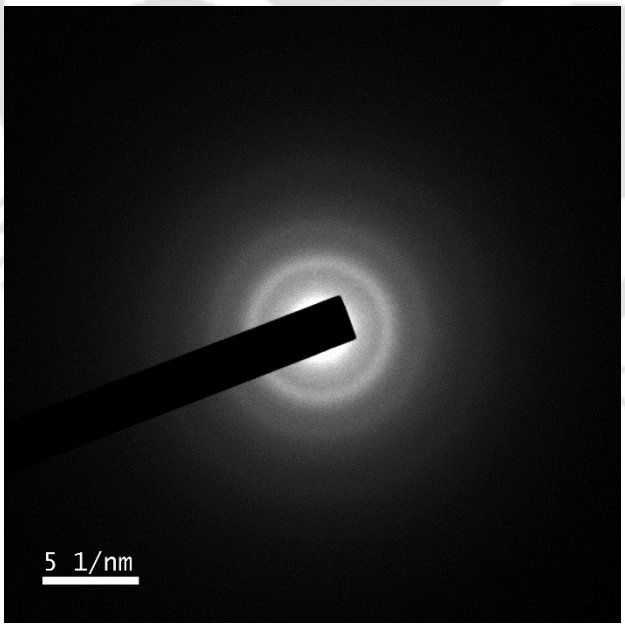

Figure 2.28. Selected Area Electron Diffraction analysis. SAED pattern of Lac_AuNC.

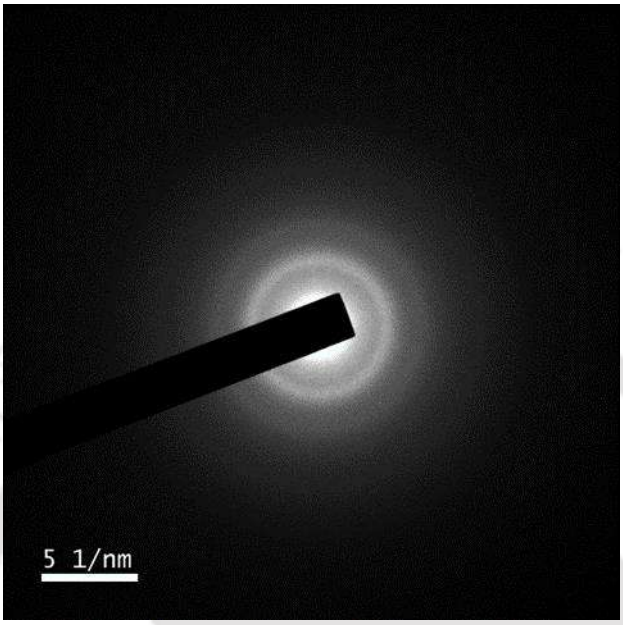

Figure 2.29. Selected Area Electron Diffraction analysis. SAED pattern of 1st sub-culture progeny of Lac_AuNC.

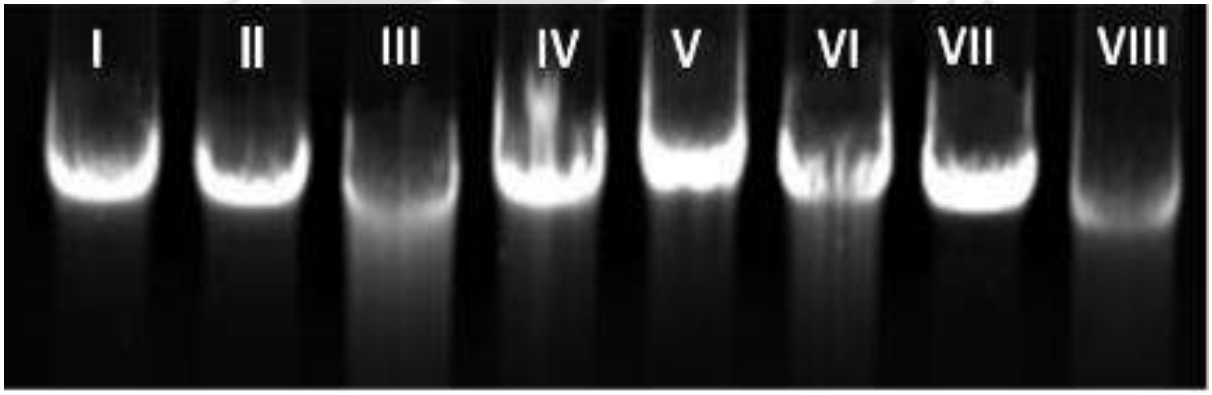

Figure 2.30. Total DNA isolation band patterns of(I) Lac_AuNC(II) Control *L.rhamnosus,* (III)1st sub-culture, (IV) 2ndsub-culture, (V) 3rdsub-culture, (VI) 4th sub-culture, (VII)'5th sub-culture(VIII)6th sub-culture.

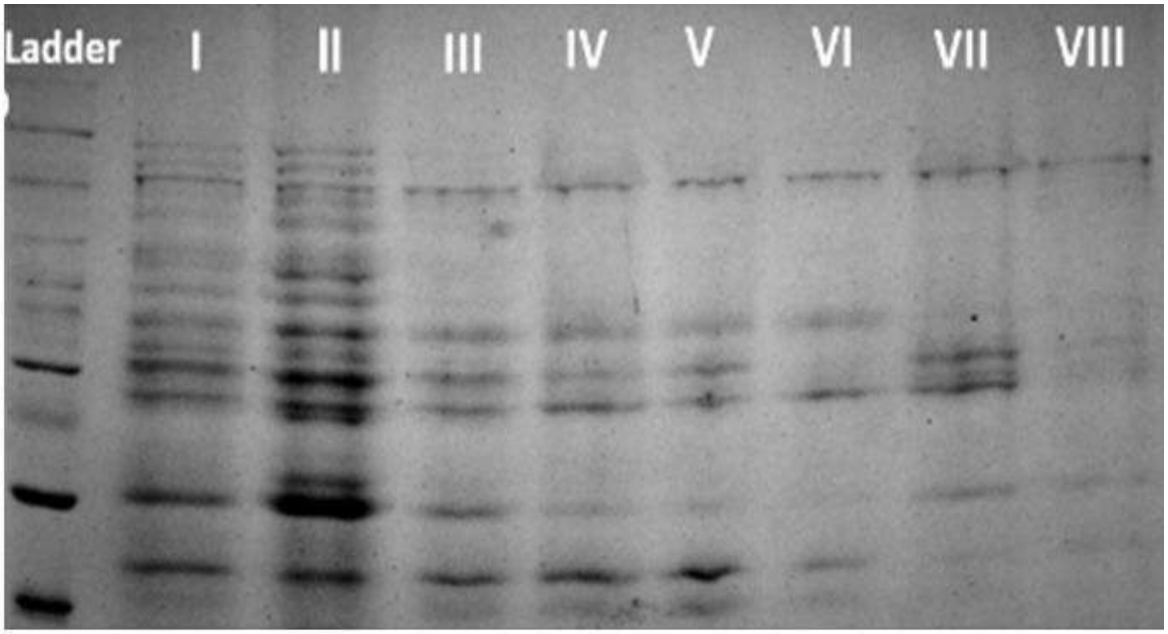

Figure 2.31. Total protein isolation bands of (I)Lac_AuNC (II)Control *L.rhamnosus* (III)1st sub-culture (IV)2nd sub-culture(V)3rd sub-culture(VI)4th sub-culture (VII)'5th sub-culture(VIII)6th sub-culture.

The bacterial cell wall is a reservoir of peptidoglycan and techoic acid, in addition to the presence of constituent proteins. Thus when $AuCl_4^-$ and MPA are added to the bacteria in absence of the medium, the salt is reduced to Au(0). The Au nanoclusters so formed on the surface of the bacteria were possibly stabilized by the carboxylates and thiol groups present on the outer walls and MPA. That the Au nanoclusters were formed and stabilized on the bacterial cell walls was supported by spectroscopic and microscopic analyses mentioned before. Moreover, the bacteria were alive and viable even after the multistep process of gold nanocluster synthesis.The as-synthesized Au nanoclusters on the bacteria were luminescent and spread over the cell wall surface. On the other hand, the nanoclusters were aggregated into larger forms in the next six subcultures and they were devoid of luminescence. Even though they were aggregated particles, there was no signature (such as the presence of localized surface plasmon resonance band) of the formation of Au nanoparticles. Thus, it may be argued that during cell divisions, remodelling of cell walls led to the formation of such structures in the progeny cells. It is known that there is a peptidoglycan turnover of about 25-50% per generation, suggesting the persistence of cell wall components of the parent generation during cell division. The current findings support the idea that some of the cell wall components of the parent generation - that had Au nanoclusters on them - were passed on to the subsequent generation as a part of cell wall remodelling. The different sizes and sites of these structures could be attributed to the membrane remodelling process involving cell elongation, cell division or stress management. Since in each generation newly formed peptidoglycans are also synthesised and replaced with the older once in a make-before-break fashion. thus, there were certain number of bacteria in all the sub-cultures that did not receive enough amount of those nanoclusters and this is why some of them did not have any of those bigger agglomerations while others had few to many over their surfaces at different sites. The reduction in photoluminescence intensity of subsequent generations could be attributed to the decrease in number of remnant nanoclusters while going

down the generation. Thus, the synthesised Au nanoclusters were present on the surface of the parent generation of bacteria, which eventually kept on being passed on to generation after generation via the processes of membrane remodelling. The presence, size, shape and distribution on the cell walls of subsequent generations were dependent on the initial number of nanocluster containing bacteria in the previous generation and the process of the bacterial elongation and cell division.

2.4 Conclusions

In conclusion, a method of generation of photoluminescent Au nanoclusters on outer cell walls of living bacteria was devel. The nanoclusters were passed on the subsequent generations of bacteria as agglomerated non-luminescent larger Au-containing particles on the cell surface. The results also indicated that during cell wall remodelling the peptidoglycans that are transferred to the next generations may help carry the nanoclusters. Cell wall elongation and division leads to the formation of larger particles in subsequent generation and in that process the luminescence is also lost without the formation of plasmonic Au nanoparticles. The current study provides a new path to understanding of passing of nanoscale particles in bacterial generations that are expected to contribute to their use as in drug delivery. This study may also provoke new studies for better understanding of the fate of nanoparticles in the living environment.

2.5 References

(1) Rajamani, S.; Kuszpit, K.; Scarff, J. M.; Lundh, L.; Khan, M.; Brown, J.; Stafford, R.; Cazares, L. H.; Panchal, R. G.; Bocan, T. Bioengineering of Bacterial Pathogens for Noninvasive Imaging and in Vivo Evaluation of Therapeutics. *Sci. Rep.* **2018**, *8* (1), 1–11.

(2) Liang, K.; Liu, Q.; Li, P.; Han, Y.; Bian, X.; Tang, Y.; Kong, Q. Endostatin Gene Therapy Delivered by Attenuated Salmonella Typhimurium in Murine Tumor Models. *Cancer Gene Ther.* **2018**, No. iv.

(3) Pálffy, R.; Gardlík, R.; Hodosy, J.; Behuliak, M.; Reško, P.; Radvánský, J.; Celec, P. Bacteria in Gene Therapy: Bactofection versus Alternative Gene Therapy. *Gene Ther.* **2006**, *13* (2), 101–105.

(4) Hu, Q.; Wu, M.; Fang, C.; Cheng, C.; Zhao, M.; Fang, W.; Chu, P. K.; Ping, Y.; Tang, G. Engineering Nanoparticle-Coated Bacteria as Oral DNA Vaccines for Cancer Immunotherapy. *Nano Lett.* **2015**, *15* (4), 2732–2739.

(5) Luo, C. H.; Huang, C. T.; Su, C. H.; Yeh, C. S. Bacteria-Mediated Hypoxia-Specific Delivery of Nanoparticles for Tumors Imaging and Therapy. *Nano Lett.* **2016**, *16* (6), 3493–3499.

(6) Akin, D.; Sturgis, J.; Ragheb, K.; Sherman, D.; Burkholder, K.; Robinson, J. P.; Bhunia, A. K.; Mohammed, S.; Bashir, R. Bacteria-Mediated Delivery of Nanoparticles and Cargo into Cells. *Nat. Nanotechnol.* **2007**, *2* (7), 441–449.

(7) Fan, J. X.; Li, Z. H.; Liu, X. H.; Zheng, D. W.; Chen, Y.; Zhang, X. Z. Bacteria-Mediated Tumor Therapy Utilizing Photothermally-Controlled TNF-α Expression via Oral Administration. *Nano Lett.* **2018**, *18* (4), 2373–2380.

(8) Song, J.; Zhang, Y.; Zhang, C.; Du, X.; Guo, Z.; Kuang, Y.; Wang, Y.; Wu, P.; Zou, K.; Zou, L.; Lv, J.; Wang, Q. A Microfluidic Device for Studying Chemotaxis Mechanism of Bacterial Cancer Targeting. *Sci. Rep.* **2018**, *8* (1), 1–9.

(9) Zhou, S.; Gravekamp, C.; Bermudes, D.; Liu, K. Tumour-Targeting Bacteria Engineered to Fight Cancer. *Nat. Rev. Cancer.* **2018**, *18* (12), 727–743.

(10) Larsen, M. D. B.; Griesenbach, U.; Goussard, S.; Gruenert, D. C.; Geddes, D. M.; Scheule, R. K.; Cheng, S. H.; Courvalin, P.; Grillot-Courvalin, C.; Alton, E. W. F. W. Bactofection of Lung Epithelial Cells in Vitro and in Vivo Using a Genetically Modified Escherichia Coli. *Gene Ther.* **2008**, *15* (6), 434–442.

(11) Zhu, H.; Li, Z.; Mao, S.; Ma, B.; Zhou, S.; Deng, L.; Liu, T.; Cui, D.; Zhao, Y.; He, J.; Yi, C.; Huang, Y. Antitumor Effect of SFlt-1 Gene Therapy System Mediated by Bifidobacterium Infantis on Lewis Lung Cancer in Mice. *Cancer Gene Ther.* **2011**, *18* (12), 884–896.

(12) Wong, S.; Slavcev, R. A. Treating Cancer with Infection: A Review on Bacterial Cancer Therapy. *Lett. Appl. Microbiol.* **2015**, *61* (2), 107–112.

(13) Vassaux, G.; Nitcheu, J.; Jezzard, S.; Lemoine, N. R. Bacterial Gene Therapy Strategies. *J. Pathol.* **2006**, *208* (2), 290–298.

(14) Roy, S.; Trinchieri, G. Microbiota: A Key Orchestrator of Cancer Therapy. *Nat. Rev. Cancer.* **2017**, *17* (5), 271–285.

(15) Iida, N.; Dzutsev, A.; Stewart, C. A.; Smith, L.; Bouladoux, N.; Weingarten, R. A.; Molina, D. A.; Salcedo, R.; Back, T.; Cramer, S.; Dai, R. M.; Kiu, H.; Cardone, M.; Naik, S.; Patri, A. K.; Wang, E.; Marincola, F. M.; Frank, K. M.; Belkaid, Y.; Trinchieri, G.; Goldszmid, R. S. Commensal Bacteria Control Cancer Response to Therapy by Modulating the Tumor Microenvironment. *Science.* **2013**, *342* (6161), 967–970.

(16) Gamallat, Y.; Meyiah, A.; Kuugbee, E. D.; Hago, A. M.; Chiwala, G.; Awadasseid, A.; Bamba, D.; Zhang, X.; Shang, X.; Luo, F.; Xin, Y. *Lactobacillus Rhamnosus* Induced Epithelial Cell Apoptosis, Ameliorates Inflammation and Prevents Colon Cancer Development in an Animal Model. *Biomed. Pharmacother.* **2016**, *83*, 536–541.

(17) Fang, J.; Liao, L.; Yin, H.; Nakamura, H.; Shin, T.; Maeda, H. Enhanced Bacterial Tumor Delivery by Modulating the EPR Effect and Therapeutic Potential of Lactobacillus Casei. *J. Pharm. Sci.* **2014**, *103* (10), 3235–3243.

(18) Ryan, R. M.; Green, J.; Lewis, C. E. Use of Bacteria in Anti-Cancer Therapies. *BioEssays* **2006**, *28* (1), 84–94.

(19) Park, J. T.; Uehara, T. How Bacteria Consume Their Own Exoskeletons (Turnover and Recycling of Cell Wall Peptidoglycan)†. **2008**, *72* (2), 211–227.

(20) Bacteria's Different Ways to Recycle Their Own Cell Wall _ Elsevier Enhanced Reader.Pdf.

(21) Reith, J.; Mayer, C. Peptidoglycan Turnover and Recycling in Gram-Positive Bacteria. *Appl. Microbiol. Biotechnol.* **2011**, *92* (1), 1–11.

(22) Goswami, U.; Basu, S.; Paul, A.; Ghosh, S. S.; Chattopadhyay, A. White Light Emission from Gold Nanoclusters Embedded Bacteria. *J. Mater. Chem. C.* **2017**, *5* (47), 12360–12364.

(23) He, F. *E. coli* Genomic DNA Extraction. *Bioprotocol.* **2011**, *1 (14)* (1–3). https://bio-protocol.org/bio101/e97.

Chapter 3

Living Gut Bacteria Functionalized with Gold Nanoclusters and Drug for Facile Cancer Theranostics

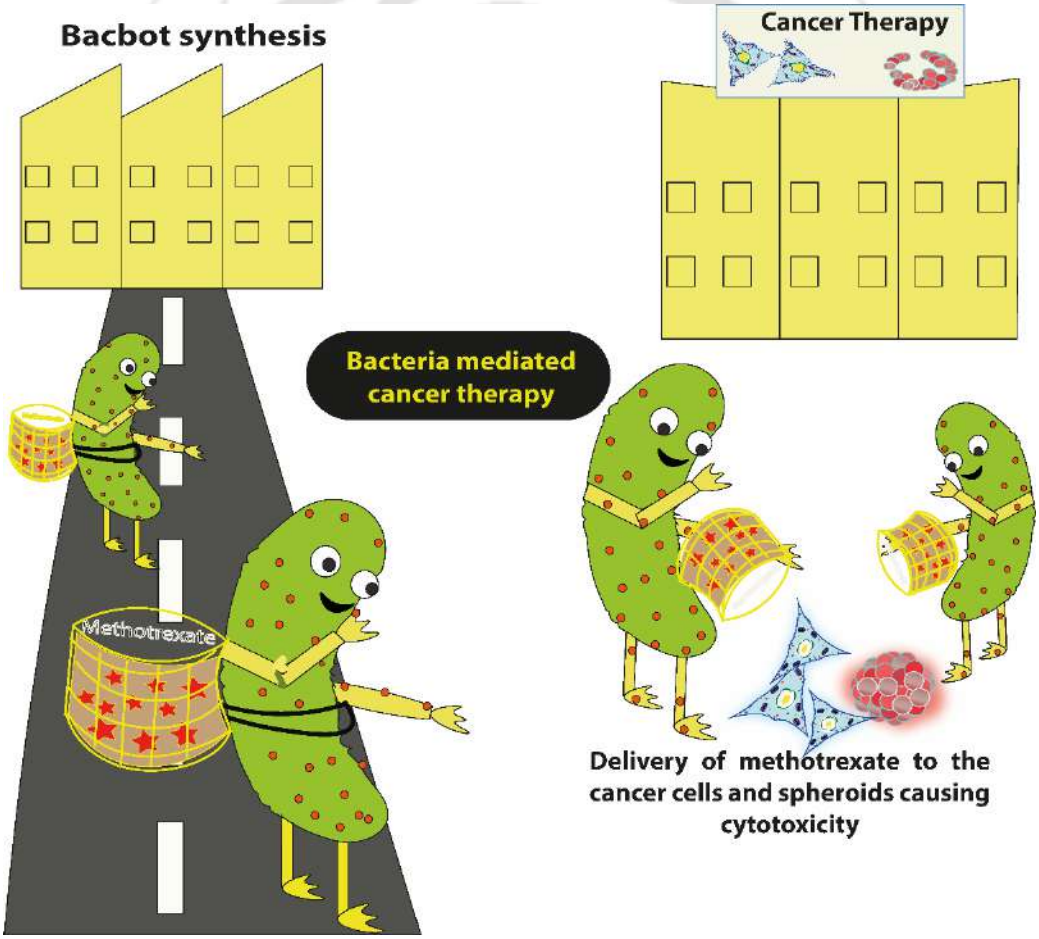

(This chapter has been published in *ACS Applied Biomaterials*)

(https://pubs.acs.org/doi/10.1021/acsabm.2c00911)

Abstract

Bacbots are potent self- propelling vehicles for targeted therapy that can be guided by chemical and biochemical stimuli of the host. In addition, they can be guided externally by the use of magnetic field or other physical forces. The challenge is to incorporate drugs and diagnostic tools in living bacteria with retention of theranostic activity till reaching the targets and easy clearance of the remainder following the treatment. We report that living *Lactobacillus rhamnosus* - when functionalized with photoluminescent Au nanoclusters and anticancer drug methotrexate - was cytotoxic to monolayer and spheroids of cancer cells (HeLa and HT29) even at low dose of bacteria used (10^7 cfu/mL). The observed cell death was nearly 90% in HeLa spheroids and 70% in HT29 spheroids. Further, functionalization of the bacterial surface with the nanoclusters helped incorporate the drug onto their cell surfaces. The drug and nanocluster-loaded bacteria annihilated the cells and the spheroids in a rather short time (6 h) that revealed the specificity and effectiveness of the bacbots. The bacbots exhibited synergistic toxicity on the cells as their effect was more than the drug and the bacteria individually. This higher toxicity could be associated with elevated levels of reactive oxygen species generated in the bacbot-treated cells. The multifunctional bacbots reported here provide an option for guided therapy with the natural variant of the human gut-friendly living bacteria without the need of attenuation or genetic modification.

3.1 Introduction

The imagination that future nanoscale robots will hover around the human body in order to identify and cure diseases - without direct human intervention - has persistently sprang many a development in theranostics. While electronic fabrication practices are yet to reach the level of precision needed to manufacture a functional robot at that scale, synthetic chemistry and biology have provided novel opportunities for molecular scale bottom-up assembly of functional components of nanoscale drug delivery vehicles. The parallel developments in the allied fields also have resulted in conjugation of principles and practices of down-scale manufacturing that aims to fulfil the promise. In this regard, an attractive option may involve the use of living bacteria in conjunction with nanoscale materials and molecular drugs.

Fortuitously, the therapeutic potential of bacteria against cancer - as such and as vectors - has been well-established now. The mechanisms of their action are also fairly known. The tumor targeting bacteria reach, when injected intravenously, both the normal and cancerous cells. However, in the normal cells they are knocked down by the immune system and those which reach the tumors, reside and multiply in the hypoxic cores. The immunosuppression mechanism of the hypoxic tumor cores masks the bacteria from getting eliminated.[1] The anaerobic bacteria especially take advantage of this mechanism. Since they possess an inherent tumor preference over normal cells, they continue to inhabit the core and thus eliminate the cancer cells as a virtue of their anti-cancer property. The preferred choices for this purpose are *Bifidobacterium*, *Clostridium*, *Salmonella* and *E.coli*.[2,3] *Listeria monocytogenes* , *Pseudomonas* and *Yersinia* and magnetotactic bacteria.[4] The bacteria have also been genetically modified to act as vectors for cancer vaccine.[5]

It is important to mention here that the choice of the strain is critical to the success of bacteria-based therapy. For example, the gut microbiota plays a vital role in drug metabolism, cancer

metastasis and progression in multiple ways. Strains such as *Helicobacter pylori*, *Helicobacter hepaticus* and *Fusobacterium nucleatum* are associated with colon cancers. Additionally, they are known to initiate tumors in distant locations as well. Whereas, *Lactobacillus acidophilus* is known for their anti-proliferative activity[6] and for complementing the anticancer drugs for enhanced efficacies [7] *Lactobacillus rhamnosus* GG is known to have anti-proliferative activities against hepatocellular carcinoma. It is also known to induce proinflammatory responses leading to apoptosis in case of colon cancers.[8,9] Similar activities are known to be exhibited by *Lactobacillus casei and Lactobacillus reuteri.* The lactic acid bacteria induce anti-proliferative activities by mechanisms such as activation of natural-killer cells, releasing iron scavengers and by maturation of dendritic cells.[10] Further, co-culturing of *Lactobacillus* sp. with colon cancer cells shows apoptotic cytotoxicity.[11] However, the route of administration also decides the potential of the anticancer activities.[12] For example, in the case of colitis, the therapeutic efficacy improves upon oral administration of bioengineered *Lactobacillus lactis.* Similarly, the administration of genetically modified *Streptococcus gordonii* has better outcomes through nasal route than the others in treatment of meningitis. In some special cases intratumoral or direct injection into central nervous system resulted into improved efficiency as compared to the conventional routes of administration.[13]

Genetically engineered bacteria help attenuate the virulent genes and achieve targeted delivery of therapeutic modules such as proteins, prodrug - enzymes, genes[14], gene silencers specific to cancer metastasis, target molecules and drugs.[15,16,17,18,19] In addition, activating desired anti-proliferative pathways, enhancing efficacy of combination therapy[20], imaging and real-time tracking of the bacteria through a reporter gene such as that for luciferase provide novel opportunities in bacteria-based theranostics.[21,22,23] Further, the antibody-mediated bacterial targeting of tumors reduces the risks to the normal cells. The mechanism-based approach in theranostics has added to the repertoire of current developments in cancer specific remedy[3].

While bacteria-based therapy provides unique opportunities in cancer treatments, there are still avenues for significant improvements in order for them to be fully potent. First of all, use of only bacteria may not annihilate all cancer tissues and thus there would be a chance of resistance and recurrence.[24] Further, high bacterial doses (10^8 or 10^9 cfu/mL) that are typically used for therapy may be toxic to the patients. Importantly, oral administration of the bacteria is not effective owing to the acidic pH of the gut.[24] Additionally, the clearance of the bacteria from the body and effect of the remaining attenuated bacteria, after majority of them being flushed out of the body by antibiotics, remain unclear. The target specificity is often achieved by pursuing genetic modifications of attenuated strains[25], which is a rather involved process. In such a situation, combination therapy using molecular or nanoscale drugs[26] and the bacteria may be more effective. Some of the early results affirm the superiority of this approach.[27,28] Thus, the chemistry needs to be worked out for easy incorporation of molecular or nanoscale drugs inside or on the surface of living bacteria. The conjugation of bacterial therapy with molecular or nanoscale modules may address the limitations associated with any of the approaches. For example, issues related to drug resistance, targeted delivery of therapeutic payloads and renal clearance post treatments may have higher success rates in a combinatorial approach as opposed to the individual treatments. Further,

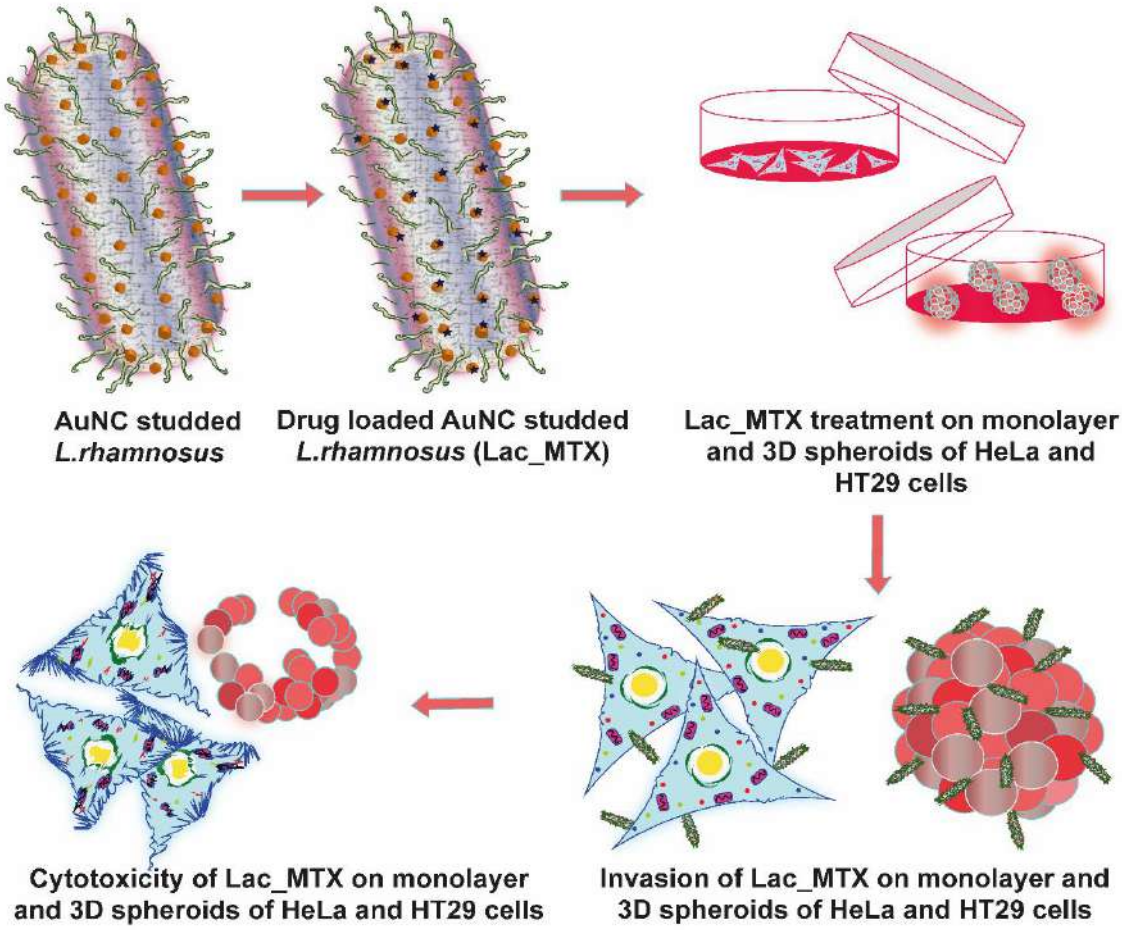

Scheme 3.1. Schematic Representation of Synthesis of Au Nanoclusters on the Surface of *Lactobacillus rhamnosus* (Lac_AuNC) Followed by Loading of Methotrexate (MTX) on the Bacteria (Lac_MTX), the Treatment of these Drug Loaded Bacteria on Monolayer Cultures and 3D spheroids of Cervical Cancer and Colon Cancer Cell Lines Showing Significant Increase in Cytotoxicity in Comparison to the Drug Alone.

the combination therapy may also be able to take advantage of photodynamic and photothermal therapy practices in order to deliver precision medicine.[26, 27,29,30,31] The current study was attempted to address some of the issues raised above while developing a bacterium embedded with photoluminescent Au nanoclusters and anticancer drug. Firstly, the bacterial bot (bacbot) is developed based on a human-gut friendly strain of bacteria *Lactobacillus rhamnosus*, thus addressing the issues of clearance from the body and antagonistic affects following treatment. The use of naturally occurring living bacteria is expected to make the module easier to fabricate and to eliminate their population using antibiotics following treatment. The delivery system - that consisted of *Lactobacillus rhamnosus* bacteria, 1.8 nm (approximate) Au nanoclusters (AuNCs) and anticancer drug methotrexate - took 1.5 h to construct following minimal steps. The current study revealed that the bacbot had a specific affinity towards cancer cells as compared to the healthy cells (Scheme 3.1).

The acidic pH 3 tolerance of the strain makes it suitable to be used for oral administration. There have been no reports of loading of drugs directly on the live bacteria. The study showed for the first time that methotrexate loaded live *Lactobacillus rhamnosus* of population 10^4 unit could be efficiently cytotoxic to cervical as well as colon cancer cells in just 6 h of treatment on monolayer and 3D spheroids that mimic the tumor microenvironment. Further, upon use of the bacbot up to the concentration of 10^7 exhibted less than 13% viability of the spheroids of HeLa cells, thus, reducing chances of recurrence. The photoluminescent nature of the bacteria and the AuNCs – in addition – helped in probing the cells and the spheroids thus providing a novel theranostic module.

3.2 Materials and Methods

3.2.1 Synthesis of gold nanocluster and methotrexate encapsulation on living bacteria

The gold nanoclusters were synthesized on late log phase grown *Lactobacillus rhamnosus* (10^9 cfu/mL) by following a previously described protocol.[32] The methotrexate drug was loaded on the bacteria by incubating 5 μM of the drug with the nanocluster studded bacteria (10^8 cfu/mL) at 37 °C for 1 h. The product medium was then centrifuged at 10,000 rpm for 10 min for obtaining the MTX loaded bacteria that were devoid of unreacted MTX.

3.2.2 Invasion assay

The cancer cells (HeLa, HT29) were grown at a density of 10^5 cells/35 mm tissue culture plates at 5% CO_2 and 37 °C growth conditions in DMEM inside a humidified incubator. After 24 h, the cells were incubated with 10^7 number of bacteria- bearing AuNC and methotrexate on their outer surface (Lac_MTX), at a multiplicity of infection rate of 100:1. This was done such that approximately 100 bacteria are available to invade into each cell (the bacterial dilutions were made in antibiotic free DMEM before carrying out infection on the cells). The invasion was allowed to continue for two different time intervals (2 h and 6 h, separately). After the completion of each time interval, the medium was discarded in order to remove the surplus extracellular bacteria from the medium, which was followed by PBS (1X) wash twice to remove any leftover bacteria. The cells were then ruptured using 0.1X Triton-X in order to collect the bacteria that actually invaded the cells and entered inside. The collected lysate was serially diluted and 100 μL of these diluted lysates were spread- plated on MRS agar plates and were incubated at 37 °C for 48 h. Thus, the number of bacteria (cfu/mL) that invaded the cells were calculated from the grown colonies.

3.2.3 Spheroid formation

The three-dimensional spheroids of cancer cells (HeLa, HT29) were formed by seeding 20,000 cells/well in the 96-well plate. The bottoms of the wells were pre-coated with 1.5% agarose dissolved in serum free and antibiotic free DMEM to prepare a non-adherent substratum. This was followed by centrifugation of the 96 well plate at 700 rcf for 10 min in order to bring the cells to close proximity for spheroid formation. The cells were then allowed to incubate at 37 °C in presence of 5% CO_2 for 96 h in a humidified incubator to form three dimensional spheres.

3.2.4 Characterization study of Lac_MTX

The transmission electron microscopy (TEM) and field emission scanning electron microscopy (FESEM) analyses were carried out by diluting Lac_MTX with de-ionized water and making a drop-cast on carbon coated copper grid (for TEM) and on silicon wafer (for FESEM); the samples were allowed to dry thoroughly before the analysis. The drop-cast was analyzed under the microscopes, and for a comparative study similar drop-casts of control *Lactobacillus rhamnosus* and Lac_AuNC were made and analyzed.

3.2.5 Cytotoxicity assay on monolayer of cells

Cell cytotoxicity of Lac_MTX was determined by growing monolayer of HeLa and HT29 cells in antibiotic free DMEM at 37 °C in the presence of 5% CO_2 in a humidified incubator. For the further experiments, these monolayers were trypsinized and the cells were seeded at a density of 10^4 cells/well in a 96 well plate (in separate 96 well plates for both the cell lines) and were allowed to attach. After 24 h, the cells were co-cultured with four treatment groups (control *Lactobacillus rhamnosus*, Lac_AuNC, Lac_MTX and only MTX) that consisted of (a) different numbers of control bacteria (10^4, 10^5, 10^6 and 10^7 cfu/mL of control *Lactobacillus rhamnosus*; that means here the multiplicity of infection - MOI - was as low as 1:1 and 1:10 and as high as 1:100 and 1:1000) ; (b) Lac_AuNC (10^4, 10^5, 10^6 and 10^7 cfu/mL of bacteria bearing AuNC); (c) Lac_MTX (10^4, 10^5, 10^6 and 10^7 cfu/mL of bacteria bearing AuNC and MTX) and (d) 1.8 μM of MTX. All the dilutions were prepared in antibiotic free DMEM. The co-culturing was allowed to continue for 6 h. The viability of the cells was determined by MTT assay. This assay is based on the principle of reduction of tetrazolium dye to formazan crystals in presence of mitochondrial enzymes of live cells.The cell viability was determined by measuring the absorbance at 570 nm and keeping a reference filter of 655 nm in a micro titer plate reader. The treatment groups consisted of live bacteria (control *Lactobacillus rhamnosus*, Lac_AuNC and Lac_MTX) by which the dye could be taken up and otherwise interfere with the measurements of the absorbance. Hence, simultaneously MTT assay was carried out for these treatment groups, serving as control groups, without being co-incubated with the cells but keeping all of the parameters same as that of co-culturing experimental conditions. The final calculations were carried out based on the difference of absorbance of treatment groups and control groups.

3.2.6 Cytotoxicity assay on 3D spheroids

Cell cytotoxicity of Lac_MTX was determined on spheroids by growing three-dimensional spheroids of HeLa and HT29 cells in antibiotic free DMEM at 37 °C in the presence of 5% CO_2 in a humidified incubator. The spheroids were co-incubated for 6 h with four treatment groups similar to the treatment groups used in the case of the cytotoxicity assay of the monolayer of the cells. The viability of the spheroids was determined by alamar blue assay in which the non-fluorescent resazurin dye is reduced to a fluorescent form by live cells producing a visible color change from blue to highly fluorescent pink color. The spectroscopic analysis was carried out by measuring the absorbance at 570 nm and reference filter of 655 nm in a micro titer plate reader.

The alamar blue assay of the treatment groups only without co-incubation with spheroids was also carried out that served as the control group for accurate calculation of the viability without any interference from the living bacteria of the treatment groups.

3.2.7 Live/dead staining assay of monolayer and 3D spheroids

The live dead staining in monolayer and 3D spheroids were carried out by using propidium iodide and acridine orange staining protocols. The monolayer and 3D spheroids were treated with the above mentioned four different treatment groups similar to the cytotoxic assays of monolayer and spheroids. These were allowed to incubate for 6 h. After the completion of the treatment, the media containing the bacteria were removed and the monolayer cells and spheroids were carefully subjected to PBS wash twice to remove any leftover extracellular bacteria. Further, the monolayer cells and spheroids were incubated with 10 µL of 1 mg/mL of acridine orange for staining the live cells that was followed by incubation with propidium iodide (10 µL of 1 mg/mL) for staining the dead cells. The monolayer cells and spheroids were further analyzed in confocal laser scanning microscope. The cells were illuminated with 488 nm laser to visualize the live cells that fluoresce green and the dead cells that fluoresce red upon illumination with 488 nm and 514 nm laser respectively.

3.2.8 ROS generation analysis

The ROS assay was carried out by seeding 10^4 cells/well in a 96 well plate at 37 °C in the presence of 5% CO_2 in a humidified incubator. The cells were treated with the similar treatment groups that were used for cytotoxicity assays. The treatment was allowed to continue for 6 h that was followed by addition of 10 µM of non-fluorescent 2,7-dichlorofluoresceindiacetate (DCHFDA) dye to each well, which was then allowed to incubate at room temperature for 30 min. The dye hydrolyzes to 2′,7′-dichlorodihydrofluorescein (DCFH) which oxidizes to 2', 7' – dichlorofluorescein (DCF), in presence of ROS, on diffusing into cells and emits green fluorescence. The spectroscopic analysis was carried out using 488 nm excitation and 530 nm emission wavelengths. The treatment groups, without co-culturing with the cells, were considered as the control groups. Apart from these, a positive control treatment group was taken by treating the cells and spheroids with hydrogen peroxide in order to determine the extent of change ROS generation of the cells after being subjected to the four treatment groups.

3.3 Results and Discussion

3.3.1 Synthesis and characterization of Au nanoclusters on living *Lactobacillus rhamnosus*

The synthesis of Au nanoclusters on *Lactobacillus rhamnosus* was carried out by chemical reduction of $HAuCl_4$ using 3-mercaptopropionic acid as reported earlier.[1] The characterization of the Au nanoclusters based on spectroscopic analyses using UV–visible, photoluminescence, X-ray photoelectron and energy dispersive X-ray spectroscopy (XPS and EDX) confirmed the synthesis of fluorescent AuNCs on the surface of the live bacteria. The microscopic analyses using transmission electron microscopy (TEM), field emission scanning electron microscopy (FESEM), atomic force microscopy (AFM), and confocal laser scanning microscopy (CLSM) further supported the presence of the luminescent AuNCs (typically of 1.3 nm size) on the bacteria. The

Au nanocluster loaded bacteria (Lac_AuNC) showed orange luminescence upon visualization over UV transilluminator. A similar but dimmer luminescence was observed in the methotrexate loaded Au nanocluster embedded bacteria (Lac_MTX); however, no such luminescence was observed in the case of control bacteria (Figure 3.2d). The fluorescence emission spectrum of the Lac_AuNC consisted of two peaks - the broad peak in the range of 200- 400 nm is attributed to the proteins present in the bacteria and the second peak with the maximum at 580 nm could be attributed to the Au nanoclusters synthesized on the bacterial surface. The Lac_MTX exhibited a similar fluorescence spectrum as Lac_AuNC except for a weaker peak maximum at 580 nm that could have been due to the interaction between methotrexate and the AuNCs (Figure 3.2c). The UV-visible spectrum of the control bacteria however had only a single broad peak in the region of 200-400 nm. The TEM images of Lac_AuNC revealed the presence of AuNCs on the outer surface of bacteria. An additional layer-like deposition could be observed in the images of Lac_MTX that could be due to the deposition of methotrexate over the surfaces of Lac_AuNC (Figure 3.2 b). The FESEM images of Lac_AuNC and Lac_MTX supported the findings with the TEM images. The

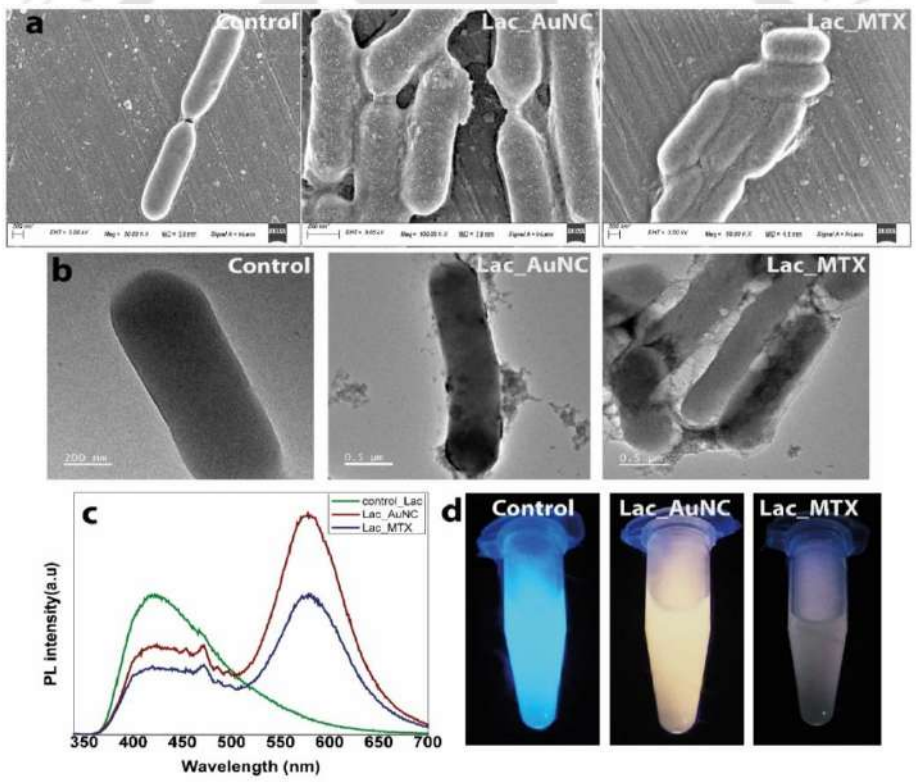

Figure 3.2. Characterization study of Lac_MTX. (a) Transmission electron microscopy images of control bacteria, Lac_AuNC and Lac_MTX, (b) field emission scanning electron microscopy images of control bacteria, Lac_AuNC and Lac_MTX, (c) photoluminescence intensity spectra of control bacteria, Lac_AuNC and Lac_MTX, and (d) digital photographic

AuNCs were observed to be distributed all over the surface of bacteria and an apparent thin layer of additional materials was present over bacteria in FESEM images of Lac_MTX (Figure 3.2a).

3.3.2 Methotrexate encapsulation/ adsorption on Lac_AuNC

The AuNC embedded living *Lactobacillus rhamnosus* were motile and viable. Initially, the cytotoxicity of Lac_AuNC on cancer cells was confirmed through MTT assay (the details have been discussed in later section of the Results and Discussions). A similar cytotoxic effect of Lac_AuNC and *Lactobacillus rhamnosus* was observed on the cancer cells as discussed later. Thus, the prevailing cytotoxicity of Lac_AuNC could be attributed to the inherent anti-cancer property of *Lactobacillus rhamnosus* that was not discernibly affected following incorporation of AuNCs on the bacteria. The therapeutic efficiency was enhanced by encapsulating a well-known anti-cancer drug methotrexate on their surface without hampering their motility or viability. The drug is known to inhibit the tumor growth by interfering with the nucleic acid synthesis in tumor cells.

Prior to the encapsulation of the drug, the minimum inhibitory concentration (MIC) of methotrexate on *Lactobacillus rhamnosus* was determined to understand whether there was an adverse effect of the drug on the bacteria itself. It was established that there was no significant inhibition of growth of *Lactobacillus rhamnosus* in the range of 100 nM to 500μM concentration of MTX (Figure 3.3c). The results suggested that MTX drug could safely be incorporated into the nanocluster studded bacteria (Figure 3.3d). The encapsulation was carried out by incubating different concentrations of the drug (100 nM to 5 μM) with Lac_AuNC in presence of MRS medium (the number of bacteria was kept constant in each of the medium; 10^8 cfu/mL) at 37 °C for 1 h. The drug encapsulation efficiency was calculated on the basis of change in photoluminescence peak maximum of Lac_AuNCs at 580 nm, for each concentration of drug used for encapsulation. It was observed that with the increasing concentration of the drug in the medium, the intensity of the peak maximum at 580 nm was decreasing (Figure 3.4a). This indicated that the dimmer fluorescence of Lac_MTX was due to the interaction between the drug molecules and AuNCs on bacterial surface (Figure 3.2d). The maximum encapsulation % (Figure 3.4b) was calculated to have been approximately 36% (1.8 μM approx.) using the formula in equation 1.

$$\text{Drug encapsulation} = \frac{\text{PL intensity of Lac\_AuNC} - \text{PL intensity of Lac\_MTX}}{\text{PL intensity of Lac\_AuNC}} * 100$$

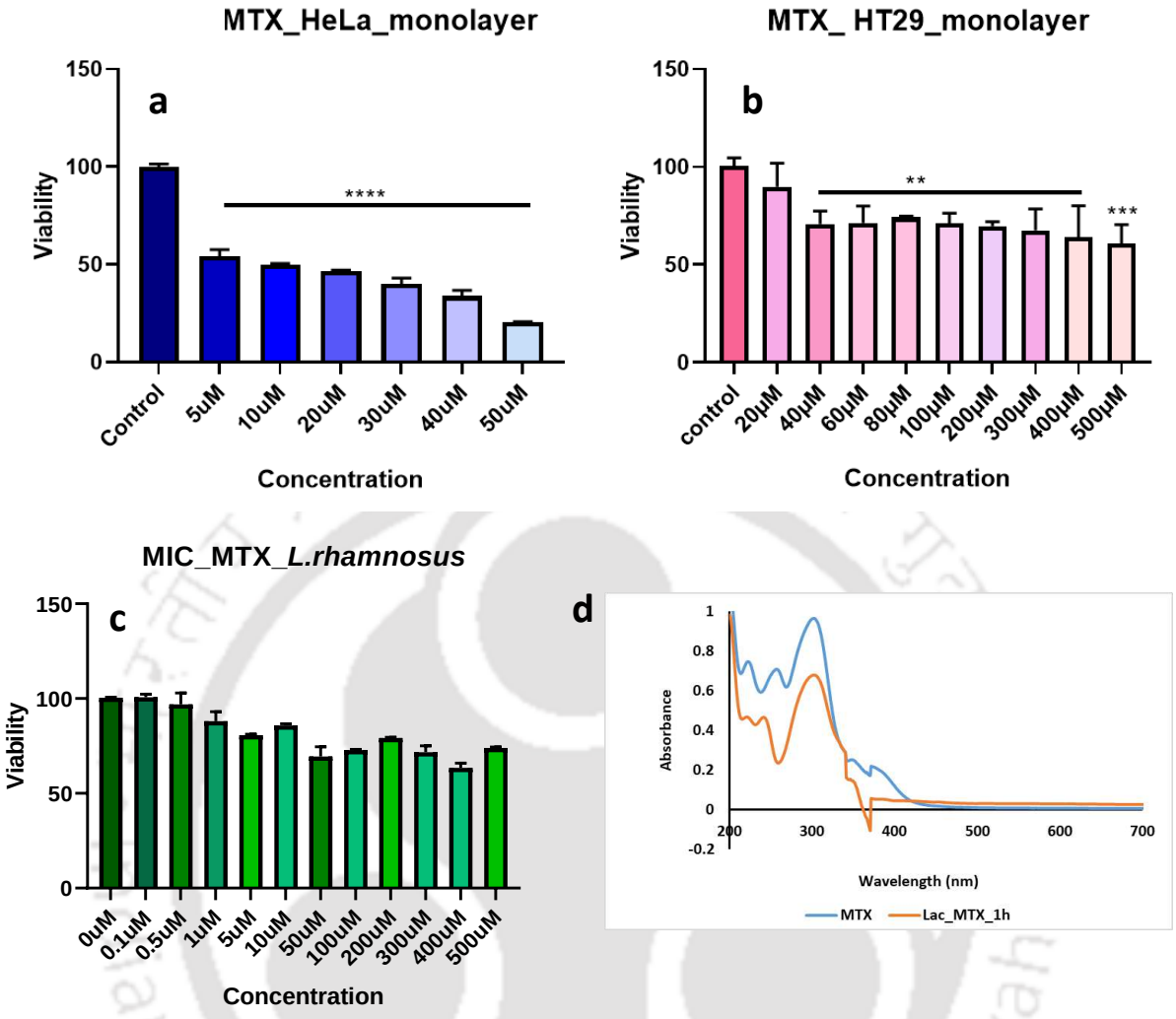

Figure 3.3. Cell cytotoxicity assay (a) MTT assay of methotrexate on monolayer of HeLa cells, (b) MTT assay of methotrexate on monolayer of HT29 cells. (c) MIC of methotrexate on control *Lactobacillus rhamnosus*, and (d) UV-visible absorbance spectra of MTX and Lac_MTX. Statistical significance is represented by ** ($p<0.01$), *** ($p < 0.001$), and **** ($p < 0.0001$). The values are represented as mean ± standard deviation (SD) of three individual experiments.

The viability was confirmed by inoculating 1% of freshly prepared Lac_MTX in MRS medium that were allowed to incubate for 48 h at 37 °C. The resultant turbid medium was analyzed for absorbance at 590 nm for the presence of live bacteria. This was reaffirmed by plating the Lac_MTX on MRS agar plates. The cfu/mL were calculated to be 10^7 (cfu/mL of Lac_AuNC- 10^8 and *Lactobacillus rhamnosus* - 10^9) (Figure 3.5a). Thus, the resultant Lac_MTX were alive, viable, self-driven, therapeutic carrier systems that were labelled with photoluminescent nanoclusters (Video1_Lac_MTX).

3.3.3 Invasion assay

As discussed before, the lactic acid bacteria are known to have affinity towards cancer cells. The colonization of bacteria inside the host depends on its invasion capabilities. Thus, in the current study the validation of the invading competency of *Lactobacillus rhamnosus* into the cancer cells was an important aspect to have been determined. The invasion assay was designed such that the cervical cancer cells (HeLa) and colon cancer cells (HT29) were allowed to be invaded by Lac_MTX for two different time periods.

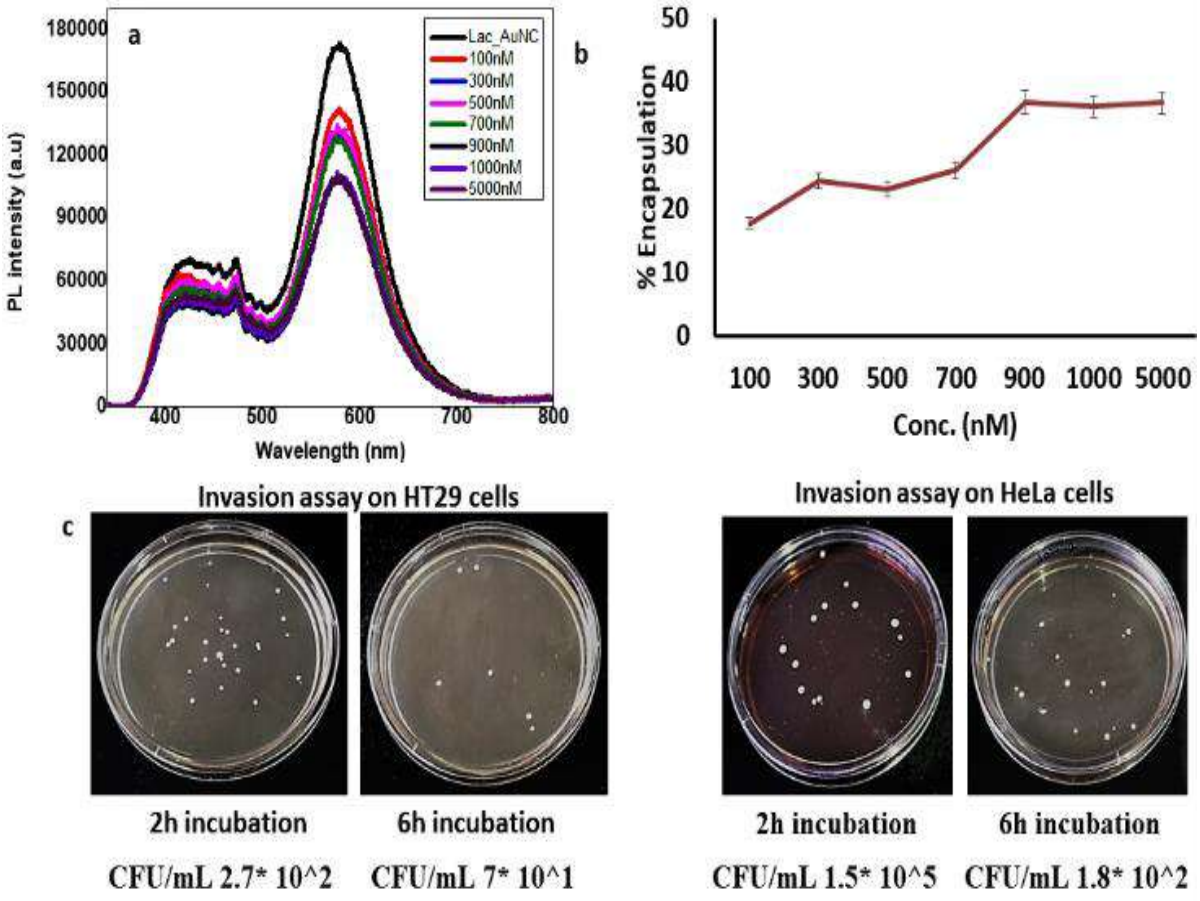

Figure 3.4. (a) Photoluminescence spectra of Lac_AuNC loaded with different concentrations of MTX, (b) drug loading efficiency on Lac_AuNC as a function of concentration of MTX, (c) agar plates with bacterial colonies grown from cell lysates obtained after invasion assay as carried out on HT29 cells and HeLa cells for 2 h and 6 h of time intervals.

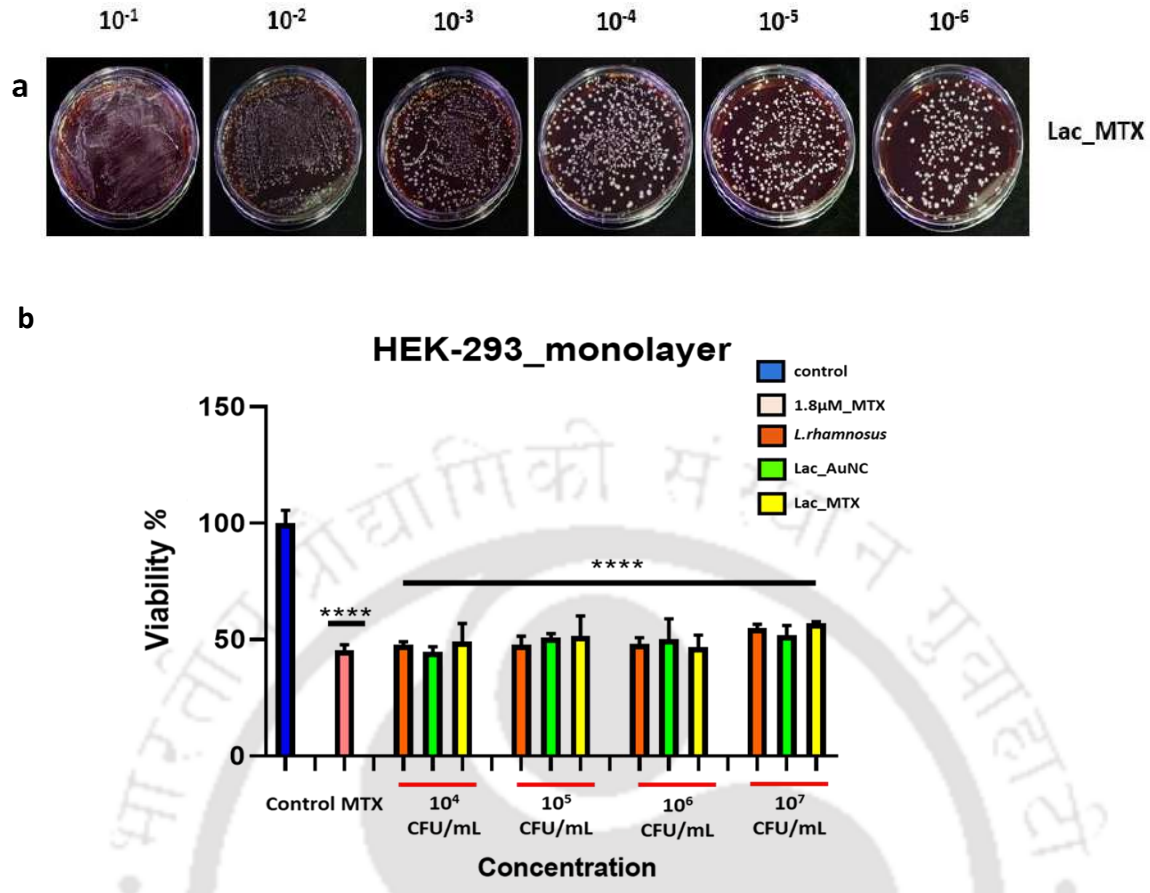

Figure 3.5. Colony forming unit and Cell cytotoxicity assay. (a) colony forming unit/mL of Lac_MTX with serially diluted concentration of bacteria as described in legends (b) MTT assay of control *Lactobacillus rhamnosus*, Lac_AuNC, Lac_MTX and methotrexate (MTX) on monolayer of HEK_293 cells. Statistical significance is represented by **** ($p < 0.0001$). The values are represented as mean ± standard deviation (SD) of three individual experiments.

Here, the two different types of cancer cells were grown separately on 35 mm tissue culture plates in DMEM at 37 °C and 5% CO_2 in a humidified incubator. The cell density was kept 10^5 cells/ plate for both the cell lines. The Lac_MTX were freshly prepared and were diluted to a density of 10^7 cfu/mL. This was done so that approximately 100 bacteria were to invade each cell i.e., the Multiplicity of Infection (MOI) was 100:1. The bacterial dilutions were made in antibiotic free DMEM media so that they themselves do not get eliminated in presence of antibiotics. Following invasion for 2 or 6 h, the extracellular bacteria were removed by PBS wash twice. The cells were trypsinized and were counted. The number of HeLa cells after 2 h of treatment were found to be 10^3 cells/mL and after 6 h of treatment the cell number were found to be $1.2*10^2$ cells/mL. The number of HT29 cells after 2 h of treatment were found to be $5.7*10^4$ cells/mL and after 6 h of treatment the cell number were found to be $1.9*10^4$ cells/mL. Further, the invading bacteria were collected by rupturing the cells following incubation with a mild concentration of Triton X (0.1X) for 30 s. The collected lysate was serially diluted using antibiotic free medium and 100 µL of this was spread plated on MRS agar plates followed by an incubation period of 48 h at 37 °C. The cfu/mL was counted to calculate the number of bacteria that invaded the cells. They were $1.5*10^5$

cfu/mL and $1.8*10^2$ cfu/mL in case of 2 h and 6 h incubations, respectively in HeLa cells. Similarly, the values were $2.7*10^2$ cfu/mL and $7*10^1$ cfu/mL in case of 2 h and 6 h incubations, respectively in HT29 cells. The lesser number of cfu/mL in case of 6 h of incubation of Lac_MTX with both the cell lines could be due to lesser number of live cells available as compared to 2 h incubation. The results indicated that the bacteria had indeed invaded the cells and had released the drug in the vicinity or inside of the cells during the 6 h of incubation, leading to killing of the cells. Since the dead cells got detached from the extracellular matrix, they were washed away along with the extracellular bacteria during PBS wash (Figure 3.4c). The higher value of cfu/mL in HeLa as compared to that for HT29 cells mean better invasion of Lac_MTX in HeLa cells.

3.3.4 Cytotoxicity assay on monolayer of cells

Prior to the cytotoxicity assay of Lac_MTX on cancer cells, the cell viability and IC50 values of MTX on HeLa cells and HT29 cells were determined. The IC50 value of MTX on monolayer of HeLa was found to be 10 µM and on the HT29 cells it was 2.1 mM (Figure 3.2a and Figure 3.2b). At first, for determining the specificity of Lac_MTX, the non-cancerous cell line HEK-293 was treated with control *Lactobacillus rhamnosus* and Lac_AuNC and Lac_MTX (10^4, 10^5, 10^6 and 10^7 cfu/mL). The reason for selecting the cells of different origin was to have a comparative analysis of the cytotoxicity of bacbots on non-cancerous and cancerous cells. That would highlight the specificity of action of these bacbots. Further, the effect of bacbots on cells of similar origin (HT29) and different origin (HeLa) would help to understand the affinity of the bacbots for a particular of cell line. The HEK-293 cells are isolated from human embryonic kidney. The renal clearance of any therapeutic entity is an important aspect of the overall treatment regimen. The study of cytotoxicity of bacbots on kidney derived cell line also showed that the kidney cells might not be targeted by the bacbots. The treatment was done for a time interval of 6 h at 37 °C and 5% CO2 in a humidified incubator. The cell viability was determined through MTT assay. It was observed that the cell viability on treatment with all of these groups was nearly 50%. This affirmed the cytotoxicity of the bacteria on the mammalian non-cancerous cells (Figure 3.5b). Now, the therapeutic efficacy of Lac_MTX was evaluated by treating the cells with the above-mentioned treatment groups under the same experimental conditions. It was observed that the viability of monolayer of HeLa cells on treatment with control *Lactobacillus rhamnosus* (10^4 cfu/mL) was 34.8%. Further, there was no conspicuous change observed in the viability of cells that were treated with a higher concentration of bacteria (10^5, 10^6 and 10^7 cfu/mL). It remained nearly constant i.e., 30-35%. This could be due to the inherent toxicity of the bacteria that led to the killing of the cells that did not deviate much on varying the bacterial concentrations. A possible reason for limited effect of higher cfu/mL of bacteria on the cells could be the attainment of a threshold number of bacteria being bound to the limited number of available receptor sites on the cell surface[33]. This could also be due to threshold level of released metabolites[24] that are secreted by the bacteria that causes toxicity in the cells. In other words, even if cfu/mL of bacteria is increased the concentration of metabolites surrounding the cells may not vary significantly especially at the Lac_AuNC was 28.7 % (10^4 cfu/mL), 34.5 % (10^5 cfu/mL), 32.8% (10^6 cfu/mL) and 30.5% (10^7 cfu/mL). The viability of Lac_AuNC treated cells was marginally lower than the control bacteria treated cells. This means the synthesized AuNCs had not affected the inherent anti-cancer

properties of the bacteria. However, the cells treated with different concentrations of Lac_MTX were far less viable. The observed viabilities were 13% (10^4 cfu/mL), 14.5% (10^5 cfu/mL), 9.2% (10^6 cfu/mL) and below detectable value for 10^7 cfu/mL of bacteria. Later, the cell viability of the above- mentioned treatment groups was also determined on monolayer of HT29 colon cancer higher number of bacteria. The cell viability on treatment with different concentrations of the cells. Here, the viabilities of control *Lactobacillus rhamnosus* treated cells were observed to have been 48.0 % (10^4 cfu/mL), 42.3 % (10^5 cfu/mL), 48.3% (10^6 cfu/mL) and 49.5 % (10^7 cfu/mL). It was thus evident that the cytotoxicity of control *Lactobacillus rhamnosus* was more on HeLa cells as compared to HT29 cells. The Lac_AuNC treated HT29 cells had left 31.6 % (10^4 cfu/mL), 28.9 % (10^5 cfu/mL), 27.9% (10^6 cfu/mL) and 30.5 % (10^7 cfu/mL) viable cells after treatment. The HT29 cells that were treated with Lac_MTX had lesser number of viable cells when compared to Lac_AuNC and control bacteria treated cells. The results showed 17.7% (10^4 cfu/mL), 21.4% (10^5 cfu/mL), 13.06% (10^6 cfu/mL) and 8.03 % (10^7 cfu/mL) viabilities. In both of the monolayer of cells, the effect of 1.8 μM of MTX left nearly 80-90% of cells viable showing the ineffectiveness of the drug at such a low concentration (Figure 3.6a and 3.6b). The inherent toxicity of the bacteria towards the cancer cells was clearly higher than that of the drug alone. But the efficacy of Lac_MTX was superior to the bacteria and the drug, when treated individually on cells. This enhanced efficiency was achieved by loading the drug on the bacteria. This established that the bacteria and the drug have acted upon the cells showing a synergistic effect. The motile nature of Lac_MTX had possibly made the drug more available to the cells. There was more affinity of the control *Lactobacillus rhamnosus* on the cancerous cells as compared to the non-cancerous cells which is evident by the difference in viability of the two cell lines after the treatment. The *Lactobacillus* sp. as discussed earlier are known to have toxicity on colon cancer cells. In a previous study, it was reported that the incubation of 10^8 cfu/mL or 10^9 cfu/mL number of *Lactobacillus casei* killed nearly all the cells on incubation for 48 h and about 78% killing was observed on co-incubation of up to 24 h (cells density was 5000 and 200000 cells/well).[11] Each species of *Lactobacillus* has different mechanism and efficiency of anti-cancer activity. However, in the current study an incubation of 10^7 number of Lac_MTX with HT29 cells have shown killing (92%) with a co-incubation time of only 6 h, thus demonstrating the drug and AuNC loaded bacteria as potential carrier and therapeutic modules.

3.3.5 Cytotoxicity assay on 3D spheroids

The cytotoxic effect of Lac_MTX was further investigated on 3D spheroids of HeLa and HT29 cells. The spheroids resemble the tumor microenvironment and provide a more realistic experimental condition as compared to the monolayers of cell cultures. The drug loaded live bacteria were allowed to invade the spheroids and the treatment was carried out for 6 h in both the cell lines. The cell viability of control *Lactobacillus rhamnosus*, Lac_AuNC and Lac_MTX treated 3D spheroids of HeLa cells at a concentration of 10^4 cfu/mL (33.09%: control bacteria, 33.2%: Lac_AuNC, 31.2%: Lac_MTX) and 10^5 cfu/mL of bacteria (35.3%; control bacteria, 27.7%; Lac_AuNC, 29.9%; Lac_MTX) had less variations. As the concentration of the bacteria was further increased, the viabilities of control *Lactobacillus rhamnosus* treated spheroids were found to be 37.5% (10^6 cfu/mL of bacteria) and 30.4 % (10^7 cfu/mL of bacteria). The viability of the

Lac_AuNC treated spheroids were found to vary marginally (25.6% in case of 10^6 cfu/mL of bacteria and 22.08 % in case of 10^7 cfu/mL of bacteria) irrespective of the concentration of the bacteria used. A similar cell viability profile was obtained in case of monolayer cells of HeLa treated with control bacteria and Lac_AuNC. More importantly, the cytotoxic effect of Lac_MTX seemed to increase with higher doses of bacteria and 19% (10^6 cfu/mL) and 12% (10^7 cfu/mL) viabilities in spheroids were observed. It was evident that there was a toxic effect of the control bacteria on the spheroids that remained unaffected by the synthesis of AuNCs on the bacteria. The drug loaded bacteria had more profound effect on the spheroids, which was concentration dependent. Similarly, on treatment with control *Lactobacillus rhamnosus*, the observed viabilities of the HT29 spheroids were 54% (10^4 cfu/mL), 51.4% (10^5 cfu/mL), 48.5% (10^6 cfu/mL) and 44.6 % (10^7 cfu/mL). The viability of Lac_AuNC treated cells were 58.1% (10^4 cfu/mL), 50.9% (10^5 cfu/mL), 49.4% (10^6 cfu/mL) and 45.9 % (10^7 cfu/mL). There was an increase in cytotoxicity with increasing concentration of the Lac_MTX treatment. The viabilities were 49.0% (10^4 cfu/mL), 42.1% (10^5 cfu/mL), 33.4% (10^6 cfu/mL) and 28 % (10^7 cfu/mL). The cell viabilities of 1.8 µM

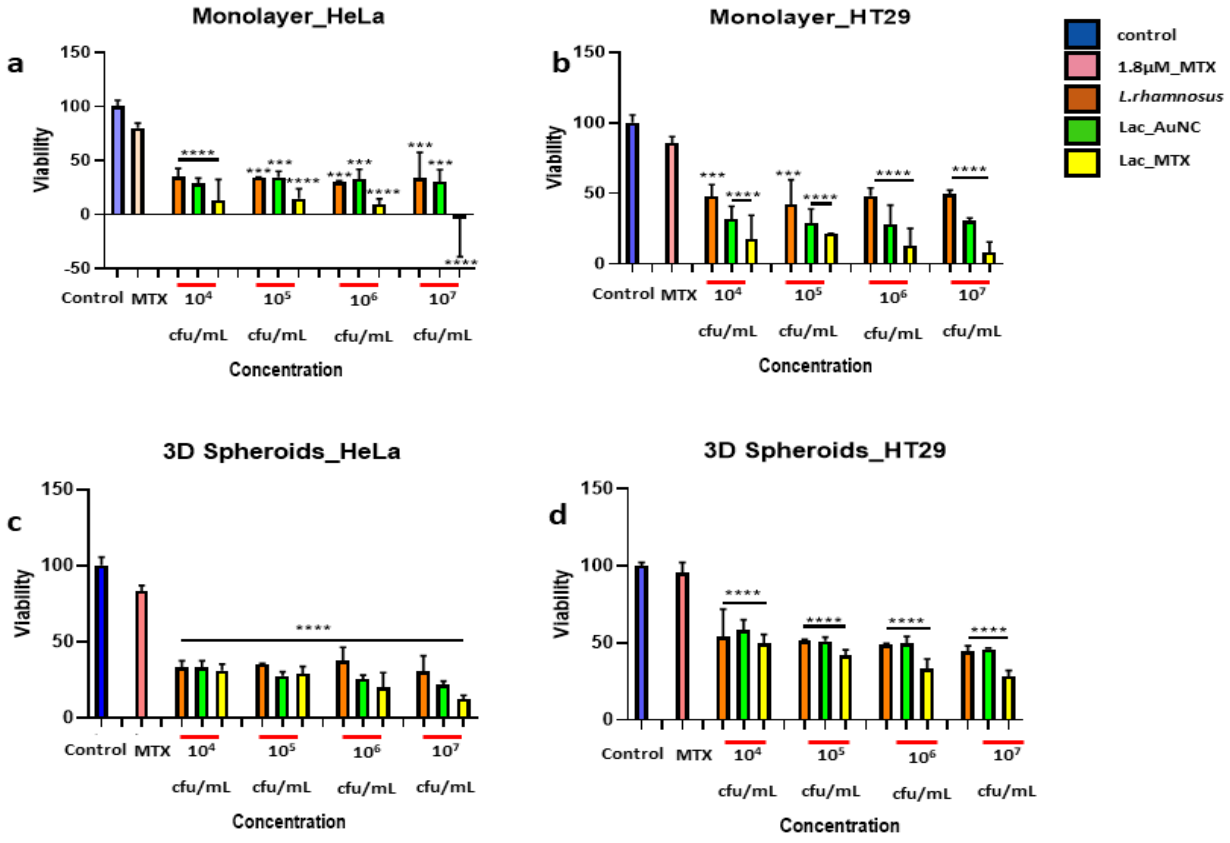

Figure 3.6. Cell viability of (a) monolayer of HeLa cells treated with control bacteria, MTX, Lac_AuNC and Lac_MTX, (b) monolayer of HT29 cells treated with control bacteria, MTX, Lac_AuNC and Lac_MTX, (c) 3D spheroids of HeLa cells treated with control bacteria, MTX, Lac_AuNC and Lac_MTX and (d) 3D spheroids of HT29 cells treated with control bacteria, MTX, Lac_AuNC and Lac_MTX on 3D spheroids of HT29 cells. Duration of the treatment was 6 h. Statistical significance is represented by *** ($p < 0.001$), and **** ($p < 0.0001$). The values are represented as mean ± standard deviation (SD) of three individual experiments.

MTX treated HeLa and HT29 spheroids were 83.4% and 95%, respectively. The spheroids have a hypoxic core at the center that remains surrounded by the cells so it is difficult to be reached. The higher level of toxicity caused by the drug loaded bacteria could be of great significance as they can reduce the chances of recurrences. Clearly, the synergistic effect of the bacteria and the drug is the cause of the enhanced cytotoxicity. The anti-cancer effect of Lac_MTX was more profound on spheroids of HeLa cells in comparison to HT29 spheroids. This re-affirms the finding of the studies conducted on monolayer of HeLa and HT29 cells suggesting specificity of Lac_MTX more towards HeLa cells (Figure 3.6c and 3.6d). This specificity could be the result of higher affinity of the metabolites released from the bacteria towards a specific type of cells (HeLa cells in the current study). The particular metabolite that causes this affinity and its properties are yet to be studied in details.[34,35]

3.3.6 Live/dead staining assay of on monolayer of cells

The cytotoxic effects of Lac_MTX on monolayers of HeLa and HT29 cells were further evaluated by dual staining of live and dead cells after treatment. Propidium iodide was used to specifically stain the dead cells and acridine orange was used to stain the live cells. The stained cells were visualized in confocal laser scanning microscope. The laser wavelengths were set at 488 nm for visualizing the live cells and at 514 nm to visualize the dead cells. The images showed that the red fluorescent labelled cells were more in number than the green fluorescent labelled cells. This revealed that the number of dead cells were very high in comparison to the number of live cells. The cells treated with only MTX were primarily of live cells. The images were in accordance with the results of cytotoxicity assay on monolayer of HeLa and HT29 cells (Figure 3.7 to Figure 3.12).

3.3.7 Live/dead staining assay of on 3D spheroids of cells

The treated spheroids were incubated with acridine orange and propidium iodide dye for specific staining of the live and dead cells, respectively. Then the images were obtained by exposure of 488 nm and 514 nm lasers for live (green fluorescence) and dead cells (red fluorescence) respectively. The images depicted the presence of higher number of dead cells in spheroids of both the cell lines that were treated with Lac_MTX as compared to the MTX, control bacteria and Lac_AuNC treated spheroids. The images of spheroids of HT29 cells revealed that the higher number of dead cells were inside the core of the spheroids. The results showed the ability of *Lactobacillus rhamnosus* to invade to the core of the spheroids. On the other hand, the spheroids of Hela cells were destroyed completely and the spheroids were not intact. Hence, there was no distinction between the core and peripheral cells (Figure 3.13a, 3.13b and 3.13c). The results were in accordance with the cytotoxicity assays which confirmed a more profound effect of Lac_MTX on the HeLa cells than on the HT29 cells (Figure 3.14 to Figure 3.16). The 3D spheroids in combination and Z-stack view of combination field reveal that the spheroids were invaded by the bacbots thus both PI stained dead cells and acridine orange stained live cells could be seen. The HeLa cells on treatment with Lac_MTX were also observed under confocal laser scanning microscope. For this single cells were focused with 63X magnification and 405 nm laser specific to AuNCs on bacterial surface was used. The bacbots were distinctly fluorescent by virtue of the AuNCs and were found on the surface

of the cell indicating the intrusion of cells by the bacteria (Figure 3.21). Since, majority of them were sticking to the membrane it could be inferred that the bacteria would have released the drug near or on the cell membrane leading to its easy uptake. Further, majority of the bacteria were seen to cling on the cells and very few of them were away from the cells, this could be attributed to the affinity of the bacteria towards the cancer cells. It may be also added here that a few of the bacteria had indeed invaded the cells adding to higher efficacy (Video 2 _Hela_Lac_MTX).

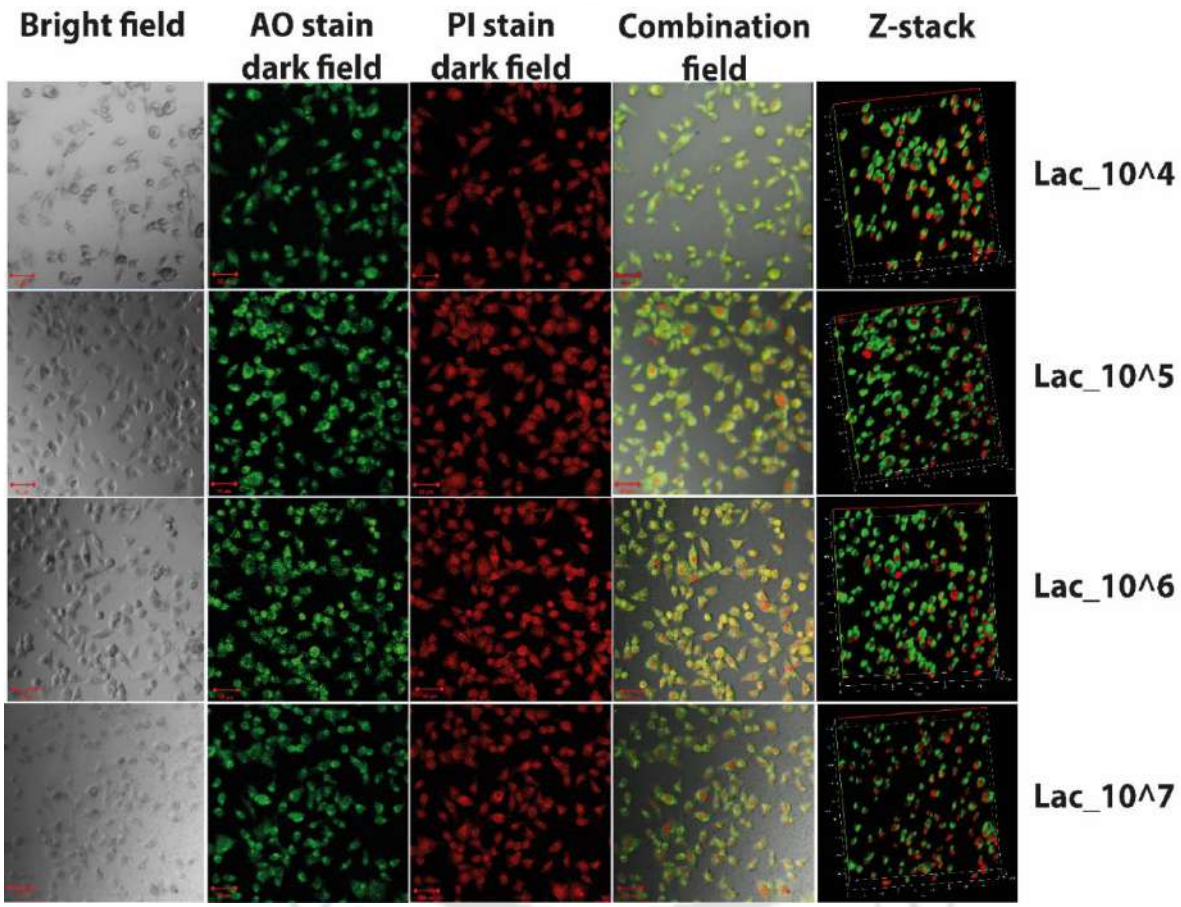

Figure 3.7. Confocal laser scanning microscopy. Propidium iodide/acridine orange dual staining images of live (green channel) and dead (red channel) monolayer of HeLa cells treated with different concentrations of control *Lactobacillus rhamnosus* (as described in the legends).

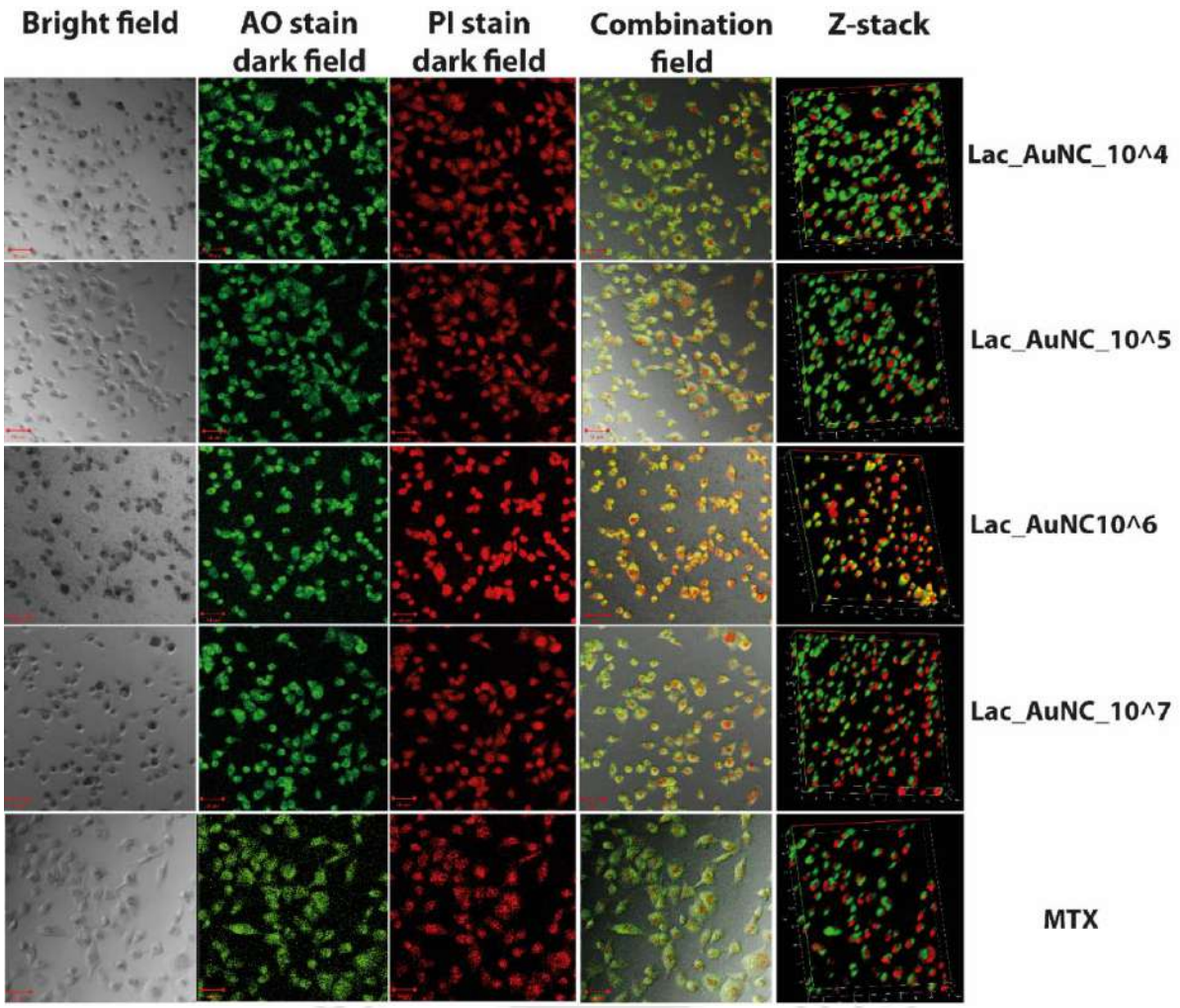

Figure 3.8. Confocal laser scanning microscopy. Propidium iodide/acridine orange dual staining images of live (green channel) and dead (red channel) monolayer of HeLa cells treated with different concentrations of control Lac_AuNC (as described in the legends).

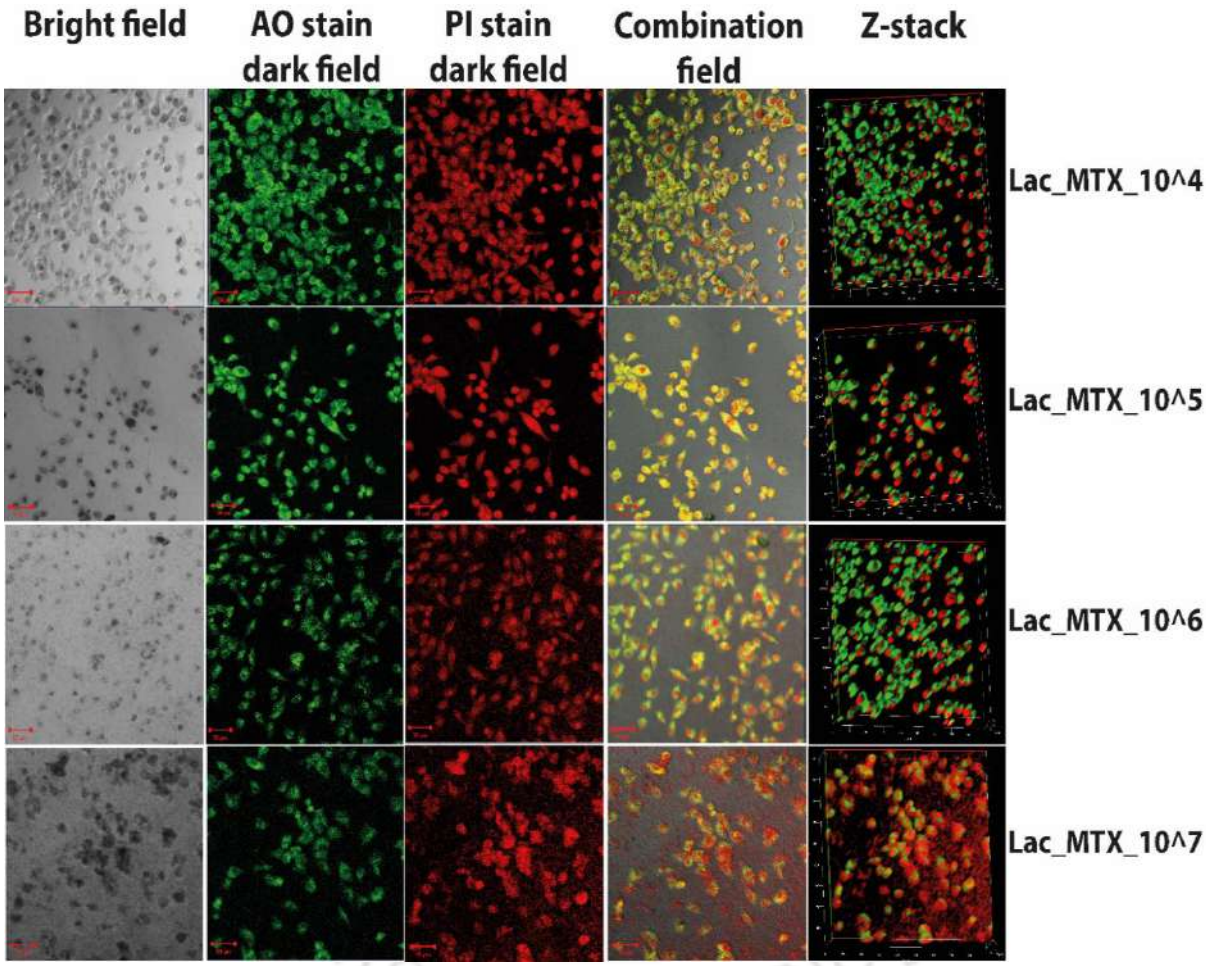

Figure 3.9. Confocal laser scanning microscopy images of monolayer of HeLa cells treated with control bacteria and Lac_MTX at different number of bacteria (10^4,10^5,10^6 and 10^7). The dead cells were stained with propidium iodide and the live cells were stained with acridine orange.

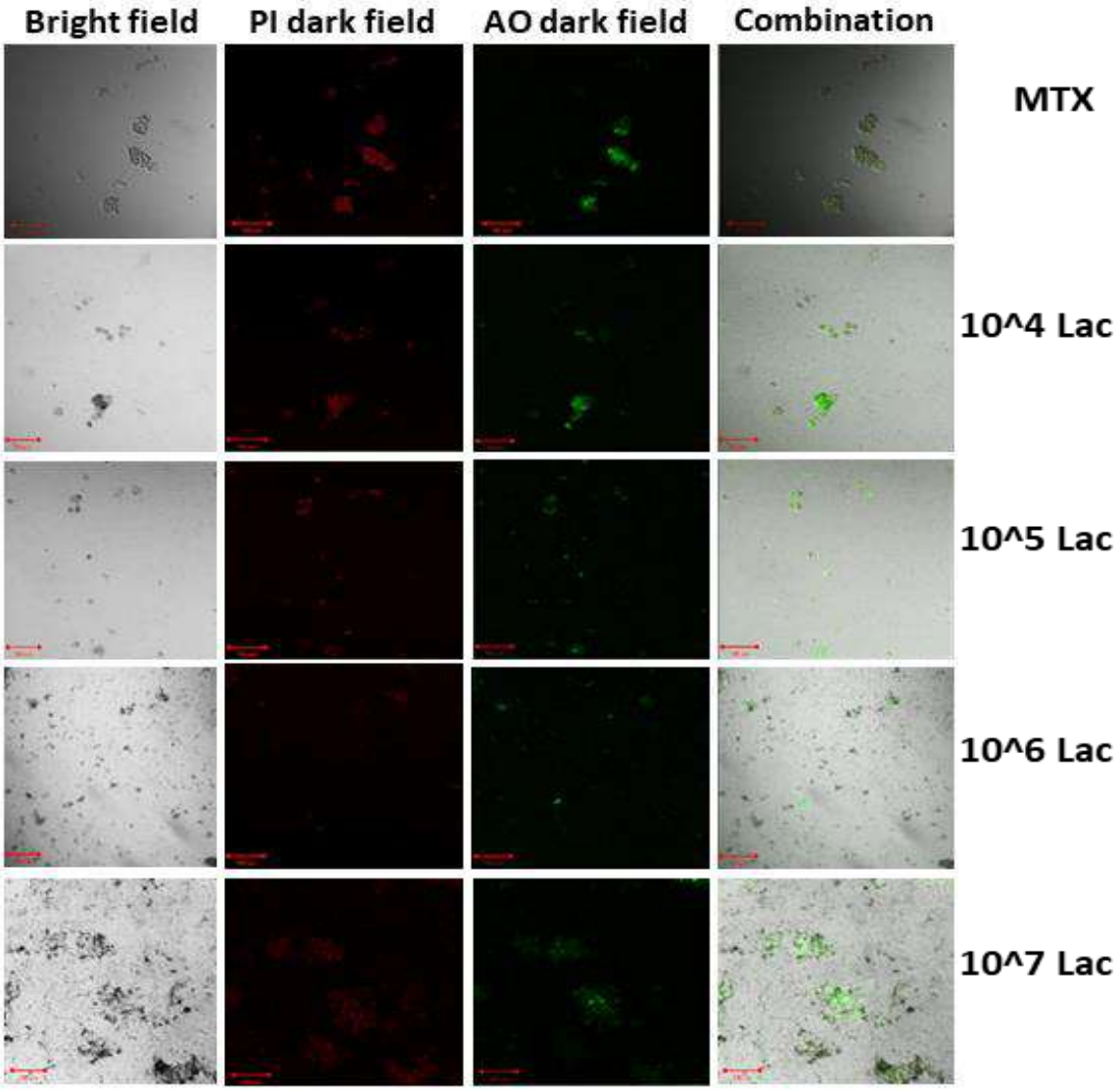

Figure 3.10. Confocal laser scanning microscopy. Propidium iodide/acridine orange dual staining images of live (green channel) and dead (red channel) HT29 monolayer cells treated with different concentrations of control *Lactobacillus rhamnosus* (as described in the legends).

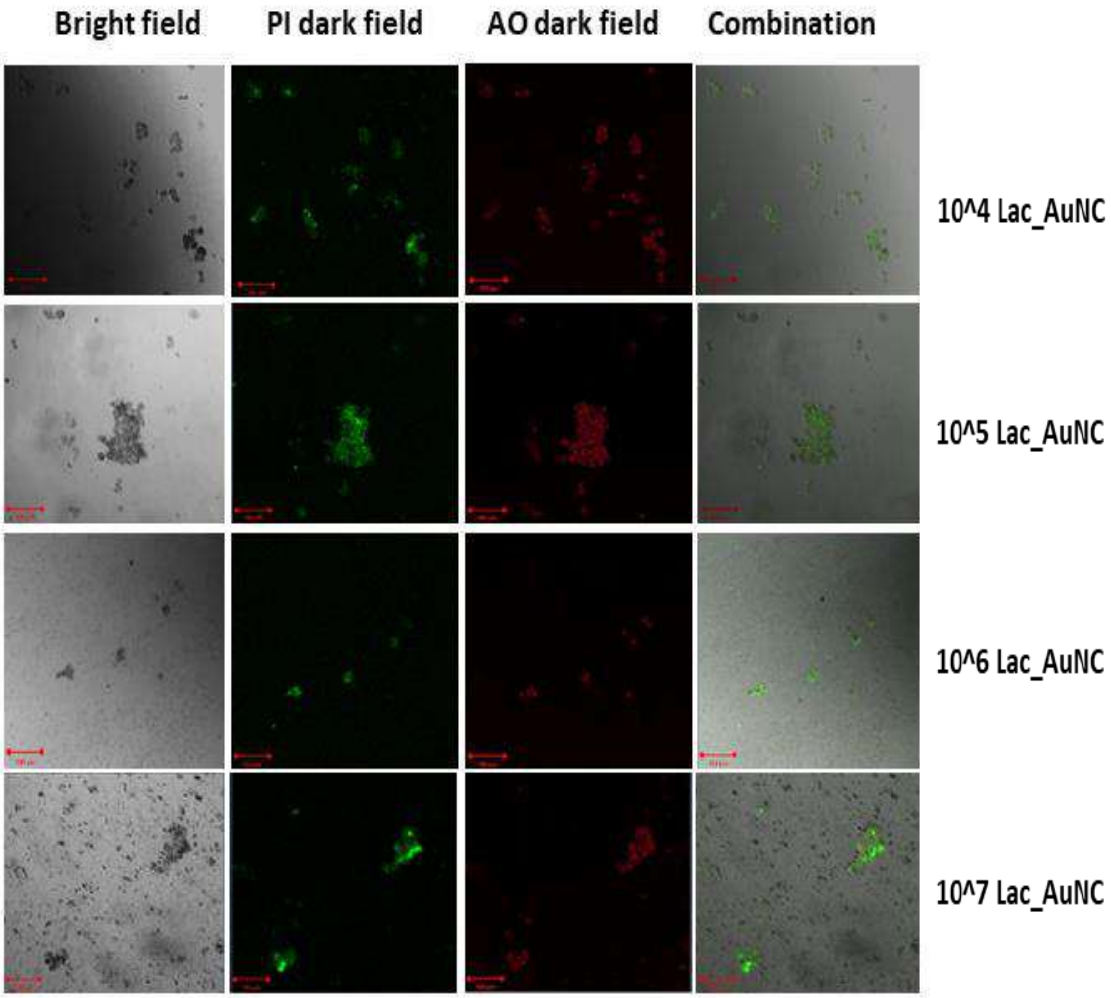

Figure 3.11. Confocal laser scanning microscopy. Propidium iodide/acridine orange dual staining images of live (green channel) and dead (red channel) HT29 monolayer cells treated with different concentrations of Lac_AuNC (as described in the legends).

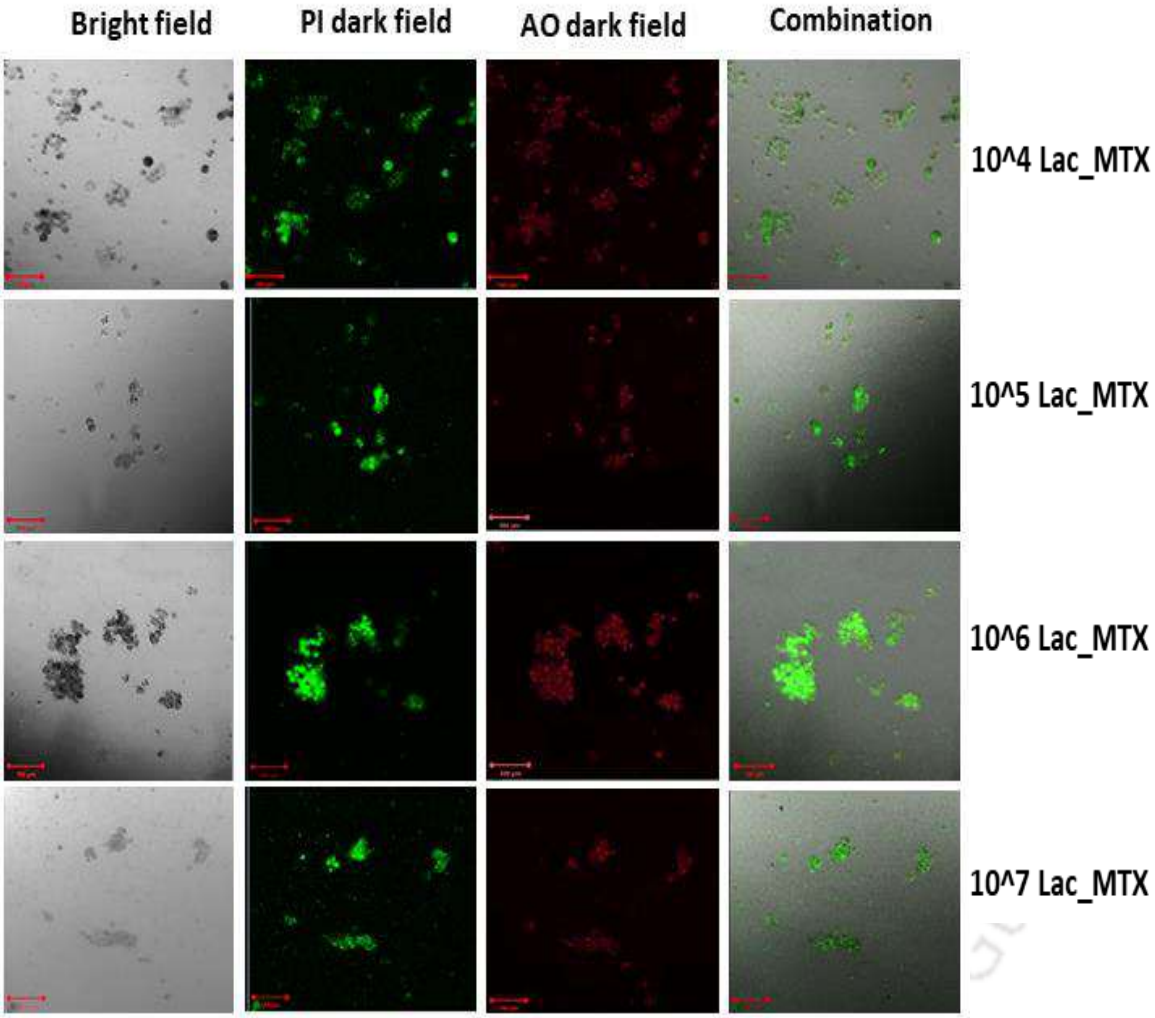

Figure 3.12 Confocal laser scanning microscopy. Propidium iodide/acridine orange dual staining images of live (green channel) and dead (red channel) HT29 monolayer cells treated with different concentrations of Lac_MTX (as described in the legends).

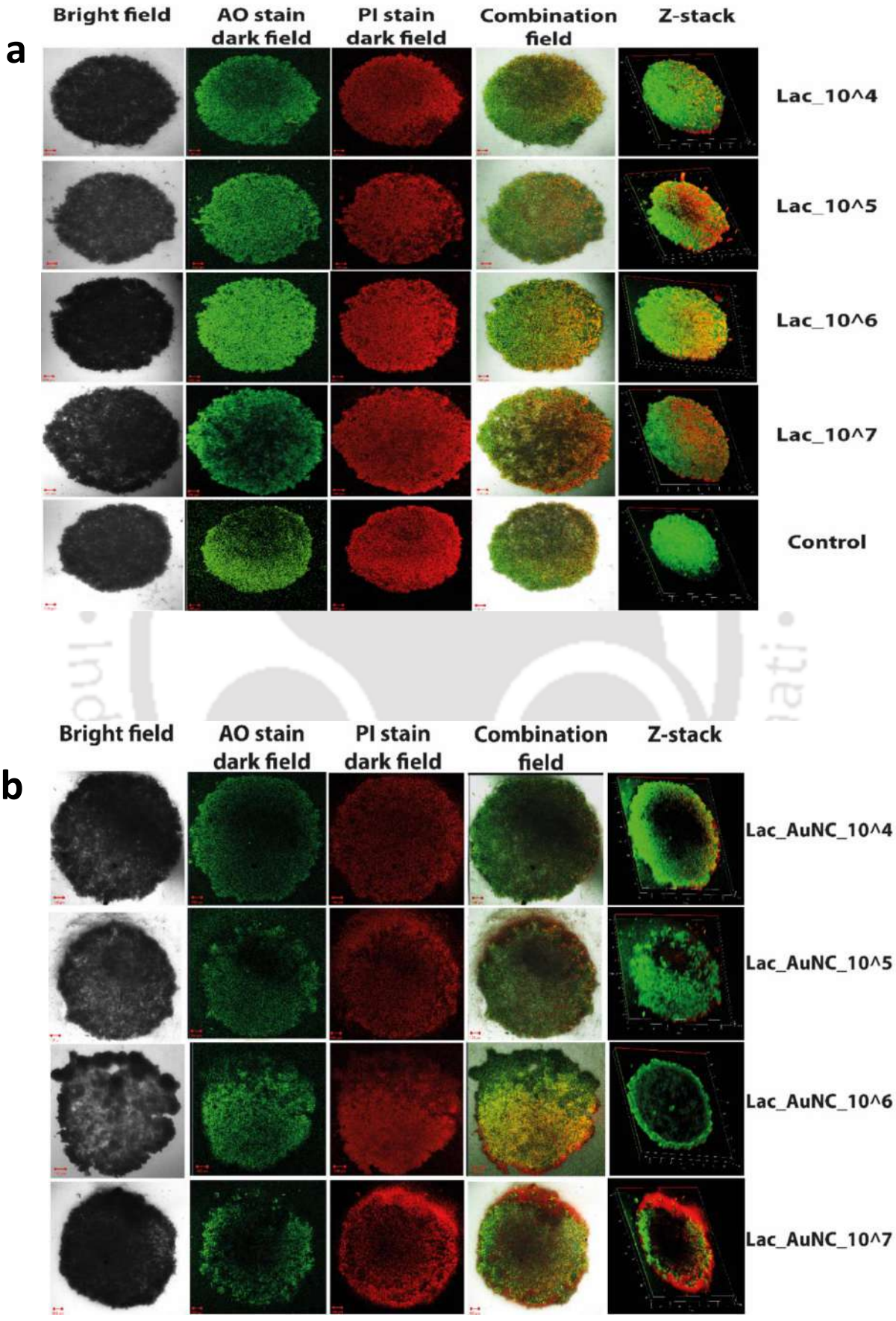

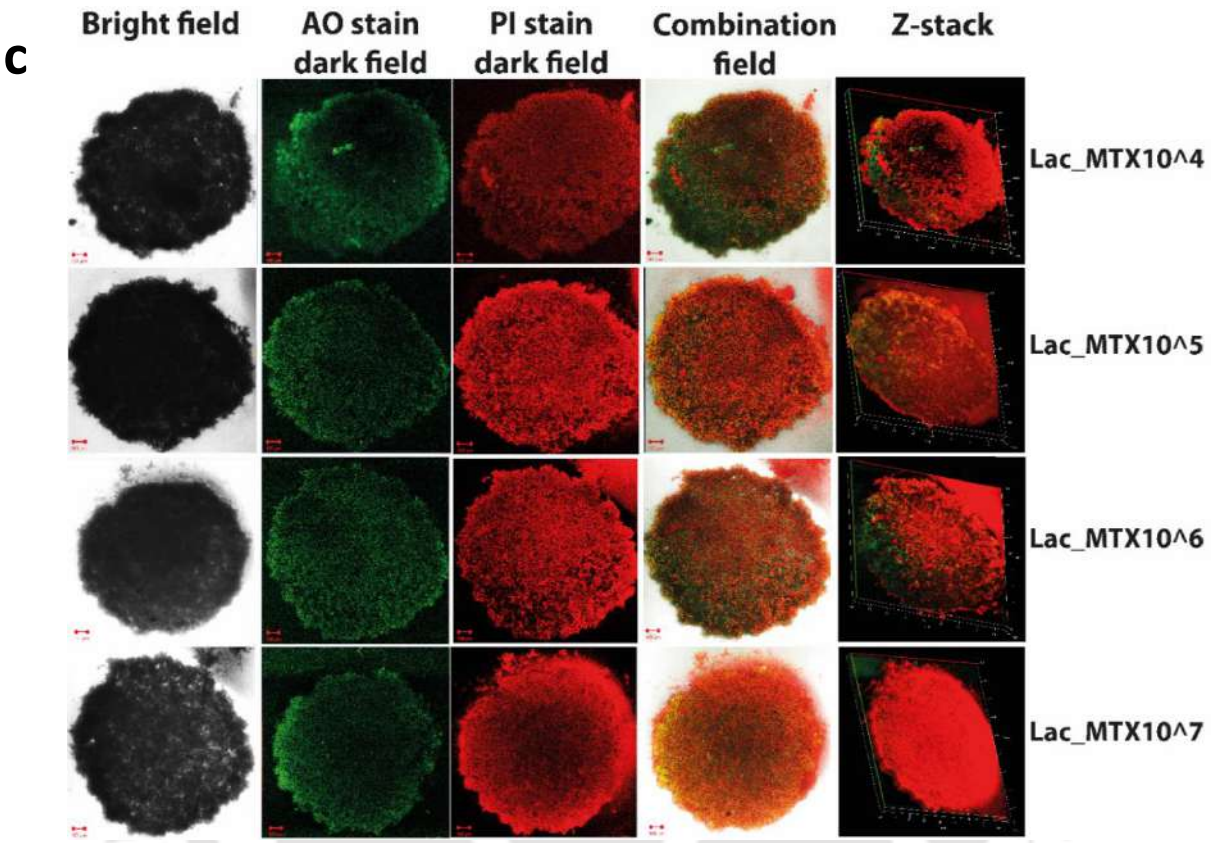

Figure 3.13. Confocal laser scanning microscopy images of (a) 3D spheroids of HeLa cells treated with different concentrations of control bacteria as described in legends, (b) 3D spheroids of HeLa cells treated with different concentrations of Lac_AuNC as described in legends and (c) 3D spheroids of HeLa cells treated with different concentrations of Lac_MTX as described in legends.

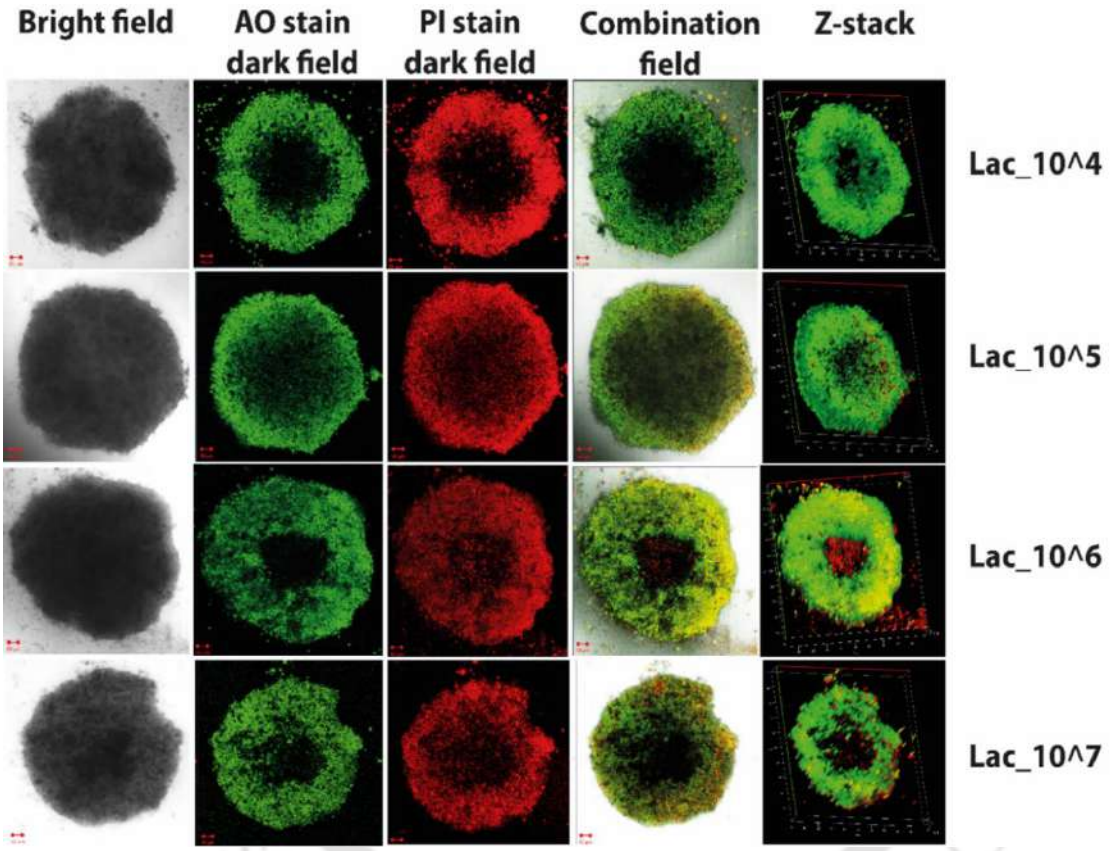

Figure 3.14. Confocal laser scanning microscopy. Propidium iodide/acridine orange dual staining images of live (green channel) and dead (red channel) spheroids of HT29 cells treated with different concentrations of control *Lactobacillus rhamnosus* (as described in the legends)

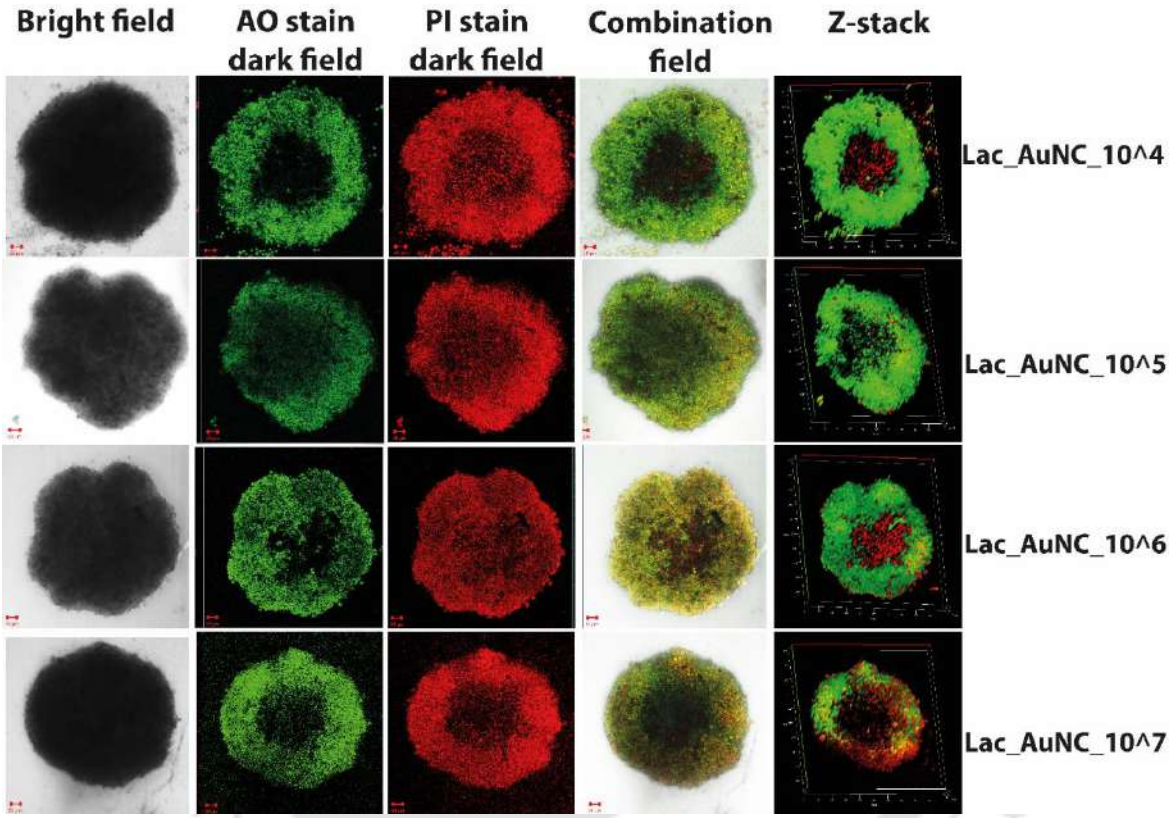

Figure 3.15. Confocal laser scanning microscopy. Propidium iodide/acridine orange dual staining images of live (green channel) and dead (red channel) spheroids of HT29 cells treated with different concentrations of Lac_AuNC (as described in the legends).

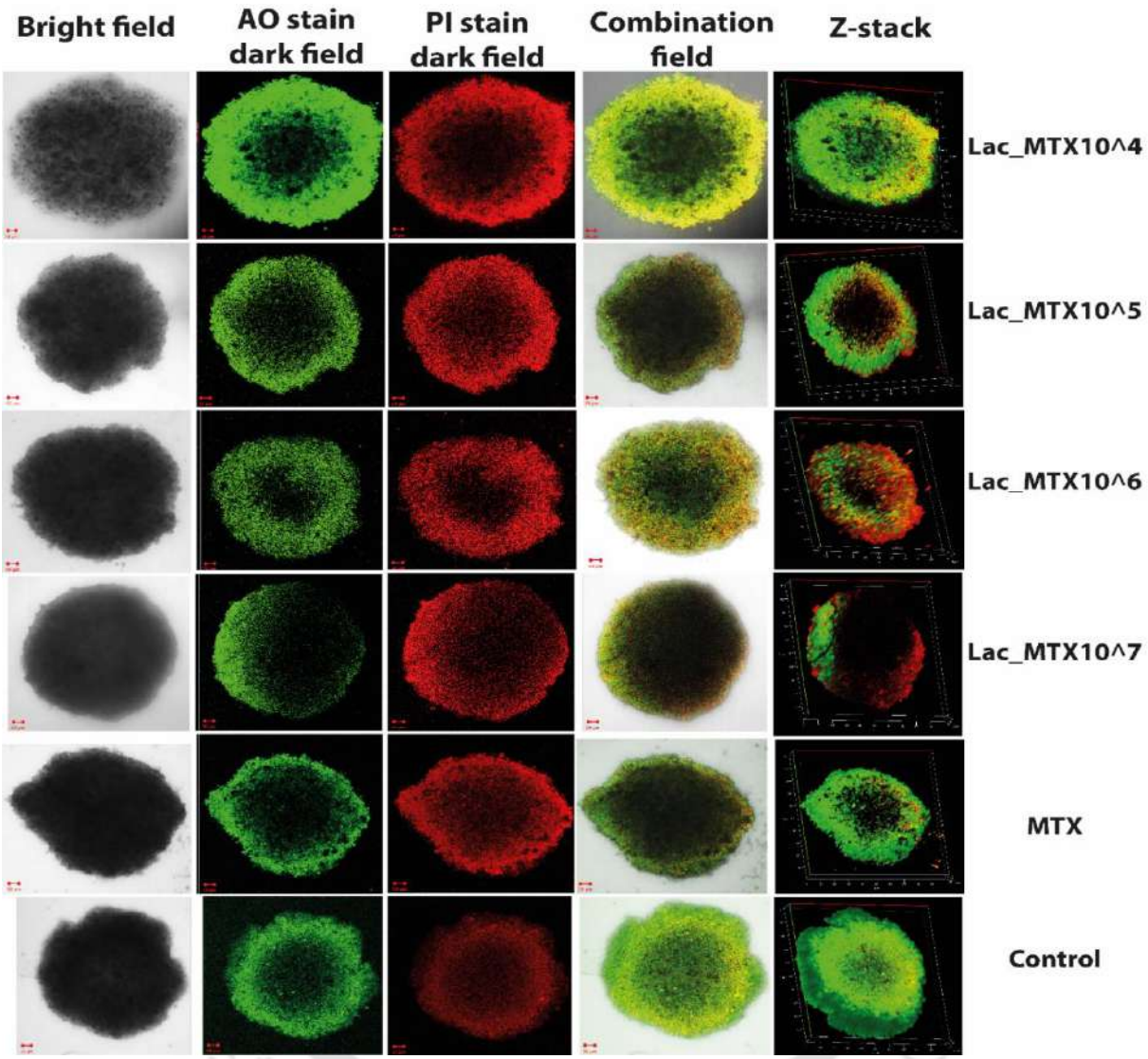

Figure 3.16. Confocal laser scanning microscopy. Propidium iodide/acridine orange dual staining images of live (green channel) and dead (red channel) spheroids of HT29 cells treated with different concentrations of Lac_MTX (as described in the legends).

3.3.8 ROS generation by Lac_MTX on monolayer and 3D spheroids of cells

The studies on mechanism of action by which the Lac_MTX acted on the cells was an important aspect to be determined. To investigate the role of production of reactive oxygen species (ROS) in the cells due to Lac_MTX, the cells treated with control *Lactobacillus rhamnosus*, Lac_AuNC and Lac_MTX and MTX were subjected to incubation with ROS sensing dye 2',7'-dichlorofluorescin diacetate (DCFHDA) that on diffusion into cells gets converted into full name (DCFH), which is a green fluorescent molecule. On excitation at 488 nm laser the fluorescence of DCFH was measured using a microtiter plate reader. The cells treated with Lac_MTX showed nearly 1.3 times and 2 times increase in ROS generations in both the monolayer and spheroids of HeLa and HT29 cells. The control *Lactobacillus rhamnosus* and Lac_AuNC treated cells also showed detectable levels of ROS in them that were similar to ROS generated from untreated cells. This could be due to the amount of ROS generated in the cells as a result of various metabolic activities. However, the elevated levels of ROS in Lac_MTX treated cells were due to the cytotoxicity. The ROS generation in MTX treated monolayer cells and spheroids were similar to that of the control cells. So, it can be concluded that the treatment of Lac_MTX on the spheroids and monolayer of both HT29 and HeLa cells had generated about twice as much as compared to control bacteria and Lac_AuNC (Figure 3.17 to Figure 3.20). Some studies suggest that the colon cancer regression by *Lactobacillus rhamnosus* GG occurs via downregulation of NFkB through ROS generation and hence causes apoptosis.[8] In correlation with the study it may be concluded that the ROS generation could have led to the cell death in the present cases. Although ROS generation could be only one of the factors leading to the cytotoxicity but seems to play vital role in cell killing.

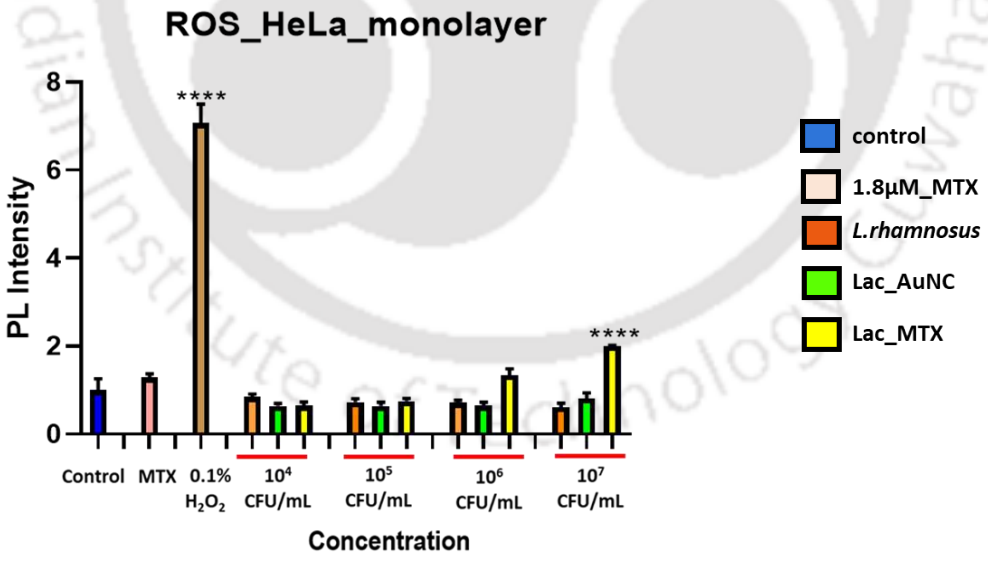

Figure 3.17. Reactive oxygen species generation assay. Determination of ROS generation on monolayer of HeLa cells treated with different concentration of *Lactobacillus rhamnosus,* Lac_AuNC and Lac_MTX (as described in the legends). Statistical significance is represented **** ($p < 0.0001$). The values are represented as mean ± standard deviation (SD) of three individual experiments.

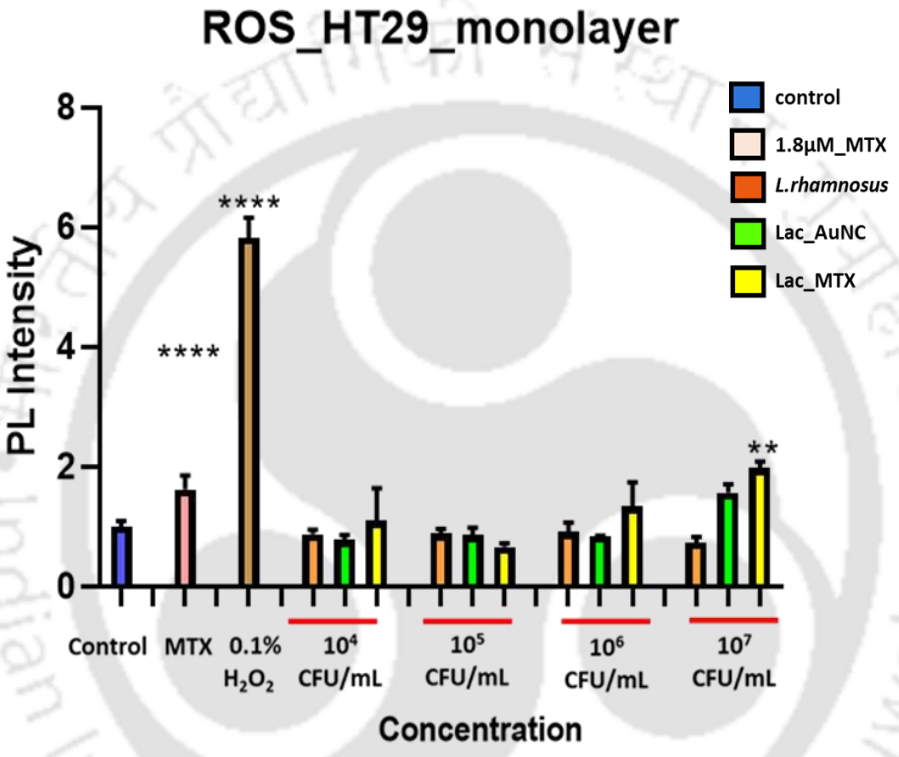

Figure 3.18. Reactive oxygen species generation assay. Determination of ROS generation on spheroids of HeLa cells treated with different concentration of *Lactobacillus rhamnosus*, Lac_AuNC and Lac_MTX (as described in the legends). Statistical significance is represented by ** ($p<0.01$), *** ($p < 0.001$), and **** ($p < 0.0001$). The values are represented as mean ± standard deviation (SD) of three individual experiments.

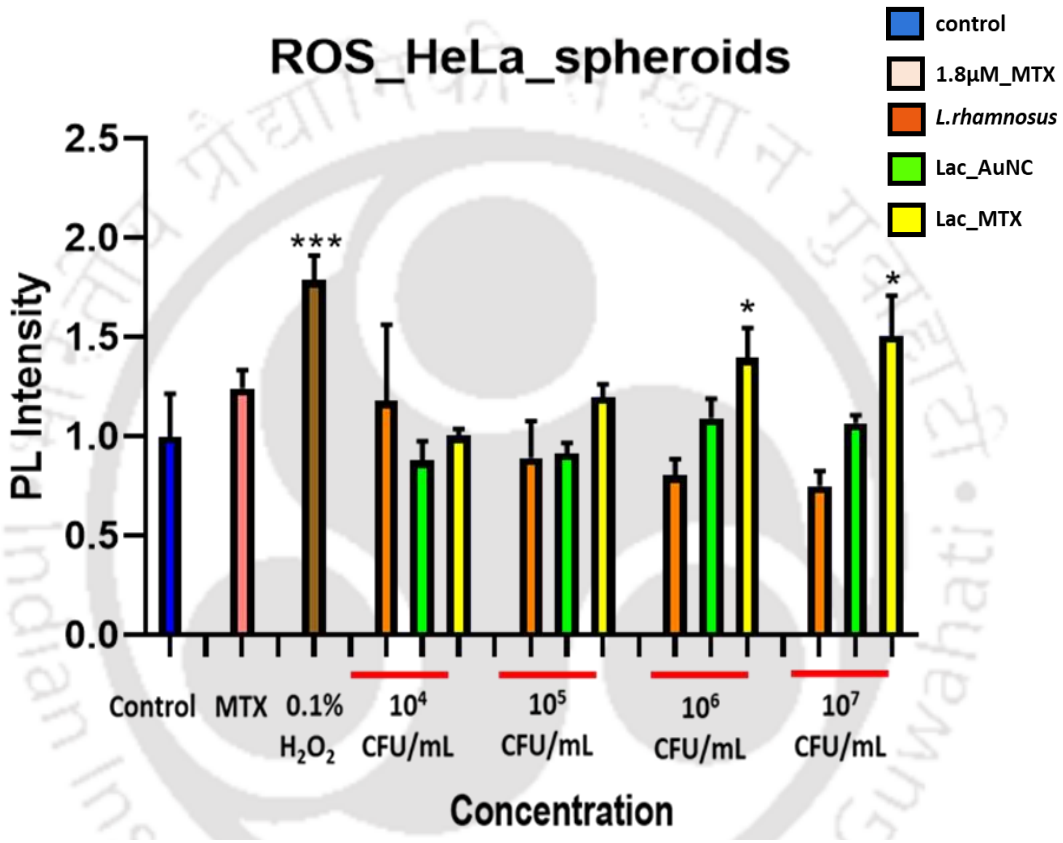

Figure 3.19. Reactive oxygen species generation assay. Determination of ROS generation on monolayer of HT29 cells treated with different concentration of *Lactobacillus rhamnosus*, Lac_AuNC and Lac_MTX (as described in the legends). Statistical significance is represented by ** ($p<0.01$), *** ($p < 0.001$), and **** ($p < 0.0001$). The values are represented as mean ± standard deviation (SD) of three individual experiments.

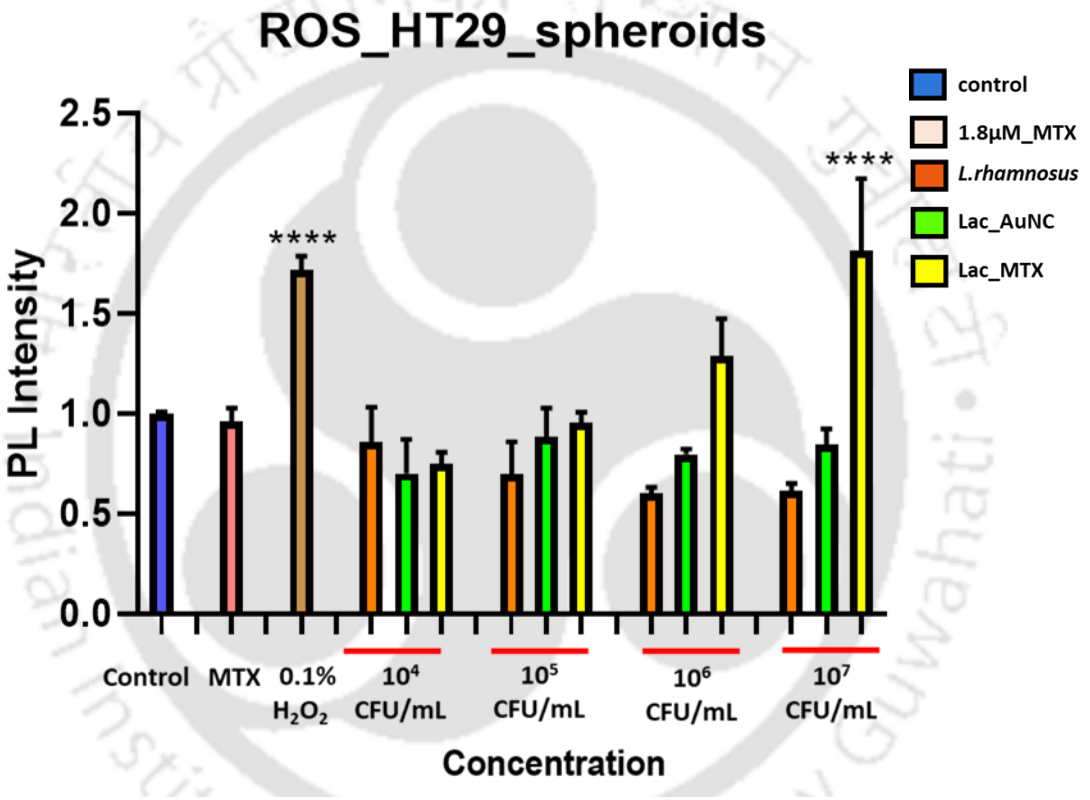

Figure 3.20. Reactive oxygen species generation assay. Determination of ROS generation on spheroids of HT29 cells treated with different concentration of *Lactobacillus rhamnosus*, Lac_AuNC and Lac_MTX (as described in the legends). Statistical significance is represented by ** ($p<0.01$), *** ($p < 0.001$), and **** ($p < 0.0001$). The values are represented as mean ± standard deviation (SD) of three individual experiments.

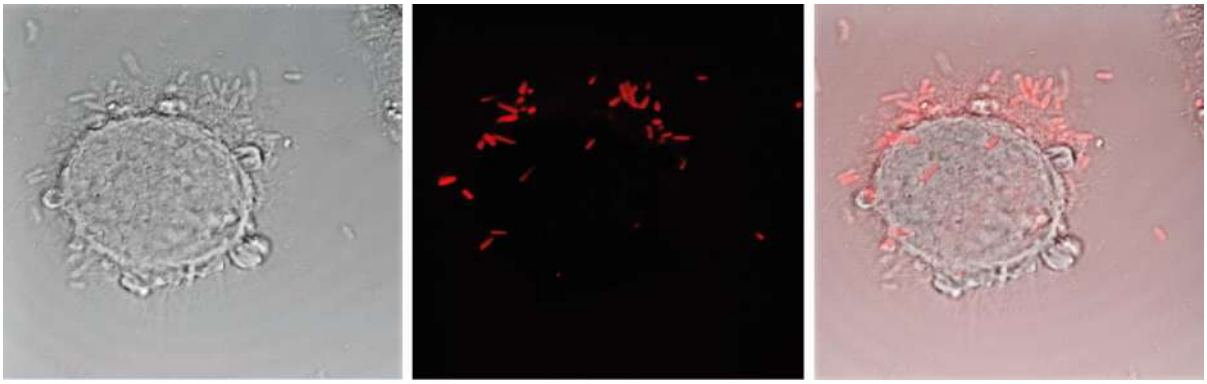

Figure 3.21. Confocal laser scanning microscopy. CLSM images of Lac_MTX treated Hela cells.

3.4 Conclusions

The current study reported the development of a bacteria mediated drug delivery system that consisted of human gut friendly bacteria *Lactobacillus rhamnosus*, AuNCs and anticancer drug MTX loaded on them. The lactic acid bacteria are safer strains to work with and have inherent anti-cancer and anti-proliferative properties. Additionally, the wildtype bacteria used reduces the time and complexity of attenuating the bacterial strain for practical usage. AuNCs were synthesized on the outer surface of the bacteria, following chemical reduction method, that rendered them fluorescent. Further, MTX was loaded on the nanocluster studded living bacteria and they were used to deliver the drug to the monolayer and 3D spheroids of cervical cancer cells and colon cancer cells. The cytotoxicity of the drug loaded bacteria (Lac_MTX) was evaluated by MTT assay (monolayer of cells) and alamar blue assay (spheroids). The results affirmed that the Lac_MTX treatment caused the maximum cytotoxicity on the monolayer and spheroids of cancer cells as compared to only drug, control bacteria and Lac_AuNC. Further, as the results suggested, the ROS generation by Lac_MTX could have interfered with the intracellular activities and caused the enhanced toxicity. The high toxicity of Lac_MTX at lower concentration of bacteria (10^4 to 10^7) projects a possibility of reduced risk of recurrences. The current work demonstrated the ability of drug encapsulation onto the bacteria directly -via the use of AuNCs- without hampering their viability and efficiency. This study establishes a novel method of using non-genetically modified living bacteria that can serve as a model drug delivery system ('bacbot'), which invades targeted cells and tissues while being alive upon incorporation of nanoscale metal particles and anticancer drug. Thus, the model bacbots presented here hold promise for furthering the field of nanomedicine with the ease of multifunctionality, enhancing efficiency and target specificity.

3.5 References

(1) Zhou, S.; Gravekamp, C.; Bermudes, D.; Liu, K. Tumour-Targeting Bacteria Engineered to Fight Cancer. *Nat. Rev. Cancer.* **2018**, *18* (12), 727–743.

(2) Liang, K.; Liu, Q.; Li, P.; Han, Y.; Bian, X.; Tang, Y.; Kong, Q. Endostatin Gene Therapy Delivered by Attenuated Salmonella Typhimurium in Murine Tumor Models. *Cancer Gene Ther.* **2018**, 25(7-8):167-183.

(3) Gao, Z.; Zhang, E.; Zhao, H.; Xia, S.; Bai, H.; Huang, Y.; Lv, F.; Liu, L.; Wang, S. Bacteria-Mediated Intracellular Click Reaction for Drug Enrichment and Selective Apoptosis of Drug-Resistant Tumor Cells. *ACS Appl. Mater. Interfaces.* **2022**, *14* (10), 12106–12115.

(4) Chen, C.; Wang, P.; Chen, H.; Wang, X.; Halgamuge, M. N.; Chen, C.; Song, T. Smart Magnetotactic Bacteria Enable the Inhibition of Neuroblastoma under an Alternating Magnetic Field. *ACS Appl. Mater. Interfaces.* **2022**, *14* (12), 14049–14058.

(5) Toussaint, B.; Chauchet, X.; Wang, Y.; Polack, B.; Gouëllec, A. Le. Live-Attenuated Bacteria as a Cancer Vaccine Vector. *Expert Rev. Vaccines.* **2013**, *12* (10), 1139–1154.

(6) Azam, R.; Ghafouri-Fard, S.; Tabrizi, M.; Modarressi, M. H.; Ebrahimzadeh-Vesal, R.; Daneshvar, M.; Mobasheri, M. B.; Motevaseli, E. Lactobacillus Acidophilus and Lactobacillus Crispatus Culture Supernatants Downregulate Expression of Cancer-Testis Genes in the MDA-MB-231 Cell Line. *Asian Pacific J. Cancer Prev.* **2014**, *15* (10), 4255–4259.

(7) Roy, S.; Trinchieri, G. Microbiota: A Key Orchestrator of Cancer Therapy. *Nat. Rev. Cancer.* **2017**, *17* (5), 271–285.

(8) Gamallat, Y.; Meyiah, A.; Kuugbee, E. D.; Hago, A. M.; Chiwala, G.; Awadasseid, A.; Bamba, D.; Zhang, X.; Shang, X.; Luo, F.; Xin, Y. *Lactobacillus Rhamnosus* Induced Epithelial Cell Apoptosis, Ameliorates Inflammation and Prevents Colon Cancer Development in an Animal Model. *Biomed. Pharmacother.* **2016**, *83*, 536–541.

(9) Wong, S. H.; Yu, J. Gut Microbiota in Colorectal Cancer: Mechanisms of Action and Clinical Applications. *Nature Reviews Gastroenterology and Hepatology*. *Springer US*. 2019, 690–704.

(10) Zitvogel, L.; Daillère, R.; Roberti, M. P.; Routy, B.; Kroemer, G. Anticancer Effects of the Microbiome and Its Products. *Nat. Rev. Microbiol.* **2017**, *15* (8), 465–478.

(11) Tiptiri-Kourpeti, A.; Spyridopoulou, K.; Santarmaki, V.; Aindelis, G.; Tompoulidou, E.; Lamprianidou, E. E.; Saxami, G.; Ypsilantis, P.; Lampri, E. S.; Simopoulos, C.; Kotsianidis, I.; Galanis, A.; Kourkoutas, Y.; Dimitrellou, D.; Chlichlia, K. Lactobacillus Casei Exerts Anti-Proliferative Effects Accompanied by Apoptotic Cell Death and up-Regulation of TRAIL in Colon Carcinoma Cells. *PLoS One.* **2016**, *11* (2), 1–20.

(12) Jacouton, E.; Michel, M. L.; Torres-Maravilla, E.; Chain, F.; Langella, P.; Bermúdez-Humarán, L. G. Elucidating the Immune-Related Mechanisms by Which Probiotic Strain *Lactobacillus Casei* BL23 Displays Anti-Tumoral Properties. *Front. Microbiol.* **2019**, 1–10.

(13) Shende, P.; Basarkar, V. Recent Trends and Advances in Microbe-Based Drug Delivery Systems. *DARU, J. Pharm. Sci.* **2019**, *27* (2), 799–809.

(14) Isabella, V. M.; Ha, B. N.; Castillo, M. J.; Lubkowicz, D. J.; Rowe, S. E.; Millet, Y. A.; Anderson, C. L.; Li, N.; Fisher, A. B.; West, K. A.; Reeder, P. J.; Momin, M. M.; Bergeron, C. G.; Guilmain, S. E.; Miller, P. F.; Kurtz, C. B.; Falb, D. Development of a Synthetic Live Bacterial Therapeutic for the Human Metabolic Disease Phenylketonuria. *Nat. Biotechnol.* **2018**, *36* (9), 857–867.

(15) Herrera Estrada, L.; Padmore, T. J.; Champion, J. A. Bacterial Effector Nanoparticles as Breast Cancer Therapeutics. *Mol. Pharm.* **2016**, *13* (3), 710–719.

(16) Riglar, D. T.; Silver, P. A. Engineering Bacteria for Diagnostic and Therapeutic Applications. *Nat. Rev. Microbiol.* **2018**, *16* (4), 214–225.

(17) Chen, H.; Li, Y.; Wang, Y.; Ning, P.; Shen, Y.; Wei, X.; Feng, Q.; Liu, Y.; Li, Z.; Xu, C.; Huang, S.; Deng, C.; Wang, P.; Cheng, Y. An Engineered Bacteria-Hybrid Microrobot with the Magnetothermal Bioswitch for Remotely Collective Perception and Imaging-Guided Cancer Treatment. *ACS Nano.* **2022**, *16* (4), 6118–6133.

(18) Akin, D.; Sturgis, J.; Ragheb, K.; Sherman, D.; Burkholder, K.; Robinson, J. P.; Bhunia, A. K.; Mohammed, S.; Bashir, R. Bacteria-Mediated Delivery of Nanoparticles and Cargo into Cells. *Nat. Nanotechnol.* **2007**, *2* (7), 441–449.

(19) Swofford, C. A.; St. Jean, A. T.; Panteli, J. T.; Brentzel, Z. J.; Forbes, N. S. Identification of *Staphylococcus aureus* α-Hemolysin as a Protein Drug That Is Secreted by Anticancer Bacteria and Rapidly Kills Cancer Cells. *Biotechnol. Bioeng.* **2014**, *111* (6), 1233–1245.

(20) Akolpoglu, M. B.; Alapan, Y.; Dogan, N. O.; Baltaci, S. F.; Yasa, O.; Tural, G. A.; Sitti, M. Magnetically Steerable Bacterial Microrobots Moving in 3D Biological Matrices for Stimuli-Responsive Cargo Delivery. *Sci. Adv.* **2022**, *8* (28), 1–15.

(21) Sedighi, M.; Zahedi Bialvaei, A.; Hamblin, M. R.; Ohadi, E.; Asadi, A.; Halajzadeh, M.; Lohrasbi, V.; Mohammadzadeh, N.; Amiriani, T.; Krutova, M.; Amini, A.; Kouhsari, E. Therapeutic Bacteria to Combat Cancer; Current Advances, Challenges, and Opportunities. *Cancer Med.* **2019**, *8* (6), 3167–3181.

(22) Jiang, T.; Yang, X.; Li, G.; Zhao, X.; Sun, T.; Müller, R.; Wang, H.; Li, M.; Zhang, Y. Bacteria-Based Live Vehicle for in Vivo Bioluminescence Imaging. *Anal. Chem.* **2021**, *93* (47), 15687–15695.

(23) Zhan, Y.; Fergusson, A.; McNally, L. R.; Davis, R. M.; Behkam, B. Robust and Repeatable Biofabrication of Bacteria-Mediated Drug Delivery Systems: Effect of Conjugation Chemistry, Assembly Process Parameters, and Nanoparticle Size. *Adv. Intell. Syst.* **2022**, *4* (3), 2100135.

(24) Yang, M.; Yang, F.; Chen, W.; Liu, S.; Qiu, L.; Chen, J. Bacteria-Mediated Cancer Therapies: Opportunities and Challenges. *Biomater. Sci.* **2021**, *9* (17), 5732–5744.

(25) Zhang, Y.; Pan, T.; Li, C. X.; Zheng, D.; Sun, Y.; Zhang, X. Z. Double Bacteria Synergistic Catalytic Reduction System for Heavy Metal Detoxification Treatment. *Nano Lett.* **2022**, *22* (13), 5575–5583.

(26) Reghu, S.; Miyako, E. Nanoengineered Bifidobacterium Bifidum with Optical Activity for Photothermal Cancer Immunotheranostics. *Nano Lett.* **2022**, *22* (5), 1880–1888.

(27) Fan, J. X.; Li, Z. H.; Liu, X. H.; Zheng, D. W.; Chen, Y.; Zhang, X. Z. Bacteria-Mediated Tumor Therapy Utilizing Photothermally-Controlled TNF-α Expression via Oral Administration. *Nano Lett.* **2018**, *18* (4), 2373–2380.

(28) Mi, Z.; Guo, L.; Liu, P.; Qi, Y.; Feng, Z.; Liu, J.; He, Z.; Yang, X.; Jiang, S.; Wu, J.; Ding, J.; Zhou, W.; Rong, P. 'trojan Horse' Salmonella Enabling Tumor Homing of Silver Nanoparticles via Neutrophil Infiltration for Synergistic Tumor Therapy and Enhanced Biosafety. *Nano Lett.* **2021**, *21* (1), 414–423.

(29) Zheng, P.; Fan, M.; Liu, H.; Zhang, Y.; Dai, X.; Li, H.; Zhou, X.; Hu, S.; Yang, X.; Jin, Y.; Yu, N.; Guo, S.; Zhang, J.; Liang, X. J.; Cheng, K.; Li, Z. Self-Propelled and Near-Infrared-Phototaxic Photosynthetic Bacteria as Photothermal Agents for Hypoxia-Targeted Cancer Therapy. *ACS Nano.* **2021**, *15* (1), 1100–1110.

(30) Pan, P.; Dong, X.; Chen, Y.; Zeng, X.; Zhang, X. Z. Engineered Bacteria for Enhanced Radiotherapy against Breast Carcinoma. *ACS Nano.* **2022**, *16* (1), 801–812.

(31) Fan, J. X.; Li, Z. H.; Liu, X. H.; Zheng, D. W.; Chen, Y.; Zhang, X. Z. Bacteria-Mediated Tumor Therapy Utilizing Photothermally-Controlled TNF-α Expression via Oral Administration. *Nano Lett.* **2018**, *18* (4), 2373–2380.

(32) Debasmita, D.; Ghosh, S. S.; Chattopadhyay, A. Hierarchical Passage of Gold Nanoclusters in Living Bacteria. *ACS Appl. Bio Mater.* **2022**. *5*(6), 2543–2548.

(33) Kusters, J.G.; Mulders-Kremers, G.A.W.M.; Doornik, C.E.M.V.; Zeijst, B.A.M.V. Effects of multiplicity of infection, bacterial protein synthesis and growth phase on adhesion to and invasion of human cell lines by *Salmonella typhimurium*. Infect.Immun. **1993**, *61*(12), 5013-5020.

(34) Nouri, Z.; Karami, F.; Neyazi, N.; Modarressi, M. H.; Karimi, R.; Khorramizadeh, M. R.; Taheri, B.; Motevaseli, E. Dual Anti-Metastatic and Anti-Proliferative Activity Assessment of Two Probiotics on HeLa and HT-29 Cell Lines. *Cell J.* **2016**, *18* (2), 127–134.

(35) Azam, R.; Ghafouri-Fard, S.; Tabrizi, M.; Modarressi, M. H.; Ebrahimzadeh-Vesal, R.; Daneshvar, M.; Mobasheri, M. B.; Motevaseli, E. Lactobacillus Acidophilus and Lactobacillus Crispatus Culture Supernatants Downregulate Expression of Cancer-Testis Genes in the MDA-MB-231 Cell Line. *Asian Pacific J. Cancer Prev.* **2014**, *15* (10), 4255–4259.

Chapter 4

Nano-Enabled Bacbots for *S.aureus* Biofilm Eradication

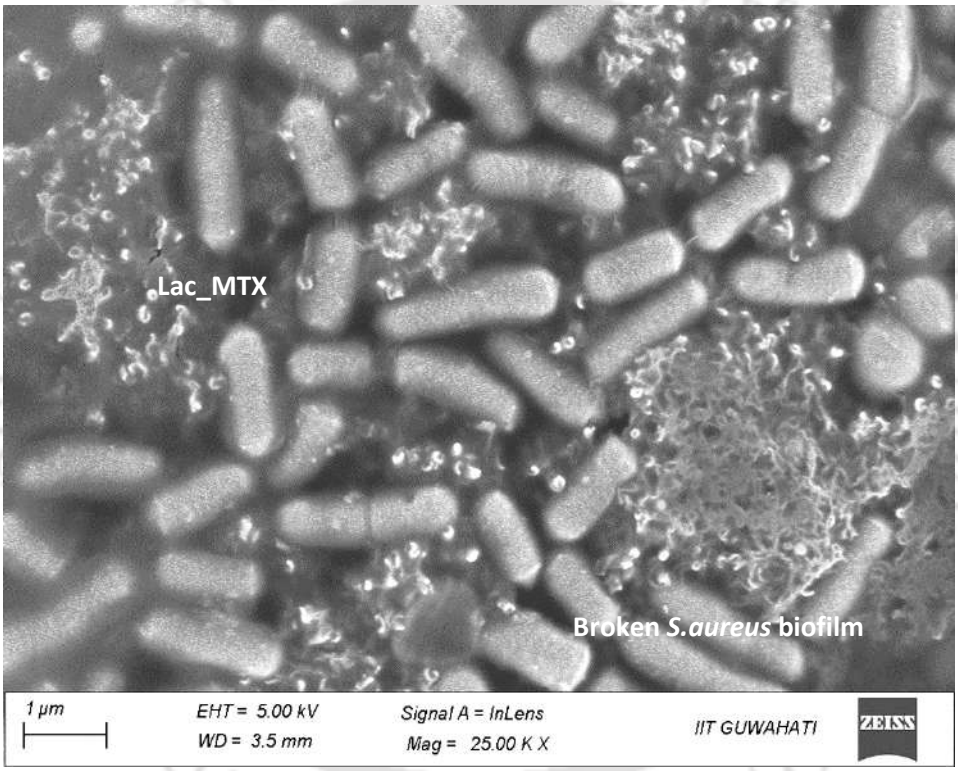

Abstract

The onset of cancer gets aggravated with the advent of secondary infections such as those caused by microbes. The prevalent pathogens are *S.aureus, P.aeruginosa, Klebseilla*, and *Streptococcus*. The havoc created by *S.aureus* is frequently observed in cancer patients who are immunocompromised, co-morbid, and are repeatedly exposed to the pathogen. The resistant strains are difficult to fight with the high doses of antibiotics as the health of the individuals is jeopardized. The challenge can be mitigated with therapeutic options to which resistance would not be developed easily. The *Lactobacillus* strains are mechanized against the *S.aureus* pathogen. The current study was taken up to explore the application of live *Lactobacillus* based bacbots that were fabricated with gold nanoclusters and methotrexate to combat the pathogen synergistically. The bacbots were motile and self- propelling by virtue of the bacteria used. The gold nanoclusters on the bacterial surface rendered them fluorescence and were helpful for the incorporation of the drug. These bacbots were effective against the planktonic *S. aureus* and also eradicated their biofilms up to 90-95% by a concentration of 10^7cfu/mL used against the consortium of biofilm. In our previous study, these bacbots had showed their anti-cancer effects on spheroids of cancers. It can be inferred that, these bacbots can be effective as a therapeutic module that can act on cancer and prevent secondary infections.

4.1 Introduction

Biofilms are physically distinct microhabitats where microbes establish interactions, accumulate and exchange nutrients and build a physicochemical environment among themselves. The extra polymeric substance (EPS) provides a matrix for the biofilm such that the microbes reside in as micro-colonies [1]. The biofilm formation is a multi-step process. In the beginning, the microbe attaches to a suitable substratum and establishes interactions with the previously existing microbes and forms micro-colonies. There are motile members in the biofilm that occasionally move out and swims to form the biofilm at a new site. Thus, planktonic stage is achieved again. The EPS gives firmness to the biofilm by acting as a scaffold [2]. The environmental factors (presence of glucose and citrate in substrate; presence of other microbial species) also play vital role in triggering the biofilm initiation mediated via second messenger molecules [3]. The biofilms provide anti-biotic resistance [4] to the sessile bacterium that is 10-1000 times more than the planktonic counterpart and they are responsible for nosocomial infections, corrosions and bio-fouling [5]. *S.aureus,* a gram positive bacteria, throws major challenge as far as biofilm eradication is concerned [6,7]. They can form films on medical devices such as central venous catheter [8]. The pathogenic bacteria cause bacteremia in cancer patients who are more susceptible due to repeated exposures to invasive procedures, medical visits, and immunocompromised state due the chemotherapy. The blood stream infection (BSI) is a major contributor of secondary infections in cancer patients [9, 10, 11] . Sometimes the absence of proper guidelines for antineoplastic chemotherapy (leads patients' to immunocompromised state) has been noticed in patients infected with multi-drug resistant *S.aureus* (MRSA) [12]. There is a paucity of required information about the central venous catheter system and its management during bacteremia in cancer patients. The samples collected from such patients showed presence of MRSA. Thus, a scanty amount of data is available about the management of secondary infections. The major treatment regimen includes use of antibiotics,

that fail miserably in case of drug resistant strains, or vaccines. The timings and related outcomes of the vaccines are not well standardized so an effective solution is still lacking.

Lactic acid bacteria are known to produce bacteriocin against *Staphylococcus aureus* [13, 14, 15, 16]. The bacteriocins of *Lactobacillus rhamnosus* are the reason of the anti-biofilm effect. *Lactobacillus rhamnosus* can form biofilm if grown in MRS media without any glucose supplements [17]. The mechanism of anti-biofilm activity is either shift in the pH or the proteins produced by the lactic acid bacteria [18]. The *Lactobacillus casei* and *Lactobacillus acidophilus* inhibit the growth of *Staphylococcus aureus* [19, 20,21]. The bacteria often develops resistance against antibiotics [22]. When different strains of bacteria reside in same habitat, they compete for resources. This competition can either be exploitative or interfering. The exploitative mode of competition represents one strain completely syphoning the nutrition and deplete the others. On the other hand, the interference mode means producing antagonistic effects on the other strains in order to lag their growth. However, some bacteria have developed mechanism to build competitive fitness by producing antibiotics, sporulation, and biofilm formation [23].

Herein, a bacbot has been developed based on living *Lactobacillus rhamnosus* bearing gold nanoclusters and anticancer drug methotrexate. The drug doesn't have profound inhibitory effect on the *Lactobacillus* but has anti-staphylococcal effects. The anti-bacterial properties of the bacbots were studied that led to the extensive study of their effect on the *S.aureus* biofilms. The drug loaded on the bacteria showed a synergistic effect on the *Staphylococcus aureus* biofilm. The lawn culture (10^9 cfu/mL) had a zone of inhibition created by treatment of bacbot (10^7 cfu/mL) that counts for a multiplicity of infection of 0.01 (100 *Staphylococcus aureus* bacterium per bacbot). The bacbots were able to efficiently eradicate the biofilms up to 90-95%. This bacbot was previously studied as an anti-cancer agent and the current study enlightens the anti-biofilm effect of these bacbots. Thus, a two-in-one therapeutic module was developed for simultaneously using for cancer and cancer associated infections caused by *S.aureus* in future.

4.2 Materials and Methods

4.2.1 Bacterial culture maintenance

The bacterial cultures of *Staphylococcus aureus* MTCC 96 and *Lactobacillus rhamnosus* MTCC 1408 were procured from MTCC. The *Staphylococcus aureus* culture was grown in brain heart infusion (BHI) broth at 37 °C and 180 rpm for 12 h. Whereas, the *Lactobacillus rhamnosus* culture was grown in MRS medium at 37 °C and 180 rpm for 48 h. The late log phase grown cultures were stored at 4 °C and were sub-cultured at a time interval of 10-15 days. Every time the experiments were executed using fresh cultures of the bacteria.

4.2.2 Synthesis of gold nanoclusters on living *Lactobacillus rhamnosus*

The *Lactobacillus rhamnosus* culture grown in MRS medium were taken and centrifuged at 10,000 rpm for 5 min. The pellet was washed thrice using double autoclaved deionized water. Then 2mM of $HAuCl_4$ was added on to the pellet re-suspended with de-ionized water. Then 3-mercaptopropionic acid was added to the mixture and was allowed to incubate for 5 min at 37 °C

in a water bath and then the product medium was centrifuged to get rid of the unreacted components. The residual pellet was collected for further use (Lac_AuNC).

4.2.3 Determination of minimum inhibitory concentration of methotrexate on *Lactobacillus rhamnosus*

The *Lactobacillus rhamnosus* culture was inoculated (1% inoculum) in to freshly prepared MRS medium. This was allowed to grow at 37 °C and 180 rpm for 48 h and served as the control group of the experiment. Simultaneously, 1% inoculum were added to MRS medium containing different concentrations of the methotrexate (MTX) drug in separate test tubes. The absorbance of the cultures was measured at 595 nm. The absorbance of the culture grown in MTX free MRS medium served as the control. The viability% of the treatment groups was calculated to determine the minimum inhibitory concentration of methotrexate (MTX) on *Lactobacillus rhamnosus*.

4.2.4 Encapsulation of MTX on Synthesized Lac_AuNC

The encapsulation of methotrexate (MTX) was done by incubating 5µM of methotrexate with Lac_AuNC for 1h at 37 °C and the unreacted components were centrifuged and discarded. The pellet containing MTX bound Lac_AuNC were collected for further use (Lac_MTX).

4.2.5 Medium compatibility of *Lactobacillus rhamnosus*

The compatibility of *Lactobacillus rhamnosus* in BHI medium was determined by inoculating 1% of the culture in to both MRS and BHI media. The culture tubes were allowed to incubate for 48 h at 37 °C. The absorbance of both the cultures was measured at 595 nm.

4.2.6 Anti-bacterial effect of Lac_MTX

The late log phase grown *Staphylococcus aureus* were inoculated (1%) into BHI medium containing 1% of different concentration (10^4,10^5,10^6 and 10^7 cfu/mL) of *Lactobacillus rhamnosus*, Lac_AuNC and Lac_MTX. The *Staphylococcus aureus* cultures were allowed to grow for 12 h at 37 °C. The absorbance was measured at 595 nm. The absorbance of the control groups containing only the *Lactobacillus rhamnosus*, Lac_AuNC and Lac_MTX without *Staphylococcus aureus* were also measured for accurate measurement of actual *Staphylococcus aureus* growth in presence of the treatment groups. The final calculations were made by subtracting the absorbance of the treatment groups alone from the absorbance of co-cultured groups.

4.2.6 Determination of Zone of Inhibition (ZOI)

The effect of *Lactobacillus rhamnosus*, Lac_MTX and 1.8 µM of MTX on the *Staphylococcus aureus* culture was determined by plating *Staphylococcus aureus* on BHI agar plates to this 100 µL of the treatment groups (10^7 cfu/mL of *Lactobacillus rhamnosus*, 10^7 cfu/mL of Lac_MTX and 1.8 µM of MTX) at the center of the plates, separately. The plate was incubated for 12 h at 37 °C. The zone of inhibition was measured by considering the center of the plate as the reference.

4.2.8 Formation of *Staphylococcus aureus* biofilm

Staphylococcus aureus culture was grown at 37 °C and 180 rpm for 12 h in BHI medium. The late log phase grown culture was serially diluted to obtain 10^6 cfu/mL of bacteria. The serial dilution was done using BHI medium supplemented with 0.25% of Dextrose to aid in biofilm formation. In a 96-well plate, 200 µL of the 10^6 cfu/mL *Staphylococcus aureus* were seeded in each well and the plate was incubated for 24 h at 37 °C in a humidified incubator.

4.2.9 Anti-biofilm Assay

The *Staphylococcus aureus* biofilm was formed in wells of a 96-well plate and the medium was discarded after 24 h. The un-adhered planktonic bacteria were discarded along with the medium. The formed biofilm was treated with 1.8 µM of MTX, different concentrations of control *Lactobacillus rhamnosus,* Lac_AuNC, and Lac_MTX (10^4, 10^5, 10^6 and 10^7 cfu/mL) and the biofilm without any treatment served as the control group for the assay. All the dilutions of the treatment groups were prepared in BHI medium. The treatment was allowed to occur for 24 h. The medium was removed carefully in order to get rid of the treatment groups i.e 1.8 µM of MTX, control *Lactobacillus rhamnosus,* Lac_AuNC, and Lac_MTX and the remaining planktonic *Staphylococcus aureus.* The treated biofilms were washed with double autoclaved de-ionized water to remove the remnant planktonic bacteria. 0.1% of crystal violet was added very carefully to each well and was allowed to stain the biofilm for 30 min at 37 °C. After the incubation, the excess crystal violet wasremoved carefully leaving the stained biofilm undisturbed. Simultaneously, the treatment groups without being added to the biofilms were also stained with the crystal violet for the accurate calculation of the viability% of the biofilm. Finally, 200 µL of 100% ethanol was added to each well containing the stained biofilms to dissolve the crystal violet absorbed by the biofilm. The ethanol immersed biofilms were incubated for 15 min at room temperature. The absorbance of the resultant medium containing the dissolved crystal violet was measured at 595 nm.

4.2.10 Confocal Laser Scanning Microscopy of Live/Dead cells in biofilm

The treated biofilms were washed twice using double autoclaved de-ionized water. Then 10 µL of 1 mg/mL of acridine orange was added to the biofilm and was allowed to incubate at room temperature for 15 min. The excess dye was removed and 10 µL of 1 mg/mL of propidium iodide was added to the biofilm to selectively stain the dead bacteria. The excess dye was removed after 15 min of incubation followed by imaging in CLSM using 488 nm laser for acridine orange and 514 nm for propidium iodide.

4.2.11 ROS assay of *S.aureus* biofilm treated with Lac_MTX

The *S.aureus* biofilms were prepared on a 96-well plate following the previously described method. Then the biofilms were treated with freshly prepared 10^7 cfu/mL of 1.8 µM of MTX, control *Lactobacillus rhamnosus,* Lac_AuNC, and Lac_MTX. The treatment was allowed to occur for 6 h. The treatment groups without being added to the biofilms served as the control groups as the treatment group has live bacteria that could interfere with the results. Then the biofilms were treated with a ROS detection dye 2,7-dichlorofluoresceindiacetate (DCHFDA). The dye is non-fluorescent but oxidizes to 2', 7' –dichlorofluorescein (DCF) in presence of ROS emitting green

fluorescence. 10 µM of DCHFDA was added to each well containing the treated biofilms and also to the treatment groups alone that served as the control. The dye was allowed to incubate with the samples for 30 min at room temperature. The fluorescence analysis was carried out using 488 nm excitation and 530 nm emission wavelengths. The final calculations were made by subtracting the fluorescence emission of control treatment groups from the treated groups.

4.2.12 Field emission scanning electron microscopy analysis of *S.aureus* biofilm treated with Lac_MTX

The biofilms were prepared of cover slips keeping them in 6-well plate tissue culture plates. The biofilms were treated with the treatment groups as described earlier for anti-biofilm assay. The treatment was allowed to happen for 24 h followed by careful washing of the treated biofilms by PBS. The coverslips were recovered gently from the 6-well plate tissue culture plates and were kept under the laminar airflow for drying. The dried samples were analyzed under FESEM(Zeiss).

4.3 Results and Discussion

4.3.1 Synthesis of gold nanoclusters on living *Lactobacillus rhamnosus*

The gold nanoclusters were synthesized on living bacterium following a previously standardized protocol [24]. The resultant Lac_AuNCs were fluorescent and showed fluorescence spectrum with two peak maxima (420 nm and 580 nm). The broad peak at 420 nm corresponds to the protein present in the bacterium and the peak a 580 nm can be attributed to the gold nanoclusters synthesized on the surface of the bacterium. The microscopic images (TEM, FESEM) confirmed the presence of gold nanoclusters on the outer surface of the intact bacterium. The confocal laser scanning microscopy images of Lac_AuNC confirms the fluorescent nature of the bacteria due to the presence of the nanoclusters. Moreover, the bacteria were alive and viable as was evident from the cfu/mL counting of the bacteria and video of live bacteria taken using confocal microscope. The encapsulation of MTX was carried out on the bacteria in order to develop bacbots with therapeutic efficiency [25].

4.3.2 Minimum inhibitory concentration (MIC) of MTX on *Lactobacillus rhamnosus*

The minimum inhibitory concentration is the lowest concentration of the drug required to reduce the inoculum viability. The lower the MIC the lesser amount of drug is required to prevent the growth of the bacteria[26]. The determination of the MIC of MTX on *Lactobacillus rhamnosus* was taken up cto confirm the effect of the drug on the bacterium and to determine whether MTX was suitable for encapsulation on the living Lac_AuNC. The incubation of the bacterial inoculum in presence of different concentration of MTX was continued for 48 h. The viability of the bacteria in presence of up to 20 µM of MTX suggested that the lower concentrations of the drug were able to have a tolerable inhibitory effect (nearly 28%) on the bacteria. However, nearly 48% inhibition on the bacterial growth was observed in presence of 500 µM of MTX. The MIC of the drug was found to be 427.5 µM. Thus, the drug was considered suitable for the encapsulation as it would not hinder in the viability of the bacterium at lower concentration of the drug (Figure 4.1a). The

field emission scanning electron microscopy images also showed the bacteria clubbed together that could be attributed to the additional layer of deposition. Thus, the additional layer covering the Lac_AuNC surface could be the layer of MTX (Lac_MTX) (Figure 4.2).

4.3.3 Encapsulation of MTX on Lac_AuNC

The MTX was encapsulated on the gold nanocluster studded bacteria (Lac_AuNC) by incubating different concentrations of the drug with 10^8 cfu/mL of Lac_AuNC in separate vials for 1 h at 37 °C. The encapsulation was ensured by the change in the fluorescence peak at 580 nm. The decrease in the intensity of the fluorescence of Lac_AuNC in presence of higher concentrations of drug could be attributed to the interaction of the drug with the gold nanoclusters on the surface of the bacteria [25]. The transmission electron microscopy images of the resultant product showed an additional layer of deposition on the bacterial surface which was otherwise absent on Lac_AuNC.

4.3.4 Medium compatibility analysis

The *S.aureus* biofilm formation was carried out using BHI medium for the current study and the recommended growth medium for *Lactobacillus rhamnosus* is MRS medium. In order to confirm if the treatment group for the anti-bacterial and anti-biofilm study would be able to thrive in presence of a different medium, the *Lactobacillus rhamnosus* was inoculated into BHI medium at 1% concentration. The bacteria were allowed to incubate for 48 h which is the recommended growth period for the strain. The turbidity in the BHI medium indicated the growth of *Lactobacillus rhamnosus*. The UV-absorbance at 595 nm was found to be close to the absorbance of the bacteria grown in MRS medium. For further support, the FESEM imaging of the bacteria

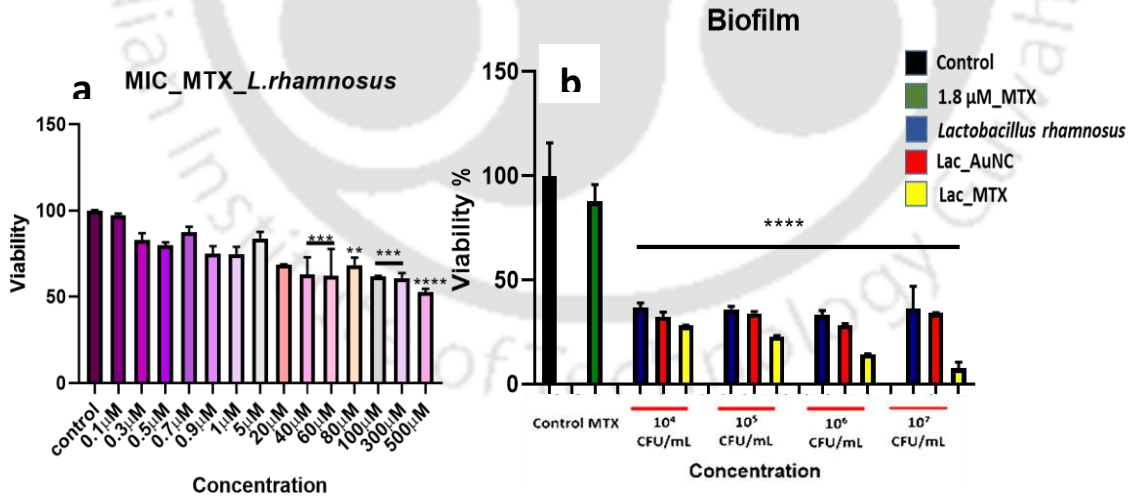

Figure 4.1. (a) Minimum inhibitory concentration determination of methotrexate on control *Lactobacillus rhamnosus*, (b) viability assay of *S.aureus* biofilm treated with different concentration of on control *Lactobacillus rhamnosus*, Lac_AuNC and Lac_MTX as described in the legends. Statistical significance is represented by *** ($p < 0.001$), and **** ($p < 0.0001$). The values are represented as mean ± standard deviation (SD) of three individual experiments.

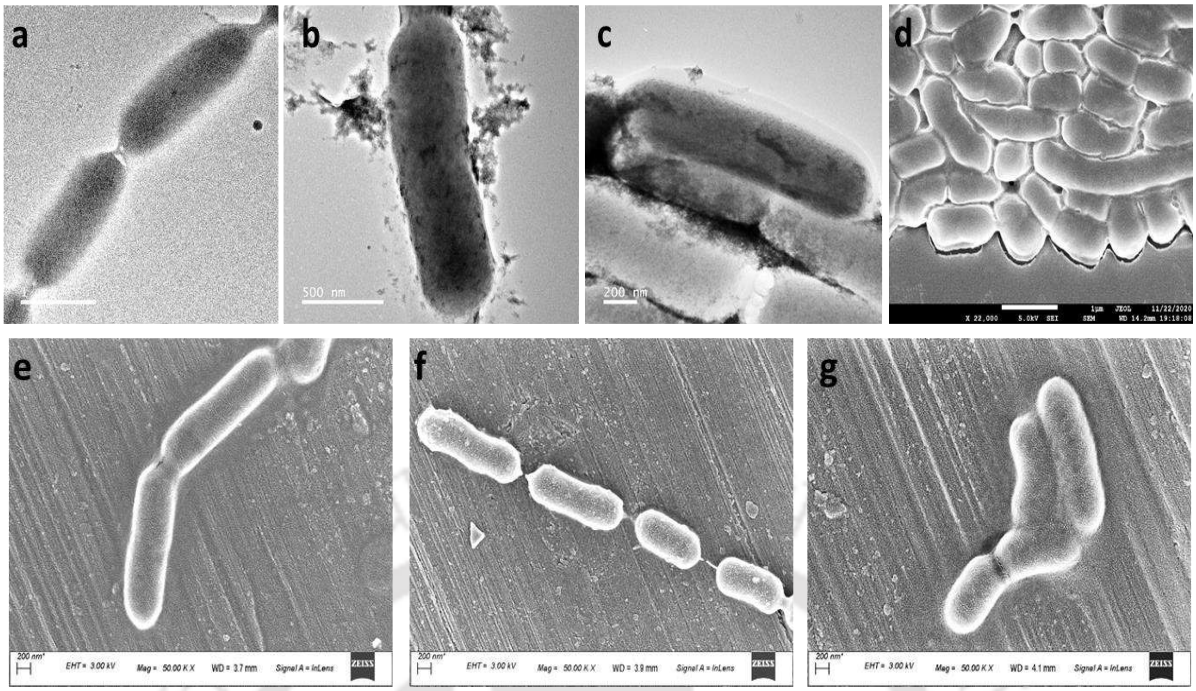

Figure 4.2. Characterization study (a) transmission electron microscopy image of control *Lactobacillus rhamnosus*, (b) transmission electron microscopy image of Lac_AuNC, (c) transmission electron microscopy image of Lac_MTX, (d) field emission electron scanning microscopy image of control *Lactobacillus rhamnosus* grown in BHI medium, (e) field emission electron scanning microscopy image of control *Lactobacillus rhamnosus*, (f) field emission electron scanning microscopy image of Lac_AuNC, and (g) field emission electron scanning microscopy image of Lac_MTX.

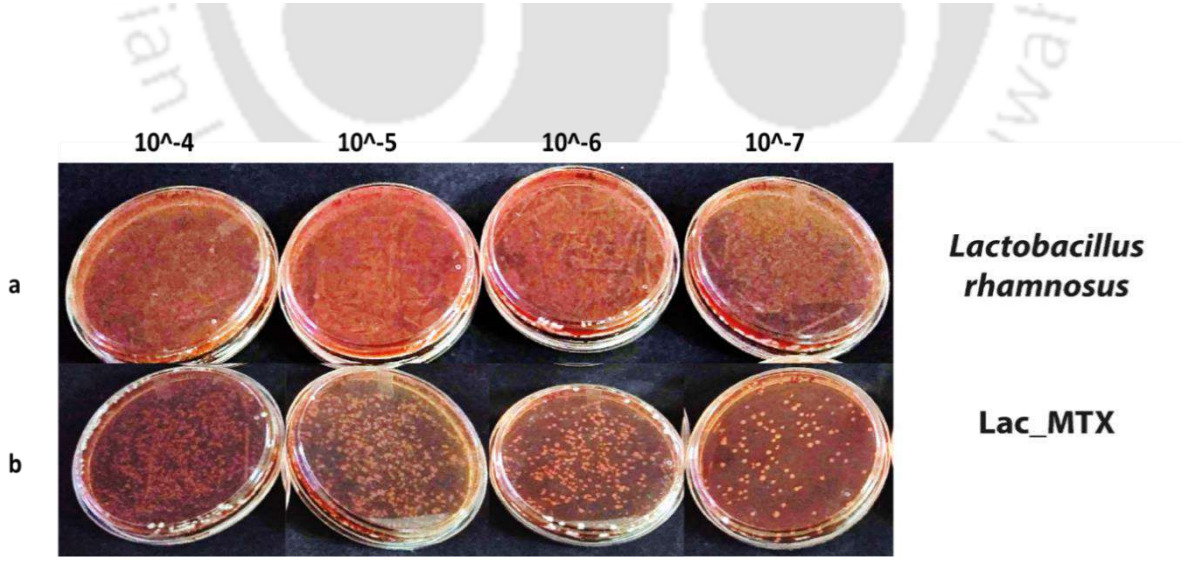

Figure 4.3. Colony forming unit determination of (a) control *Lactobacillus rhamnosus*, and (b) Lac_MTX with serial dilutions as described in legends.

was carried out and the images confirmed the presence of intact *Lactobacillus rhamnosus*. Similar to the ones grown in MRS medium. The colony forming unit/mL of Lac_MTX were also determined (Figure 4.2d and Figure 4.3).

4.3.5 Determination of anti-bacterial activity of Lac_MTX

The anti-bacterial property of the Lac_MTX was determined by co-incubating the *Staphylococcus aureus* inoculum (1%) with different concentration of *Lactobacillus rhamnosus*, Lac_AuNC, and Lac_MTX and 1.8μM of MTX. Each of the treatment group was freshly prepared and were diluted to concentrations of 10^4 cfu/mL, 10^5 cfu/mL, 10^6 cfu/mL, and 10^7 cfu/mL using BHI medium for compatibilty. In different test tubes containing BHI medium, 1% of *S.aureus* inoculums were added and to the respective test tubes 1% inoculum of the treatment groups were added simultaneously. The same amount of inoculum of these treatment groups were added in to separate test tubes where *S.aureus* was not added. These tubes served as the control groups. All the test tubes were allowed to incubate at 37 °C for 12 h in aerobic condition. The UV-absorbance of the grown bacteria were recorded at 595 nm and the final results were calculated by subtracting the absorbance of the control groups inoculated without the *S.aureus* from the co-cultured tubes for accuracy. The results showed that the viabilities of *S.aureus* in presence of the treatment groups were 81.1% (1.8 μM_MTX), 22.9 % (10^4 cfu/mL of *Lactobacillus rhamnosus*), 22.2% (10^4 cfu/mLof Lac_AuNC), and 15.1% (10^4 cfu/mL of Lac_MTX). The results further reveal that the viability was found to be 22.3 % (10^5 cfu/mL of *Lactobacillus rhamnosus*), 20.9% (10^5 cfu/mL of Lac_AuNC), and 10.8% (10^5 cfu/mL of Lac_MTX). 20.5 % (10^6 cfu/mL of *Lactobacillus rhamnosus*), 19.8% (10^6 cfu/mL of Lac_AuNC), and 5.6% (10^6 cfu/mL of Lac_MTX). 22.1 % (10^7 cfu/mL of *Lactobacillus rhamnosus*), 19.1% (10^7 cfu/mL of Lac_AuNC), and 3.8% (10^7 cfu/mL of Lac_MTX) (Figure 4.4a). The results showed that there was a dose dependent decrease of viability of *S.aureus* on treatment with Lac_MTX that gradually declines from 15.1% to 3.8%. This gradual decrease could be attribute to the inherent effect of *Lactobacillus rhamnosus* against the *S.aureus* as worked by inhibiting growth and preventing bacterial adhesion as a result of competitive exclusion [27]. However, there was a nominal change in viability of *S.aureus* in presence of increasing concentration of *Lactobacillus rhamnosus* and Lac_AuNC. In our previous study [25] the effect of Lac_AuNC and *Lactobacillus rhamnosus* on cancer cells were found to be nearly similar suggesting that the gold nanoclusters were not interfering with the properties of the bacteria. In the current study also, the effect of *Lactobacillus rhamnosus* and Lac_AuNC were found to be similar. The negligible variations in the viability although could not be understood fully, but could be attributed to the equilibrium achieved by both the bacterial strains competing for the nutrients. Since, the strains were inoculated simultaneously the depleting nutrients could have brought a state of equilibrium for both the strains. After which the viability of *S.aureus* did not change further. However, in case of Lac_MTX, the drug could have aided in causing the toxicity by posing a synergistic effect on *S.aureus*. Previous study in this field confirms the anti-Staphylococcal activity of MTX [28]. Thus, the bacbots were able to cause sufficient anti-microbial activity to suppress the growth of the strain *S.aureus* up to 97% (approx.) which is otherwise difficult to achieve by conventional means (Figure 4.4a).

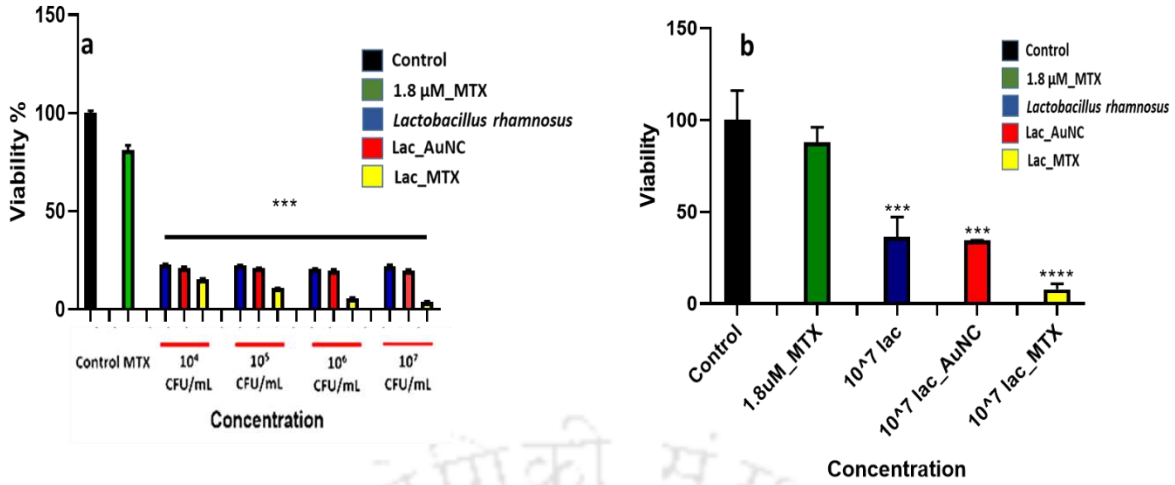

Figure 4.4. Viability assay of (a) *S.aureus* planktonic culture treated with 1.8 µM_MTX, control *Lactobacillus rhamnosus,* Lac_AuNC, and Lac_MTX at different concentrations as described in the legends, and (b) *S.aureus* biofilm treated with 1.8 µM_MTX, 10^7 cfu/mL of control *Lactobacillus rhamnosus*, 10^7 cfu/mL of Lac_AuNC, and 10^7 cfu/mL of Lac_MTX. Statistical significance is represented by *** ($p < 0.001$), and **** ($p < 0.0001$). The values are represented as mean ± standard deviation (SD) of three individual experiments.

4.3.6 Zone of Inhibition Study

The zone of inhibition measures the ability of a therapeutic agent to inhibit the growth of the microorganism. The diameter/radius of the clear zone in the agar plate allows to have a visually distinct region distinguishing the ability of the drug/ therapeutic agent to create a zone of inhibition. The *S.aureus* lawn culture was spread plated on BHI-agar plates and in the centre of the plate the treatment groups were poured. All of treatment groups were poured in separate plates with lawn culture of *S.aureus* plated over it. The zone of inhibition created by the control *Lactobacillus rhamnosus* had an average radius of 10.6 mm, the average radius created by 1.8µM of MTX was 16.72 mm and the average radius formed by 10^7 cfu/mL Lac_AuNC was 9.38 mm, and for Lac_MTX it was 19.66 mm (Figure 4.5). The zone of inhibition created by the *Lactobacillus rhamnosus* and Lac_AuNC were nearly similar and this could be due to the similar anti-bacterial properties of both the treatment groups that indicated that the gold nanoclusters did not interfere with the properties of the bacteria. Thus, the treatment showed a ZOI having a difference of merely 1.3 mm. The ZOI created by Lac_MTX was larger than that of the control *Lactobacillus rhamnosus* but there was less difference (2.94 mm) in comparison to the zone of inhibition created by the 1.8µM_MTX. This hinted towards two inferences. The first one is, the MTX loaded bacbots were more efficient than only *Lactobacillus rhamnosus*. Thus, the MTX and the *Lactobacillus rhamnosus* present in the bacbots as a single unit had a synergistic effect on the *S.aureus* lawn culture leading to a larger ZOI. The second inference that could be drawn was that the results of the effect of MTX and bacbots were close to each other due to possible restricted mobility of the bacteria (*Lactobacillus rhamnosus*, Lac_AuNC and Lac_MTX) as compared to the soluble MTX that could

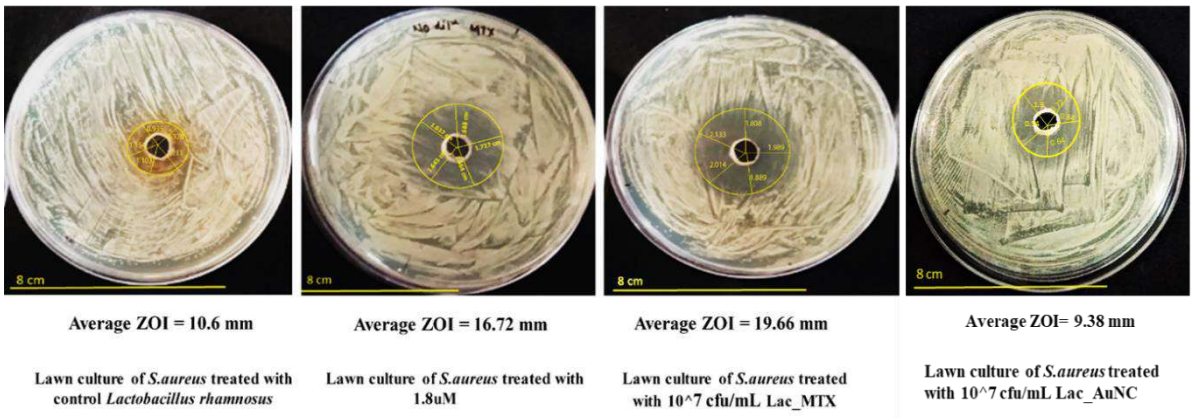

Figure 4.5. Zone of Inhibition on BHI-agar plate containing *S.aureus* lawn culture treated with (a) 10^7 cfu/mL of control *Lactobacillus rhamnosus*, (b) 1.8 µM_MTX, (c) 10^7 cfu/mL of Lac_MTX, and (d) 10^7 cfu/mL of Lac_AuNC.

have swiftly seeped in to the agar plate creating a ZOI. These results indicated that the drug itself had similar impact on lawn culture of *S.aureus* as that of the bots. Taking these results in to account further studies on viability of *Staphylococcus aureus* biofilms treated with bacbots were pursued.

4.3.7 Determination of anti-biofilm activity of Lac_MTX

The biofilms are the aggregates of any microorganisms that remain together by producing extra cellular matrix with their own extra polymeric substances. They represent a complex system that bear high cell density of nearly 10^8 to 10^{11} per gram wet weight [1]. *S.aureus* causes acute soft tissue infections in cancer patients by forming biofilms [29]. Hence, the effect of the developed bots against the biofilms was studied to determine whether these can be used to deal with these infections. The biofilms were formed using the previously described protocol. Then were incubated with 10^4, 10^5, 10^6 and 10^7 cfu/mL of control *Lactobacillus rhamnosus*, Lac_AuNC, and Lac_MTX and 1.8 µM-MTX. The treatment continued for 24 h. The viability of the biofilms was determined following crystal violet assay protocol (Figure 4.6). The biofilm viabilities were found to be 87.8 % (1.8 µM_MTX), 36.7 % (10^4 cfu/mL of *Lactobacillus rhamnosus*), 32.5% (10^4 cfu/mL of Lac_AuNC), and 28.2% (10^4 cfu/mL of Lac_MTX); 36.1 % (10^5 cfu/mL of *Lactobacillus rhamnosus*), 34.2% (10^5 cfu/mL of Lac_AuNC), and 23% (10^5 cfu/mL of Lac_MTX); 33.4 % (10^6 cfu/mL of *Lactobacillus rhamnosus*), 28.5% (10^6 cfu/mL of Lac_AuNC), and 14.5% (10^6 cfu/mL of Lac_MTX); 36.5 % (10^7 cfu/mL of *Lactobacillus rhamnosus*), 34..4% (10^7 cfu/mL of Lac_AuNC), and 7.8% (10^7 cfu/mL of Lac_MTX) (Figure 4.1b and Figure 4.4b).Here, the results showed a similar pattern to that of the anti-bacterial assay. There was a nominal difference in the viability of biofilm on treatment with *Lactobacillus rhamnosus* and Lac_AuNC. This could be also attributed to the probable equilibrium that was set between the two strains struggling for the limited available nutrients. That led to a limit of toxicity beyond which the increased *Lactobacillus rhamnosus* and Lac_AuNC amount also did not exert much effect. However, due to the synergistic effect of anti-staphylococcal MTX and *Lactobacillus rhamnosus* of the bacbots, a dose dependent toxicity and

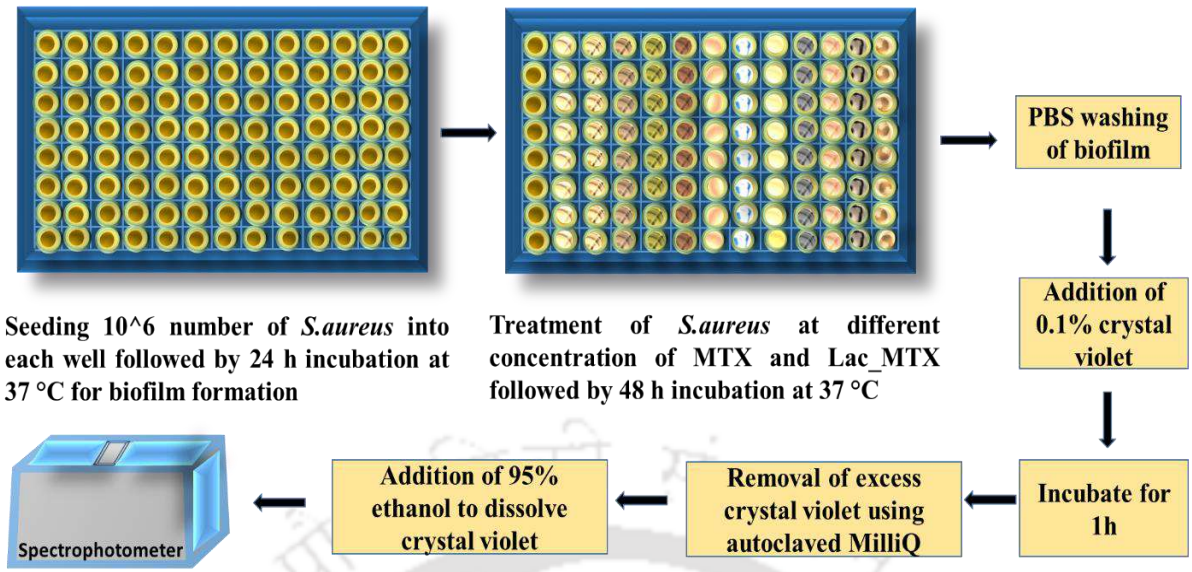

Figure 4.6. Schematic representation of procedure of crystal violet assay for determining the viability % of *S.aureus* biofilm.

anti-biofilm effect was observed. The live bacbots have made the drug more available to the intricate networks of the biofilm and the motile nature of the live bacbots could have aided in this. Thus, the developed bacbots were capable of combating biofilms and eradicate up to 90% of them.

4.3.8 Confocal Laser Scanning Microscopy analysis

To obtain qualitative analysis of the activity of bacbots against the biofilm. The biofilms were prepared and treated with the treatment groups. The treated biofilms were carefully washed using double autoclaved de-ionized water to remove remnants of the treatment groups. Then the biofilms were stained with 10µL of 1mg/mL of acridine orange and incubated to stain the live bacteria and then the dead biofilm portions were stained with 10µL of 1mg/mL propidium iodide. The treatment of 10^7 cfu/mL of the control bacteria on the biofilm had obliterated 70% of the biofilm and the same concentration of Lac_MTX had destructed 90-95% of the biofilm. The confocal laser scanning microscopy images of the biofilms showed propidium iodide stained broken parts of the dead biofilm where as a scanty amount of green fluorescent portions of the live biofilms could also be seen. The images confirmed the findings of the anti-biofilm assay (Figure 4.7- Figure 4.9).

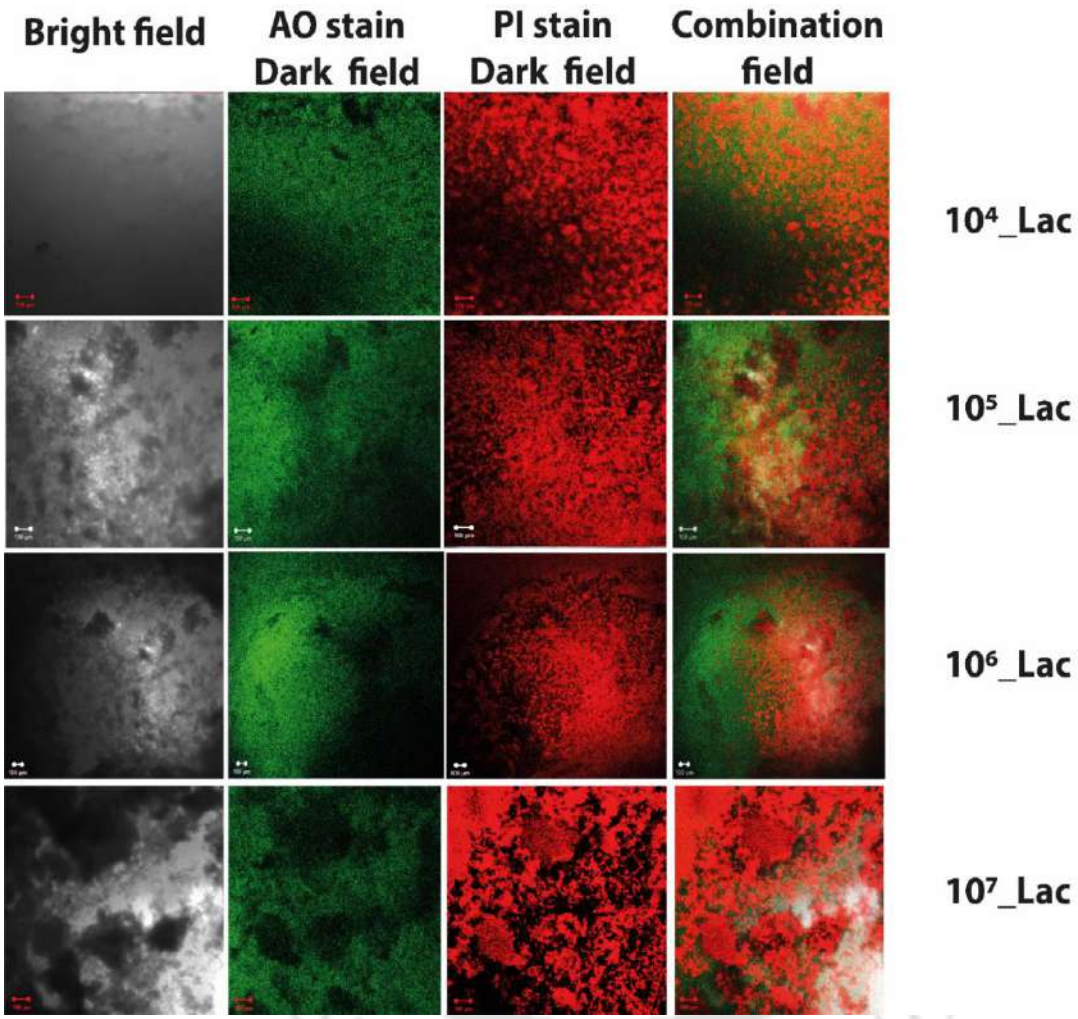

Figure 4.7. Confocal laser scanning microscopy images of *S.aureus* biofilm treated with control *Lactobacillus rhamnosus* at different concentrations as described in the legends. Acridine orange was used to stain live biofilm portions and Propidium Iodide was used to stain dead portions of the biofilm.

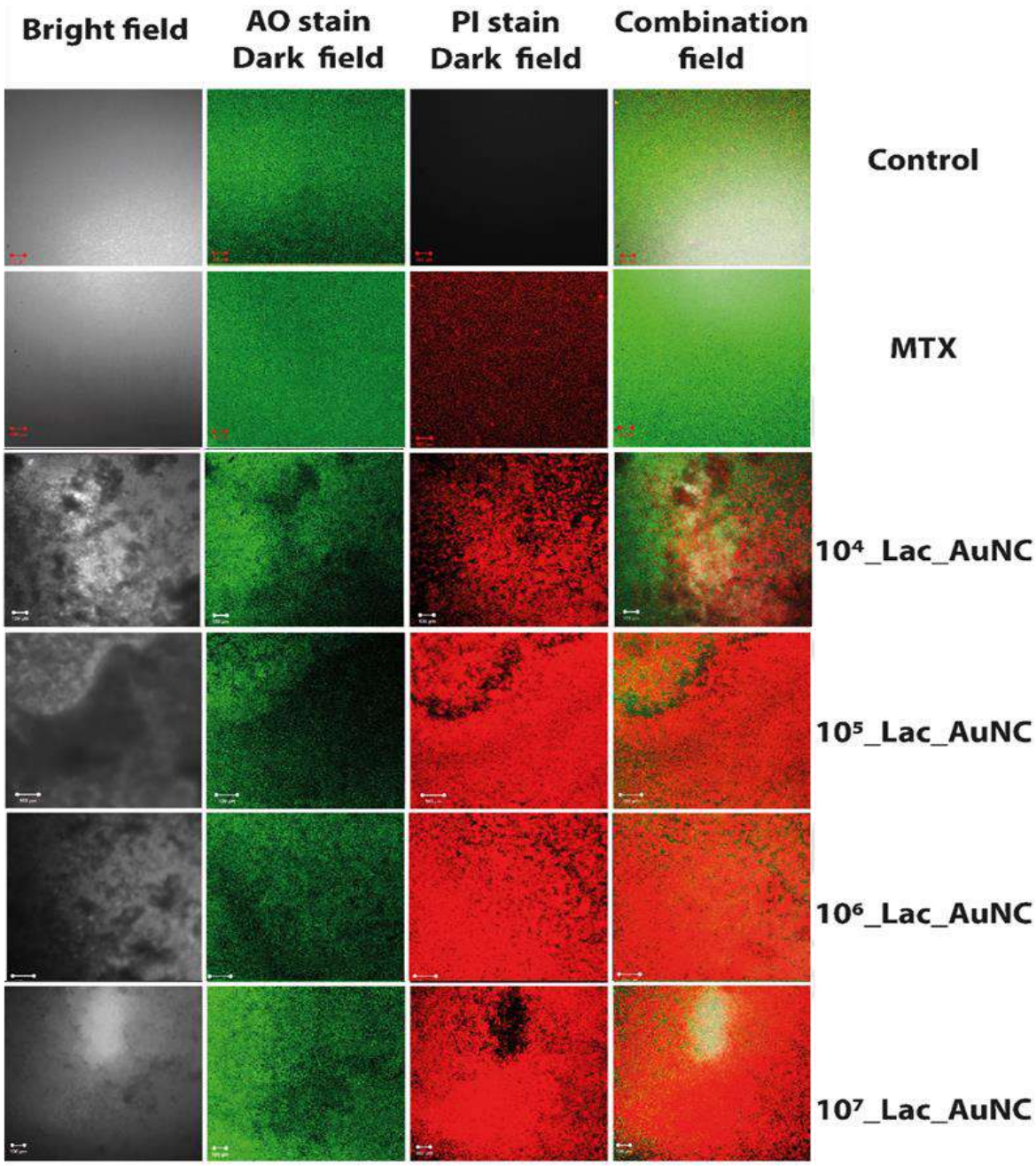

Figure 4.8. Confocal laser scanning microscopy images of untreated *S.aureus* biofilm and *S.aureus* biofilm treated with 1.8 μM_MTX and Lac_AuNC at different concentrations as described in the legends. Acridine orange was used to stain live biofilm portions and Propidium Iodide was used to stain dead portions of the biofilm.

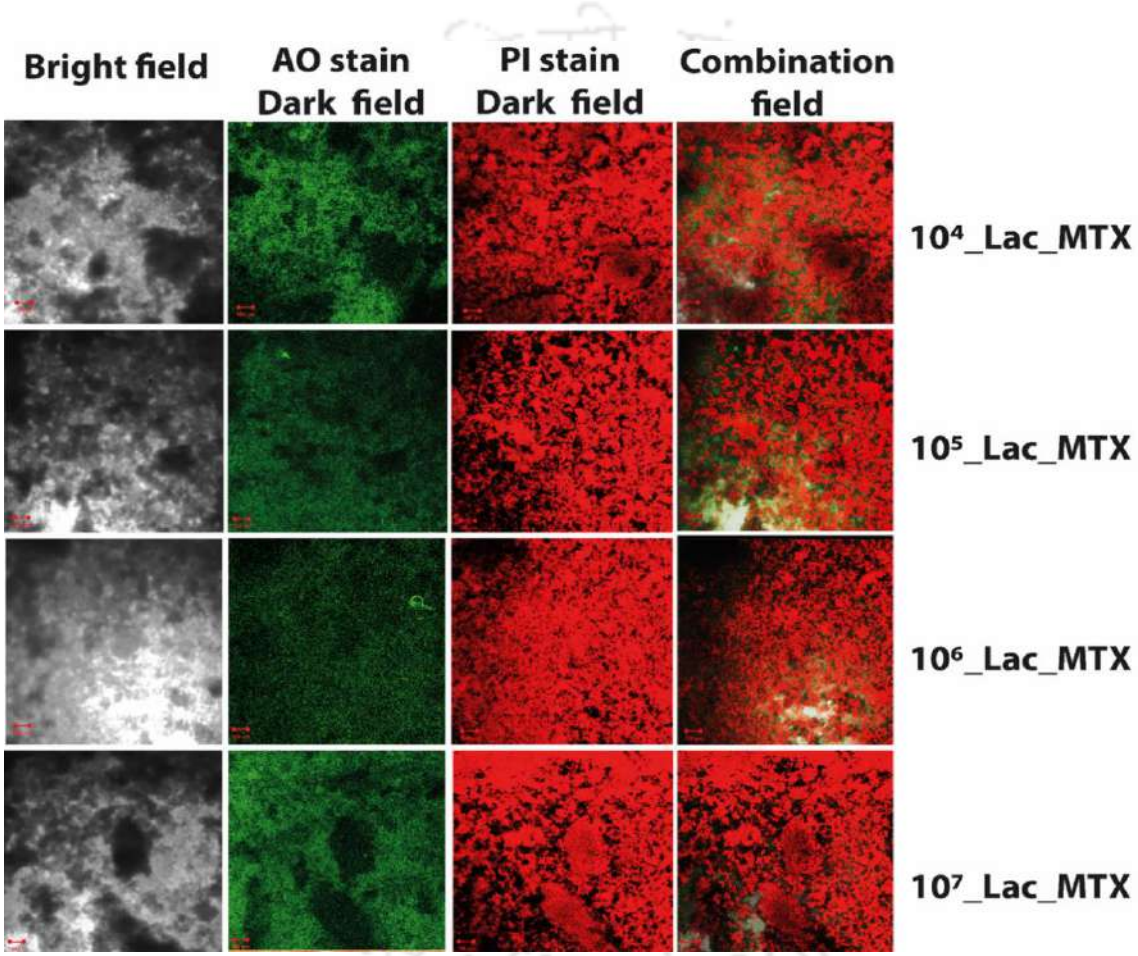

Figure 4.9. Confocal laser scanning microscopy images of *S.aureus* biofilm treated with Lac_MTX at different concentrations as described in the legends. Acridine orange was used to stain live biofilm portions and Propidium Iodide was used to stain dead portions of the biofilm.

4.3.9 Field emission scanning electron microscopy of *S.aureus* biofilm treated with bacbots

The treated biofilms were washed using PBS to remove the remainder treatment groups and the biofilms were dried thoroughly. The biofilms were analysed under FESEM (Zeiss Sigma 300). The untreated biofilm, served as the control, seemed intact with no visible breakage. The treated biofilms were broken into chunks of heterogeneous sizes and in some cases the chunks were so fragile that they were washed out during the PBS wash. The FESEM images showed that majority of the biofilms were destroyed due to treatment with the bacbots in comparison to the other treatment groups (Figure 4.10 - Figure 4.13). Thus, the images reinforced the outcomes of the crystal violet assay.

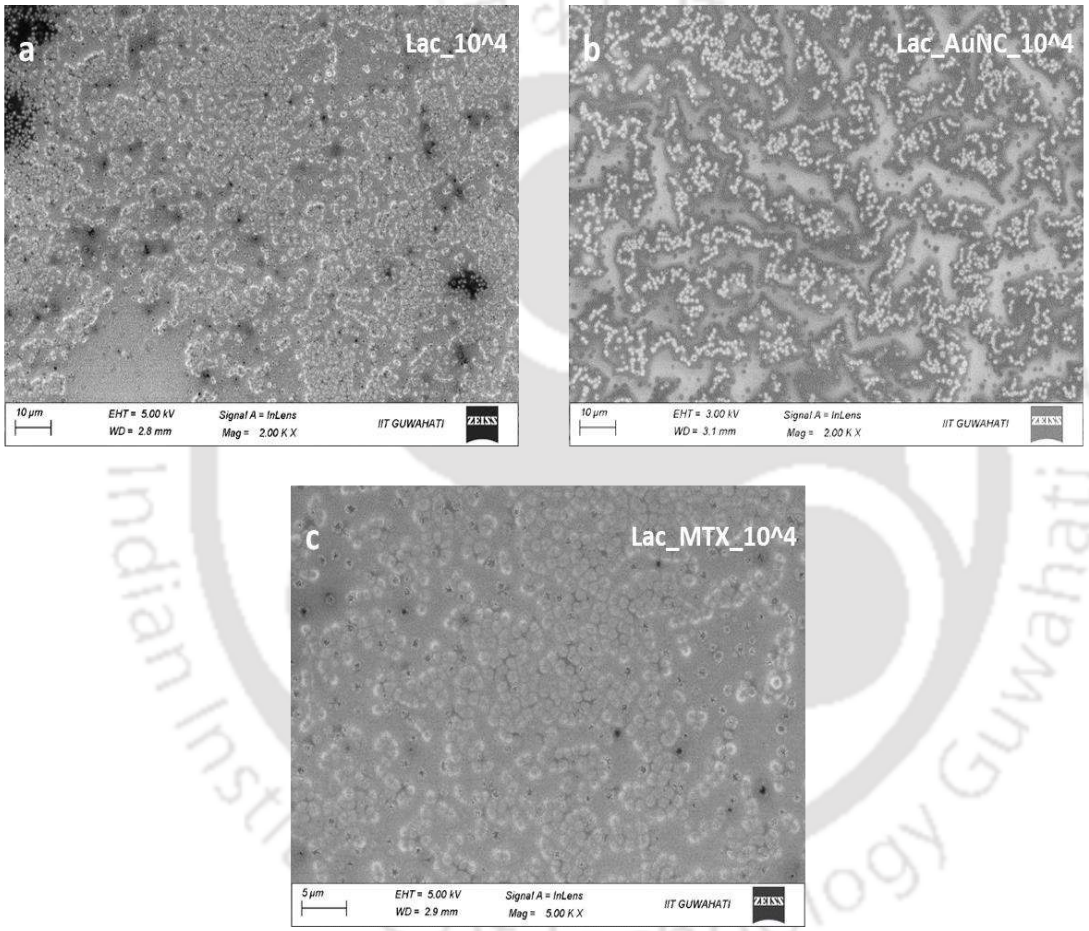

Figure 4.10. Field emission scanning microscopy images of *S.aureus* biofilm treated with (a) control *Lactobacillus rhamnosus*, (b) Lac_AuNC, and (c) Lac_MTX at 10^4 cfu/mL concentration..

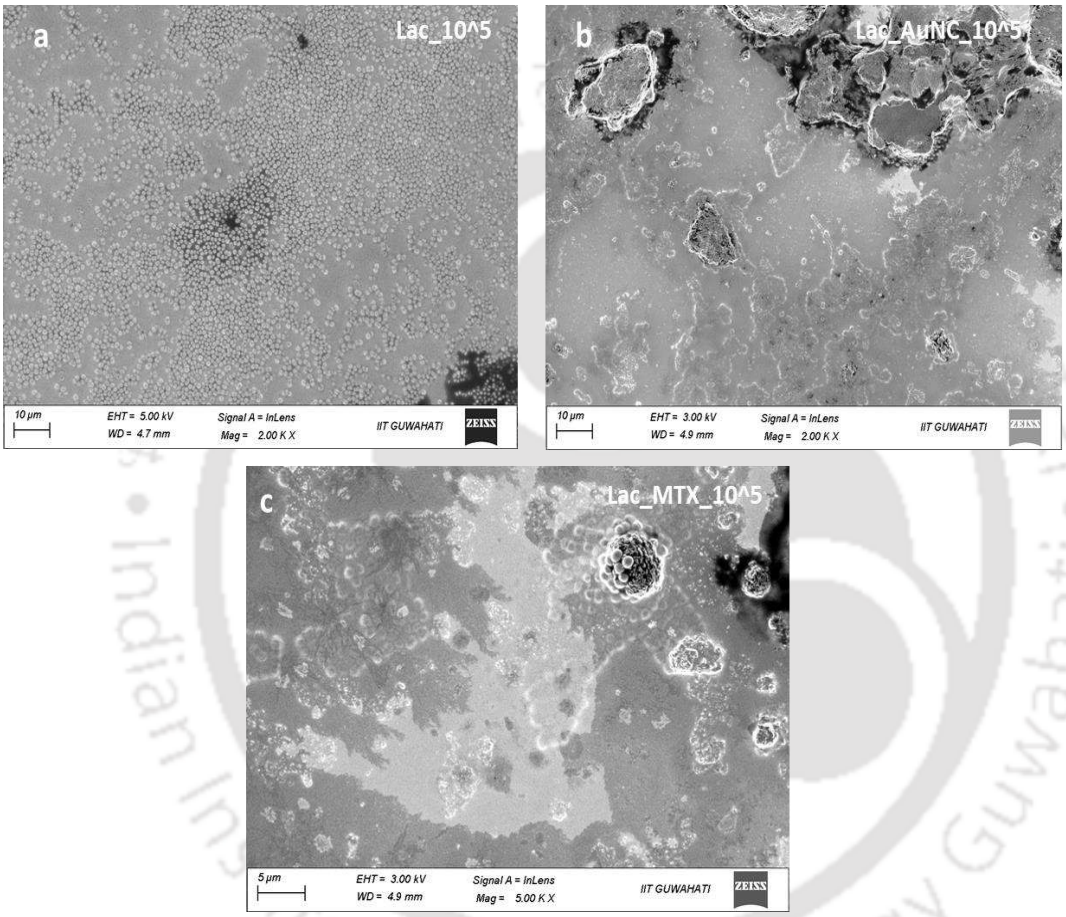

Figure 4.11. Field emission scanning microscopy images of *S.aureus* biofilm treated with (a) control *Lactobacillus rhamnosus*, (b) Lac_AuNC, and (c) Lac_MTX at 10^5 cfu/mL concentration..

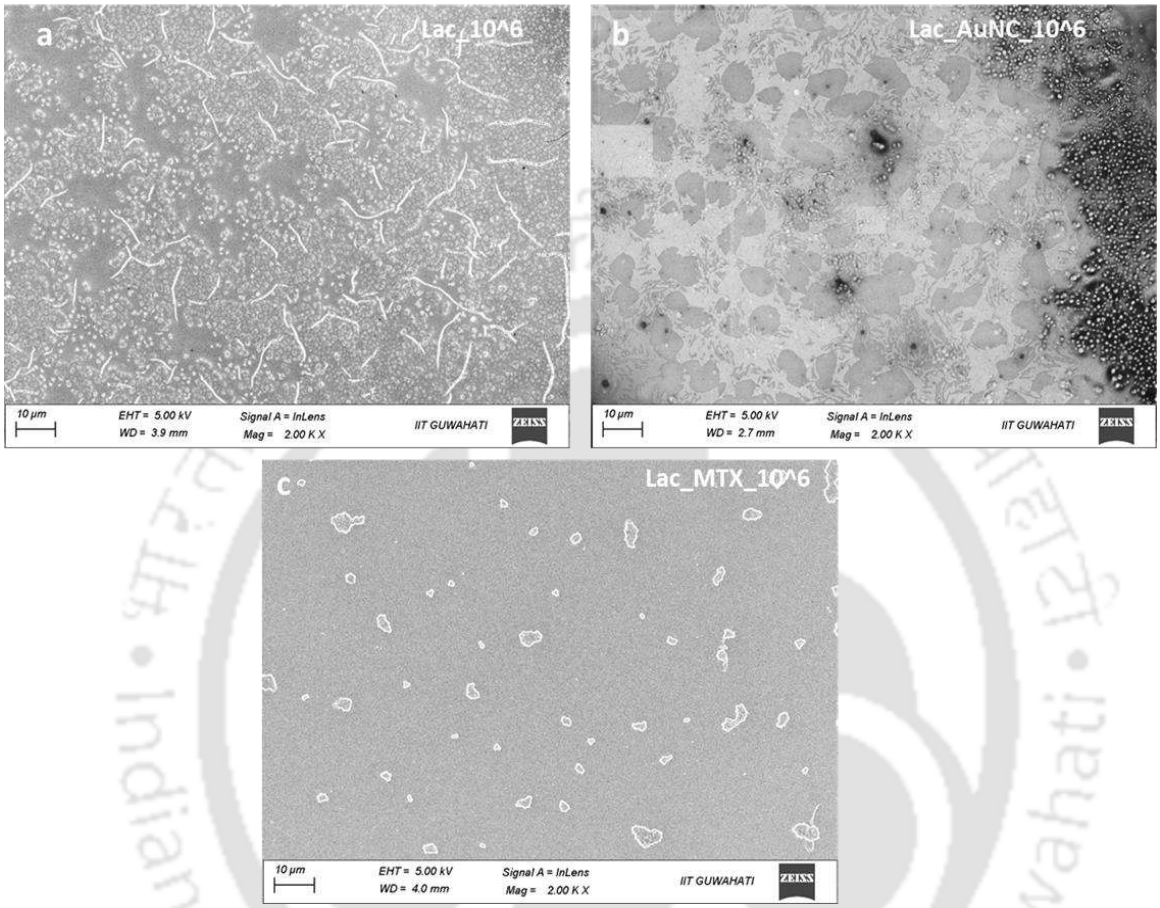

Figure 4.12. Field emission scanning microscopy images of *S.aureus* biofilm treated with (a) control *Lactobacillus rhamnosus,* (b) Lac_AuNC, and (c) Lac_MTX at 10^6 cfu/mL concentration..

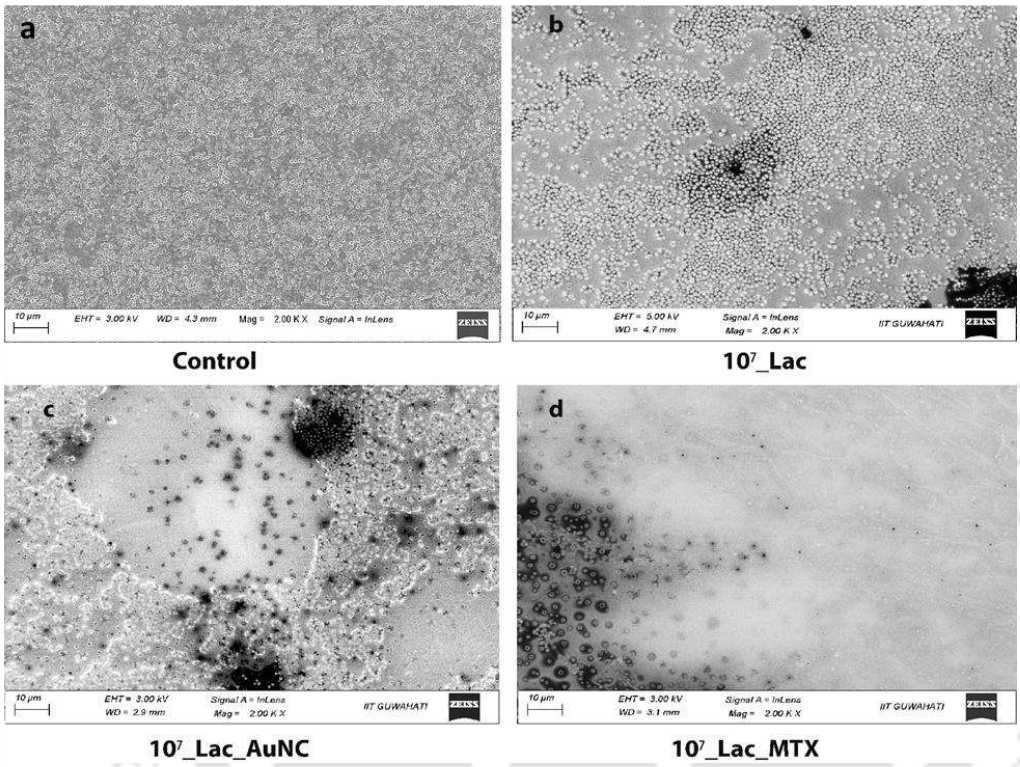

Figure 4.13. Field emission scanning electron microscopy images of (a) untreated *S.aureus* biofilm (b) biofilm treated with control *Lactobacillus rhamnosus*, (c) biofilm treated with Lac_AuNC, and (d) biofilm treated with Lac_MTX at 10^7 cfu/mL concentrations each.

4.3.10 ROS assay of *S.aureus* biofilm treated with bacbots

The ROS generated by the bacbots during the treatment was measured by treating the biofilm with 10^7 cfu/mL of *Lactobacilus rhamnosus*, Lac_AuNC and Lac_MTX for 6 h. The ROS detecting dye DCFHDA gets converted from non-fluorescent compound to a fluorescent one on getting oxidized in presence of ROS [30]. The ROS over production causes loss of biofilm integrity, the polysaccharides, eDNA and protein of biofilm are degraded due to ROS [31]. *Lactobacillus* strains are known to generate ROS. The generated ROS was quantified spectroscopically by using an excitation wavelength of 488 nm and at an emission wavelength of 535 nm. The amount of ROS generated by 1.8 µM_MTX, *Lactobacillus rhamnosus*, and Lac_AuNC wwere nearly similar to each other and were quite close to the amount of ROS produced by the untreated biofilm as a result of normal cellular activities. However, the amount of ROS produced by the bacbot treated biofilm was 1.7 times more than the untreated biofilm (Figure 4.14). This suggests that there was an important role being played by ROS during the treatment of bacbots. Though ROS production may not be the sole mechanism for the anti-biofilm effect of the bacbots but the contribution of ROS generation is noteworthy.

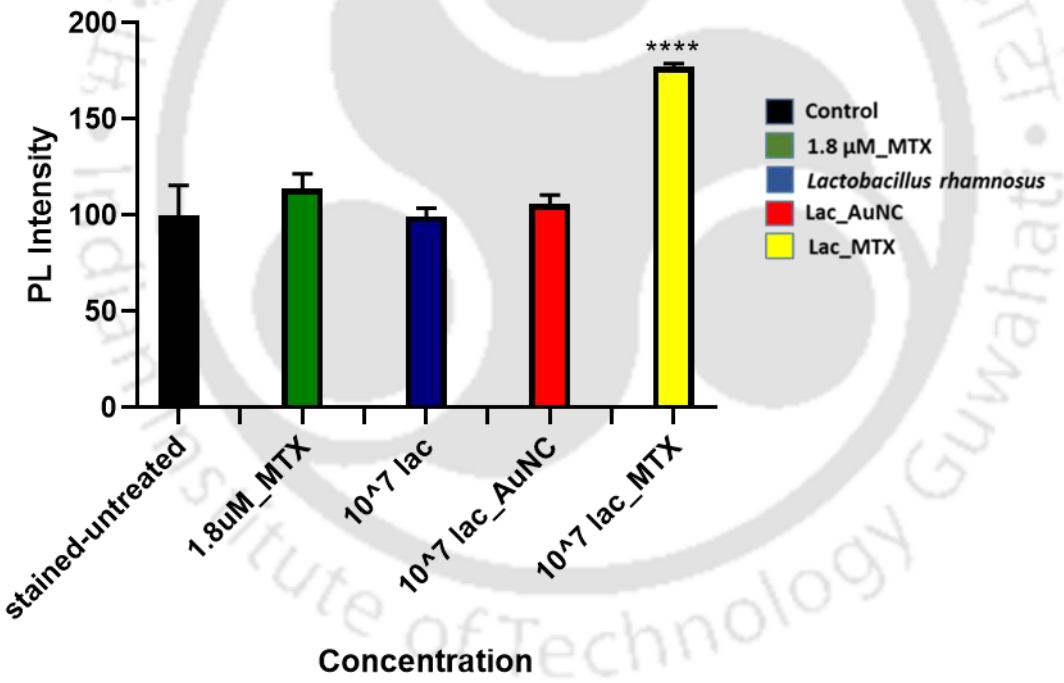

Figure 4.14. ROS assay of (a) *S.aureus* biofilm treated with 1.8 µM_MTX, control *Lactobacillus rhamnosus*, Lac_AuNC, and Lac_MTX at 10^7 cfu/mL. Statistical significance is represented by **** ($p < 0.0001$). The values are represented as mean ± standard deviation (SD) of three individual experiments.

4.4 Conclusions

In conclusion, a drug encapsulated bacbot was fabricated with gold nanoclusters. The bacbots were alive and viable and showed anti-bacterial properties against the deadly bacteria *S.aureus*. The bacteria are responsible for nosocomial infections and is regarded as one of the deadly bacteria causing secondary infections in cancer patients. The bacbots were able to eradicate the biofilm of *S.aureus* by nearly 90-95%. This brings out a great two-in-one solution in the form of the bacbots as in our previous studies the bacbots were shown to have tremendous cytotoxicity against spheroids and monolayer cultures of cancer cells. In the current study the anti-bacterial and anti-biofilm effects of the bacbots were also explored in details. Thus, the bacbots provide dual therapeutic solutions and can be considered as a viable two-in-one solution for cancer and cancer associated secondary infections caused by *S.aureus*.

4.5 References

(1) Flemming, H. C.; Wingender, J.; Szewzyk, U.; Steinberg, P.; Rice, S. A.; Kjelleberg, S. Biofilms: An Emergent Form of Bacterial Life. *Nat. Rev. Microbiol.* **2016**, *14* (9), 563–575.

(2) Watnick, P.; Kolter, R. Biofilm, City of Microbes. *Journal of Bacteriology*. **2000**, 2675–2679.

(3) Coenye, T. Bio Fi Lm. *Biofilm.* **2021**, *3*, 100043.

(4) Li, J.; Xie, S.; Ahmed, S.; Wang, F.; Gu, Y.; Zhang, C.; Chai, X.; Wu, Y.; Cai, J.; Cheng, G. Antimicrobial Activity and Resistance: Influencing Factors. *Front. Pharmacol.* **2017**, *8* , 1–11.

(5) Rumbaugh, K. P.; Sauer, K. Biofilm Dispersion. *Nat. Rev. Microbiol.* **2020**, *18* , 571–586.

(6) Avila-Novoa, M. G.; Iñíguez-Moreno, M.; Solís-Velázquez, O. A.; González-Gómez, J. P.; Guerrero-Medina, P. J.; Gutiérrez-Lomelí, M. Biofilm Formation by *Staphylococcus aureus* Isolated from Food Contact Surfaces in the Dairy Industry of Jalisco, Mexico. *J. Food Qual.* **2018**, *2018*, 1746139.

(7) Bhattacharjee, B.; Das, A.; Das, G.; Ramesh, A. Urea-Based Ligand as an Efflux Pump Inhibitor: Warhead to Counter Ciprofloxacin Resistance and Inhibit Collagen Adhesion by MRSA. *ACS Appl. Bio Mater.* **2022**, *5* (4), 1710–1720.

(8) Kokare, C. R.; Chakraborty, S.; Khopade, A. N.; Mahadik, K. R. Biofilm: Importance and Applications. *Indian Journal of Biotechnology*. **2009**, 159–168.

(9) Li, Z.; Zhuang, H.; Wang, G.; Wang, H.; Dong, Y. Prevalence, Predictors, and Mortality of Bloodstream Infections Due to Methicillin-Resistant *Staphylococcus aureus* in Patients with Malignancy: Systemic Review and Meta-Analysis. *BMC Infect. Dis.* **2021**, *21* (1), 1–10.

(10) Grillo, S.; Cuervo, G.; Laporte-Amargós, J.; Tuells, M.; Grau, I.; Berbel, D.; Gudiol, C.; Pujol, M.; Carratalà, J. Bloodstream Infection and Endocarditis Caused by *Staphylococcus aureus* in Patients with Cancer: A Multicenter Cohort Study. *Infect. Dis. Ther.* **2022**, *11* (1), 323–334.

(11) Carney, D. N.; Fossieck, B. E. J.; Parker, R. H.; Minna, J. D. Bacteremia Due to *Staphylococcus aureus* in Patients with Cancer: Report on 45 Cases in Adults and Review of the Literature. *Rev. Infect. Dis.* **1982**, *4* (1), 1–12.

(12) Crysandt, M.; Lemmen, S. W.; Jost, E.; Brummendorf, T. H.; Osieka, R.; Wilop, S. Antineoplastic Chemotherapy in Cancer Patients with Methicillin-Resistant *Staphylococcus Aureus* (MRSA). *Oncol. Res. Treat.* **2010**, *33* (11), 598–603.

(13) Jiang, Y. H.; Xin, W. G.; Yang, L. Y.; Ying, J. P.; Zhao, Z. S.; Lin, L. B.; Li, X. Z.; Zhang, Q. L. A Novel Bacteriocin against *Staphylococcus aureus* from *Lactobacillus paracasei* Isolated

from Yunnan Traditional Fermented Yogurt: Purification, Antibacterial Characterization, and Antibiofilm Activity. *J. Dairy Sci.* **2022**, *105* (3), 2094–2107.

(14) Jabbar, H.; Hala, F.; Radeef, M. Capability of Lactobacillus Acidophilus Supernatant to Inhibit Production of Lipase from Methicillin-Resistant Staphylococcus Aureus. *J. Univ. Anbar Pure Sci.* **2011**, *5* (2), 1-5.

(15) Zhou, B.; Zhang, D. Antibacterial Effects of Bacteriocins Isolated from *Lactobacillus Rhamnosus* (ATCC 53103) in a Rabbit Model of Knee Implant Infection. *Exp. Ther. Med.* **2018,** *15* (3), 2985–2989.

(16) Yan, X.; Gu, S.; Cui, X.; Shi, Y.; Wen, S.; Chen, H.; Ge, J. Antimicrobial, Anti-Adhesive and Anti-Biofilm Potential of Biosurfactants Isolated from *Pediococcus acidilactici* and *Lactobacillus plantarum* against *Staphylococcus aureus* CMCC26003. *Microb. Pathog.* **2019**, *127* , 12–20.

(17) Salas-Jara, M. J.; Ilabaca, A.; Vega, M.; García, A. Biofilm Forming *Lactobacillus*: New Challenges for the Development of Probiotics. *Microorganisms* **2016**, *4* (3), 35.

(18) Kang, M. S.; Lim, H. S.; Oh, J. S.; Lim, Y. J.; Wuertz-Kozak, K.; Harro, J. M.; Shirtliff, M. E.; Achermann, Y. Antimicrobial Activity of *Lactobacillus salivarius* and *Lactobacillus fermentum* against *Staphylococcus aureus*. *Pathog. Dis.* **2017,** *75* (2), 1–10.

(19) Karska-Wysocki, B.; Bazo, M.; Smoragiewicz, W. Antibacterial Activity of *Lactobacillus acidophilus* and *Lactobacillus casei* against Methicillin-Resistant Staphylococcus Aureus (MRSA). *Microbiol. Res.* **2010**, *165* (8), 674–686.

(20) Nguyen, D.; Huynh, T.; Nguyen, T. Anti-Biofilm Activities of *Lactobacillus acidophilus* against Staphylococcus Aureus ATCC 25923. *Available online www.jocpr.com J. Chem. Pharm. Res.* 2016, *8* (8), 464–467.

(21) Dinges, M. M.; Orwin, P. M.; Schlievert, P. M. Exotoxins of *Staphylococcus aureus*. *Clin. Microbiol. Rev.* **2000**, *13* (1), 16–34.

(22) Bhattacharjee, B.; Das, A.; Das, G.; Ramesh, A. Urea-Based Ligand as an Efflux Pump Inhibitor: Warhead to Counter Ciprofloxacin Resistance and Inhibit Collagen Adhesion by MRSA. *ACS Appl. Bio Mater.* **2022**, *5* (4), 1710–1720.

(23) Stubbendieck, R. M.; Straight, P. D. Multifaceted Interfaces of Bacterial Competition. *J. Bacteriol.* **2016**, *198* (16), 2145–2155.

(24) Debasmita, D.; Ghosh, S. S.; Chattopadhyay, A. Hierarchical Passage of Gold Nanoclusters in Living Bacteria. *ACS Appl. Bio Mater.* **2022**, 5 (6), 2543–2548.

(25) Debasmita, D.; Ghosh, S. S.; Chattopadhyay, A. Living Gut Bacteria Functionalized with Gold Nanoclusters and Drug for Facile Cancer Theranostics. *ACS Appl. Bio Mater.* **2023**.

(26) Swofford, C. A.; St. Jean, A. T.; Panteli, J. T.; Brentzel, Z. J.; Forbes, N. S. Identification

of *Staphylococcus aureus* α-Hemolysin as a Protein Drug That Is Secreted by Anticancer Bacteria and Rapidly Kills Cancer Cells. *Biotechnol. Bioeng.* **2014**, *111* (6), 1233–1245.

(27) Mohammedsaeed, W.; McBain, A. J.; Cruickshank, S. M.; O'Neill, C. A. *Lactobacillus Rhamnosus* GG Inhibits the Toxic Effects of *Staphylococcus aureus* on Epidermal Keratinocytes. *Appl. Environ. Microbiol.* **2014**, *80* (18), 5773–5781.

(28) Kruszewska, H.; Zabera, T.; Tyski, S. Antimicrobial Activity of Selected Non-Antibiotics - Activity of Methotrexate against *Staphylococcus aureus* Strains. *Acta Pol. Pharm. - Drug Res.* **2000**, *57* , 117–119.

(29) Savage, V. J.; Chopra, I.; O'Neill, A. J. *Staphylococcus aureus* Biofilms Promote Horizontal Transfer of Antibiotic Resistance. *Antimicrob. Agents Chemother.* **2013**, *57* (4), 1968–1970.

(30) Dwivedi, S.; Wahab, R.; Khan, F.; Mishra, Y. K.; Musarrat, J.; Al-Khedhairy, A. A. Reactive Oxygen Species Mediated Bacterial Biofilm Inhibition via Zinc Oxide Nanoparticles and Their Statistical Determination. *PLoS One.* **2014**, *9* (11), 1–9.

(31) Qayyum, S.; Oves, M.; Khan, A. U. Obliteration of Bacterial Growth and Biofilm through ROS Generation by Facilely Synthesized Green Silver Nanoparticles. *PLoS One.* **2017**, *12* (8), 1–18.

Chapter 5

Conclusions and Future Prospects

5.1 Conclusions

The dissertation work aimed at developing a living, motile, and fluorescent drug encapsulated bacbot for effectively killing of cancer cells and eradicate the secondary infection caused by *S. aureus* biofilm. The chemical synthesis of gold nanoclusters on living bacteria was standardized in a manner that the bacteria remained intact, motile and viable. The gold nanoclusters rendered the bacteria fluorescent, making them trackable. The study was done using a wild type strain this is human friendly in nature. The study showed that a non-genetically modified wild type strain can be used against cancer.

Briefly, the gold nanoclusters were formed on the surface of the bacteria and the nanoclusters were passed to the progenies in the form of large spheres. The spheres were composed of aggregates of gold nanoclusters. As the parent bacteria divided into the progenies these clusters aggregated to form larger spheres appearing like nanoparticles. This study was up taken for six subsequent sub-cultures of the parent gold nanocluster bearing bacteria. Each sub-culture was done after an interval of 48 h incubation The doubling time of the bacteria is 1.1 h. Thus, the passage of gold nanoclusters was studied in details up to 262 cell divisions. As the sub-cultures progressed, the number of the aggregated spheres gradually decreased. The aggregations of nanoclusters could be attributed to the cell membrane remodeling during the cell division. The loss of some portions of membrane during every division made the bacteria lose some of the nanoclusters and thus the number of large aggregates decreased. This study is one of its own kind.

Next study was done to explore the anti-cancer activity of the bacbots. For this, an anti-cancer drug methotrexate was encapsulated on the bacbots and only 1.8 μM of the drug was loaded. This was much lower than the IC50 of the drug on HeLa cells. Originally the drug was not effective against HT29 cells. Hence, these two cancer cell lines were chosen and a non-cancerous cell line HEK-293 was also chosen for determining the efficiency and specificity of the bacbots. The bacbots were highly effective against cancer cells than non-cancerous cells especially towards the HeLa cells. The reason could be presence of higher affinity of the metabolites released from the bacteria towards a specific cell type. The study was not only limited to monolayer of cells rather, 3D spheroids of these cancer cells were also treated with the bacbots. The results have shown cytoxicity on spheroids in only 6 h of treatment. There are few noticeable points such as the gold nanocluster synthesis did not alter the toxicity of the bacteria against the cancer cells. The bacbots were able to selectively act on the cancer cells (especially HeLa cells) indicating their specific nature. The toxicity was seen on TME mimicking spheroids at low concentration of bacteria in just 6 h indicates the efficiency of the bacteria and drug synergistically.

Further, the study was up taken to determine the anti-bacterial and anti-biofilm effect of the bacbots on *S.aureus*. The latter being a strain associated with secondary infection in cancer patients. The bacbots were able to inhibit the growth of *S.aureus* in planktonic state and also were able to eradicate about 90-95% of the biofilm. The study shows that the synergistic effect of methotrexate and bacbots was capable to fight against the deadly pathogen. This also indicates that the developed bacbots are a two-in-one solution for the cancer and associated infections caused by *S.aureus*. Since, the bacbot has a drug and a living component, the development of resistance

against the bacbots might be difficult in future. Here, the bacbots are able to act against the pathogen an also making the drug available for action into depth of the biofilms.

5.2 Future prospects

The current study reveals that the wild type gut friendly bacteria can be used against tumors. The bacbots that were synthesized were used for achieving two different targets - one is cancer and the other is biofilms associated with cancer. In future, a much realistic model for co-infecting the cancer spheroids and *S. aureus* with the bacbots can be designed. The bacbots were fabricated with gold nanoclusters that rendered them fluorescent and provided traceability. In future, the bacbots can be used as trackers due to their specificity towards cancer cells and ability to cling on the outer surface of the cells and some of them can also invade inside. The natural specificity of the bacteria can be elevated by fabricating the bacterial surface with target specific entities such as antibodies, aptamers, receptor specific small molecules etc. The bacbots can be upgraded in future by fabricating the bacteria with iron oxide nanoparticles that would render magnetothermal therapy prospect using the bacbots. The bacbots were able to generate ROS among tumor cells and biofilm, thus, if ROS generating groups, nanoparticles, and polymers are fabricated on to the bacteria then photodynamic therapy can also be expected out of these bacbots. The bacbots are versatile in their ability as they were fluorescent, and had anti-tumour and anti-bacterial actions and also acted as drug carriers. So, the bacbots can be further modified to be responsive to external stimuli such as pH, magnetic field, radiation, temperature etc. The bacbots can also be used to develop sensors by virtue of their sensitivity towards cancer cells. Thus, the options are endless as the bacbots are highly versatile. In future, the bacbots - with appropriate modifications - can gradually overtake other therapeutic modes not only in cancer but for other diseases too.

List of Publications

- Debasmita, D.; Ghosh, S. S.; Chattopadhyay, A. Hierarchical Passage of Gold Nanoclusters in Living Bacteria. *ACS Appl. Bio Mater.* **2022,** *5*(6), 2543–2548.
- Debasmita, D.; Ghosh, S. S.; Chattopadhyay, A. Living Gut Bacteria Functionalized with Gold Nanoclusters and Drug for Facile Cancer Theranostics. *ACS Appl. Bio Mater.* **2023.** (https://pubs.acs.org/doi/10.1021/acsabm.2c00911)
- Debasmita, D.; Ghosh, S. S.; Chattopadhyay, A. Nano-Enabled Bacbots for *Staphylococcus aureus* Biofilm Eradication (**manuscript under preparation**)

List of Conferences attended

- Flash Talk presented at 7th International Conference on Nanomaterials and Nanotechnology (ICANN 2021). Organised by Centre for Nanotechnology, IIT Guwahati.
- Particiated in Zeiss Microscopy Conclave 2019. Organized at Zeiss campus, Bomasandra, Bangalore, Karnataka, India.
- Poster presented at 6th International Conference on Nanomaterials and Nanotechnology (ICANN 2019). Organised by Centre for Nanotechnology, IIT Guwahati.
- Volunteered and participated in 5th National workshop on NEMS/MEMS & Theranostic Devices (NWNTD 2019). Organized by Centre for Excellence in Research & Development of Nanoelectronic Theranostic Devices, Centre for Nanotechnology, IIT Guwahati.
- Poster presentation at 4th National workshop on NEMS/MEMS & Theranostic Devices (NWNTD 2018). Organized by Centre for Excellence in Research & Development of Nanoelectronic Theranostic Devices, Centre for Nanotechnology, IIT Guwahati.
- Particiated in Reflux 2018. Organized by Department of Chemical Engineering, IIT Guwahati.
- Demonstrated advanced equipment in TEQIP-III Short term course on "Advanced Computer Architecture". Organized by Centre for Nanotechnology, IIT Guwahati.

Permissions

Figure 1.2

Publisher: John Wiley and Sons

© 2021 The Authors. Advanced Science published by Wiley-VCH GmbH

Open Access Article

This is an open access article distributed under the terms of the Creative Commons CC BY license, which permits unrestricted use, distribution, and reproduction in any medium, provided the original work is properly cited.

You are not required to obtain permission to reuse this article.

For an understanding of what is meant by the terms of the Creative Commons License, please refer to Wiley's Open Access Terms and Conditions.

Permission is not required for this type of reuse.

Wiley offers a professional reprint service for high quality reproduction of articles from over 1400 scientific and medical journals. Wiley's reprint service offers:

- Peer reviewed research or reviews
- Tailored collections of articles
- A professional high quality finish
- Glossy journal style color covers
- Company or brand customisation
- Language translations
- Prompt turnaround times and delivery directly to your office, warehouse or congress

Please contact our Reprints department for a quotation. Email corporatesaleseurope@wiley.com or corporatesalesusa@wiley.com or corporatesalesDE@wiley.com.

JOHN WILEY AND SONS LICENSE TERMS AND CONDITIONS

Chapter 2

ACS PUBLICATION LICENCE TERMS AND CONDITIONS

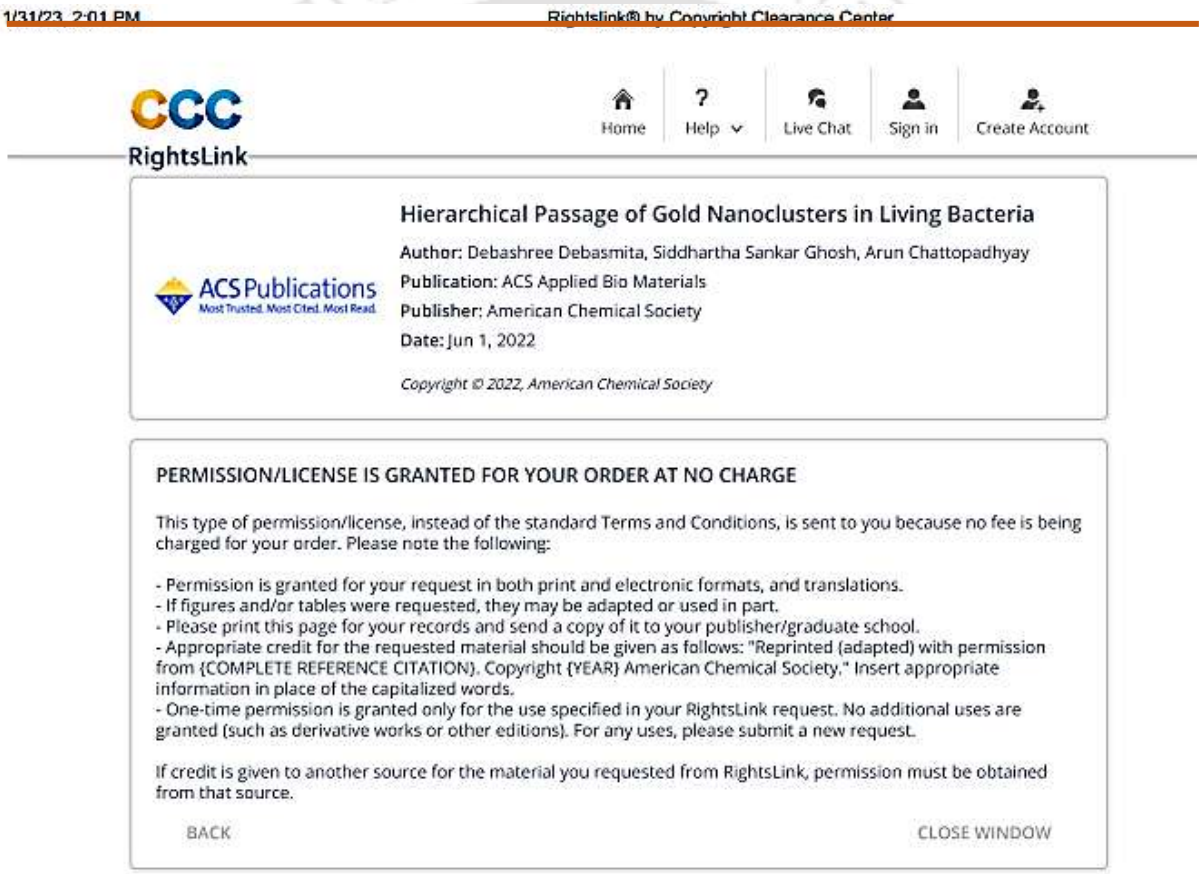

1/31/23, 2:01 PM Rightslink® by Copyright Clearance Center

CCC RightsLink

Home | Help | Live Chat | Sign in | Create Account

ACS Publications
Most Trusted. Most Cited. Most Read.

Hierarchical Passage of Gold Nanoclusters in Living Bacteria

Author: Debashree Debasmita, Siddhartha Sankar Ghosh, Arun Chattopadhyay
Publication: ACS Applied Bio Materials
Publisher: American Chemical Society
Date: Jun 1, 2022

Copyright © 2022, American Chemical Society

PERMISSION/LICENSE IS GRANTED FOR YOUR ORDER AT NO CHARGE

This type of permission/license, instead of the standard Terms and Conditions, is sent to you because no fee is being charged for your order. Please note the following:

- Permission is granted for your request in both print and electronic formats, and translations.
- If figures and/or tables were requested, they may be adapted or used in part.
- Please print this page for your records and send a copy of it to your publisher/graduate school.
- Appropriate credit for the requested material should be given as follows: "Reprinted (adapted) with permission from {COMPLETE REFERENCE CITATION). Copyright {YEAR} American Chemical Society." Insert appropriate information in place of the capitalized words.
- One-time permission is granted only for the use specified in your RightsLink request. No additional uses are granted (such as derivative works or other editions). For any uses, please submit a new request.

If credit is given to another source for the material you requested from RightsLink, permission must be obtained from that source.

BACK CLOSE WINDOW